Departement für Chemie
Universität Freiburg (Schweiz)

Complexation and Protonation Behaviour of Chiral Tetradentate Polypyridines Derived from *α*-Pinene

INAUGURAL-DISSERTATION

zur Erlangung der Würde eines Doctor rerum naturalium der Mathematisch-Naturwissenschaftlichen Fakultät der Universität Freiburg in der Schweiz

vorgelegt von

MATHIAS DÜGGELI

aus Malters (LU)

Diss. Nr. 1382
UniPrint
Freiburg, Juli 2002

Von der Mathematisch-Naturwissenschaftlichen Fakultät der Universität Freiburg in der Schweiz angenommen auf Antrag der Jury:

Prof. Dr. Carl-Willhelm Schläpfer, Departement für Chemie, Universität Freiburg (Jurypräsident).

Prof. Dr. Alexander von Zelewsky, Doktorvater, Departement für Chemie, Universität Freiburg.
Prof. Dr. Peter Belser, Departement für Chemie, Universität Freiburg.
Prof. Dr. Helen Stoeckli-Evans, Institut de chimie, Université de Neuchâtel.

Fribourg, 19. Juli 2002

Prof. Dr. Alexander von Zelewsky
Dissertationsleiter und Dekan

Prof. Dr. Jean-Pierre Métraux
Vizedekan

Diese Arbeit wurde vom Schweizerischen Nationalfonds unterstützt.

MEINEM VATER GEWIDMET

“Scio me nihil scire“

(Ich weiss, dass ich nichts weiss)

Sokrates

(469 – 399 v.Chr.)

Dankesworte

Der grösste Dank gebührt Herrn Prof. Dr. Alex von Zelewsky. Er hat mich freundlicherweise in seiner Forschungsgruppe aufgenommen und mich wohlwollend durch die Doktorandenjahre begleitet. Seine Grosszügigkeit, sein Ideenreichtum und die Forschungsfreiheit, die er mir gewährte, machten diese Arbeit zum Vergnügen. Vor allem schätzte ich seine motivierende Unterstützung in “schwierigeren Zeiten“. Für all das ein herzliches Vergelts Gott.

Von ganzem Herzen danke ich Herrn Prof. Dr. Peter Belser, dass es sich als interner Experte zur Verfügung gestellt hat. Seine Kompetenz im praktischen und synthetischen Bereich haben viel zum erfolgreichen Abschluss dieser These beigetragen. Auch die zahlreichen Diskussionen um 9 Uhr bei Kaffee und Gipfeli waren immer eine Bereicherung.

Frau Prof. Dr. Helen Stoeckli-Evans spreche ich meinen herzlichen Dank aus, nicht nur für die Messungen und Auswertungen von Kristallstrukturen, sondern auch für die Beurteilung meiner Arbeit als externe Expertin.

Herrn Prof. Dr. C. W. Schläpfer möchte ich für die zahlreichen Diskussionen und Auswertungen von Messdaten danken. Ebenfalls gedankt sei für die Möglichkeit, als Assistent zu arbeiten.

Hernn Prof. Dr. Jenny möchte ich für Diskussionen über NMR-Spektren danken.

Herrn Prof. Dr. Gossauer sei gedankt für die Möglichkeit, als Assistent zu arbeiten.

Ganz speziell danken möchte ich Herrn Dr. Detlef Moskau von Bruker Biospin in Fällanden für die Möglichkeit, einige Messungen in Fällanden durchzuführen und für die zahlreiche Ratschläge bei technischen Problemen mit dem NMR-Spektrometer.

Ein kollegialer Dank geht an meinen langjährigen Labor- und Studienkollege Dr. Didier Lötscher. Wir durften viele unvergessliche Stunden miteinander erleben. Herzlichen Dank, Didier. Auch möchte ich Dir, für das Durchlesen und Korrigieren des Manuskriptes danken.

Einen herzlichen Dank geht auch an Dr. Manel Querol, der mich durch zahlreiche Diskussionen immer wieder motiviert hat. Danke auch für das kritische Durchlesen des Manuskriptes.

Danken möchte ich für die guten Diplomarbeiten von Christophe Bonte, Tobias Christen und David Mauron (†). David, ich denke viel an das letzte Bier, das wir zusammen getrunken haben.

Ich möchte auch Michael Wälchli, unserem Lehrling danken. Er war nicht nur wegen seines Humors eine Bereicherung in unserem Labor.

Speziell erwähnen möchte ich folgende Personen: Dr. Gregory Malaisé, Boris Quinodoz, Dr. Marielle Loi, Dr. Liam Gilby und Manuel Raemy. Sie alle haben Zeit gefunden, mein Manuskript durchzulesen und zu korrigieren. Herzlichen Dank, zudem durfte ich mit Ihnen zahlreiche gemütliche Stunden ausserhalb der Uni verbringen.

Herzlichen Dank, Dr. Liz Kohl. Deine Einführungen für die Benutzung der NMR-Geräte waren sehr kompetent und angenehm. Danke auch für die Literatursuche.

Für zahlreiche analytische Messungen danke ich auch Inge Müller, Felix Fehr und Fredy Nydegger.

Ein grosser Dank auch dem Zentraldienst: Philippe Rime, Noëlle Chassot, Lucienne Rouiller, Hubert Favre und Alphonse Crottet. Eure Bemühungen haben meine Arbeit um einiges erleichtert.

Für die Erledigung der administrativen Dinge und für die Organisation von Weihnachtsfesten danke ich Emerith Brügger herzlich.

Ein Merci an alle meine Studentinnen und Studenten, die immer genug Geduld mit mir hatten.

Ich möchte den Forschungsgruppen von Prof. Dr. Alex von Zelewsky, Prof. Dr. Peter Belser und der ganzen anorganische Sektion für die angenehme Arbeitsatmosphäre danken. Dank geht an Prof. Dr. Franzpeter Emmenegger, Prof. Dr. Claude Daul, Dr. Brunhilde Kolb, Dr. Cathy Goujon-Ginglinger, Dr. Dominique Suhr, Dr. Ilaria Ciofini, Dr. Jorge A. Parola, Dr. Liana Ghizdavu, Dr. Magali Palacio, Dr. Mattieu Buchs, Dr. Olimpia Mamula, Dr. Sandrine Fraysse, Dr. Ulrich Knof, Anita Mader, Bilijana Bozic, Cedric Rauzy, Danut Bilc (†), Dominik Wuest, Dusan Drahonovsky, Fabio Mariotti, Laure-Emmanuelle Perret-Aebi, Michel Piccand, Nunzio Salluce, Pio Bättig, Sarah Richard-Ducotterd, Silvia Roma, Simona Ciobanu, Thomas Bark, Valery Weber, Vincenzo Adamo, Yoel Chirqui.

Zum Schluss möchte ich ganz herzlich meiner Familie und meiner Verlobten danken, die mich während dem ganzem Doktorat unterstützt haben.

ABSTRACT

In the scope of this thesis, enantiomerically pure 5'- and 6'-substituted pinene-fused-bipyridine- (pinene-bpy-derivatives) and *N*-pyridine ligands (pinene-*N*-py derivatives) have been prepared. The 6'-bromo-substituted pinene-bpy derivatives can act as precursors for the synthesis of several 6'-subsituted pinene-bpy derivatives. Tetradentate ligands have been prepared starting from these 5' and 6'-substutiuted pinene-bpy derivatives, the pinene-bpy moieties are linked either directly or with a *p*-xylyl-bridge. All ligands have been entirely characterized, some of them with X-ray analysis.

The tetradentate ligands containing a *p*-xylyl-bridge were used for the formations of supramolecular aggregates such as hexanuclear, circular helicates, which were characterized in solution. The tetradentate ligands, where the two bipyridine moieties are directly linked, were used for the formation of mononuclear silver(I)-complexes.

An extended protonation study was carried out with the non-substituted bi- and tetradentate pinene-bpy-derivatives. In one case, it was shown, that a proton can fix the ligand in a conformation analogous to that of metal complexes.

ZUSAMMENFASSUNG

Im Rahmen der vorliegenden Arbeit wurden neue enantiomerenreine 5'- und 6'-substituierte, mit Pinen annellierte Bipyridin- (Pinen-bpy Derivate) und *N*-Pyridin-Liganden (Pinen-N-py Derivate) hergestellt. Die 6'-Brom substituierten Pinen-bpy Derivate stellen dabei geeignete Zwischenstufen für die Synthese von weiteren 6'-substituierten Pinen-bpy Derivate dar. Tetradentate Liganden konnten ausgehend von diesen Pinen-bpy-Derivaten hergestellt werden, wobei die beiden Pinen-bpy Einheiten direkt oder über eine *p*-Xylyl-Brücke verbunden sind. Alle diese Liganden konnten vollständig charakterisiert werden, einige auch mittels Röntgenstrukturanalyse.

Die mit *p*-Xylyl verbrückten tetradentaten Liganden wurden für die Synthese von supramolekularen Aggregaten verwendet. Diese hexanuklearen Zirkularhelicate konnten in Lösung charakterisiert werden. Mononukleare Silber(I)Komplexe wurden mit den direkten verbrückten tetradentaten Liganden hergestellt und charakterisiert.

Eine ausgedehnte Studie über das Protonierungsverhalten wurde mit den nicht-substituierten di- und tetradentaten Pinen-bpy-Liganden durchgeführt. Dabei konnte in einem Fall gezeigt werden, dass ein Proton, analog zu Metallkationen, die Konformation eines tetradentaten Liganden fixieren kann.

SYNTHESISED LIGANDS

All ligands are listed in the general schemes below. They are numbered in the text according to these charts.

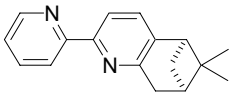

L1: [5,6]-pinene-bpy

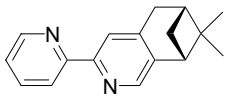

L2: [4,5]-pinene-bpy

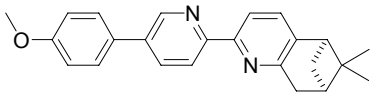

L3: {5'-*p*-MeO-Ph}-[5,6]-pinene-bpy

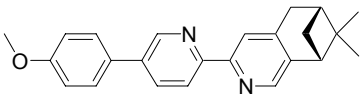

L4: {5'-*p*-MeO-Ph}-[4,5]-pinene-bpy

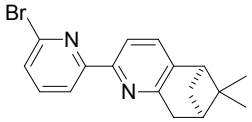

L5: {6'-Br}-[5,6]-pinene-bpy

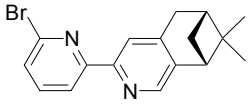

L6: {6'-Br}-[4,5]-pinene-bpy

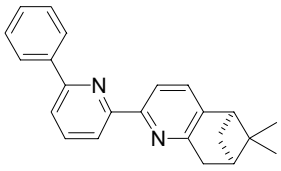

L7: {6'-Ph}-[5,6]-pinene-bpy

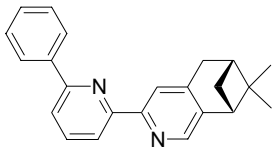

L8: {6'-Ph}-[4,5]-pinene-bpy

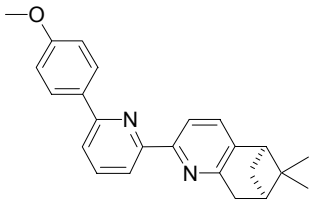

L9: {6'-*p*-MeO-Ph}-[5,6]-pinene-bpy

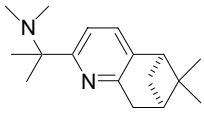

L10: {2-DAMI}-[5,6]-pinene-py

chart A: Pinene-bpy derivatives

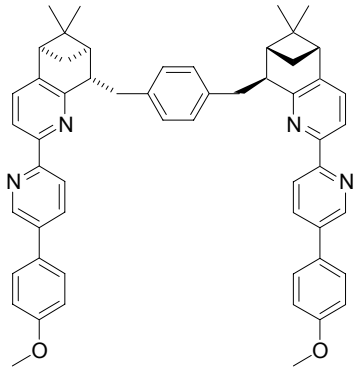

L11: {5'-*p*-MeO-Ph}-[5,6]-CHIRAGEN[*p*-xyl]

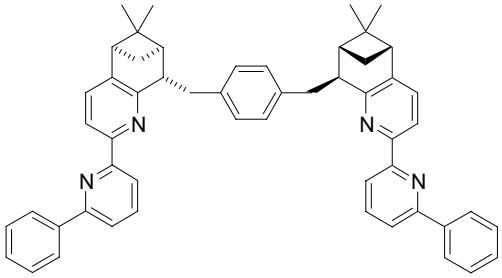

L12: {6'-Ph}-[5,6]-CHIRAGEN[*p*-xyl]

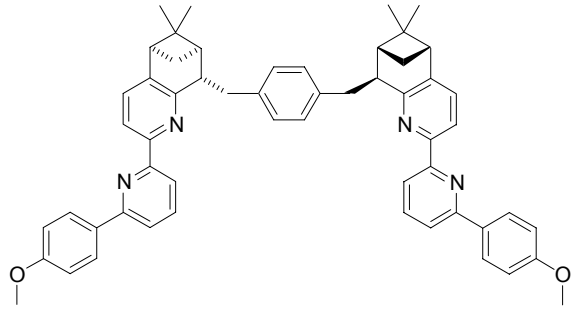

L13: {6'-*p*-MeO-Ph}-[5,6]-CHIRAGEN[*p*-xyl]

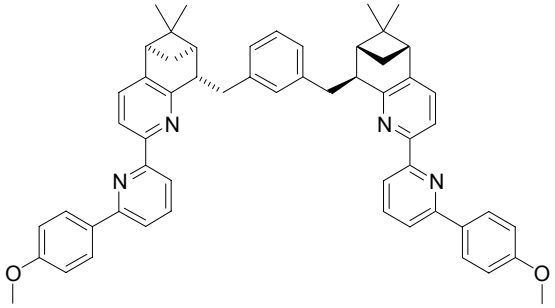

L14: {6'-*p*-MeO-Ph}-[5,6]-CHIRAGEN[*m*-xyl]

chart B: CHIRAGEN[bridge] derivatives

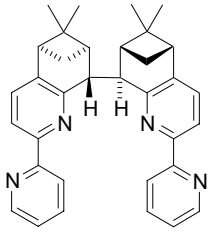

L15: [5,6]-CHIRAGEN[0]

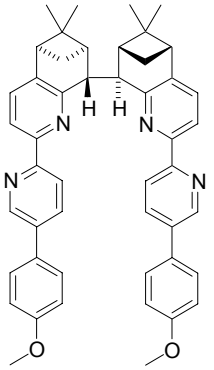

L16: {5'-*p*-MeO-Ph}-[5,6]-CHIRAGEN[0]

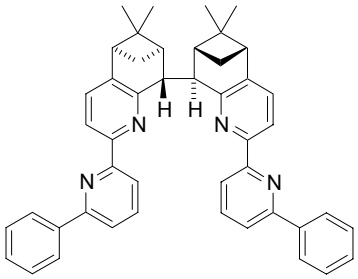

L17: {6'-Ph}-[5,6]-CHIRAGEN[0]

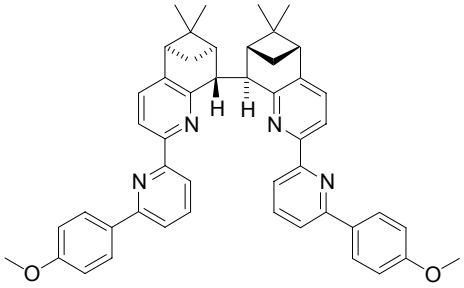

L18: {6'-*p*-MeO-Ph}-[5,6]-CHIRAGEN[0]

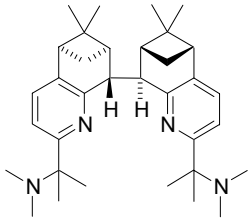

L19: {2-DAMI}-[5,6]-CHIRAGEN[0]

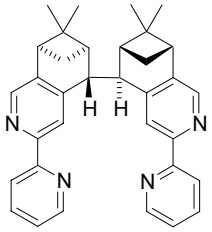

L20: [4,5]-CHIRAGEN[0]

chart C: CHIRAGEN[0] derivatives

ABBREVIATIONS

2-DAMI	2-(1-*N,N*-dimethylamino-isopropyl)-
Bpy	2,2'-bipyridine
CD	ciruclar dichroism spectroscopy
DEPT	Distortionsless Enhancement by Polarization Transfer
DMAA	*N,N*-dimethyl-acetamide
EI-MS	electron-impact ionization mass spectrosopy
ESI-MS	electrospray-mass spectroscopy
FAB-MS	fast atom bombardement mass spectroscopy
HETCOR	heteronuclear correlation experiments
HMBC	hetereonuclear multiple bond correlation
HMQC	hetereonuclear multiple quantum correlation
HOAc	acetic acid
LDA	lithium diisopropylamide
MLCT	metal to ligand charge transfer
m-xyl	*m*-xylene
NMR	nuclear magnetic resonance
NOE	nuclear Overhauser effect
Oac	acetate
Ph	phenyl
PS	proton sponge
p-MeO-Ph	*p*-methoxy-phenyl
p-xyl	*p*-xylene
Py	pyrdine
TFA	trifluoroacetic acid
THF	tetrahydrofuran
TMA	trimethylamine
TMEDA	*N,N,N',N'*-tetramethylethylendiamine
UV/Vis	ultraviolet-visible spectroscopy

TABLE OF CONTENTS

INTRODUCTION

INTRODUCTION

1. Helicity in natural and in artificial structures

A helix is a geometric motif, which is found in natural as well as in artificial structures on a macroscopic, microscopic and even on a molecular level. The definition of the word "helix" given by the American Heritage Dictionary of the English Language [1] is the following: "1. A three-dimensional curve that lies on a cylinder or cone, so that its angle to a plane perpendicular to the axis is constant (figure 1). 2. A spiral form or structure, ..." It comes from the ancient Greek word *'έλιξ*, which means "winding, convolution, spiral".

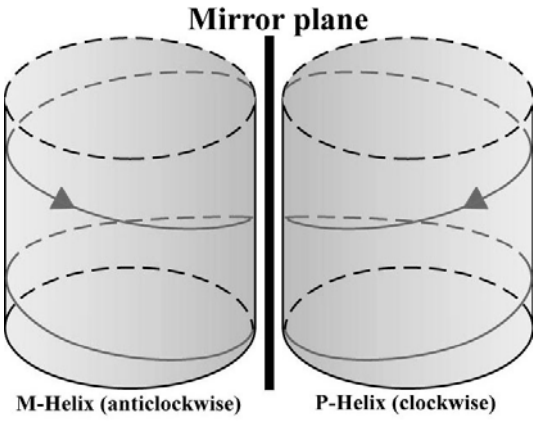

figure 1: left (*M*) and right (*P*) handed helices[1].

From the point of view of chirality* (definition: The property of any kind of object, that the object itself and its mirror image are not congruent), helices are intrinsically

* Chirality from the ancient Greek word: *χείρ:* hand. Our hands are chiral, they act as object and its mirror image. Chirality on molecular level can be defined as following: Any molecule lacking an improper symmetry axis S_n is chiral, although proper rotational axes of any rank may be present.[2] The concept of chirality is defined for the first time in Appendix H of the

chiral. The left-handed *M*-helix (minus, anticlockwise rotation) is the mirror image of the right-handed *P*-helix (plus, clockwise rotation).

Helicity can be observed in the spiral arms of galaxies, in snail shells or in microscopic structures such as right- or left-handed quartz[4] (figure 2) as well in human art, architectures and technology (figure 3).

figure 2: natural helical objects.

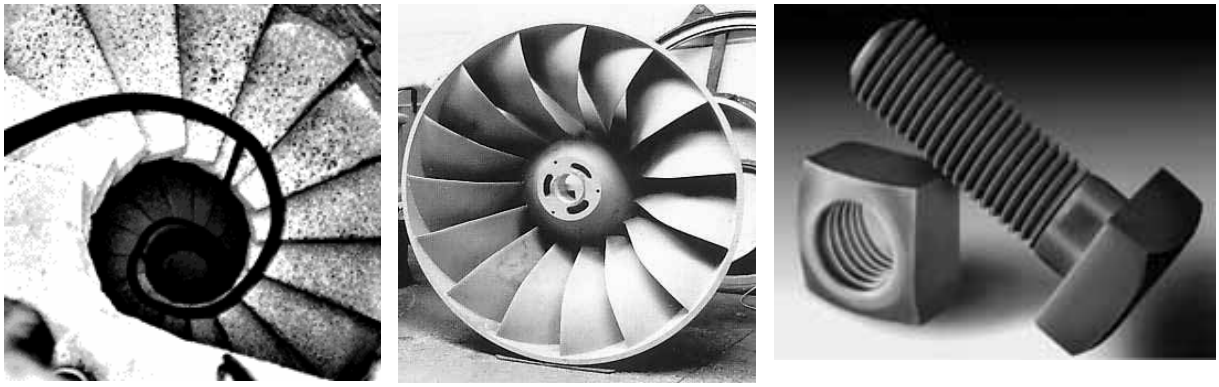

figure 3: artificial helical objects.

In chemistry or biochemistry helicity is present in various systems.[5] α-Amylose is a macromolecule with a helical structure that contains six glucose units per helical turn.[6] Deoxyribonucleic acid (DNA) exists as a double helix (figure 4) in which the two strands are connected by hydrogen bonds between complementary bases and π-stacking.[7,8] It stores and transmits our genetic make-up and therefore is essential for

---

'Baltimore Lectures' by Lord Kelvin.[3] This Appendix is the publication of a lecture given by Lord Kelvin in 1893.

life. Peptides can adopt an α-helical structure or form larger helical arrays, as found, for example found in the collagene triple helices.[9]

In artificial supramolecular architectures helicity can be introduced by conformational restrictions of macromolecules,[10] inter or intra-molecular hydrogen bonds[11,12] or coordinating metal ions.[13,14]

For the latter J. M. Lehn introduced in 1987 the term helicate for the description of a polymetallic double-stranded helical complex, actually a metal containing helix (figure 4).[15] It is formed by the contraction of the word helix with the suffix *–ate*, characterizing host-guest complexes between (pre)organized receptors (ligands) and metal ions in the same way as coron*ates* and crypt*ates*.

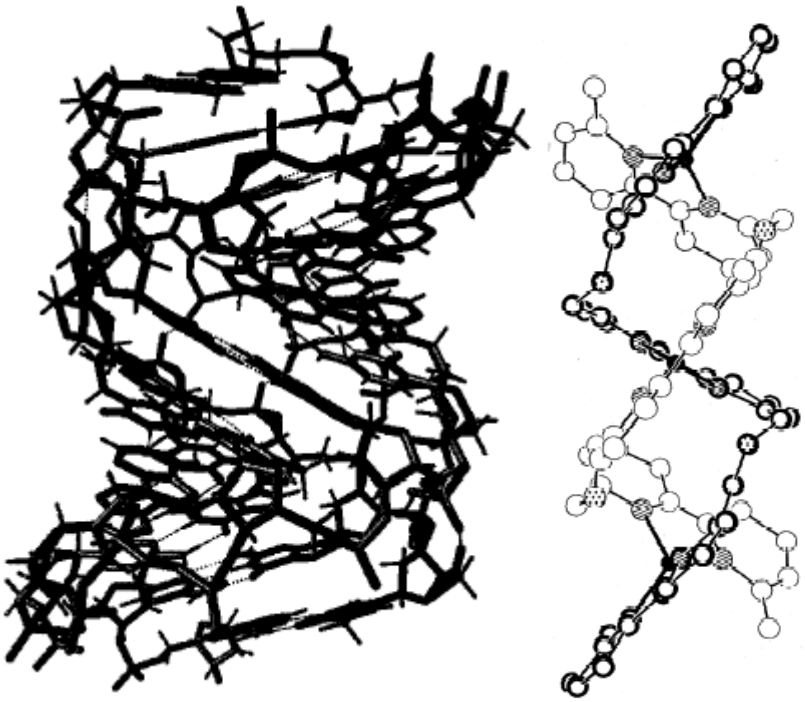

figure 4: X-ray structures of a double-stranded α-DNA[8] and a trinuclear double-stranded helicate.[15]

Nowadays the term helicate is used more generally for any metal complex, which contains at least one ligand strand and two or more metal centres.

2. Linear and circular helicates

2.1. General aspects of helicates

Since the introduction of the term helicate in 1987 (only a few double- and triple-stranded helicates were known before this date)[16-22], the research in this field has intensified and the number of publications has been increasing. Piguet[23] reviewed this subject in 1997 (containing ca. 200 references since 1987), Albrecht[24] in 2001 (containing ca. 200 references since 1997).

Mainly two different types of helicates can be distinguished: linear and circular ones. In linear helicates the metal cations define the helical axis, and the ligands wrap around these forming the helices. In circular helicates the metal cations are arranged in a circular fashion (figure 5; cf. Francis turbine in figure 2).

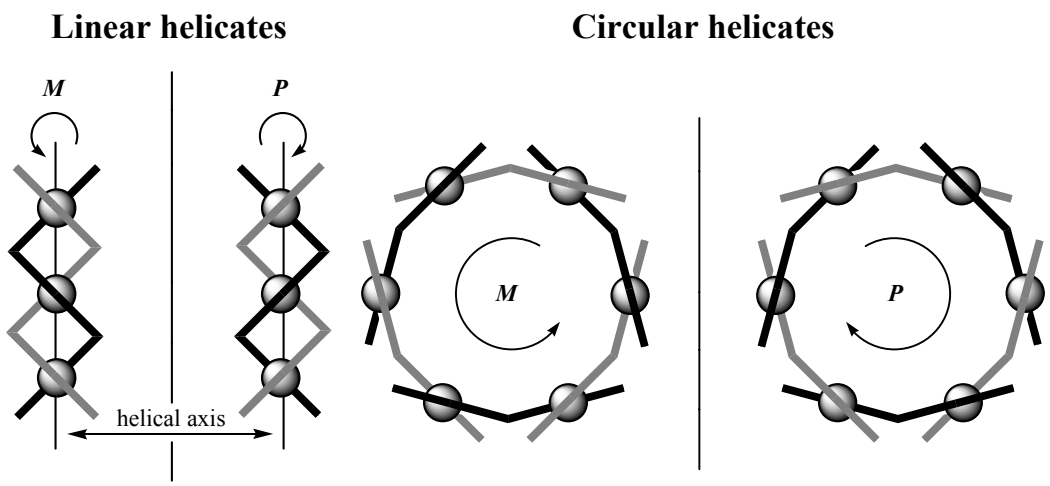

figure 5: linear and circular helicate.

In both cases two different forms of chirality can be considered. The first one is the orientation of the bridging ligands in the complex, which determines the sense of rotation of the resulting helix (figure 5). The ligands can be arranged in a clockwise (*P*-helix) or anticlockwise (*M*-helix) fashion.

The second one is the chirality at the metal centre. Already two bidentate ligands introduce helical chirality on an octahedral metal centre (figure 6). A convention can

be formulated for any complex, where two skew lines define uniquely a helical system in a coordination entity. The descriptors *Δ/Λ* (not following the CIP rule[25]) are generally used and officially recommended by IUPAC.

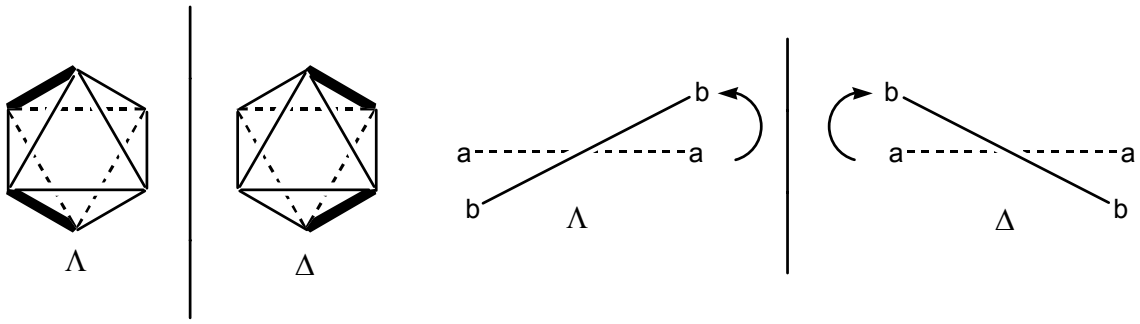

figure 6: helical chirality at an octahedral (OC-6) centre and the skew line system.

In cases of two orthogonal oriented lines (e.g. two unsymmetrical tridentate ligands on an octahedral centre in a meridional fashion (figure 7), or two bidentate ligands on a tetrahedral centre) another convention can be used for more clarity (oriented line system, chiral descriptors $\vec{\Delta}/\vec{\Lambda}$).[26]

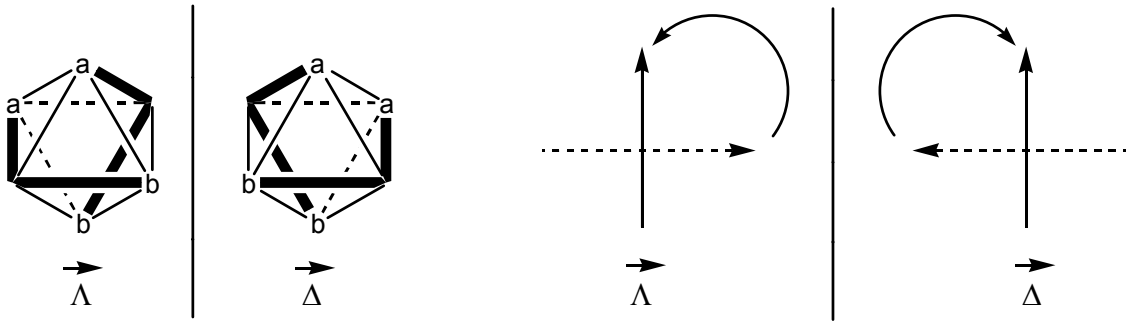

figure 7: octahedral complex with two tridentate ligands and the oriented line system.[26]

In a helicate, the metal centres possess the identical absolute configuration (homochiral, figure 8). Heterochiral systems lead either to side-by-side arrangements (alternating absolute configuration, not helical) or to irregular helicates (random absolute configuration).

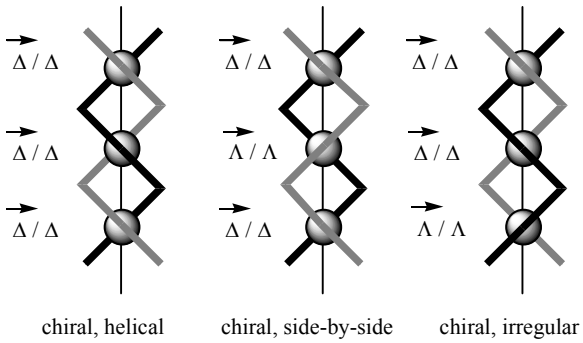

figure 8: chirality at polynuclear complexes.

Side-by-side arrangements with an even number of metal cations are achiral (mirror plane), the arrangements with an odd number of metal cations are still chiral, but not in a helical fashion. For polynuclear species, more complicated chiral and achiral, irregular helicates and side-by-side arrangements are possible due to different combinations of $\vec{\Delta}$/Δ- and $\vec{\Lambda}$/Λ- metal cations.

Achiral ligands lead to racemic mixtures of two enantiomeric helicates. Chiral enantiopure ligands are in general expected to form helicates in a more or less diastereoselective manner.

Most of the helicates published are formed by self-assembly processes, just by simple mixing of ligands and labile metal cations such as silver(I) or copper(I). These self-assembly processes are often controlled by self-recognition. If only complexes, with one kind of ligand per coordination compound (homoleptic) are formed, a sorting of the ligands proceeds by self-recognition during the self-assembly of the metallo-supramolecular aggregates. There are several different methods of controlling self-recognition: [24]

- Control by the number of binding sites: The mixing of bis-, tris- and tetra-bidentate ligands can lead only to the homoleptic, double-stranded helicates.[27]
- Control by coordination geometry: e.g. One ligand prefers a tetrahedral coordination geometry at the metal, leading to double-stranded helicates, while another can form octahedral metal complexes (→ triple-stranded helicates). The mixture of these ligands with two different metals leads to the sorting not only of the ligands, but also of the metals.[27]

- Size control: A further possibility of controlling self-recognition in the formation of helicates is to use rigid ligands with significant differences in the distances between the metal binding sites.[28]
- Self recognition by chiral ligands: another important possibility is the use of chiral centres in ligands strands. A racemic mixture of chiral ligands can lead to homoleptic helicates and therefore to diastereoselective formation of helicates.[29]
- Template control: The templating ability of counterions can control the self-recognition of the self-assembly of helicate-type ligands.[30]

2.2. Linear helicates

The characteristics of linear helicates can be described in different ways:

- Number of central atoms in the helical axis: di-, tri-, tetra- and polynuclear species (figure 9).
- Number of strands, wrapping around the helical axis: single-, double- and triple-stranded helicates (figure 9).
- Different types of strands: identical strands lead to homoleptic, different strands to heteroleptic helicates.

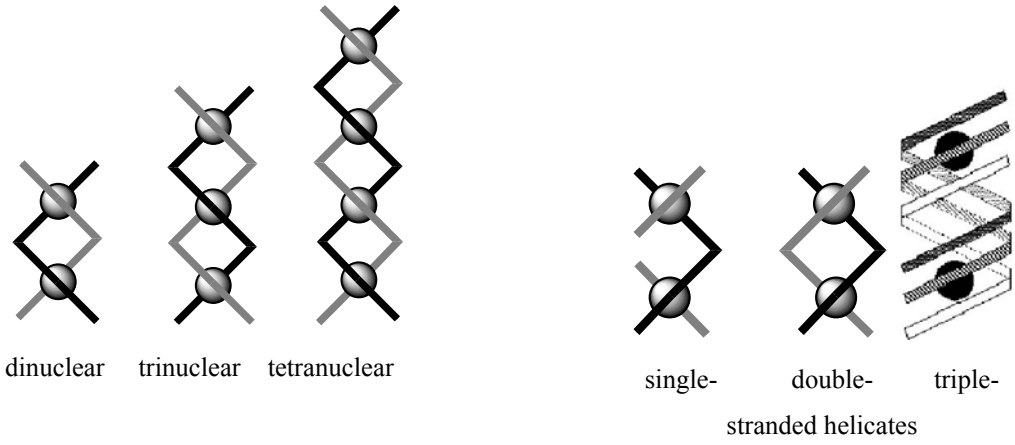

figure 9: different types of helicates.

- Binding site of strands: a strand with a sequence of similar binding units leads to homotopic helicates (figure 10). Strands possessing different binding units provide a directionality within the strands. These heterotopic helicates exist in two diastereomeric forms according to the orientation of the coordinated binding units (head-to-head or head-to-tail).
- Saturation: when the stereochemical requirements of the metal ions are fulfilled by the donor atoms of the strands, the helicate is saturated (figure 10). Unsaturated helicates need other ligands to complete the coordination sphere.

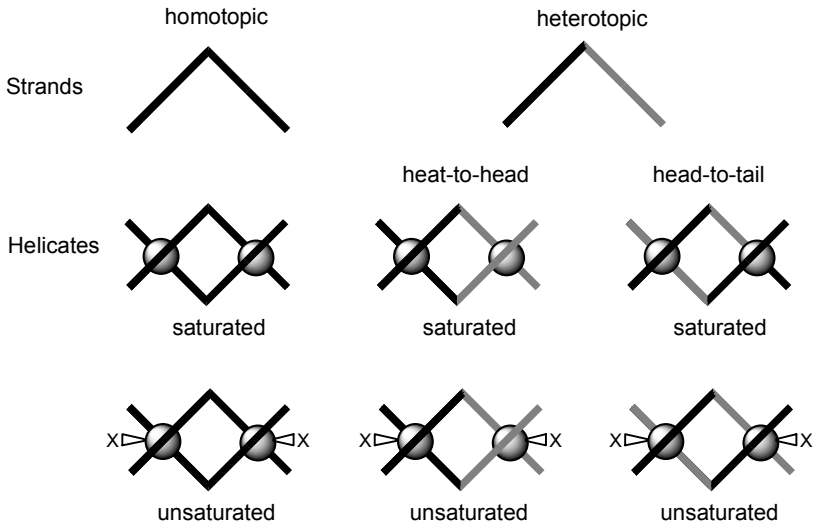

figure 10: homotopic and heterotopic strands provide different helicates

Many examples of linear helicates with nearly all variations of the points mentioned above are known and reviewed in the articles of Piguet[23] and Albrecht.[24] A few remarkable examples of linear helicates are discussed here.

First of all, a special case will be treated: single-stranded, dinuclear and trinuclear helicates. While ligands with fixed conformations (**L21)** (chart 1) lead to single-stranded dinuclear helicates[31], where the helicity can easily be attributed, a problem arises with ligands, which can still change the conformation upon complexation, such as **L22**.[32]

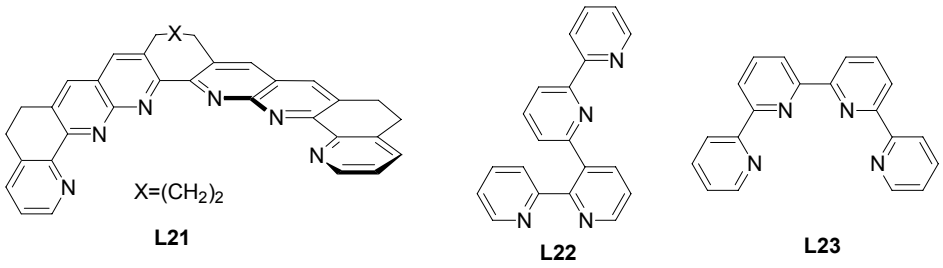

chart 1: ligands for single-stranded dinuclear complexes

The resulting hetero-dinuclear cation $[Cl(CO)_3Re(\mathbf{L22})Ru(bpy)_2]^{2+}$ (figure 11) still corresponds to the definition of a heterotopic single-stranded helicate despite the unusual conformation of the ligand strand, which is obviously not compatible with our intuitive representation of a helix (figure 1, p.2).

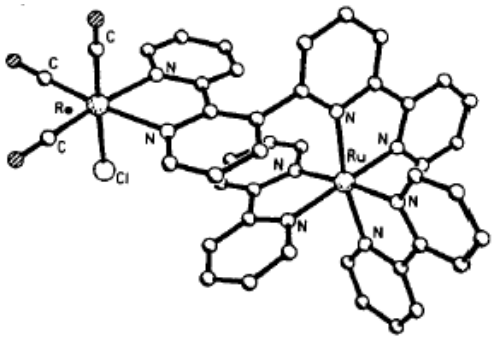

figure 11: crystal structure of $[Cl(CO)_3Re(\mathbf{L22})Ru(bpy)_2]^{2+}$. [32]

A general approach considers the segmental ligand **L22** (or its symmetrical analogue **L23**, chart 1) as a strand adopting *P* or *M* helicity (or *T* conformation) (scheme 1).[33] According to this statement, almost any dinuclear complex possessing a linear nonplanar (*P* or *M* configuration) chelating strand may loosely be described as a single-stranded helicate .[34]

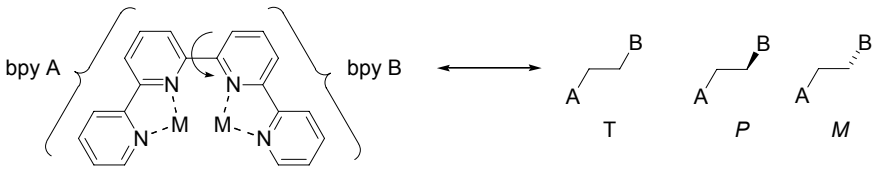

scheme 1: possible conformation of **L23** acting as bis-bidentate chelate bridging ligand.

Nevertheless, an example of a single-stranded trinuclear complex, synthesised by our group [35] and obtained in a enantiopure form should be mentioned (scheme 2).

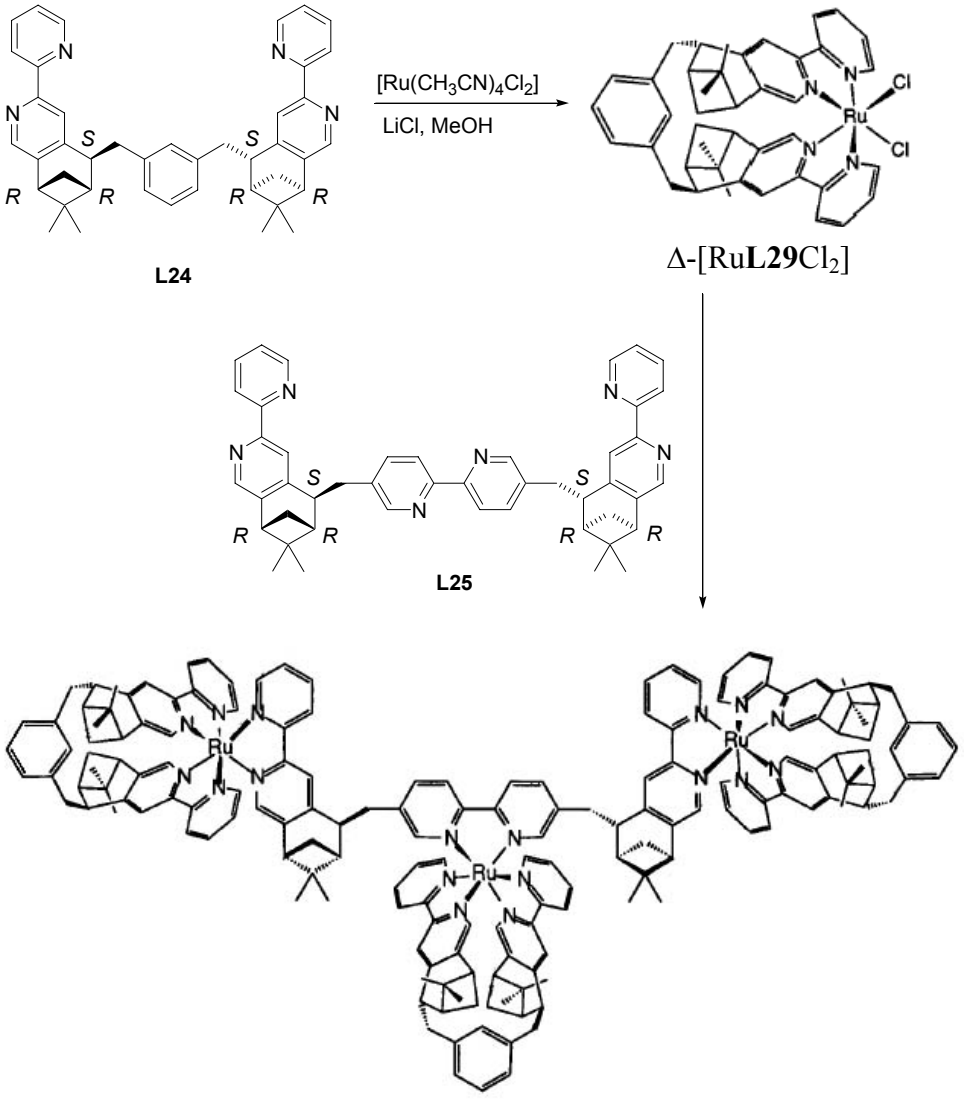

scheme 2: single-stranded, trinuclear complex [{Δ-Ru**L24**}$_3$-μ-**L25**](PF$_6$)$_6$.[36]

Starting from the enantiopure ligand **L24**, available in a few steps from myrtenal, the ruthenium complex [Ru**L24**Cl$_2$] was obtained with predefined absolute configuration.[37] By reacting this building block [Ru**L24**Cl$_2$] (3 eq.) with ligand **L25** (1 eq.), only one enantiomer of the trinuclear complex is formed. To achieve absolute control of the stereoselecetivity in this complex (it contains 27 elements of chirality!), chirality is introduced step by step. Starting from *R,R*-(-)-myrtenal (8*2 stereogenic carbon atoms have configurations determined by nature), one enantiomer of **L24**

(*RRS*,*SRR*) and **L25** (*RRS*,*SRR*) is obtained (4*2 stereogenic carbon atoms have configurations determined by stereoselective synthesis). **L24** predetermines the absolute configuration *Δ* at the metal centre. By reacting this *Δ*-building block with **L25**, the configuration at the ruthenium centres (configuration is determined at 3 metal centres by stereoselective synthesis) does not change and therefore the trinuclear species contains three homochiral metal centres (an important property of a helicate). But as already discussed above, the strand of this trinuclear complex can change the conformation, and therefore the helical wrapping of the strand around the metal is only one of several possible conformations.

The synthesis of [{Δ-Ru**L24**}$_3$-*μ*-**L25**](PF$_6$)$_6$ in six steps is in contrast with the next example discussed here: a self-assembly process published recently by Hannon *et al*.[38], where enantiopure dinuclear double-stranded helicates were synthesised by a one-pot synthesis starting from the commercially available materials for the ligands (pyridine-2-carbaldehyde and *R*- or *S*-1,1'-binaphthalene-2,2'-diamine, scheme 3) and a silver(I) source.

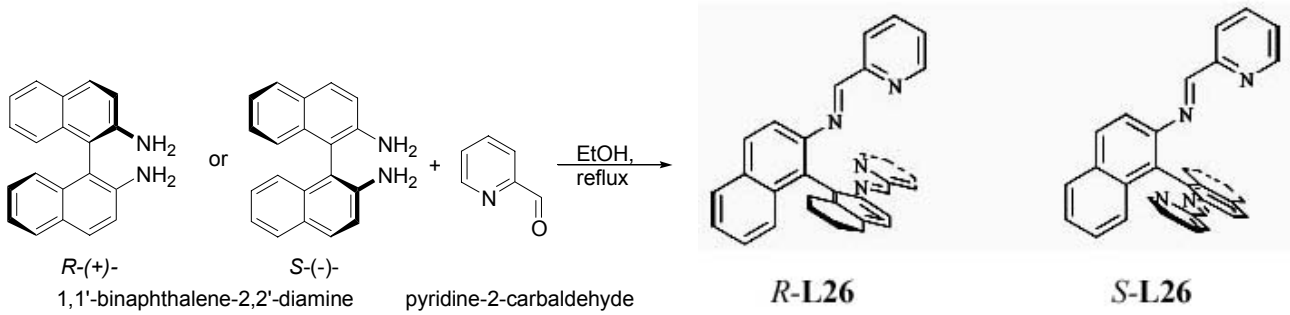

scheme 3: formation of enantiopure ligands *R*-**L26** and *S*-**L26**.

The enantiopure ligand *R*- or *S*-**L26** is formed *in-situ* and reacts readily with silver(I) acetate to form the enantiopure helicates, which precipitate by addition of ammonium hexafluorophosphate giving *PΔΔ*-[Ag$_2$(*R*-**L26**)$_2$](PF$_6$)$_2$ or *MΛΛ*-[Ag$_2$(*S*-**L26**)$_2$](PF$_6$)$_2$, respectively (figure 12). The CD-spectra[†] of both enantiomers are described and show the expected opposite signals.

[†] Circular dichroism is a standard method for detecting enantiopure, optically active species.

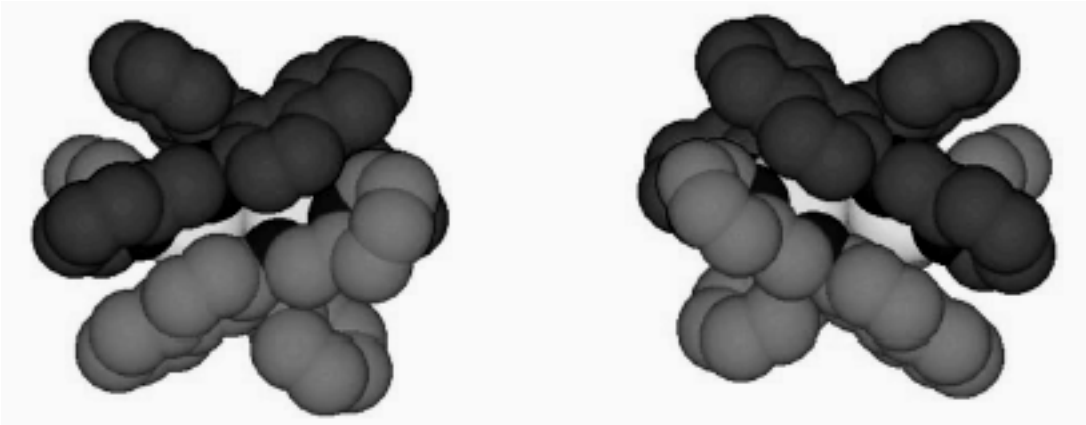

figure 12: the two enantiomers of a dinuclear, double-stranded helicates: *PΔΔ*-[Ag_2(*R*-**L26**)$_2$](PF_6)$_2$ and *MΛΛ*-[Ag_2(*S*-**L26**)$_2$](PF_6)$_2$.[38]

Another example of enantioselective synthesis of helicates were carried out by Williams *et al.*.[39,40] They used chiral bis(oxazolyl)pyridine ligands **L27**-**L29** (figure 13). These ligands were used in rhodium catalysed enantioselective hydrosilylation of ketones by Nishiyama and co-workers in 1991 to achieve high enatiomeric excess.[41] The *S,S*-enantiomer of **L27** and **L28** form the dinuclear, double-stranded helicates *PΔΔ*-[Ag_2(*S,S*-**L27**)$_2$](BF_4)$_2$ and *PΔΔ*-[Ag_2(*S,S*-**L28**)$_2$](BF_4)$_2$ (figure 13). The *R,R*-enantiomers lead to corresponding *MΛΛ*-entaniomers. When a racemic mixture of **L27** or **L28** was used, the ^{1}H-NMR-spectrum was identical to that of the pure one and no CD-signal was observed. No trace of the mixed, heteroleptic species was observed. This establishes the homochiral self-recognition during self-assembly, which means that the chirality of the first ligand to be complexed induces the choice of the chirality to the second. Another interesting feature of these helicates is the linear coordination geometry of the metal centres (L-2). It is one of the rare cases, where the linear coordination geometry reveals chiral complexes.

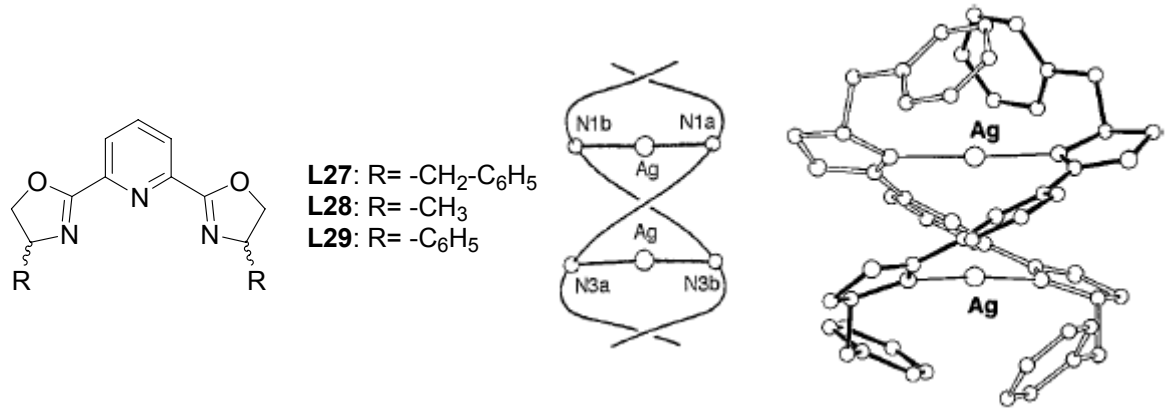

figure 13: ligands **L27**-**L29**, schematic representation of the double-stranded helicate and the X-ray structure of *PΔΔ*-$[Ag_2(S,S\text{-}\mathbf{L27})_2]^{2+}$.[39,40]

Williams *et al.* published another remarkable example of stereoselective control of the helical configuration at metals centres.[42] **L30** described in this publication comprises three bidentate sites, one bpy unit and two amino acids (figure 14). The amino acids were expected to induce stereoselectivity in the coordination of metal ions and the different binding sites should allow to complex two different metal ions. Instead, a surprising observation of diastereoselectivity was reported, only the achiral bpy chelating unit is occupied by a metal cation. Moreover, they observed anion binding at the amino acid site in the solid state (figure 14).

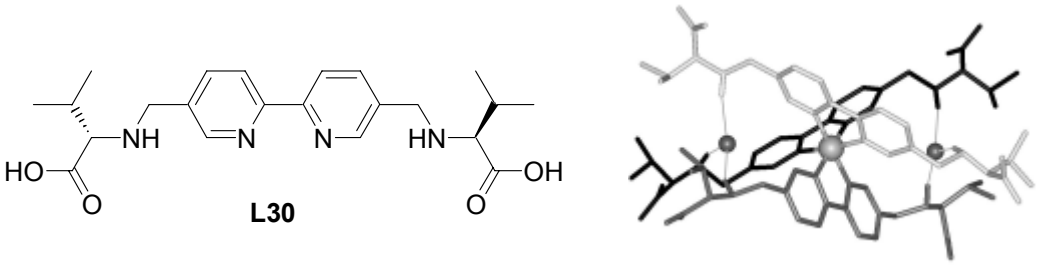

figure 14: L30 and the "pseudo-trinuclear", triple-stranded helicate $[Fe\mathbf{L30}_3]Cl_2$.[42]

The ^{1}H-NMR of the diamagnetic low spin iron (II) complex $[Fe\mathbf{L30}_3]^{2+}$ revealed a mixture of diastereomers in a ratio of 2:1, but on heating to 60 °C, the weaker set of signals disappeared, indicating a thermodynamically controlled diastereoselectivity (*Δ*-$[Fe\mathbf{L30}_3]Cl_2$). In the crystal, the structure is held together by coordinative bonds between the iron and the bpy moieties and as well as hydrogen bonds and electrostatic

interactions between the chlorides and the protonated amino residues of the ligand (figure 14).

2.3. Circular helicates

Circular helicates are oligonuclear complexes with a cyclic arrangement of metal ions and several bridging ligands wrapping around the metals centres. Only a few circular helicates have been published and all show similar characteristics.

- Firstly, the number of metal cations and the number of ligands wrapping around them are identical. Helicates with n = 3-6 are known (figure 15).
- The highest possible molecular symmetry of circular helicates is D_n (n-fold symmetry axis and n C_2-symmetry axes).

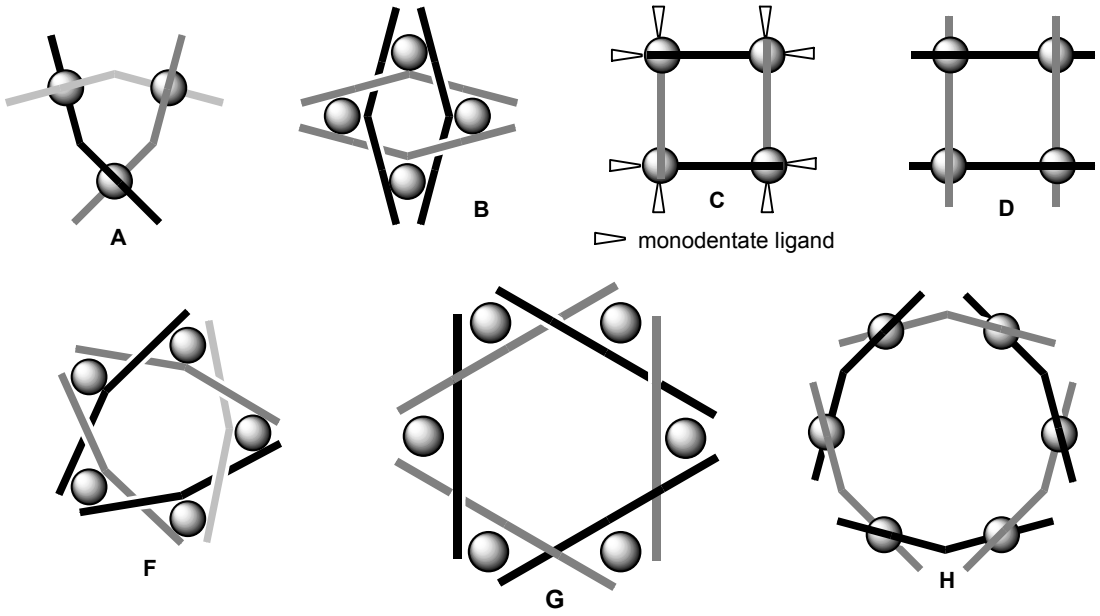

figure 15: schematic representation of circular helicates with n = 3-6.

- All ligands used in circular helicates consist at least of one C_2-symmetry axis leading always to homotopic helicates (no head-to-head or head-to-tail arrangements possible).
- As already described earlier, all metal centres in a helicate are homochiral (cf. figure 8).

- Achiral ligands lead to racemic mixtures of the helicates, chiral enantiopure ligands induce diastereoselectivity during complex formation.

2.3.1 Trinuclear, circular helicates (n = 3)

The known trinuclear helicates can be schematically represented by structure **A** (figure 15): Three ligands with two binding sites wrapping around three tetrahedral metal centres.

The first type of ligands (bis(oxazolyl)pyridine, **L27** and **L28**) have been already mentioned, they form dinuclear double-stranded helicates (figure 13)[39,40]. The slightly modified ligand *R,R*-**L29** forms the trinuclear, circular helicate *P*-[Ag_3(*R,R*-**L29**)$_3$](BF_4)$_3$ in the solid state (figure 16). The coordination geometry of the silver(I) ions is one of the rare chiral cases of A-2. An interesting feature to note is that while compound *S,S*-**L27** leads to an enantiopure *P*-helicate (figure 13), the *R,R*-enantiomer of **L29** forms as well a *P*-circular helicate. Williams *et al.* detected an equilibrium of several complexes depending on solvents, silver/ligand ratio and concentration.[39]

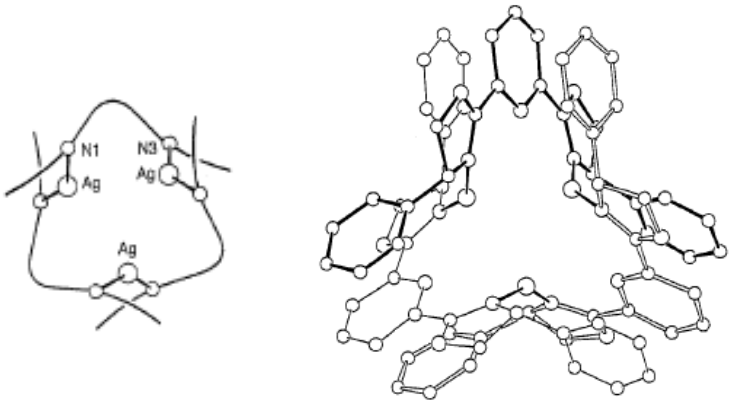

figure 16: schematic representation and X-ray structure of *P*-[Ag_3(*R,R*-**L29**)$_3$]$^{3+}$.[40]

In the same year, Lehn *et al.* published an analogous case.[43] A 1:1 mixture of ligand **L31** (figure 17) and [$Cu(MeCN)_4$]PF_6 stirred overnight leads to a mixture of three different species: the racemic dinuclear double-stranded helicate [Cu_2**L31**$_2$]$^{2+}$, the racemic trinuclear circular helicate [Cu_3**L31**$_3$]$^{3+}$ and an achiral tetranuclear side-by-side arrangement [Cu_4**L31**$_4$]$^{4+}$ (figure 17).

All these three self-assembled species convert into a single species $[Cu_2\mathbf{L31}_2](PF_6)_2$, in the solid state upon crystallisation.

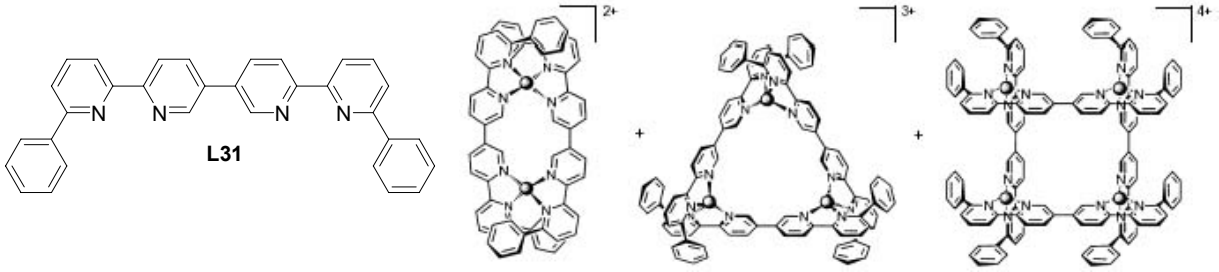

figure 17: ligand **L31** forms three different species in solution: $[Cu_2\mathbf{L31}_2]^{2+}$, $[Cu_3\mathbf{L31}_3]^{3+}$and $[Cu_4\mathbf{L31}_4]^{4+}$.[43]

The complex formation with **L32** was thoroughly studied by Constable *et al.*[44] (figure 18). This ligand forms double-stranded dinuclear helicates in methanol with a slight preference to one diastereomer (ratio 10:7). Dissolving these helicates in acetonitrile a variety of species could be observed (from dinuclear up to pentanuclear species). In the solid state a "quasi-racemic" circular helicate was obtained. The chiral substituents on the bpy units do therefore not influence the stereoselectivity (figure 18).

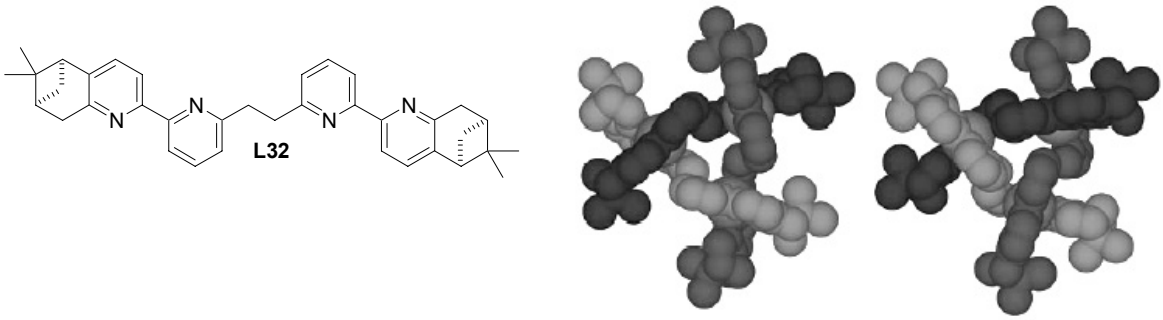

figure 18: L32 and the X-ray structure of *P*-$[Cu_3\mathbf{L32}_3]^{3+}$, *M*-$[Cu_3\mathbf{L32}_3]^{3+}$.[44]

A last example leading to a structure **A** (figure 15) was published by Thummel *et al.*. [45] The trinuclear circular helicate can be formed from ligand **L33** with tetrahedrally coordinating metal ions (Cu(I)). This achiral ligand leads to the racemic mixture of the helicate (figure 19).

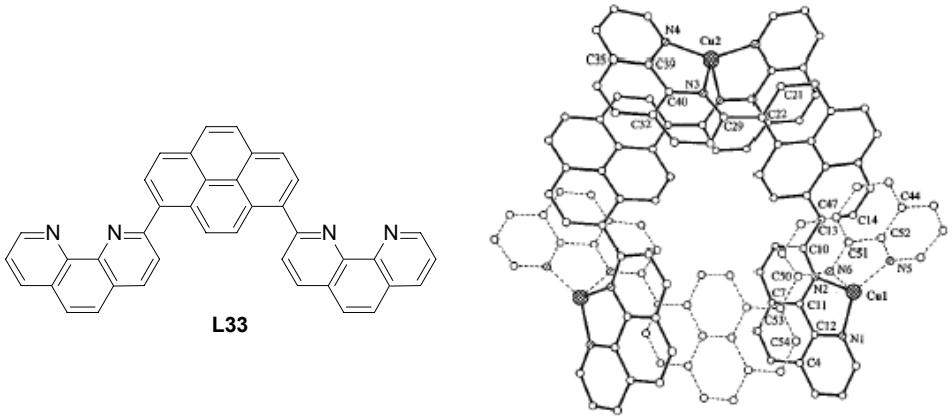

figure 19: L33 and the X-ray structure of $[Cu_3\mathbf{L33}_3]^{3+}$.[45]

2.3.2 Tetranuclear, circular helicates (n = 4)

Three different types of tetranuclear circular helicates are known to exist (figure 15). Structure **B** is formed by tris-bidentate ligands with an octahedral geometry at the metal centres. Structure **C** is the unsaturated analogue of **D**, which is formed by bis-tridentate ligands on octahedral metal centres.

The ether-linked tris(bpy) ligand **L34** (figure 20) forms a tetranuclear circular helicate $[Fe_4\mathbf{L34}_4]^{8+}$ with iron(II) ions (figure 20).

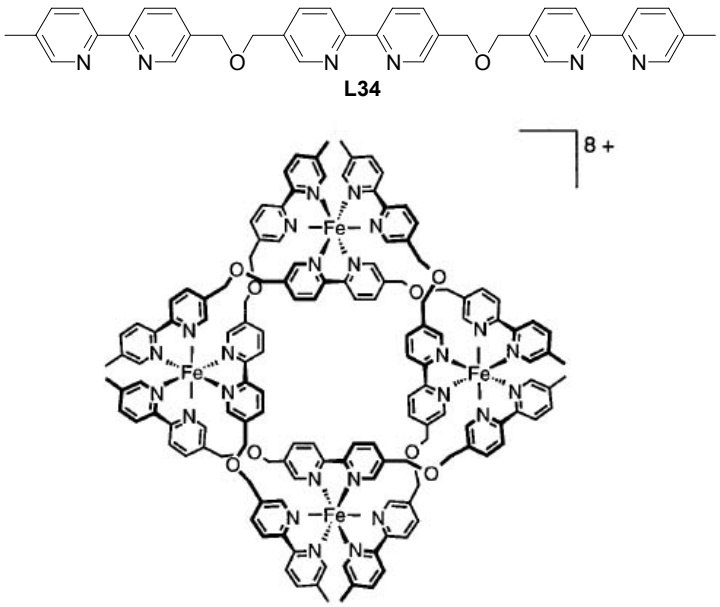

figure 20: L34 and $[Fe_4\mathbf{L34}_4]^{8+}$.[46]

Each of the metal ions possesses a pseudo octahedral coordination geometry and binds to two terminal and one central bipyridine unit of three different ligand strands **L34**, resulting in a structure similar to **B**.[46]

Ligand **L35** reacts with $[Ni(CH_3CN)_6](BF_4)_2$ to form the racemic unsaturated tetranuclear circular helicate $[Ni_4\mathbf{L35}_4(CH_3CN)_8](BF_4)_8$ (figure 21). Acetonitrile molecules acts as monodentate ligands to complete the coordination sphere.[47]

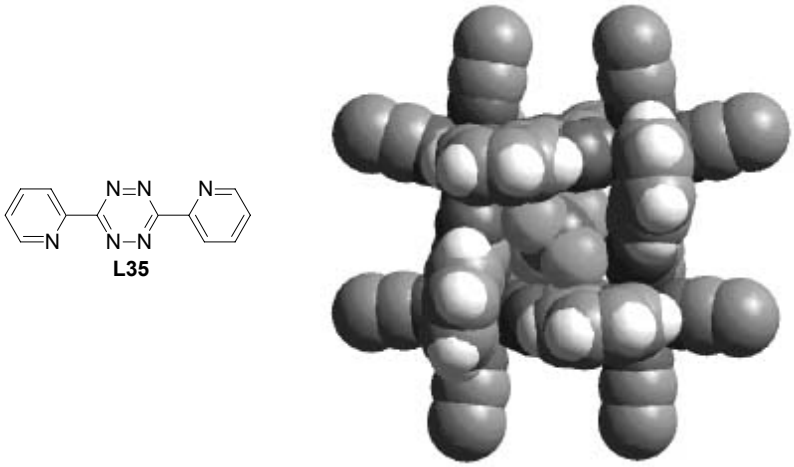

figure 21: L35 and $[Ni_4\mathbf{L35}_4(CH_3CN)_8](BF_4)_8$.[47]

The same phenomenon was observed within our group.[48] The achiral ligand **L36** leads to the racemic mixture of the circular helicate $[Zn_4\mathbf{L36}_4](PF_6)_8$, the chiral ligand **L37** to one diastereomer ($M\vec{\Delta}\vec{\Delta}\vec{\Delta}\vec{\Delta}$-$[Zn_4\mathbf{L37}_4](PF_6)_8$) in the solid state (figure 22). In solution the trinuclear helicate is formed as minor species In case of **L37,** both diastereomers are present.

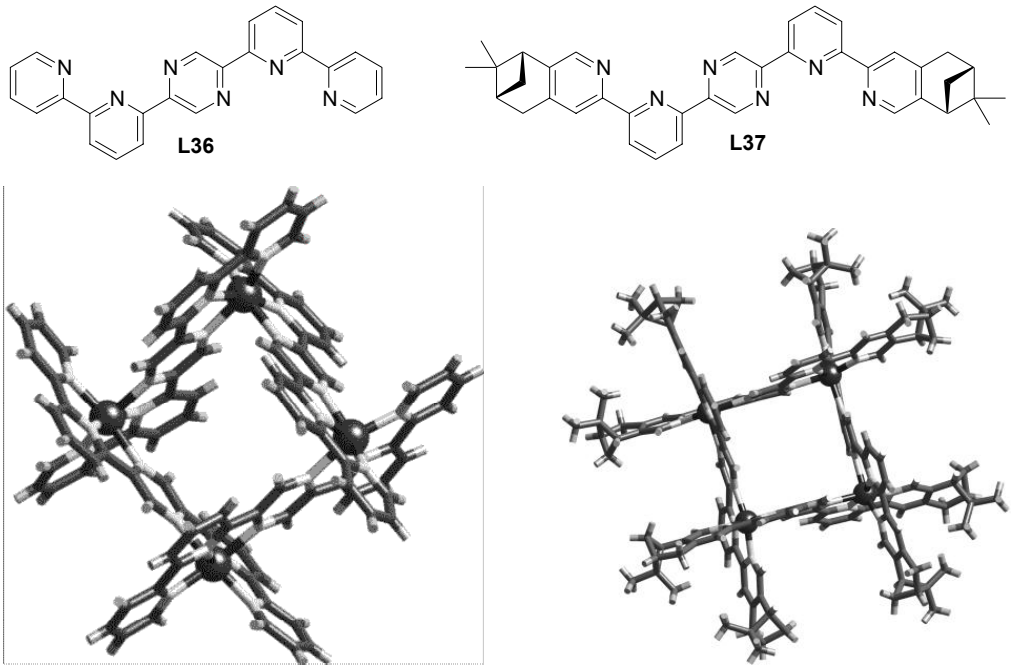

figure 22: L36, L37 and X-ray-structures of $[Zn_4\mathbf{L36}_4](PF_6)_8$ and $[Zn_4\mathbf{L37}_4](PF_6)_8$.[48]

2.3.3 Penta- and hexanuclear, circular helicates (n = 5,6)

Ligand **L38** (figure 23) reacts with nickel (II) to form a trinuclear triple-stranded helicate $[Ni_3\mathbf{L38}_3]^{6+}$ which could be structurally characterized (figure 23).[49]

With iron(II) ions a similar helicate $[Fe_3\mathbf{L38}_3]^{6+}$ is initially obtained . However, it was found that the triple-stranded helicate is the product of kinetic control of complex formation. Under thermodynamic control, the pentanuclear $[Fe_5\mathbf{L38}_5]^{10+}$ or hexanuclear circular helicates $[Fe_6\mathbf{L38}_6]^{12+}$ are obtained (figure 23).[50]

Here, the nuclearity depends on the nature of the counter-ions which can act as templates and support the formation of a defined macrocyclic helicate. The pentanuclear coordination species $[Cl\ \{Fe_5\mathbf{L38}_5\}]^{9+}$ (**F**, figure 15) is formed in the presence of chloride anions. X-ray structural analysis shows that one chloride ion is located in the interior cavity of the complex (figure 23). The coordination geometry at the iron centres is very similar to that described for $[Fe_4\mathbf{L34}_4]^{8+}$ with each iron binding to two terminal and one central bpy of three different ligands. With the larger bromide anion a mixture of pentanuclear and hexanuclear complexes is observed by ESI mass

spectrometry and the anions BF_4^-, SO_4^{2-}, and SiF_6^{2-} also support the formation of the hexanuclear circular helicate $[Fe_6\mathbf{L38}_6]^{12+}$(**G**) (figure 23).[46]

$[Fe_6\mathbf{L38}_6]^{12+}$ possesses six hexacoordinated iron centres arranged as a hexagon with ligands **L38** wrapping around those centres. This complex was not characterized by X-ray diffraction. [46]

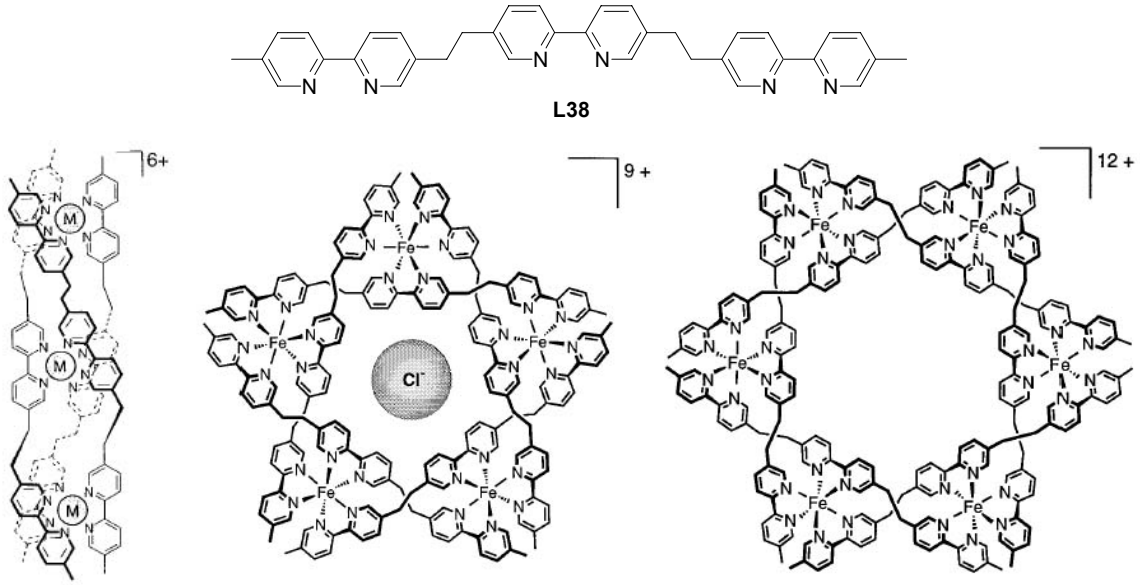

figure 23: L38 and $[M_3\mathbf{L38}_3]^{6+}$, $[Fe_5\mathbf{L38}_5]^{10+}$ and $[Fe_6\mathbf{L38}_6]^{12+}$.[27,46]

However, another hexanuclear circular helicate $[Ag_6\mathbf{L39}_6]^{6+}$ was crystallized and structurally characterized by our group (figure 24). [51] The six silver ions are pseudo-tetrahedrally coordinated by bpy units, and the six ligands **L39** have a helical arrangement around the hexagon of metal ions (**H**) (figure 15). Due to the chirality at ligand **L39**, an enantiomerically pure circular helicate (*P*)-$[Ag_6\mathbf{L39}_6]^{6+}$ is obtained. In solution, the hexanuclear circular helicate $[Ag_6\mathbf{L39}_6]^{6+}$ is in equilibrium with the corresponding tetranuclear species $[Ag_4\mathbf{L39}_4]^{4+}$. This equilibrium was shown to be pressure dependent. [52]

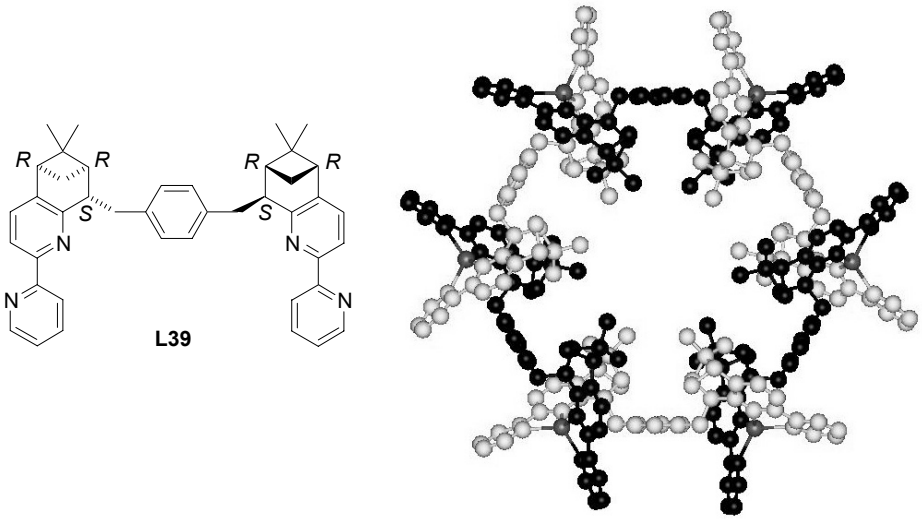

figure 24: L39 and an enantiopure hexanuclear circular helicate (*P*)-$[Ag_6\mathbf{L39}_6]^{6+}$.[51]

The octanuclear cobalt(II) complex $[Co_8\mathbf{L40}_{12}]^{4+}$ is related to the circular helicates although this coordination compound does not have the earlier mentioned characteristics of circular helicates (figure 25).[53]

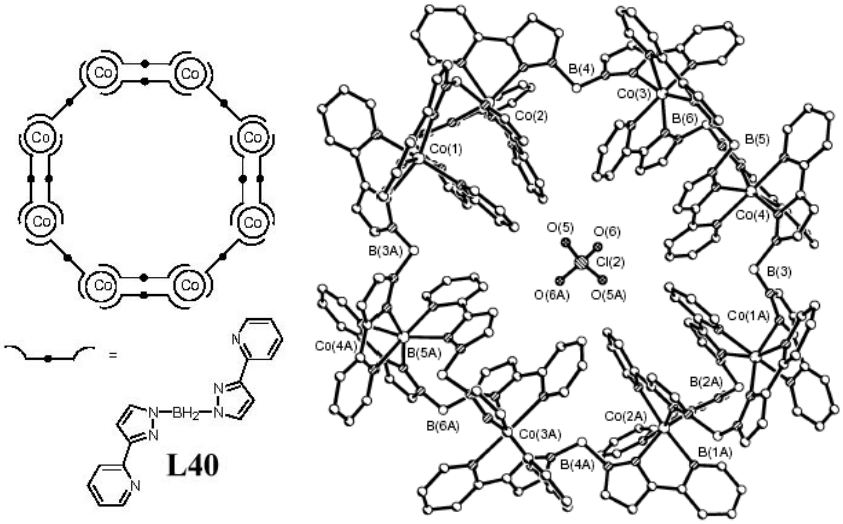

figure 25: the octanuclear Co(II)-complex.[53]

3. Mononuclear helical metal complexes

Up to now helicity has been discussed in linear and circular helicates, but it can occur readily in mononuclear complexes (described in general on page 6). The polydentate ligands, which are expected to form polynuclear complexes such as helicates or side-by-side arrangements, can also form mononuclear helical complexes. A few selected examples with polydentate ligands will be discussed here.

As mentioned earlier, ligand **L24** forms mononuclear complexes and determines moreover the chirality at an octahedral metal centre (scheme 2, p.11). The (*RRS;RRS*)-enantiomer of **L24** forms the *Δ*-enantiomer of the complex [Ru**L24**Cl_2].[37]

Constable *et al.*[54-57] and Potts *et al.*[58] have shown that the quinquepyridine **L41** and its substituted analogues **L42**-**L46** (chart 2) may act as pentadentate ligands to give mononuclear single-stranded helical racemic complexes with transition metals. Large metal cations such as silver(I) almost fit into the cavity of the quinquepyridine, leading to a slight helical twisting of the strand in the crystal structure of [Ag**L41**]$^+$ (figure 26).[54] Unsaturated complexes such as [Co**L42**Cl_2][58] and [Co**L45**(CH_3OH)(OH_2)](PF_6)$_2$[56] (figure 26) show a more pronounced shallow helical twist about the equatorial plane of a pentagonal bipyramidal seven-coordinated metal centre. The two axial coordination sites are occupied by chloride anions or solvent molecules.

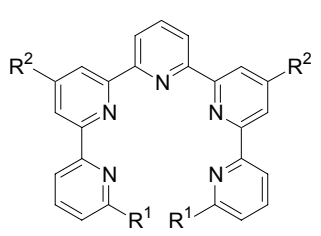

L41: R^1= H; R^2 = H
L42: R^1= H; R^2 = S-$CH_2CH_2CH_3$
L43: R^1= Me; R^2 = H

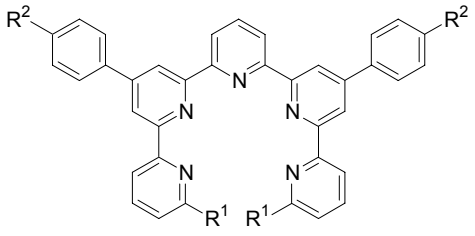

L44: R^1= H; R^2 = H
L45: R^1= H; R^2 = Cl
L46: R^1= Me; R^2 = H

chart 2: quinquepyridine derivatives for the formation of mononuclear helical complexes.

In contrast, unsaturated double-stranded helicates can be obtained by substitution at the 6, 6’’’’-position of the quinquepyridines (**L43**, **L46**)[59] or by other transition

metals such as copper(II) and nickel (II) with ligands **L42**-**L46**.[57] Surprisingly, the assembly of **L41** with cobalt(II)acetate leads to an analogous double-stranded helicate $[Co_2\mathbf{L41}_2(OAc)]^{3+}$.[55]

figure 26: [Ag**L41**]$^{+}$[54] and [Co**L45**$(CH_3OH)(OH_2)](PF_6)_2$.[56]

Within our group a whole series of mononuclear complexes were synthesised starting from diastereomeric ligands **L15** and **L47** (chart 3).[60] These ligands form with several metals saturated and unsaturated mononuclear complexes with different coordination geometries and predetermine the chirality at the metal centre. Silver(I), palladium(II) (figure 27) and zinc(II) (only with **L47**, figure 28) form saturated mononuclear complexes. The coordination geometry of these complexes can be considered as a very distorted (flattened) tetrahedron or a helically twisted square.

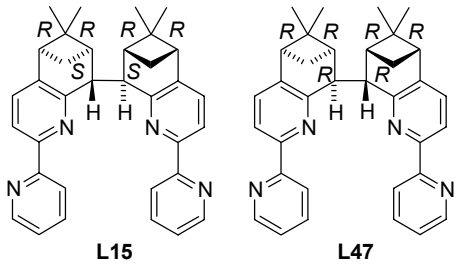

chart 3: tetradentate ligands: CHIRAGEN[0].

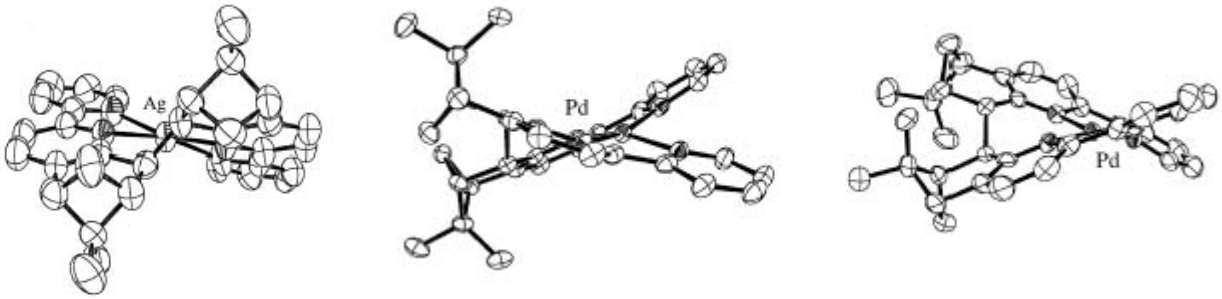

figure 27: crystal structure of [Ag**L15**]$^{+}$, [Pd**L15**]$^{2+}$ and [Pd**L47**]$^{2+}$.[60]

With other metals such as copper(II) (figure 28), cadmium(II) and zinc(II) (with **L15**, figure 28) unsaturated mononuclear complexes were obtained. Obviously, other ligands are required to fill up the coordination sphere.

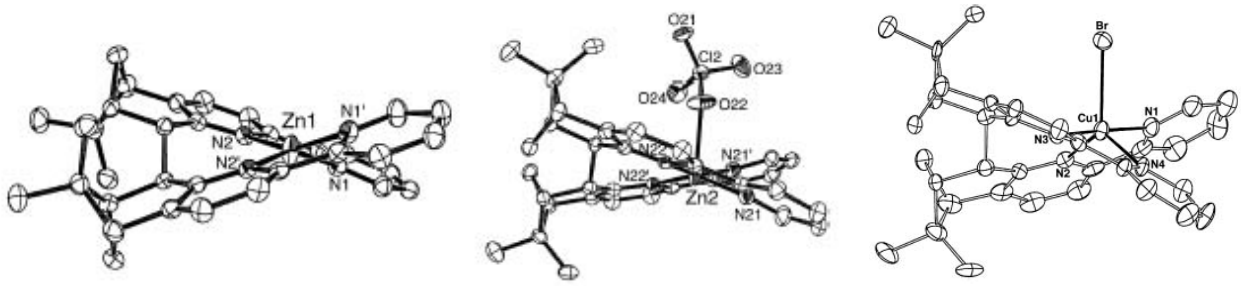

figure 28: crystal structure of $[Zn\mathbf{L47}]^{2+}$, $[Zn\mathbf{L15}ClO_4]$ and $[Cu\mathbf{L15}Br]^{+}$.[60]

4. Protons as a coordinating central cation

The smallest cation known is the proton. An interesting question is: Is it possible, that the proton can act as a coordinating centre and therefore can a ligand induce helicity to this proton core?

Only a few examples are known, where the proton is exchanged between four donor atoms of one or two ligands and the conformation of the ligand remained fixed.

Sauvage *et al.* published in 1986 a mono-protonated catenane (figure 29).[61] The macrocycles are interlocked and the 2,9-diphenyl-1,10-phenanthroline fragments are entwined. The molecular topography is strikingly similar to its copper(I)-analogue, the two phenanthroline units are facing each other with a dihedral angle of 61°. Although in the solid state, the acidic hydrogen atom is located on one of the four nitrogen sites (figure 29), the ^{1}H-NMR spectrum corresponds to a symmetrical species, indicating a fast exchange of the binding between the four nitrogen atoms.

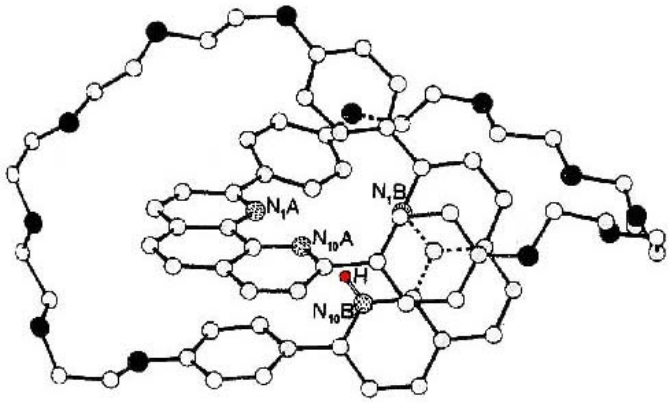

figure 29: a mono-protonated catenane.[61]

Another example, not as obvious as the previous one, was reported by Albrecht-Gary *et al.*.[62] They observed a mono-protonated species of **L48** (chart 4**)**. The ^{1}H-NMR of H**L48**$^{+}$ is highly symmetrical, consistent with a folding of the flexible strand **L48** around a single proton coordinated to two bpy subunits. This observation was confirmed by molecular modelling calculations with Hyperchem, which showed that

the most stable conformation in a vacuum was a folded structure with stacking interactions between the aromatic parts.

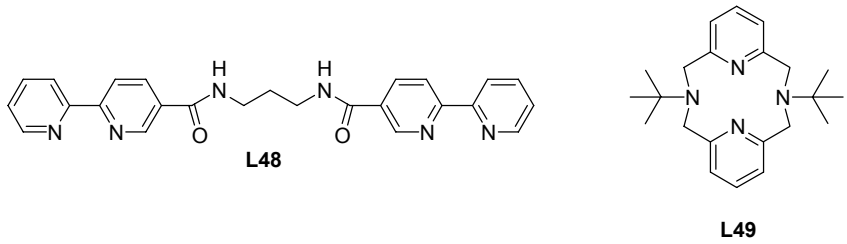

chart 4: ligand **L48** and **L49**.

The most recent example was published by Kress *et al.* in 2001.[63] These authors reported an unexpected protonation of **L49**, a well known ligand (its crystal structure was published by Che *et al.* in 1994)[64] (figure 30). This mono-protonated structure (syn boat-boat) is markedly different from the free ligand (syn chair-chair), suggesting the proton is exchanged between the four nitrogen atoms, maintaining the ligand in its unusual conformation.

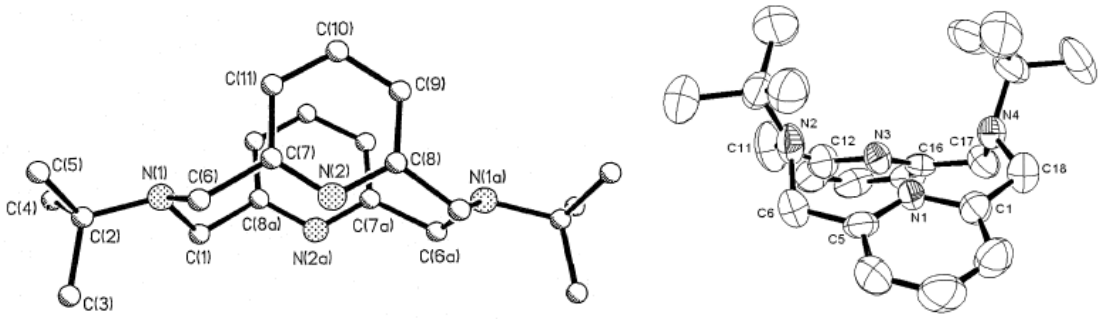

figure 30: crystal structure of **L49**[64] and its protonated form.[63]

These examples show that a proton can act in the time average as a coordinating centre for up to four nitrogen donor atoms. In one case a helical structure of two phenantroline moieties was observed[61], whereas in the other structurally characterized cases a symmetrical coordination occurs located on a mirror plane, again in the time average.

RESULTS AND DISCUSSION

RESULTS AND DISCUSSION[‡]

1. Ligand Syntheses

1.1. Introduction

The aim of Hayoz's work in 1992[65] was the development of a chiral building block of the type *cis*-[Ru(diimine)$_2$Cl$_2$] in order to synthesise enantiopure[§], polynuclear complexes (scheme 4). The ligand, which allows the formation of this building block, has to fulfil several criteria. First of all, it should contain two diimine units (strong complexation properties of diimines). Second, the bridge between these two diimine units must fix the conformation and therein contain centres of chirality, which are easy to synthesise in an enantiopure form. Finally, it should be easy to modify the length of the bridge.

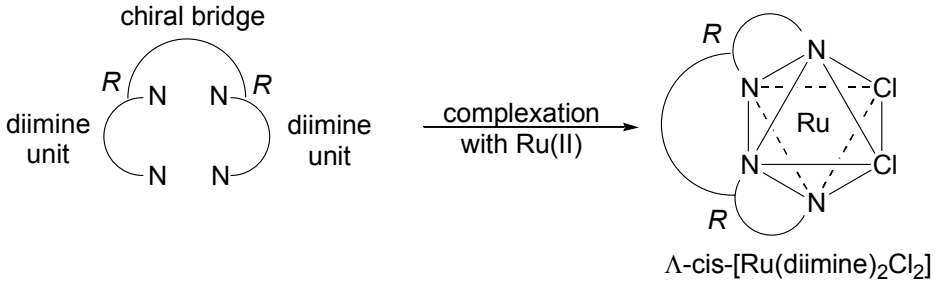

scheme 4: tetradentate ligand for the synthesis of chiral building blocks.

Hayoz therefore introduced a pinene moiety into a bpy system (scheme 5) in order to introduce chirality. Myrtenal or α-pinene (both available in nearly enantiopure form) were used as the source of chirality to synthesise the corresponding [4,5]-pinene-bpy and [5,6]-pinene-bpy derivatives, respectively. An advantage of these ligands is their

---

[‡] Some results were taken from diploma work carried out either under my supervision (Christophe Bonte, Tobias Christen) or in the group (David Mauron, deceased).

[§] Enantiopure is used in an approximate sense. In most cases terpenes of ca. 97-98% *e.e.* are used for the syntheses.

ability to be stereoselectively deprotonated and coupled via a bridge to form enantiopure tetradentate ligands: the [4,5]-CHIRAGEN[bridge] and [5,6]-CHIRAGEN[bridge] ligands. These CHIRAGEN-ligands fulfil the above mentioned and desired ligand properties. They contain two bpy units, which potentially can form complexes with one or two metal cations. Finally, different bridges between the two pinene-bpy units can be introduced in a stereoselective manner by deprotonation with a sterically demanding base such as LDA and further reactions with a dihalide compound.

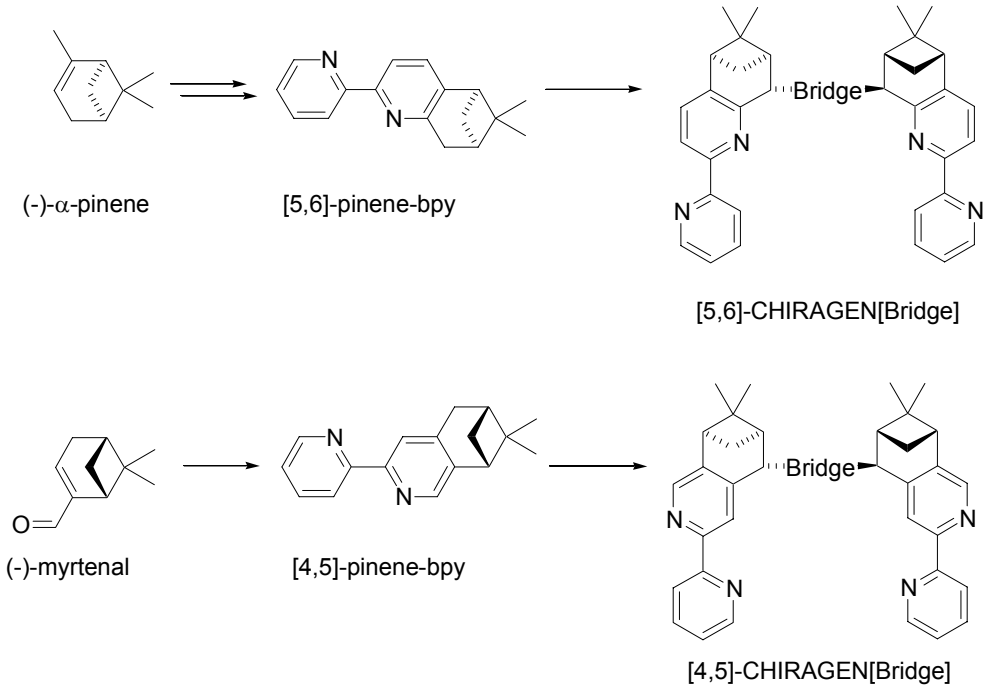

scheme 5: synthetic strategy.

1.2. New ligands

In this thesis, a new family of tetradentate ligands ([5,6]-CHIRAGEN) has been synthesised (scheme 6). On the one hand, directly bridged [5,6]-CHIRAGEN[0] derivatives were used for the formation of mononuclear metal complexes, on the other hand [5,6]-CHIRAGEN[*p*-xyl] derivatives were synthesised for self-assembly studies. All these new ligands are substituted either at the 5'-position (R^1 = H, R^2 = *p*-MeO-Ph) or at the 6'-position (R^1 = *p*-MeO-Ph, R^2 = H; R^1 = Ph, R^2 = H). CHIRAGENS with

these substituents are derived from the analogous [5,6]-pinene-bpy derivative, that means the length of bridge can be varied easily in one step. The precursors for the [5,6]-pinene-bpy derivatives are the corresponding 5- or 6- substituted 2-acetyl-pyridines.

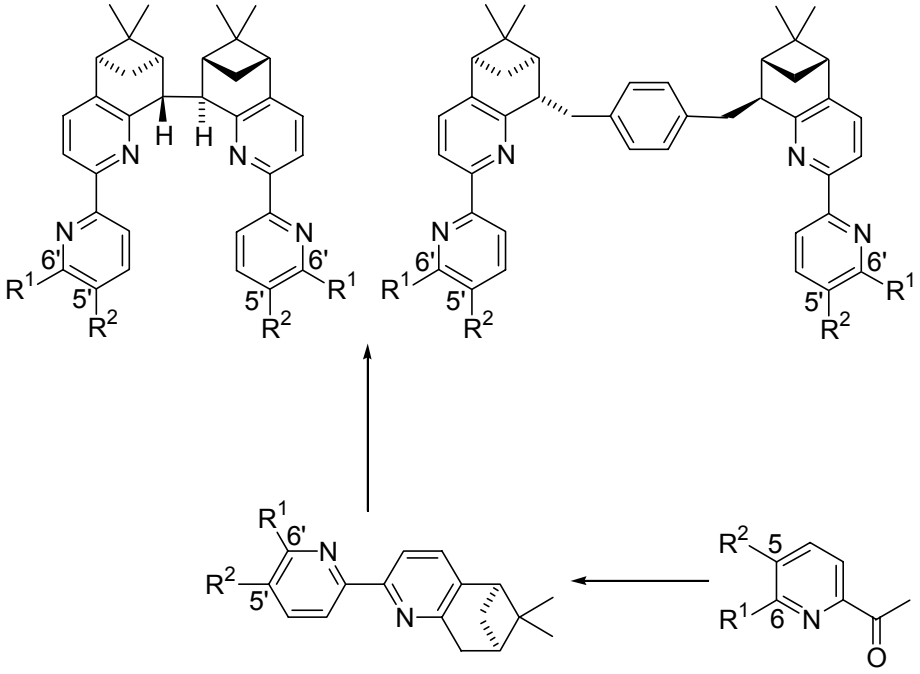

scheme 6: new ligand family.

For protonation studies, another type of tetradentate ligand was synthesised. Since 1968 [66] the remarkable basicity of 1,8-bis-(dimethylamino)-naphthalene (scheme 7) has been known and well studied [66]. This molecule was given the nick-name “proton sponge”, in accordance with its ability to take up protons. Our idea was to introduce this bis-dimethylamino moiety into our well known chiral skeleton of pinene-py derivatives to form the tetradentate ligands. This was realised with ligand **L19**, which is derived from **L10** by a direct coupling in a similar way as for the other CHIRAGEN[0] ligands (scheme 7).

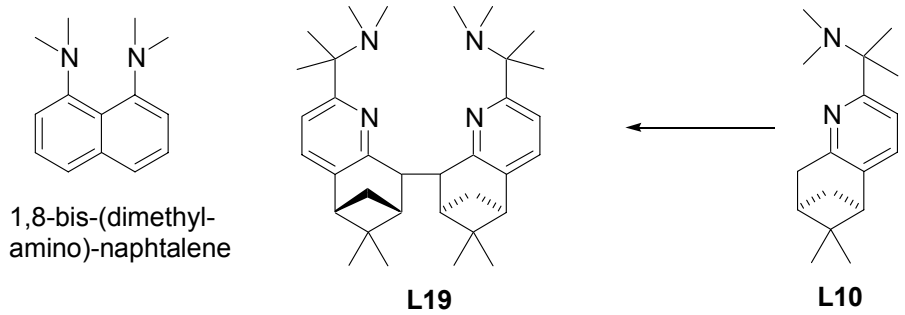

scheme 7: proton sponge analogue

1.3. Nomenclature

The skeleton of all bpy ligands are derived from pinene and bpy, therefore they are called [4,5]-pinene-bpy, [5,6]-pinene-bpy, or generally pinene-bpy derivatives** (chart 5). The connectivity between the pinene and bpy is given by the number in the square brackets, which correspond to the carbons of the bpy where the pinene unit is attached. In curly brackets, the substituent at the second pyridine ring and its position is given. The name for ligand **L10** is also mentioned in chart 5.

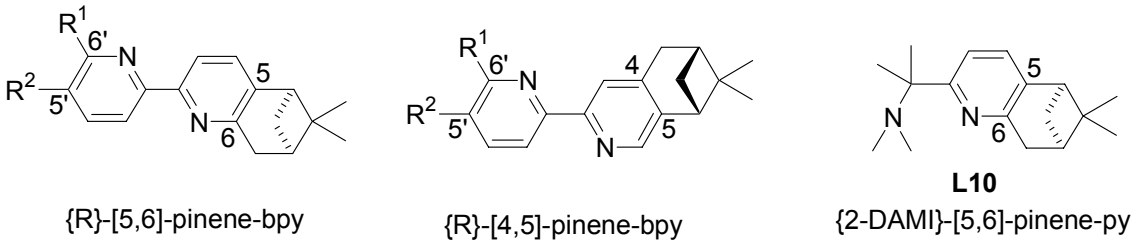

chart 5: nomenclature of pinene-bpy derivatives.

The tetradentate ligands have been called CHIRAGEN derivatives, (from **CHIRA**lity **GEN**erators) due to their ability to induce a predetermined configuration at metal

** The IUPAC name of these ligands are very complicated. E.g. [4,5]-pinene-bpy is called by IUPAC: (6*R*, 8*R*)-5,6,7,8-tetrahydro-7,7-dimethyl-3-(2'-pyridyl)-6,8-methano-isoquinoline and [5,6]-pinene-bpy (5*R*, 7*R*)-5,6,7,8-tetrahydro-6,6-dimethyl-2(2'-pyridyl)-5,7-methano-quinoline.

centres upon complexation.[37,67,68] Again the same rules mentioned above were used: in curly brackets the substituents attached to second pyridine ring is given and in square brackets, the connectivity of the pinene to the first pyridine ring. At the end of the name, the bridge between the two pinene-bpy moieties is also given in square brackets. These bridges can be either *p*- or *m*-xylene bridges [*p*-xyl] or [*m*-xyl], or the two pinene-bpy moieties are linked directly together [0]. The ligand **L19** is thus called {2-DAMI}-[5,6]-CHIRAGEN][0] (chart 6).

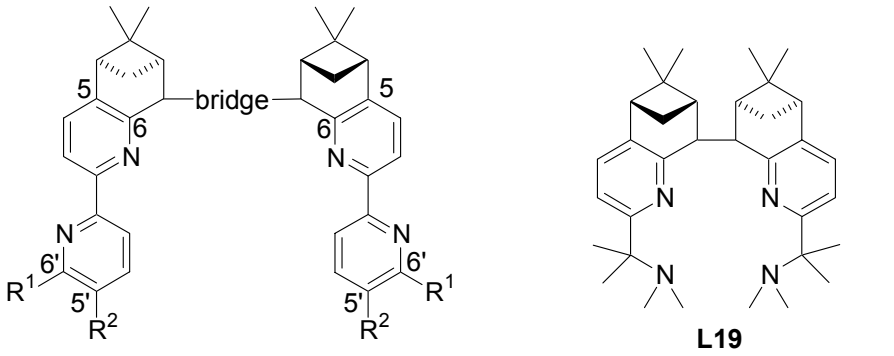

{R}-[5,6]-CHIRAGEN[bridge] {2-DAMI}-[5,6]-CHIRAGEN[0]

chart 6: nomenclature of CHIRAGEN derivatives.

1.4. Mechanistic aspects of the annellation step

The synthesis of the pinene-bpy derivatives (**L1**, **L2**) is described in the literature[69] and shown in scheme 8. Starting from acetyl-pyridine (**3**), the 1-(2-acetylpyridyl)-pyridinium bromide (**4**) was synthesised according to the improved method of Mürner[70] (the bromide salt is easier to handle compared to the originally described iodide and no side product is observed). The 1-(2-acetylpyridyl)-pyridinium bromide (**4**) reacts with pinocarvone (**1**) (oxidation of α-pinene[71]) or myrtenal (**2**) in a mixture of ammonium acetate and glacial acetic acid or formamide to give the corresponding pinene-bpy derivatives (**L1**, **L2**).

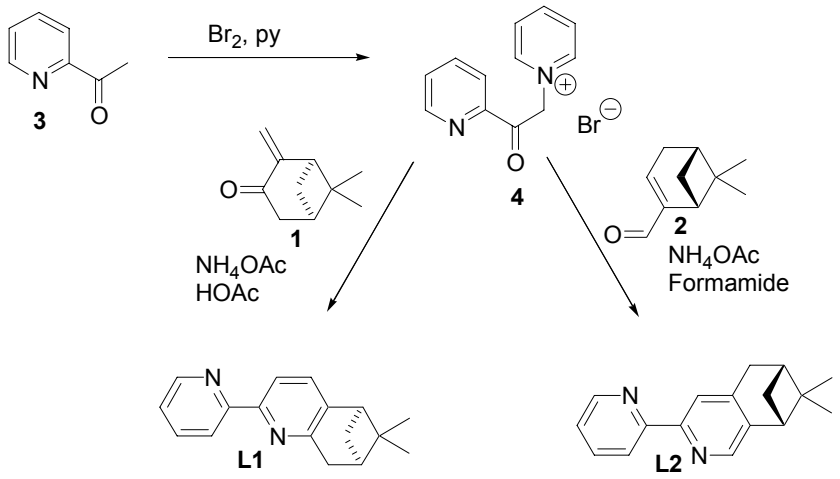

scheme 8: synthesis of pinene-bpy derivatives.

The synthesis of the substituted pyridines was reported for the first time by Kröhnke *et al.* in 1961 (scheme 9). [72-74] The pyridinium salt **5** undergoes a Michael addition with an *α,β*-unsaturated carbonyl compound **6** to form a dicarbonyl compound **7**, which can be isolated. The aza-ring closure with ammonium acetate in glacial acetic acid and the loss of the pyridinium bromide occurs, giving a 2,4,6-trisubstituted pyridine **8** (proposed mechanism of Kröhnke[75], scheme 9). Improved procedures gave better yields. For example, a one-pot synthesis with the starting materials heated in a mixture of ammonium acetate and glacial acetic acid, yielded the corresponding pyridine, without isolation of the dicarbonyl compound **7**.

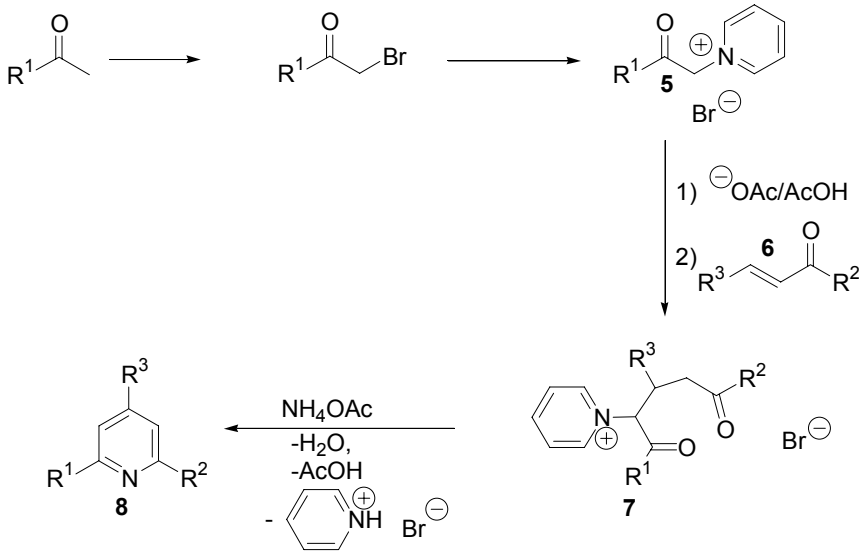

scheme 9: mechanism proposed by Kröhnke.[75]

A more detailed mechanism for the formation of pinene-bpy derivatives is shown in scheme 10. The first step starting from the 1-(2-acetylpyridyl)-pyridinium bromide (**4**) is the Michael addition. Treatment of **4** with base forms the enolate **9**, which adds to the α,β-unsaturated carbonyl compound (pinocarvone (**1**)) forming intermediate **10**. After hydrolysis the dicarbonyl compound **11** is formed. The next step is the aza- ring closure with ammonium acetate and simultaneous or subsequent loss of the pyridinium halide finally yielding the desired [5,6]-pinene-bpy (**L1**).

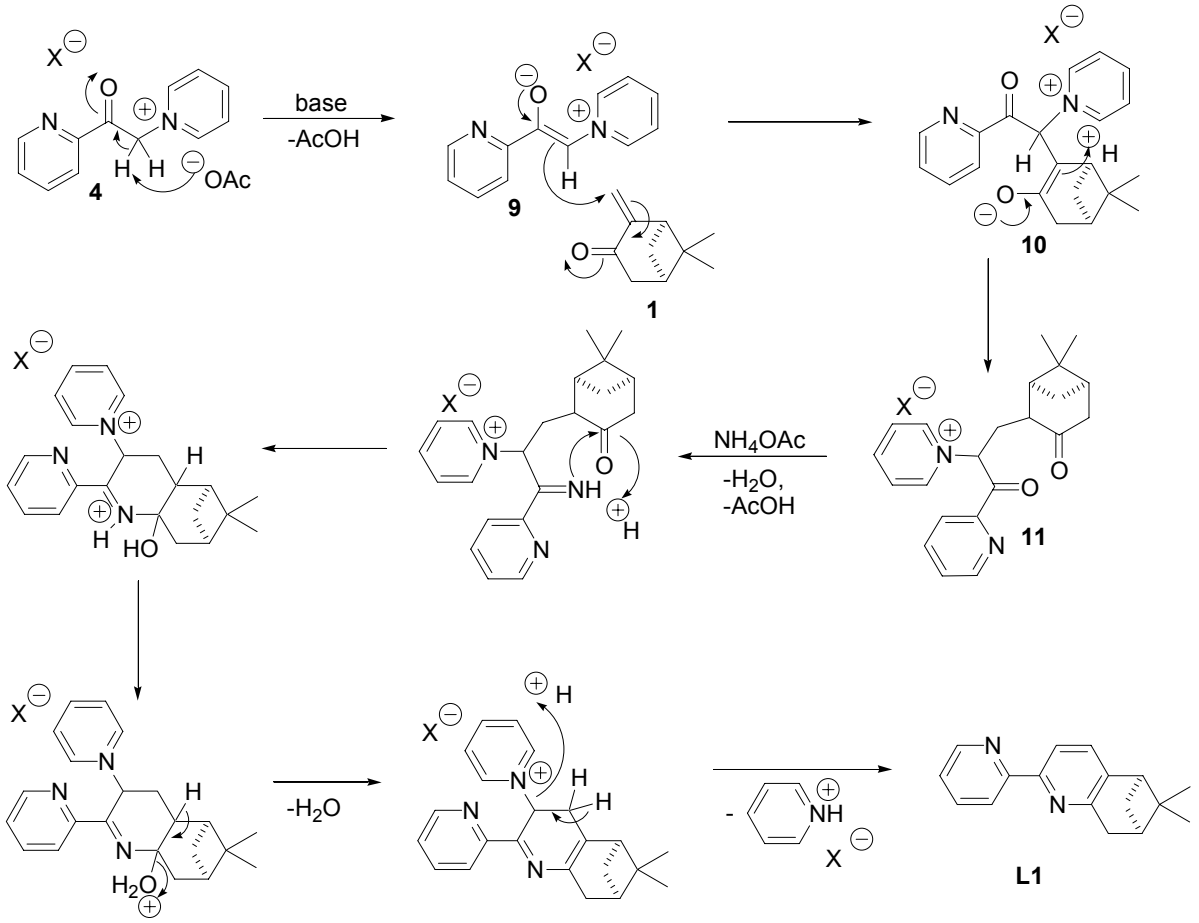

scheme 10: detailed mechanism.

1.5. Precursors for the pinene-bpy and pinene-*N*-py derivatives

The two key molecules for the formation of pinene-bpy or pinene-*N*-py derivatives are the *α,β*-unsaturated carbonyl compounds ((+)-pinocarvone (**1**) or (-)-myrtenal (**2**)) and the acetyl derivatives **3**, **12-16** (chart 7). For unsubstituted pinene-bpy derivatives (**L1**, ^{15}N-**L1** and **L2,** scheme 8), commercially available acetyl-pyridine (**3**) is used. For 5'-substituted pinene-bpy derivatives (**L3**, **L4**) 2-acetyl-5-(*p*-methoxyphenyl)-pyridine (**12**) was synthesised. 6'-substituted pinene-bpy derivatives were synthesised starting from three different acetyl compounds (**13-15**). The 2-acetyl-6-bromo-pyridine (**13**) is the precursor for the corresponding 6'-bromo-pinene-bpy derivatives (**L5**, **L6**), which can be used for the synthesis of several 6'-substituted pinene-bpy derivatives (**L5-L9**; **L54-L59**, cf. scheme 20, p. 45). An analogous species containing only one pyridine ring can be synthesised from 2-*N,N*-dimethylamino-2-methyl-butan-3-one (**16**).

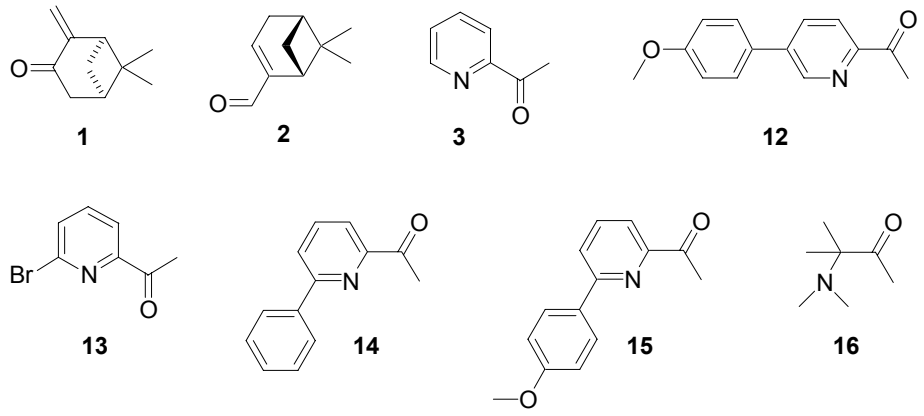

chart 7: precursors for the synthesis of pinene-bpy and pinene-*N*-py derivatives.

1.5.1 Precursors for 5'-substituted pinene-bpy

For the formation of 5'-substituted pinene-bpy derivatives, 2-acetyl-5-(*p*-methoxyphenyl)-pyridine (**12**) is used. We developed an alternative four-step synthesis (method A in scheme 11) for the acetyl-pyridine **12**, compared to the published method by Sauvage *et al.* (method B in scheme 11).[76] The iodination of the commercially available 2-amino-pyridine (**17**) was carried out according to a known

procedure[77] (I_2, DMSO). The side product, 2-amino-3,5-diiodo-pyridine, was separated from the 2-amino-5-iodo-pyridine (**18**) by an acid-base extraction. At pH 4, the desired product remains mainly in the aqueous layer, but the diiodo product transfers to the organic layer. By increasing the pH to 14, pure 2-amino-5-iodo-pyridine (**18**), also commercially available, can be extracted.

The next step, bromination of the amino function, is described in the literature for this compound (**18**) [78] and for some analogous molecules.[79-82] With sodium nitrite, a diazonium cation is formed, which reacts with HBr_3 (formed by bromine in aqueous hydrobromic acid) giving 2-bromo-5-iodo-pyridine (**19**) via an alkaline work up and destruction of bromine with sodium thiosulfate.

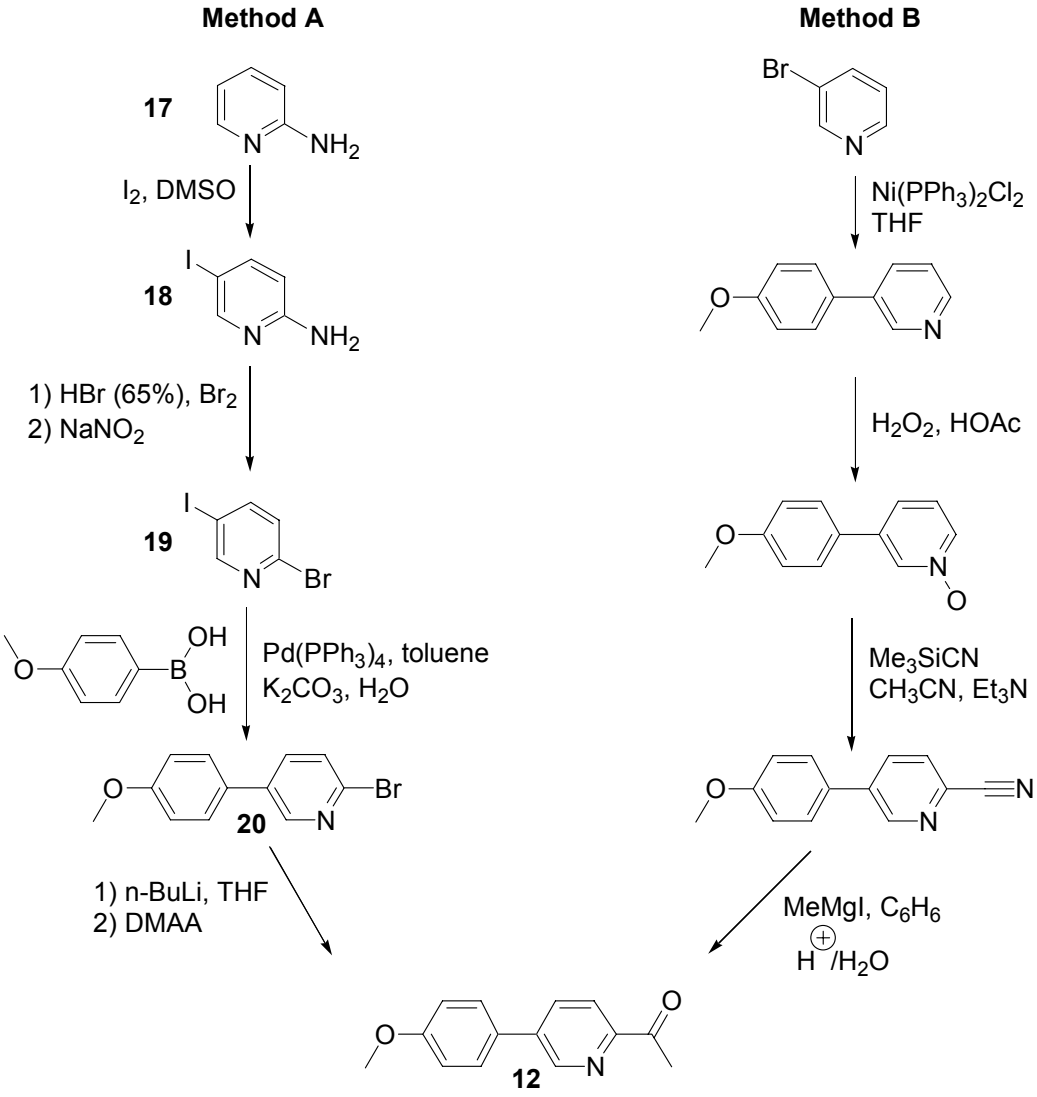

scheme 11: two different routes for the synthesis of the key intermediate **12**.

The iodo-substituted pyridine is much more reactive than the bromo-substituted one with regard to its reaction with an organoboron compound. This cross-coupling (Suzuki cross-coupling)[83-86] was the method of choice for the introduction of an aryl substituent at the 5-position of the pyridine ring. The reaction was carried out by refluxing the two starting materials in a two phase mixture (toluene/aqueous potassium carbonate) in presence of small amounts of a palladium(0)-catalyst, ($Pd(PPh_3)_4$.
Finally, the bromo-substituent (**20**) is transformed into an acetyl group according to known procedures[87,88]. Compound **20** was reacted with *n*-butyllithium to form the anion, which reacts with *N,N*-dimethyl-acetamide yielding the desired precursor **12**.

1.5.2 Precursors for the 6'-substituted pinene-bpy

The precursors for the 6'-substituted pinene-bpy were synthesised starting from 2,6-dibromo-pyridine (**21**) according to the procedures mentioned above (scheme 12). With *n*-butyllithium and *N,N*-dimethyl-acetamide the 6-bromo-2-acetylpyridine (**13**) is prepared, which can be used to synthesise either directly 6'-bromo-pinene-bpy derivatives (table 1, p.43) or 6'-substituted 2-acetyl-pyridines (**14**, **15**). The introduction of the aryl-substituent (Ph, *p*-MeO-Ph) is carried out via the Pd(0)-catalysed Suzuki cross-coupling reaction of the corresponding aryl boronic acid derivatives with 6-bromo-2-acetylpyridine (scheme 12).

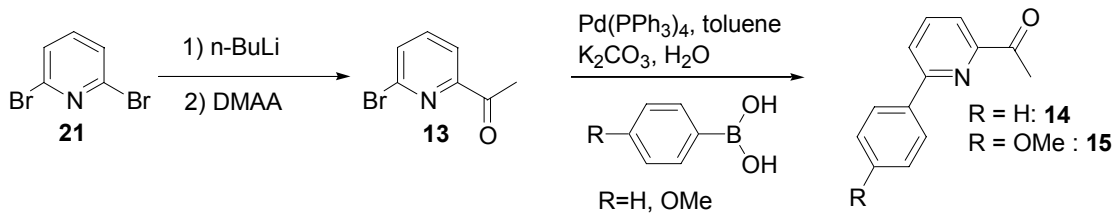

scheme 12: synthesis of the 6'-substituted acetyl-pyridines **13**, **14** and **15**.

1.5.3 Precursors for the pinene-*N*-py derivatives

When the idea to synthesise an analogue of 1,8-bis-(dimethylamino)-naphthalene (proton sponge, cf. scheme 7) to increase the basicity of the normal CHIRAGEN[0] (**L1**) emerged, ligand **L50** appeared to be the most accessible (scheme 13).

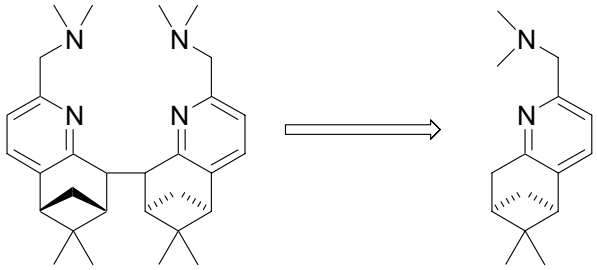

scheme 13: synthetic approach to a proton sponge analogue.

The key step for the synthesis of the ligand **L50,** would be the coupling of the pinene-*N*-py ligand **L51**. This coupling reaction (well known in our group and discussed later) consists of two steps. The first is the deprotonation with LDA, the second the coupling in presence of iodine. Deprotonation could take place at two competitive positions within **L51**, but only one would lead to the desired product **L50** (scheme 14).

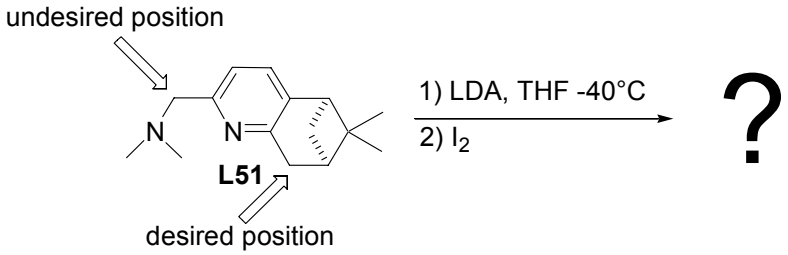

scheme 14: key step: deprotonation.

To avoid this problem, the undesired position can be substituted. Two methyl- or two phenyl-groups can protect the position against unwanted deprotonation. Therefore, the desired tetradentate ligands **L19** and **L52** should be obtained easily from the corresponding pinene-*N*-py derivatives **L10** and **L53** (scheme 15).

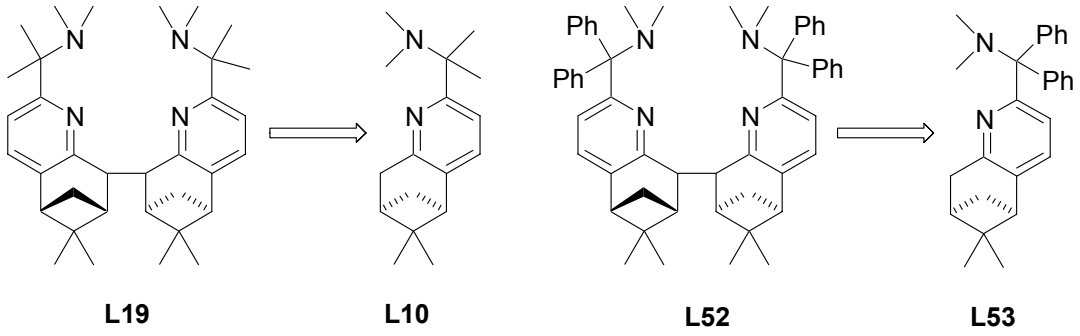

scheme 15: synthetic strategy for **L19** and **L52**.

For the preparation of these pinene-bpy derivatives, the acetyl compound **16** (scheme 16) and **27** (scheme 17) would be the precursors. 2-*N,N*-dimethylamino-2-methyl-butan-3-one (**16**) is synthesised from 3-methyl-2-butanone (**22**) in two steps by bromination and subsequent reaction with dimethylamine (scheme 16).

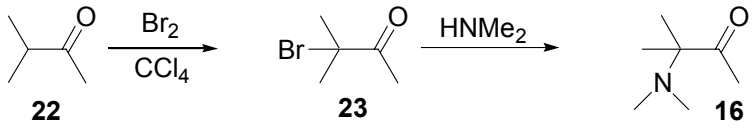

scheme 16: synthesis of 2-*N,N*-dimethylamino-2-methyl-butan-3-one (**16**).

The bromination of 1,1-diphenyl-propan-2-one (**24**) to form 1-bromo-1,1-diphenyl-propan-2-one (**25**) was carried out under analogous reaction conditions (scheme 17).

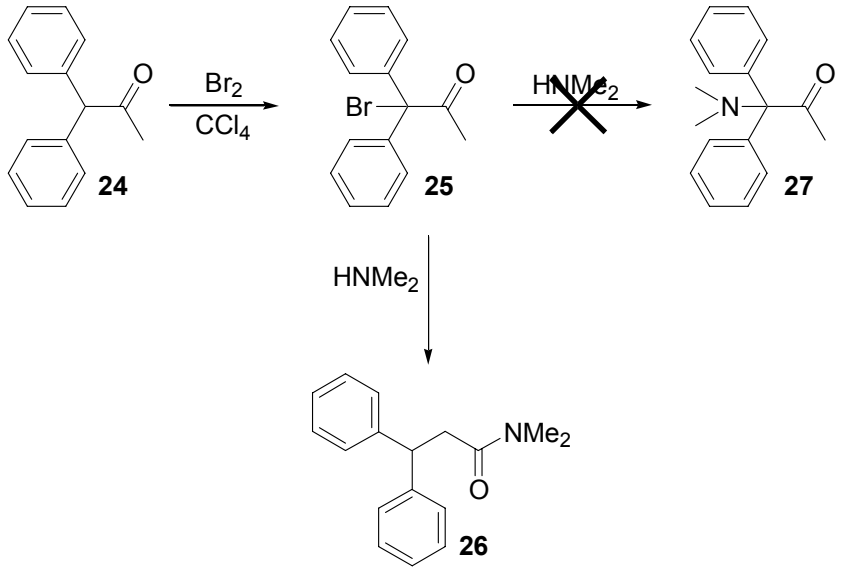

scheme 17: synthetic scheme for the formation of **26**.

But the next step (a nucleophilic substitution) to obtain 1-*N,N*-dimethylamino-1,1-diphenyl-propan-2-one (**27**) was unsuccessful. Instead of the desired product **27**, *N,N*-dimethyl- 3,3-diphenyl-propionamide (**26**) was isolated in a nearly quantitative yield (scheme 17). The spectral data for **26** corresponds to that published. [89-91]

This is a new synthetic route for the formation of **26**, which can be explained by a Favorskii rearrangement (scheme 18).[Kende, 1960 #86; Favorskii, 1985 #85] In the first step the base (dimethylamine) deprotonates compound **25** by formation of the enolate **28**, which undergoes an intramolecular substitution reaction yielding a cyclopropane **29**. By addition of the substrate (dimethylamine can act as base, but also as substrate) to the intermediate **29**, the ring opening is initiated, which leads to the more stable carbanion **30**.

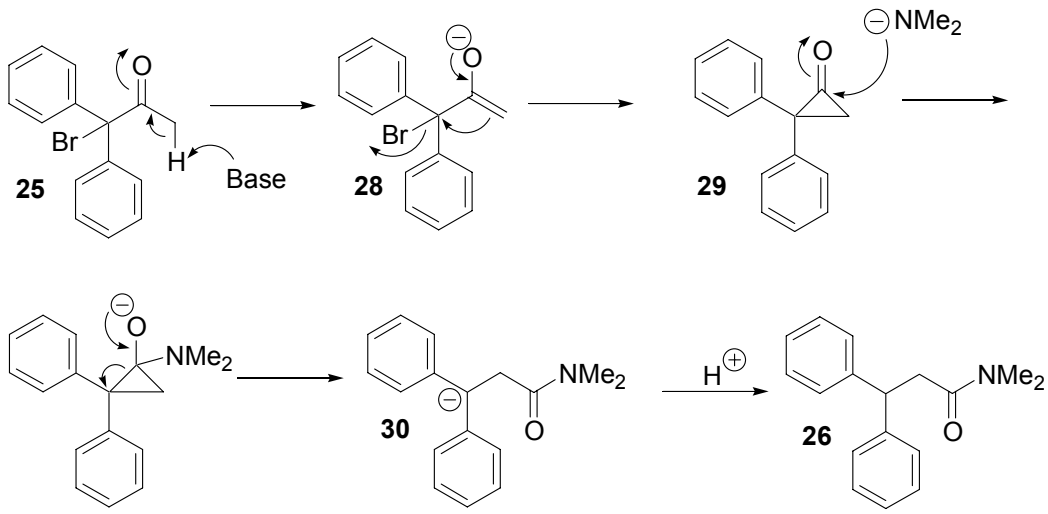

scheme 18: explanation by Favorskii rearrangement.

1.6. Syntheses of pinene-bpy and pinene-*N*-py derivatives

1.6.1 [5,6]-pinene-bpy derivatives

The syntheses of [5,6]-pinene-bpy derivatives were carried out according to the procedures for compound **L1**[69,70] (table 1). The first step is the formation of the pyridinium salts starting from the corresponding acetyl-pyridine derivatives by reaction with halogens and pyridine. The reaction with bromine is carried out in two

stages. The bromination of acetylpyridine (**3**) is followed by the reaction with pyridine yielding the pure pyridinium salt (**4**) (table 1, entries 1,2). The reaction with iodine is a one-pot synthesis (entries 3-5), adding iodine and pyridine to the acetyl derivatives and heating for two hours under reflux. By precipitation with diethyl ether, not only the desired salt, but also pyridinium iodide precipitates (the ratio of the mixture is given in table 1). The latter does not influence the following step, and it is therefore not removed. This next step is the reaction of the pyridinium salts with (+)-pinocarvone (**1**) and ammonium acetate yielding the corresponding [5,6]-pinene-bpy derivatives (for mechanistic aspects see 1.4, p.34). In entry 2, ammonium acetate with enriched ^{15}N-isotope (10%) was used.

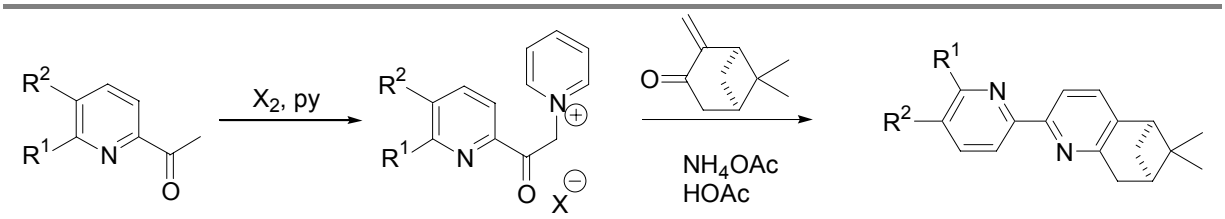

entry		R^1	R^2	salt, yield	X^-;ratio (salt : py X)	Yield
1	**3**	H	H	**4**,	Br^-; pure	**L1**, 74[1]
2	**3**	H	H	**4**,	Br^-; pure	^{15}N-**L1**, 53[2]
3	**12**	H	*p*-MeO-Ph	**31**, 85	I^-; 1.1 : 1	**L3**, 30
4	**13**	Br	H	**32**, 92	I^-; 1.1 : 1	**L5**, 50
5	**14**	Ph	H	**33**, 100	I^-; 2 : 1	**L7**, 55

[1] Synthesis described in literature[69,70]; [2] ^{15}N (10%)-labelled ammonium acetate was used;

table 1: synthesis of [5,6]-pinene-bpy derivatives.

The 6'-substituted [5,6]-pinene-bpy can be prepared in two different ways. The first (used for the synthesis of {6'-phenyl}-[5,6]-pinene-bpy (**L7**)) is described in table 1, entry 5. The other method uses the {6'-bromo}-[5,6]-pinene-bpy (**L5**) as the key intermediate (table 1, entry 4), which can be coupled with an aryl boronic acid using a Pd(0)-catalysed Suzuki cross-coupling reaction (scheme 19). {6'-p-methoxyphenyl}-[5,6]-pinene-bpy (**L9**) was synthesised in this way.

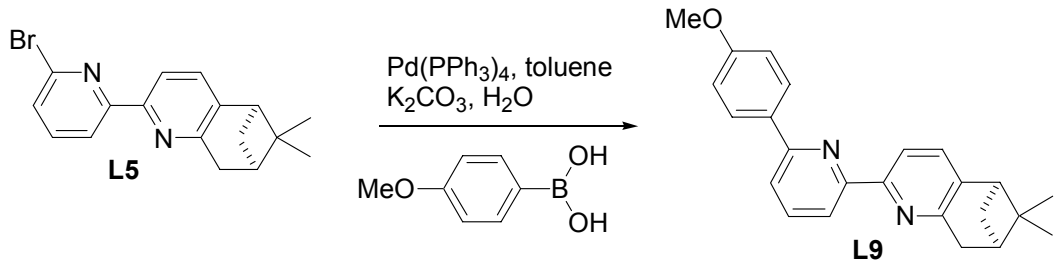

scheme 19: Suzuki cross-coupling reaction with $Pd(PPh_3)_4$.

The key intermediate **L5**[††] can be used for the preparation of several 6'-substituted [5,6]-pinene-bpy in just one step (scheme 20). In our group a variety of such ligands have been synthesised. In most of the cases the Suzuki cross-coupling reaction with $Pd(PPh_3)_4$ and a boronic acid derivative was the method of choice for the formation of these ligands. For the synthesis of **L54**, *o*-methoxy-phenyl boronic ester was used[93] and for **L56**, **L57** and **L59** *p*-phenylene-bis-boronic acid, *m*-phenylene-bis-boronic ester and 2,5-thiophenediyl-bis-boronic acid were used respectively.[94] The ligand **L58**, with the incorporated ferrocene moiety, was synthesised by Quinodoz[95] in a slightly different manner, by reaction of dilithioferrocene/TMEDA with $ZnCl_2$ and subsequent reaction with the key intermediate **L5**, the ligand **L58** was formed in the presence of a catalytic amount of $Pd(PPh_3)_4$, according to known procedures.[96-99] The quaterpyridine derivative **L55** synthesised via a double pyridinium salt by Constable *et al*[44,100-102] can be prepared by a Ni(0)-mediated coupling reaction described for other bromo compounds [103,104] starting from the key intermediate **L5**.

[††] An analogous compound was synthesised starting from *β*-pinene. [92]

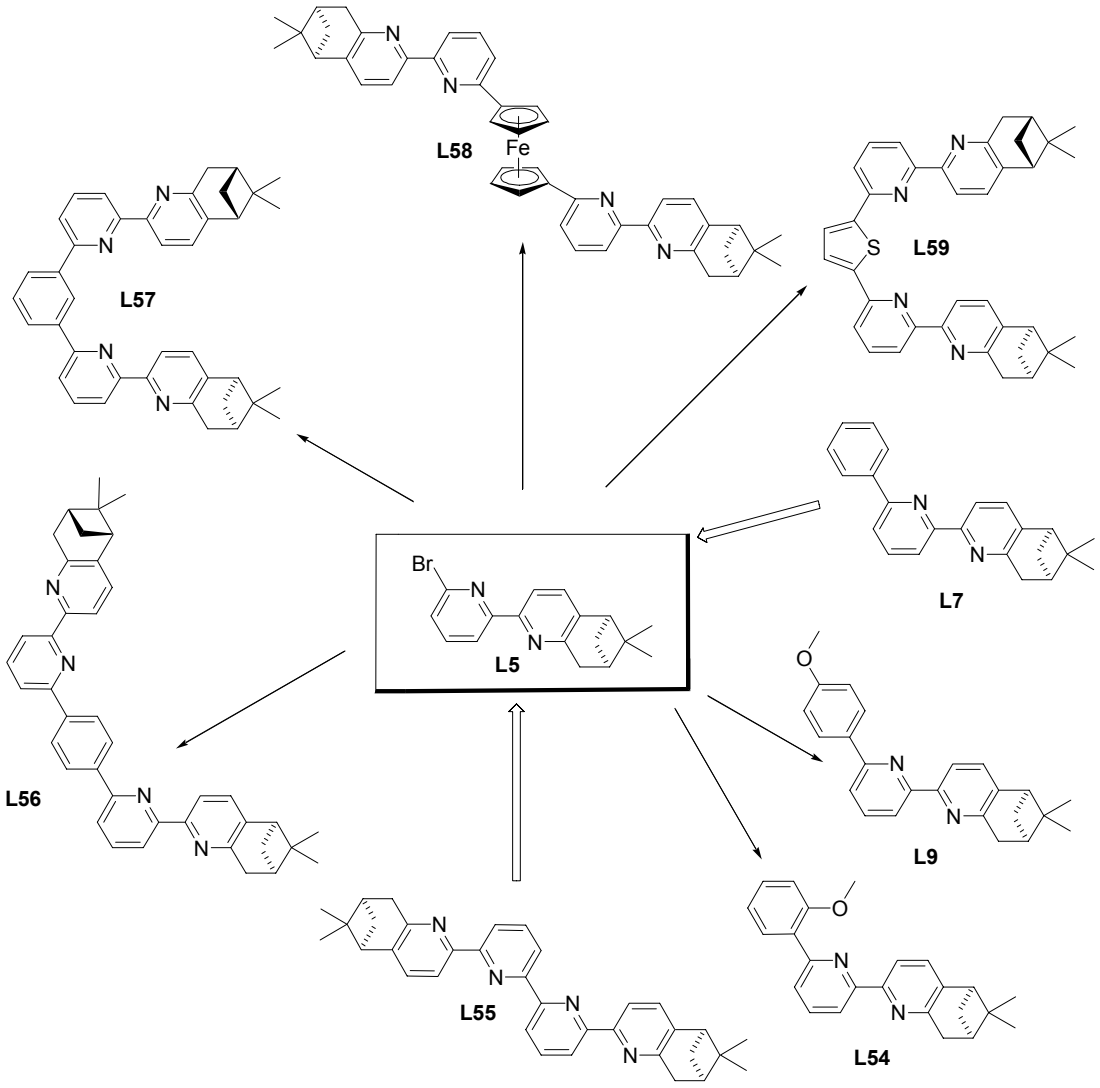

scheme 20: application for the key intermediate **L5**.

1.6.2 [4,5]-pinene-bpy-derivatives

The analogous reactions of the pyridinium salts with (-)-myrtenal (**2**) and ammonium acetate in formamide lead to the corresponding [4,5]-pinene-bpy derivatives (table 2).

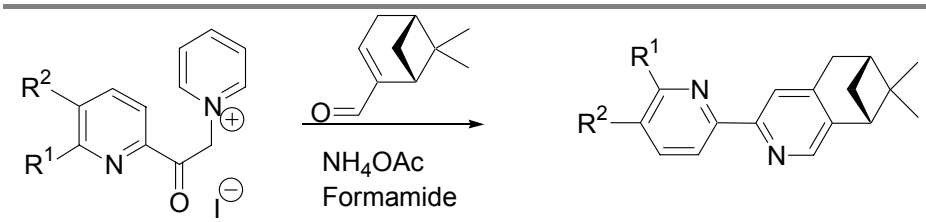

entry	Salt	R^1	R^2	Yield
1	**4**	H	H	**L2**, 65[1]
2	**31**	H	*p*-MeO-Ph	**L13**, 24
3	**32**	Br	H	**L14**, 29
4	**33**	Ph	H	**L15**, 52

[1] described in literature[69,70]

table 2: [4,5]-pinene-bpy

For 6'-bromo-[4,5]-pinene-bpy, the analogous coupling reaction as for 6'-bromo-[5,6]-pinene-bpy can in principle be carried out for the synthesis of the 6'-substitued-[4,5]-pinene-bpy analogues mentioned in scheme 20.

1.6.3 [5,6]-pinene-py-derivative

The same methodology was used for the formation of 2-substituted [5,6]-pinene-N-py derivatives such as {2-DAMI}-[5,6]-pinene-py (**L9**) (scheme 21).

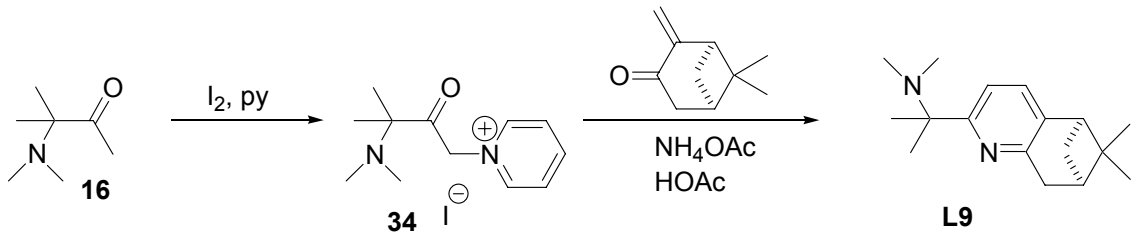

scheme 21: synthesis of the pinene-*N*-py derivative **L9**.

1.7. [5,6]-CHIRAGENS[bridge]-derivatives

The nucleophilic substitution reaction, for the formation of the [5,6]-CHIRAGEN[bridge]-derivatives (table 3), was carried out in two steps. The deprotonation of [5,6]-pinene-derivatives with a sterically demanding base, such as LDA, occurs stereoselectively (at low temperature –40° C). Reaction of this anion with a dibromo-compound (*α,α'*-dibromo-*p/m*-xylene) only one of three possible diastereomers of the corresponding tetradentate ligand is formed. The bridge is attached in anti-position with regard to the methyl-groups of the pinene moieties (*S,S*-diastereomer).

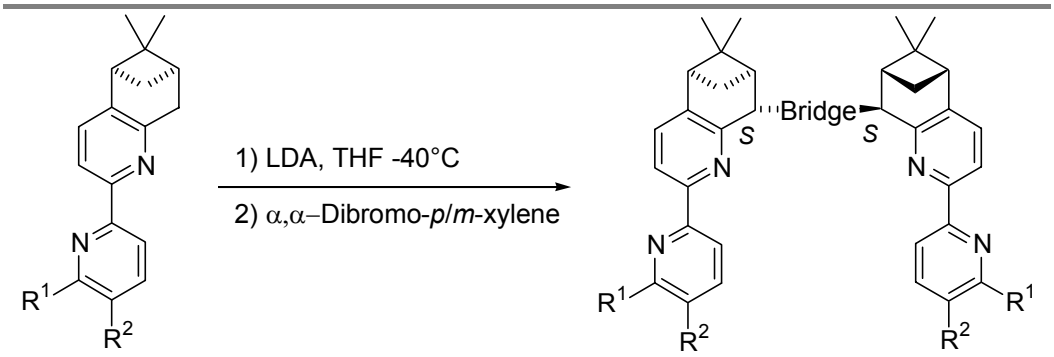

Entry		R^1	R^2	Bridge	yield (%)
1	**L4**	H	*p*-MeO	*p*-xyl	**L11,** 72
2	**L5**	Ph	H	*p*-xyl	**L12**, 68
3	**L6**	*p*-MeO	H	*p*-xyl	**L13**, 95
4	**L6**	*p*-MeO	H	*m*-xyl	**L14**, 13

table 3: {R}-[5,6]-CHIRAGEN[bridge].

1.8. CHIRAGEN[0]-derivatives

The syntheses of the CHIRAGEN[0] derivatives were carried out in analogous manner as described above (table 4). After the formation of the anion, iodine is added to form the desired CHIRAGEN[0]derivatives via an oxidative coupling reaction. The CHIRAGEN[0]derivatives are purified by recrystallisation.

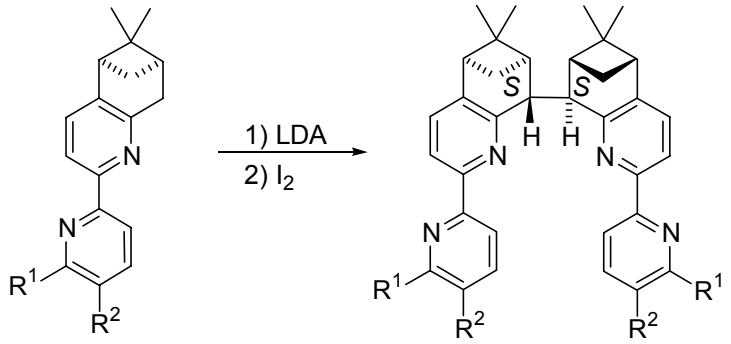

entry		R^1	R^2	yield (%)
1	**L1**	H	H	**L15**; 72
2	^{15}N-**L1**	H	H	^{15}N-**L15**; 73
3	**L3**	H	*p*-MeO	**L16**; 16
4	**L5**	Ph	H	**L17**; 68
5	**L6**	*p*-MeO	H	**L18**, 53
6	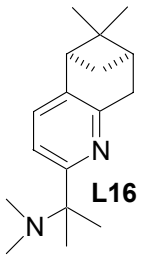			**L19**, 20

table 4: {R}-[5,6]-CHIRAGEN[0].

In contrast to the nucleophilic substitution, this oxidative coupling with iodine is not completely stereoselective. Even though the *S,S*-diastereomer is the major product, the *R,R*-diastereomer is formed in a small amount (observed by ^{1}H-NMR-spectroscopy, but not isolated). This formation of two compounds, that are configured differently at

the bridgehead, indicates that the oxidative coupling occurs via a radical intermediate (scheme 22),[60] Although the radical is configurationally less stable than the carbanion. The *R,S*-diasteromer (*meso* form) is not formed. Model studies show that the coupling most probably occurs via a Li^+-templated complex (introduced through LDA). In this template, both the *S,S*- and the *R,R*- configurations are sterically feasible, whereas the *R,S* is highly disfavoured.

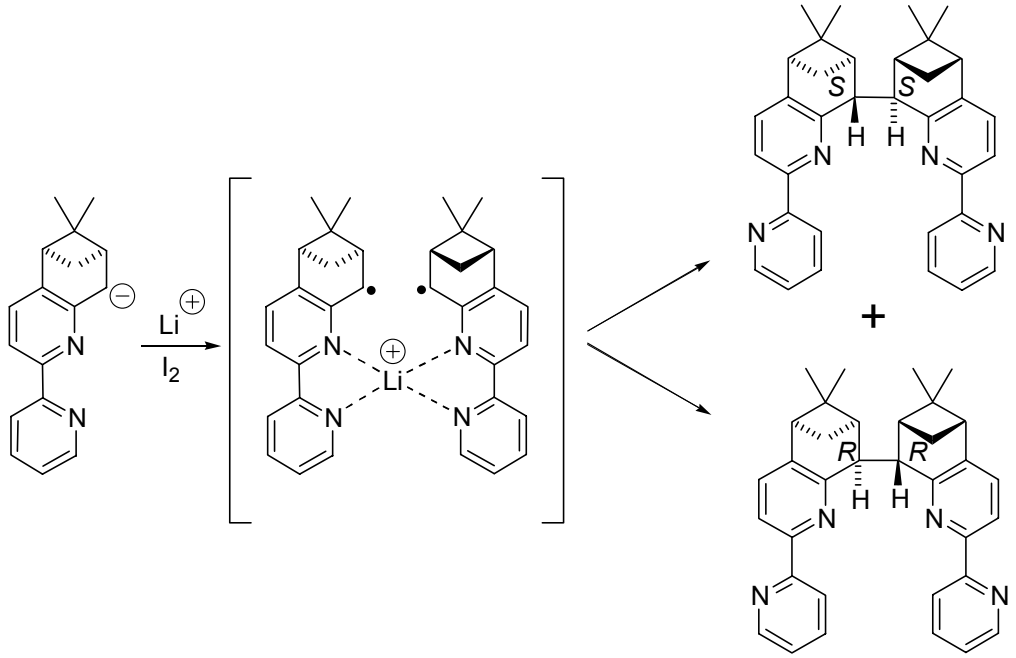

scheme 22: proposed mechanism via radical Li^+-template.

The synthesis of the [4,5]-CHIRAGEN[0] (**L20**) was carried out according to the procedures described by Fletcher [36]. The reaction mechanism is analogous to that one of the CHIRAGEN[bridge] derivatives. Only the *S,S*-isomer is formed by the oxidative coupling (scheme 23).

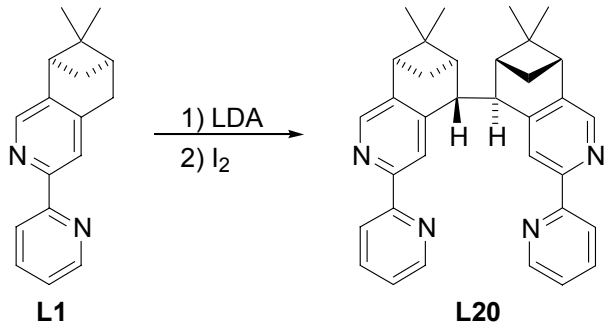

scheme 23: [4,5]-CHIRAGEN[0] (**L20**).

1.9. Characterizations of bidentate and tetradentate ligands

1.9.1 X-ray analysis

Suitable crystals for X-ray analysis were obtained from the [5,6]-pinene-bpy derivatives **L3, L5**-**L7** and **L9** and from the [5,6]-CHIRAGEN derivatives **L12**, **L18** and **L19**. The X-ray analyses were carried out by Professor Helen Stoeckli-Evans at the University of Neuchâtel.

All these ligands (figure 31-figure 35) crystallise easily in pure solvents (chloroform or acetone) or in mixture of solvents (chloroform/methanol; dichloromethane/methanol). In three cases (**L5**, **L6**, **L9**), the absolute configuration could be determined by X-ray analysis (bromide substituent for **L5** and **L6**, a chloroform molecule for **L9** in unit cell). In the other cases, the configuration is assigned to the known configuration of the *α*-pinene used. The bond lengths and the angles have the expected values. As in bpy[105], the dihedral angle between the two pyridine rings is small in ligand **L5**, **L7** and **L18**. This coplanarity is due to CH-N' interactions and to π-π-stacking.

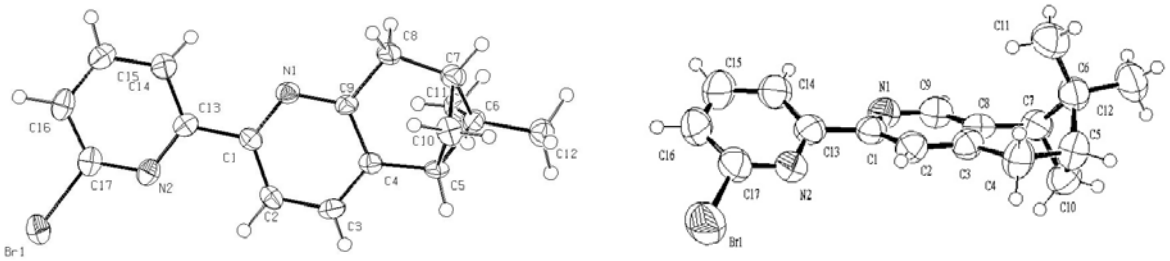

figure 31: ORTEP-plots of bromo-pinene-bpy derivatives **L5** (left) and **L6** (right).

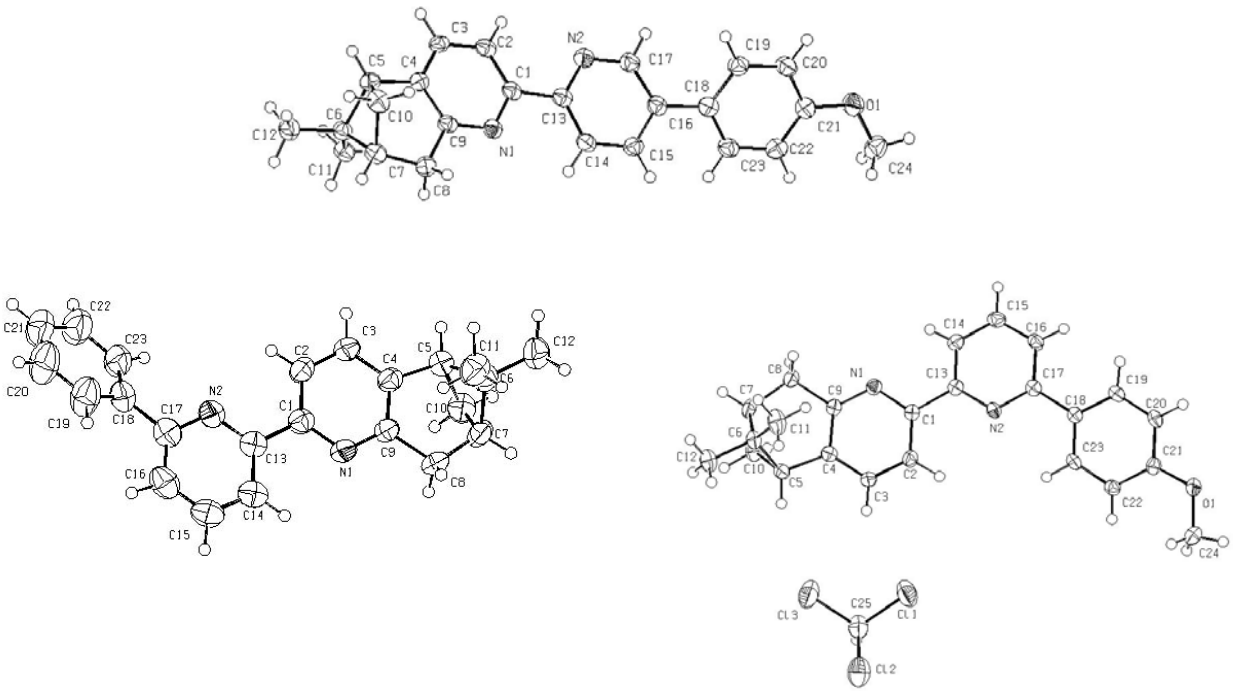

figure 32: ORTEP-plots of [5,6]-pinene-bpy derivatives **L3** (top), **L7** (left) and **L9** (right).

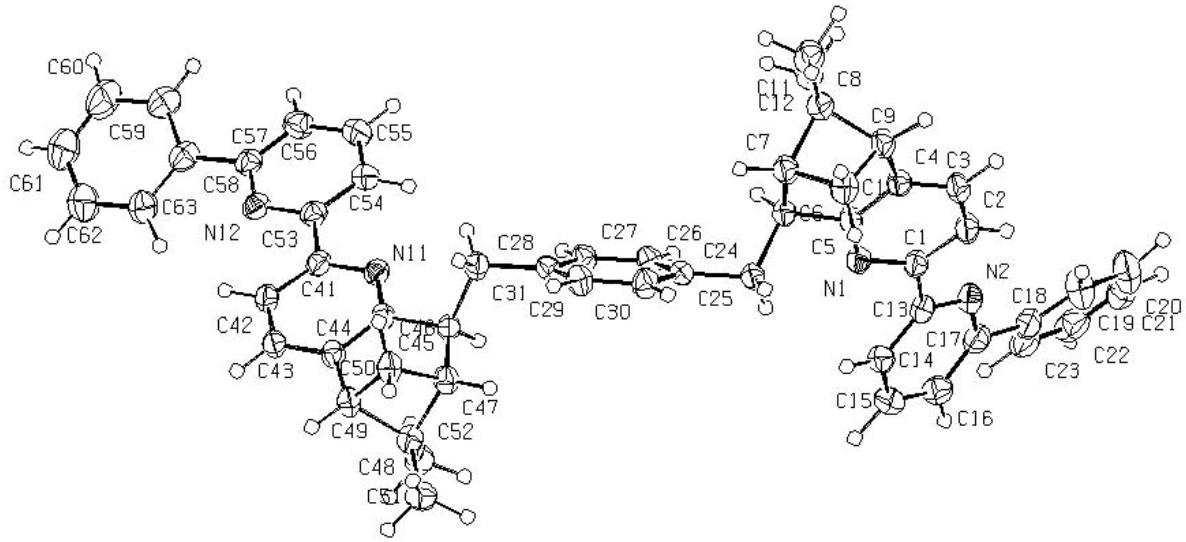

figure 33: ORTEP-plot of **L12**.

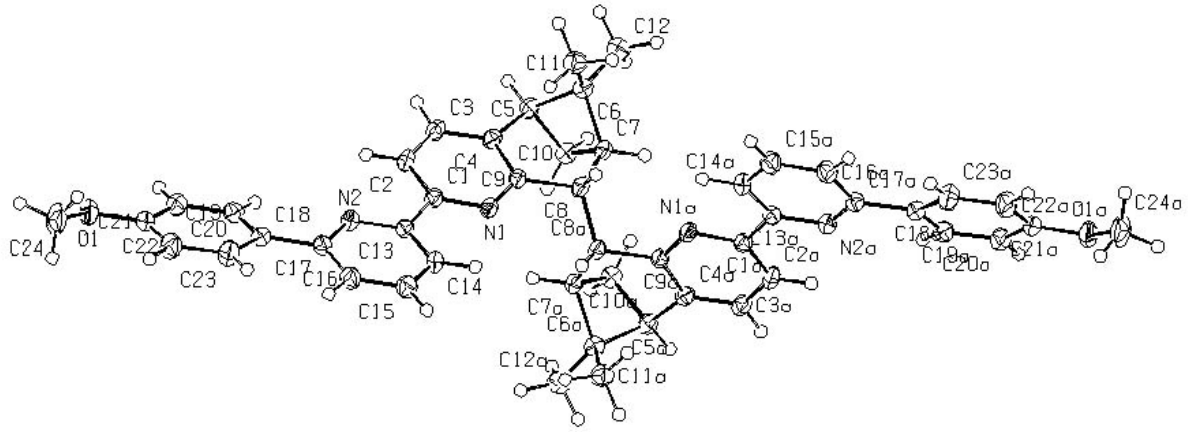

figure 34: ORTEP-plot of **L18**.

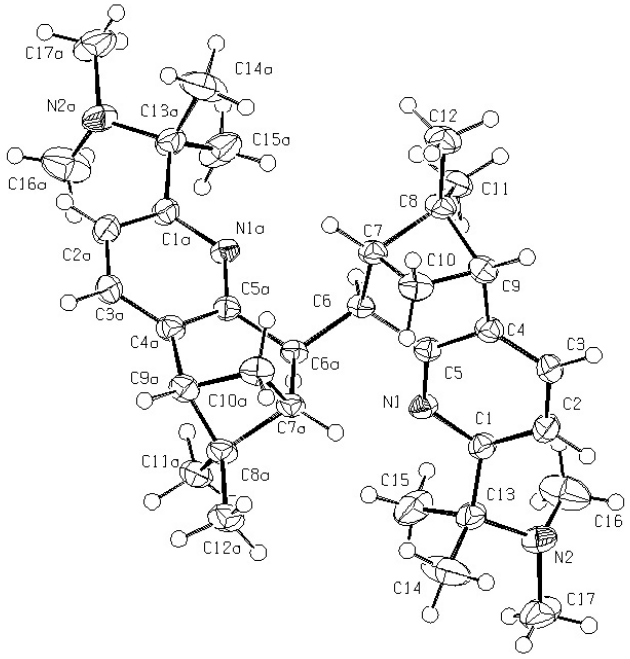

figure 35: ORTEP-plot of **L19**.

In **L3** and **L9**, as well as in [5,6]-pinene-bpy (**L1**)[106], and [5,6]-CHIRAGEN[0] (**L15**)[60], the twist angle varies from 6° to 10°, and on one of the bpy units of **L12** it amounts to 23°. For **L6** a twist angle of 29° is measured. For the 5'-substituted pinene-bpy the torsion angle between the phenyl and the pyridine is comparable to that in a biphenyl system.

	L3	**L5**	**L6**	**L7**
Empirical formula	C_{24} H_{24} N_2 O	C_{17} H_{17} Br N_2	C_{17} H_{17} Br N_2	C_{23} H_{22} N_2
Formula weight	356.45	329.24	329.24	326.43
Crystal shape	Block	Rod	Block	Block
Crystal colour	Colourless	Colourless	Colourless	Colourless
Crystal size [mm]	0.50 x 0.50 x 0.50	0.50 x 0.10 x 0.08	0.38 x 0.30 x 0.23	0.53 x 0.30 x 0.30
Crystal system	Monoclinic	Orthorhombic	Orthorhombic	monoclinic
Space group	P 2_1	P 2_1 2_1 2_1	P 2_1 2_1 2_1	P 2_1
a [Å]	9.1016(9)	6.1546(5)	6.5403(8)	10.8641(16)
b [Å]	9.3289(7)	13.5496(13)	11.3397(10)	6.3600(8)
c [Å]	11.1653(12)	17.5877(16)	20.395(2)	13.0544(17)
α [°]	90	90	90	90
β [°]	96.651(13)	90	90	90.312
γ [°]	90	90	90	90
Volume [$Å^3$]	941.64(15)	1466.7(2)	1512.6(3)	902.0(2)
Z	2	4	4	2
F(000)	380	672	672	348
Density (calculated) [g/cm^3]	1.257	1.491	1.446	1.202
Linear absorption coefficient μ [mm^{-1}]	0.077	2.794	3.619	0.070
Temperature [K]	153(2)	153(2)	293(2)	293(2)
Radiation used	Mo K_α	Mo K_α	CuK_α	Mo K_α
Wavelength [Å]	0.71073	0.71073	1.54180	0.71073
Scan method	ϕ oscillation	ϕ oscillation	ω/2Θ	ω/2Θ
No of reflections measured	7352	10465	6472	4520
No of independent reflections	3477	2871	2219	2260
No of observed reflections	2978; I> 2σ(I)	1760; I> 2σ(I)	2163I> 2σ(I)	1520; I> 2σ(I)
θ range [°]	2.74-25.94	2.32-25.96	4.34-59.60	2.43-27.48
R	0.0278	0.0315	0.0314	0.0494
wR_2	0.0639	0.0510	0.0801	0.0967
R (all data)	0.0351	0.705	0.0320	0.0850
wR_2 (all data)	0.0664	0.0574	0.0808	0.1118
Absolute structure parameter	-0.8(12)	0.002(13)	0.01(3)	0(6)

table 5: crystallographic data of the ligands **L3**, **L5-L7**.

	L9	**L12**	**L18**	**L19**
Empirical formula	C_{24} H_{24} N_2 O * CH_3Cl	C_{54} H_{50} N_4	C_{48} H_{48} N_4 O_2	C_{34} H_{50} N_4
Formula weight	475.92	754.98	710.89	514.78
Crystal shape	Plate	Rod	Rod	Rod
Crystal colour	Colourless	Colourless	Colourless	Colourless
Crystal size [mm]	0.35 x 0.30 x 0.10	0.60 x 0.20 x 0.10	0.50 x 0.30 x 0.20	0.50 x 0.15 x 0.15
Crystal system	Monoclinic	orthorhombic	monoclinic	orthorhombic
Space group	P 2_1	P 2_1 2_1 2_1	C 2	P 2_1 2_1 2
a [Å]	6.6825(5)	11.4989(5)	20.7692(18)	11.4893(8)
b [Å]	7.4085(4)	14.7712(8)	6.0863(4)	20.8542(16)
c [Å]	23.4403(18)	25.1410(16)	14.9639(13)	6.4198(4)
α [°]	90	90	90	90
β [°]	94.080(10)	90	99.673(10)	90
γ [°]	90	90	90	90
Volume [$Å^3$]	1157.52(14)	4270.3(4)	1864.7(3)	1538.19(19)
Z	2	4	2	2
F(000)	496	1608	756	564
Density (calculated) [g/cm^3]	1.365	1.174	1.266	1.111
Linear absorption coefficient μ [mm^{-1}]	0.416	0.068	0.078	0.065
Temperature [K]	153(2)	153(2)	153(2)	153(2)
Radiation used	Mo K_α	Mo K_α	Mo K_α	Mo K_α
Wavelength [Å]	0.71073	0.71073	0.71073	0.71073
Scan method	ϕ oscillation	ϕ oscillation	ϕ oscillation	ϕ oscillation
No of reflections measured	9156	31668	7379	12014
No of independent reflections	4208	8128	3471	2938
No of observed reflections	3435; I> 2σ(I)	4620; I> 2σ(I)	2907; I> 2σ(I)	1789; I> 2σ(I)
θ range [°]	2.61-25.92	2.24-25.95	1.99-25.89	1.95-25.93
R	0.0299	0.0326	0.0334	0.0417
wR_2	0.0657	0.0487	0.0819	0.841
R (all data)	0.0403	0.0760	0.0425	0.0774
wR_2 (all data)	0.0684	0.0558	0.0847	0.0926
Absolute structure parameter	-0.06(5)	2(2)	-1.4(15)	1(4)

table 6: crystallographic data of the ligands **L9**, **L12**, **L18** and **L19**.

Computational methods[107] yield a twist angle of 40° due to steric hydrogen repulsion. In the crystal structure of **L3**, a torsion angle of 34° is found. 6'-substituted-pinene-bpy derivatives have analogous structures to 2'-phenylpyridine with a calculated minimum of 25°, due to competing steric hydrogen repulsion and CH-N'-interactions. The torsion angles found in our crystals vary from 10° (**L18**) to over 14° (**L6**) and 25° (**L12**) to 32° (**L7**). The variation of all these angles is most likely the consequence of different packing in the crystals.

All three [5,6]-CHIRAGEN-ligands have a molecular C_2-axis, which is vertical to the bridge. Whereas **L18** and **L19** keep this C_2-axis in the crystal, as in the [5,6]-CHIRAGEN[0] **L15**[60], **L12** has no crystallographic C_2-axis, (one bpy conformation is coplanar, the other has a twist angle from about 23°). The plane angle between the two pyridine rings bearing the pinene moieties varies slightly, for **L15** a plane angle of 79° is found, for **L12** 81°, **L19** 81° and for **L18** 85°.

The detailed data of the crystal structure of these compounds are shown in two tables (table 5 and table 6).

1.9.2 NMR-spectroscopy

The most important method for the characterization of the ligands is the analysis by ^{1}H-NMR and ^{13}C-NMR spectroscopy. Since the structure of [5,6]-pinene-bpy and [4,5]-pinene-bpy is well characterized[65] (1D-NOE difference techniques were needed for the complete assignment), the assignment of the extended pinene-bpy systems is straightforward. All CHIRAGEN derivatives have a C_2-axis, thus the ^{1}H-NMR-spectra keep the simplicity of the pinene-bpy ligands, only the peaks of the bridge protons are added. The parts of the ^{1}H-NMR-spectra of the 5'-substituted ligands **L3**, **L11** and **L16** are shown in figure 36 (aromatic protons) and in figure 37 (aliphatic ones). Only small chemical shifts between the three different ligands could be observed, an exception is the aliphatic proton 7 at the bridge. While in **L3** the chemical shift of proton 7 is at 3.2 ppm, it is shifted downfield to 3.4 ppm in **L11** and to 4.5 ppm in **L16**. The signals of proton 3' and 7 in the CHIRAGEN[0] (**L16**) are broad, and surprisingly, they show a NOE interaction.

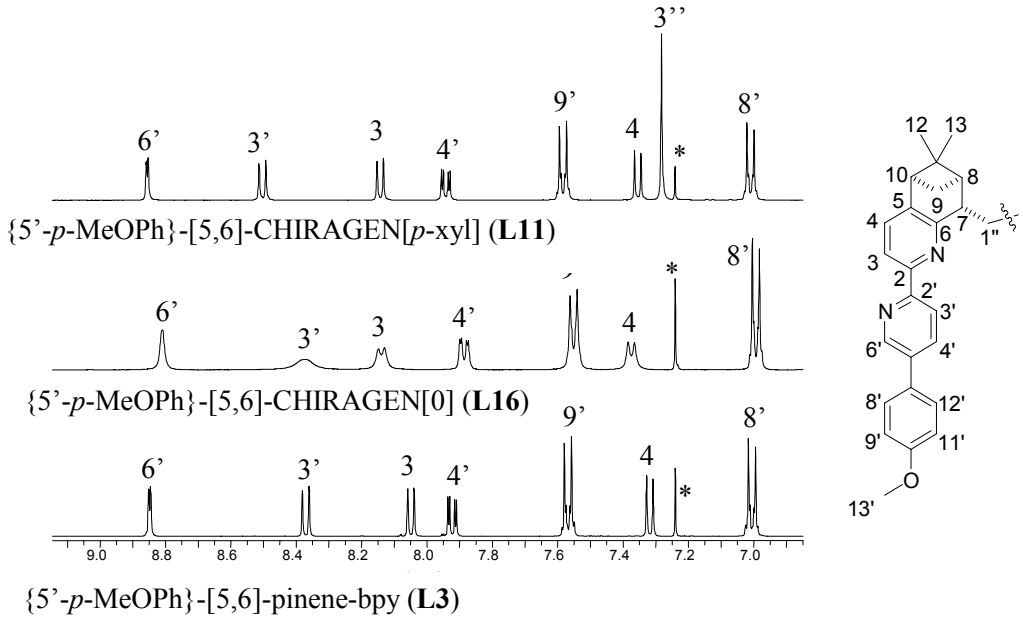

figure 36: ^{1}H-NMR-spectra of 5'-substituted derivatives.

The protons 1'' at the *p*-xylene-bridge of **L11** are diastereotopic and thus a significant difference in the chemical shift is observed. One proton is shifted up to 3.9 ppm, the other to 2.8 ppm. For the 6'-substituted [5,6]-CHIRAGEN[*p*-xyl] ligands the same phenomena are observed.

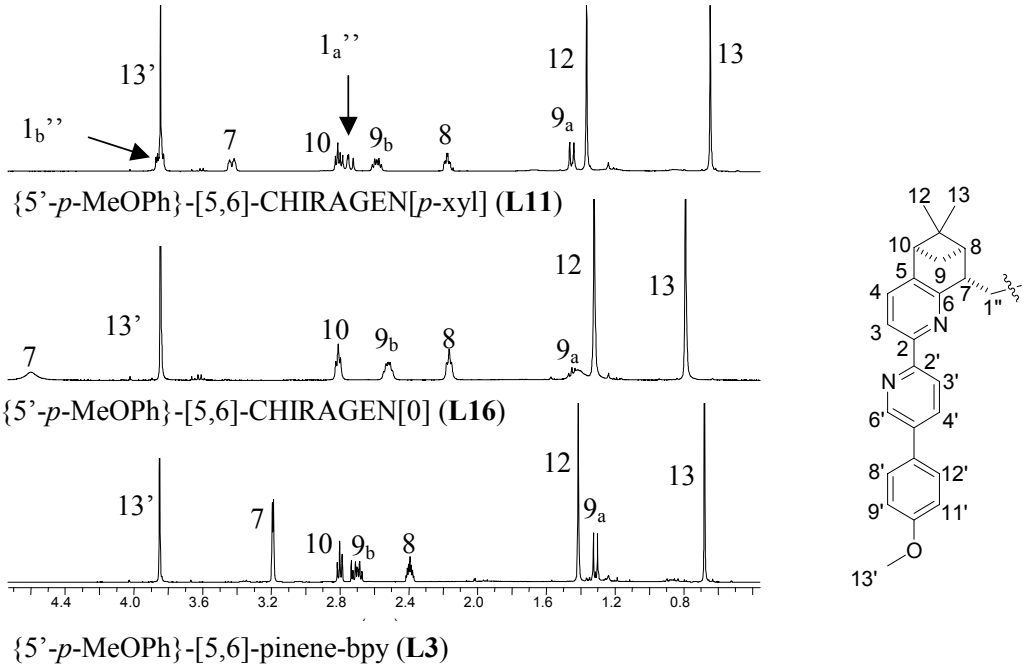

figure 37: ^{1}H-NMR-spectra of 5'-substituted derivatives.

The aromatic part of the ^{1}H-NMR spectra of the five [5,6]-CHIRAGEN[0] is shown in figure 38. As mentioned above, the signals of proton 3’ is broad in all cases.

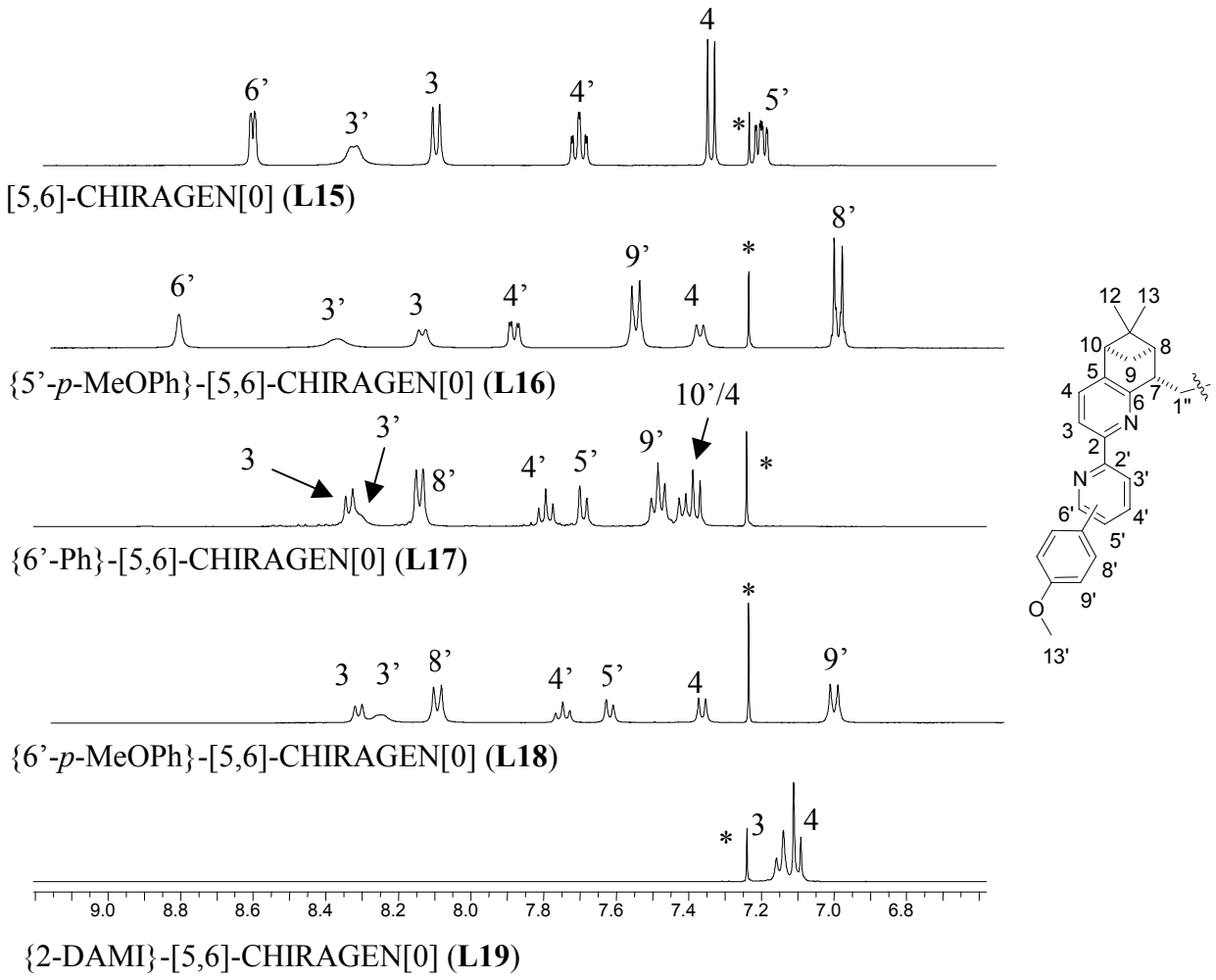

figure 38: ^{1}H-NMR-spectra of several [5,6]-CHIRAGEN[0].

1.9.3 UV/Vis spectroscopy

All ligands of the family **L1-L10** show absorptions in the UV-region, corresponding to π-π*-transitions. The spectra of the corresponding [4,5]-, and [5,6]-pinene-bpy derivatives are very similar. The spectra of **L1** and **L6** are shown in figure 39, the spectra of **L3**, **L8** and **L9** in figure 40. The spectra of the CHIRAGEN derivatives show all absorptions at the same wavelengths as the corresponding [5,6]-pinene-bpy derivatives, with ε-values nearly doubled.

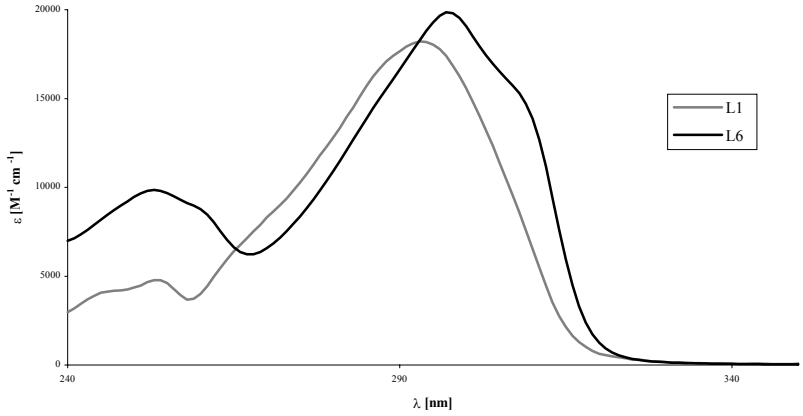

figure 39: UV/Vis-spectra of **L1** and **L6**.

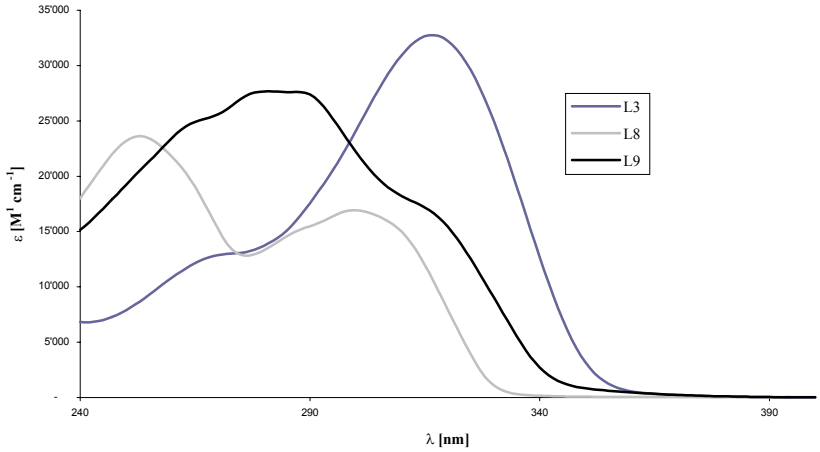

figure 40: UV/Vis-spectra of **L3**, **L8** and **L9**.

1.9.4 CD spectroscopy

As previously observed[36], pinene-bpy derivatives and CHIRAGEN[bridge] derivatives are nearly void of any CD-activity. CHIRAGEN[0]-ligands, however, show distinct exciton couplets in the range of the π-π*-absorptions (figure 41 and figure 42). The most pronounced CD-activity is measured in the spectrum of **L16** (figure 42), which can be explained by the hypothesis of an intramolecular π-stacking of the two methoxy-phenyl-groups.

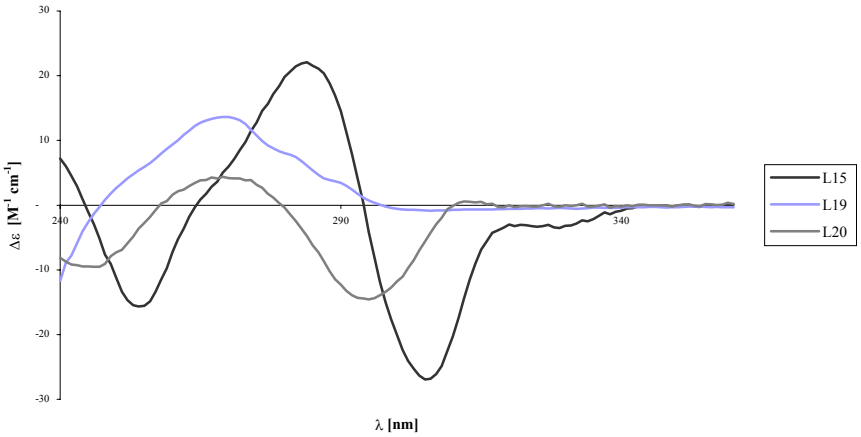

figure 41: CD-spectra of CHIRAGEN[0]derivatives **L16**, **L19** and **L20**.

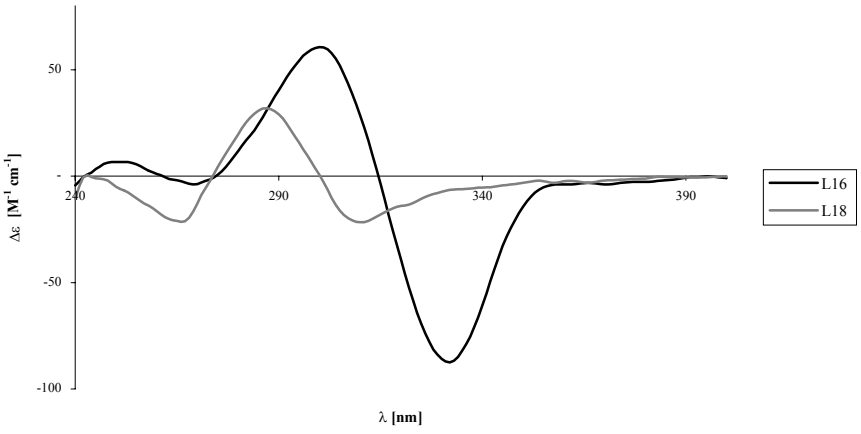

figure 42: CD-spectra of CHIRAGEN[0]derivatives **L16** and **L18**.

2. Complex formation and characterization

The tetradentate [5,6]-CHIRAGEN derivatives can be divided into two different groups depending on the bridge between the two [5,6]-pinene-bpy moieties. The first group contains those ligands with a *p*-xylene bridge. The inclusion of the bridge leads to the formation of polynuclear species and prevents intramolecular, mononuclear complexation. The second group is formed by directly bridged two [5,6]-pinene-bpy moieties. These [5,6]-CHIRAGEN[0] derivatives can be used for the formation of mononuclear complexes.[60]

2.1. Complexes with CHIRAGEN[*p*-xyl]-derivatives

It is well known, that the [5,6]-CHIRAGEN[*p*-xyl] (**L39**) forms a hexanuclear circular helicate with labile metals such as silver(I) and copper(I) (scheme 24),[51] where the chirality of the ligand predetermines the configuration at the six homochiral metal centres and furthermore the chirality of the circular helicate.

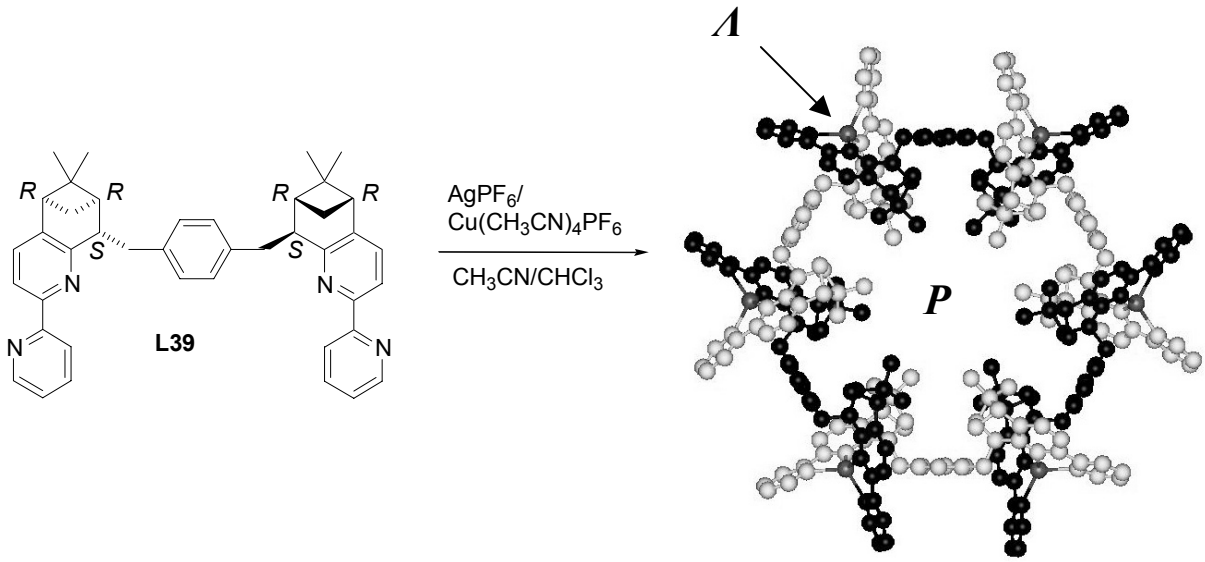

scheme 24: synthesis of the hexanuclear, circular helicate **C1** (with Ag(I)) and **C2** (with Cu(I)).[51]

The enantiopure ligand **L39** leads to a *Λ*-configuration at the metal centres and therefore to a *P*-helicate (self-recognition by self-assembly).

2.1.1 Synthesis

Herein we present similar hexanuclear circular helicates with the synthesised [5,6]-CHIRAGEN[*p*-xyl] derivatives (**L11**, **L12**, **L13**) described in the previous chapter using silver(I) or copper(I). From **L11** the complexes **C3** ($[Ag_6\mathbf{L11}_6)](PF_6)_6$) and **C4** ($[Cu_6\mathbf{L11}_6)](PF_6)_6$) were obtained (scheme 25), from **L13** **C5** ($[Cu_6\mathbf{L13}_6)](PF_6)_6$) (scheme 26) and from **L12** **C6** ($[Cu_6\mathbf{L12}_6)](ClO_4)_6$) (scheme 27).

The silver(I) complex **C3** (scheme 25) was obtained by reaction of the ligand **L11** (dissolved in $CHCl_3/CH_3CN$) with an equimolar amount of $AgPF_6$ salt (dissolved in CH_3CN). After 10 minutes the solvent was evaporated under reduced pressure and the complex **C3** was obtained in almost quantitative yield and no further purification was needed. The analogous copper(I)-complex **C4** was obtained in the same manner using the precursor $[Cu(CH_3CN)_4]PF_6$[108] as metal cation source (yield: 99%). By addition of the ligand (dissolved in $CHCl_3/CH_3CN$) to the copper(I)-solution in CH_3CN, a deep red colour appeared immediately, the characteristic colour for a copper(I) complex with bpy ligands.

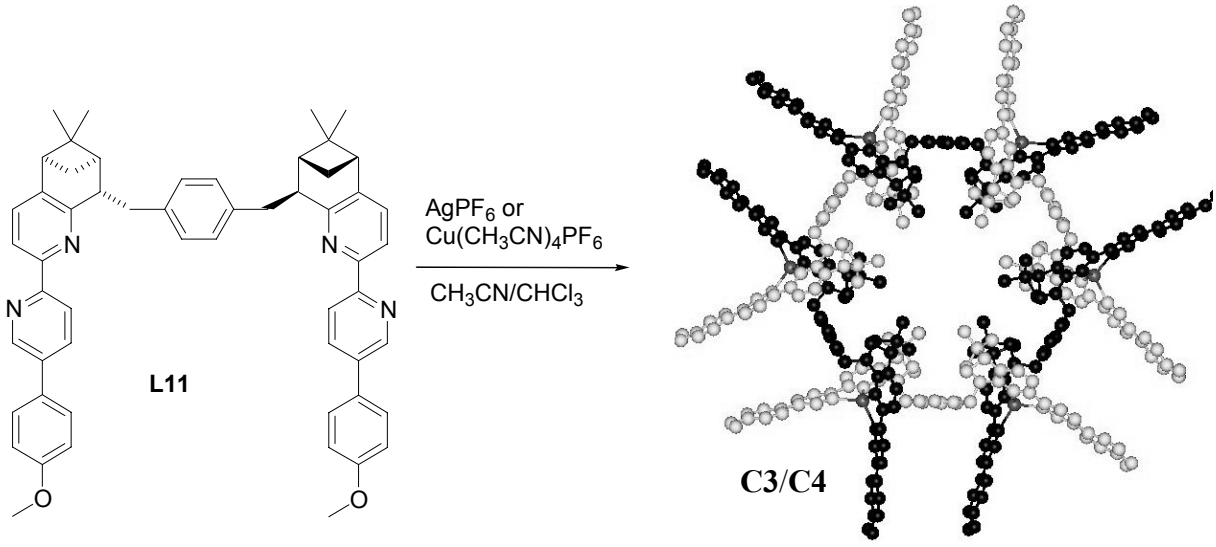

scheme 25: synthesis of **C3** and **C4** with ligand **L11**.

For the complex **C5** (scheme 26), the same method described above was used. The metal source was the $[Cu(CH_3CN)_4]PF_6$-salt.[108] The complex was isolated by precipitation with diethyl ether to remove traces of free ligand and it showed again the characteristic deep red colour.

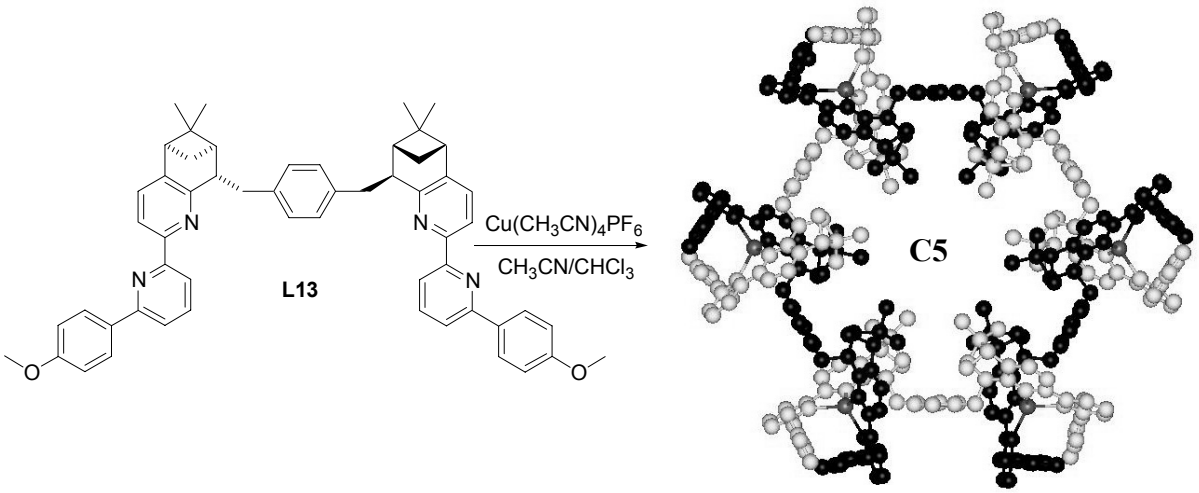

scheme 26: synthesis of **C5** with ligand **L13**.

The complex **C6** was obtained by using another metal cation source such as $[Cu(CH_3CN)_4]ClO_4$ (scheme 27).[109] The complex **C6** was isolated by precipitation with diethyl ether (yield 99 %).

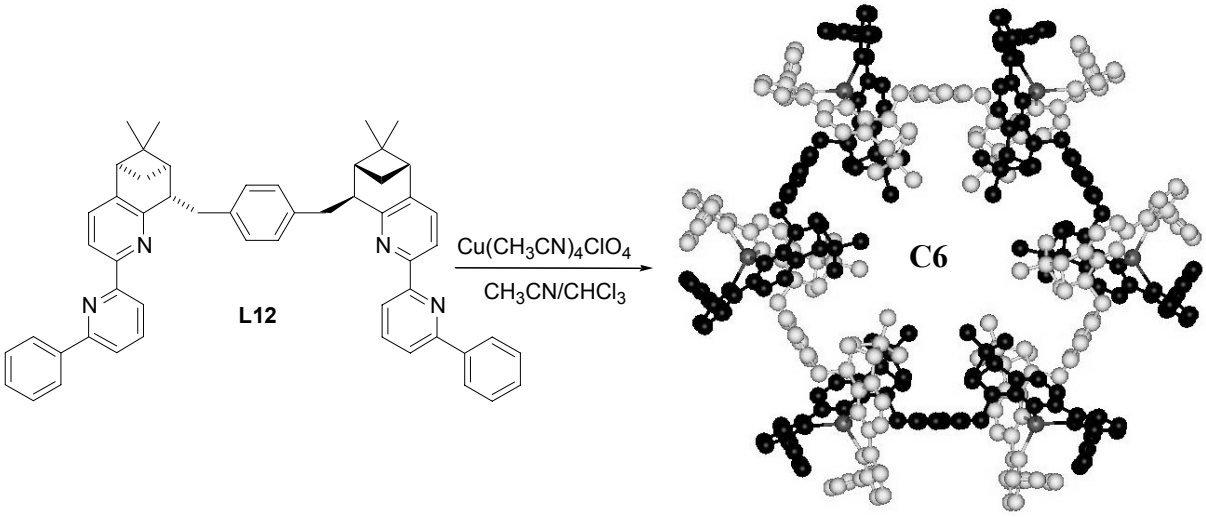

scheme 27: synthesis of **C6** with ligand **L12**.

Crystals suitable for X-ray analysis for these complexes could not be isolated. The structure representations in scheme 25 to scheme 27 show computer models using the program Molden.[110] The X-ray data of **C1** were used as starting point. But the structures can be analysed in solution and deduced by analogy to the known complexes **C1** and **C2**.

2.1.2 Characterization of the silver(I)-complex C3

The length of the bridge between the two pinene-bpy moieties of all [5,6]-CHIRAGEN[*p-xyl*] (**L11**-**L13**) was designed for the formation of polynuclear species and it should inhibit the formation of mononuclear complexes. The ^{1}H-NMR-spectrum of the silver(I)-complex **C3** shows a symmetrical species (figure 43b), which cannot be attributed to a mononuclear complex. The assumed polynuclear complex is highly symmetrical, all ligands wrapping around the metal centres are chemically equivalent. The C_2-symmetry of the free ligand (figure 43a) is preserved in the complex.

Comparing the complex with the free ligand, the largest shift in the ^{1}H-NMR-spectrum ($\Delta\delta$=1.33 to high field) is due to the aromatic protons on the bridge (3'', 4'', 5'' and 6'' chemically equivalent), associated with a dramatic change of the chemical environment. Other protons such as 7 and 8 are shifted to high field by a significant amount. The protons of the bridge and most of the aliphatic ones are broad at 25° C, indicating a fast exchange between two or more different species.

The comparison of the chemical shifts of the complexes **C1** and **C3** shows only slight changes, assuming both complexes have a similar structure (table 7). The structure of **C1** was determined by X-ray analysis and showed a hexanuclear circular helicate. The protons 6' ($\Delta\delta$=0.30) and 4' ($\Delta\delta$=0.16) show the largest difference in chemicals shifts, which is caused by the influence of the methoxy-phenyl group attached at carbon 5'.

	6'	5'	4'	3'	3	4	3''	7	8	9a	9b	10	12	13	1a''	1b''
C1	8.44	7.43	7.98	8.27	8.21	7.83	5.89	2.82	1.39	1.57	2.55	3.01	1.17	0.08	2.41	3.73
C3	8.74	---	8.14	8.24	8.29	7.85	5.95	2.89	1.22	1.60	2.59	2.97	1.22	0.14	2.46	3.83
Δδ	0.30	---	0.16	-0.03	0.08	0.02	0.06	0.07	-0.17	0.03	0.04	-0.04	0.05	0.06	0.05	0.10

table 7: comparison of the chemical shifts of **C1**[51] and **C3**.

The broadening of the signals in ^{1}H-NMR-spectrum was also observed in **C1**, where the hexanuclear species is in equilibrium with a tetranuclear one depending on concentration, temperature and pressure.[52]

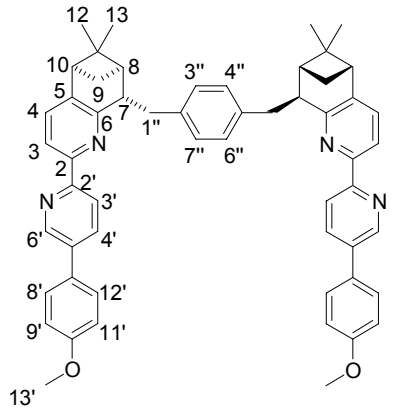

chart 8: numbering of the ligand **L11**.

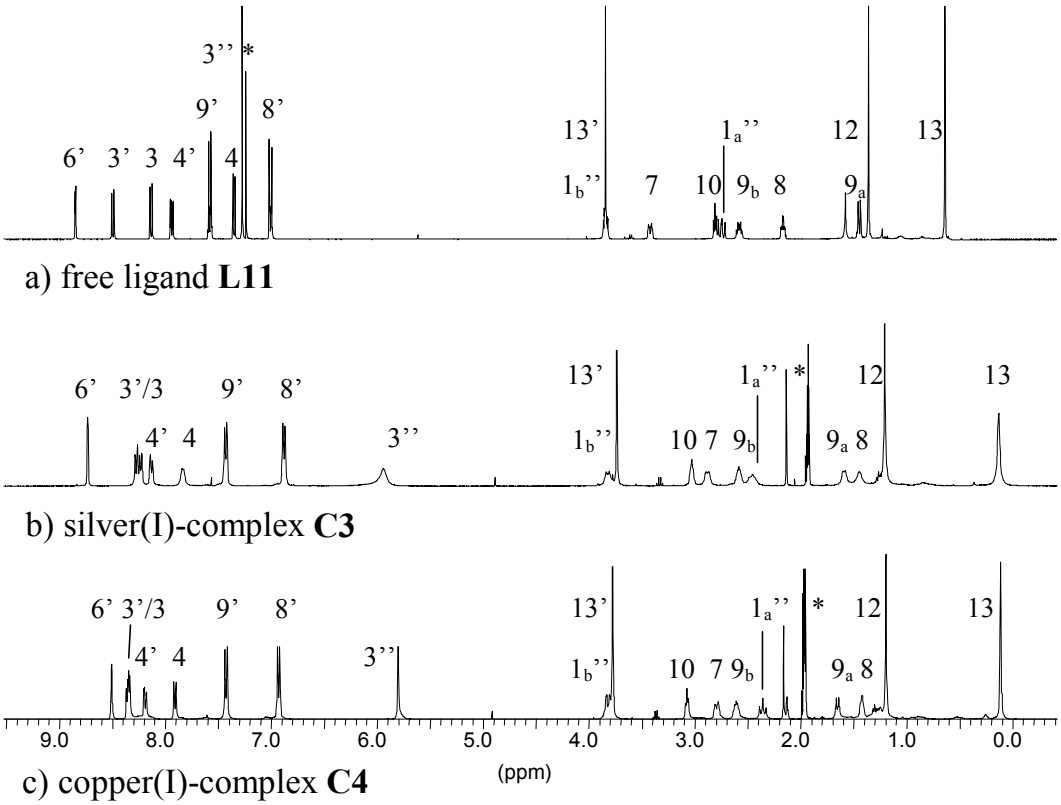

figure 43: ^{1}H-NMR-spectra of the ligand **L11** in $CDCl_3$ and the complexes **C3** and **C4** in CD_3CN.

^{1}H-NMR-measurements of **C3** were carried out at different temperatures (figure 44). At 60 °C all signals sharpened, the hexanuclear form is favoured at higher temperature. At lower temperatures (0 - 40 °C) a doubling of the signals attributed to the protons at the bridge concomitant with a broadening of all signals is observed. The exchange between the two species slowed down and the signals of the second species becomes observable (at least for the signals of the protons 3'').

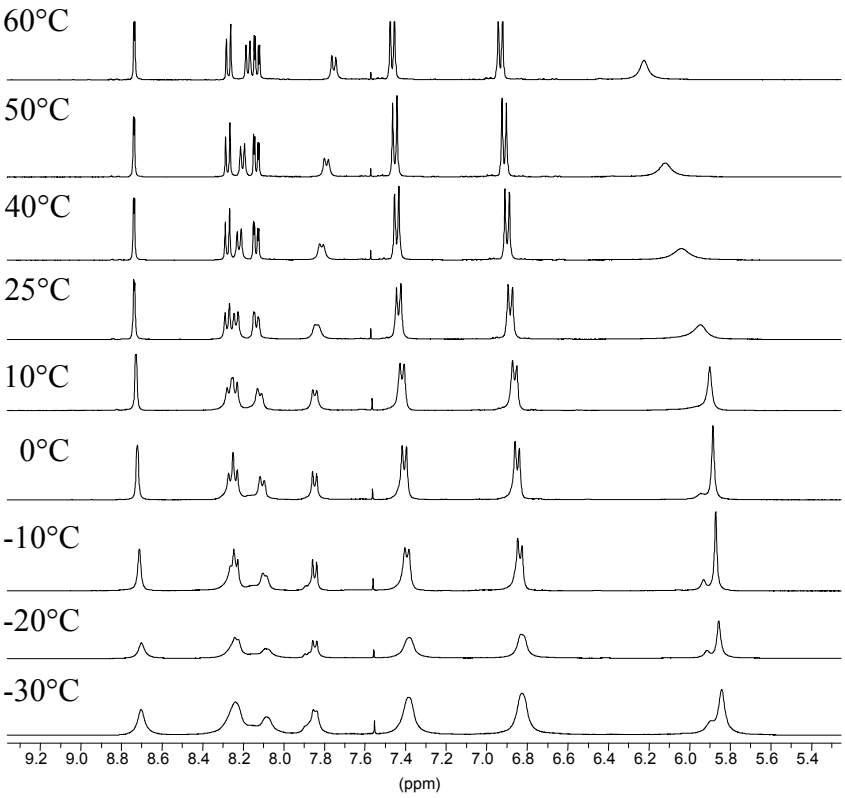

figure 44: temperature dependence of ^{1}H-NMR-measurements of **C3** in acetonitrile at 25 °C.

A doubling of all signals (the aromatic part is shown in figure 45) occurs on changing the solvent. The non-coordinating solvent nitromethane inhibits the fast exchange of the two species in equilibrium.

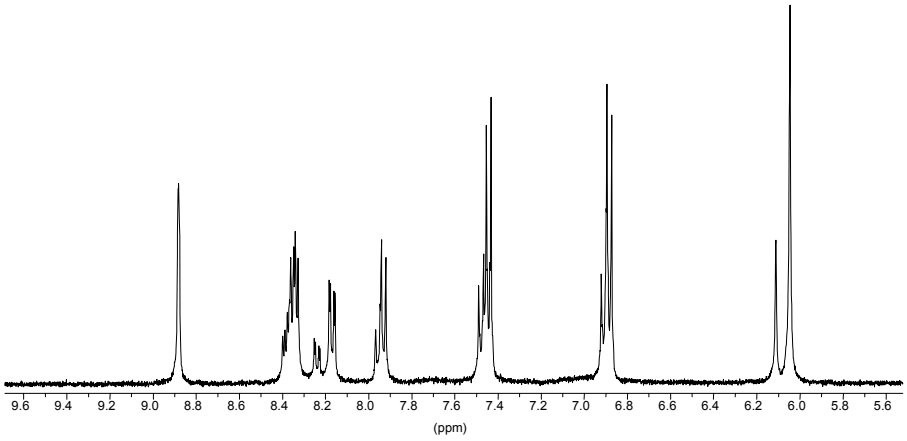

figure 45: aromatic part of the ^{1}H-NMR of **C3** in nitromethane.

Electrospray mass spectroscopy is the method of choice for the analysis of helicates, which are kinetically labile species. With this technique species in solution can be determined in a qualitative way.

In complex **C1** (structurally analysed in the solid state as hexanuclear circular helicate), electrospray mass spectroscopy shows several species present in solution. $[Ag_6\mathbf{L39}_6](PF_6)_3^{3+}$, $[Ag_4\mathbf{L39}_4]PF_6^{2+}$ and $[Ag_2\mathbf{L39}_2]^{+}$ appear all at the same nominal mass (1566.5), showing however different isotopic pattern. The same is observed for $[Ag_6\mathbf{L39}_6](PF_6)_2^{4+}$ and $[Ag_3\mathbf{L39}_3]PF_6^{2+}$ at a mass of 1138.6. Other signals are due to $[Ag_6\mathbf{L39}_6]PF_6^{5+}$ (881.9), $[Ag_5\mathbf{L39}_5]PF_6^{4+}$ (924.7), $[Ag_5\mathbf{L39}_5](PF_6)_2^{3+}$ (1281.2) and $[Ag_4\mathbf{L39}_4]PF_6^{3+}$ (995.6). Always present are as well the peak $Ag\mathbf{L39}^{+}$ at 711.2 (the isotopic pattern corresponds to several species $[Ag_n\mathbf{L39}_n]^{n+}$) and $Ag\mathbf{L39}_2^{+}$ at 1313.9.

In the case of **C3** only a few peaks could be observed (figure 46). $Ag\mathbf{L11}^{+}$ ($\hat{=}[Ag_n\mathbf{L11}_n]^{n+}$ at 922.5) and $Ag\mathbf{L11}_2^{+}$ (at 1737.5) have high intensities. Two other peaks correspond to the hexanuclear species. The study of the isotopic pattern of the peak at 1457.95 shows an overlapping of two species, one corresponds to the hexamer ($[Ag_6\mathbf{L11}_6](PF_6)_2^{4+}$), the other one to the trimer ($[Ag_3\mathbf{L11}_3]PF_6^{2+}$).

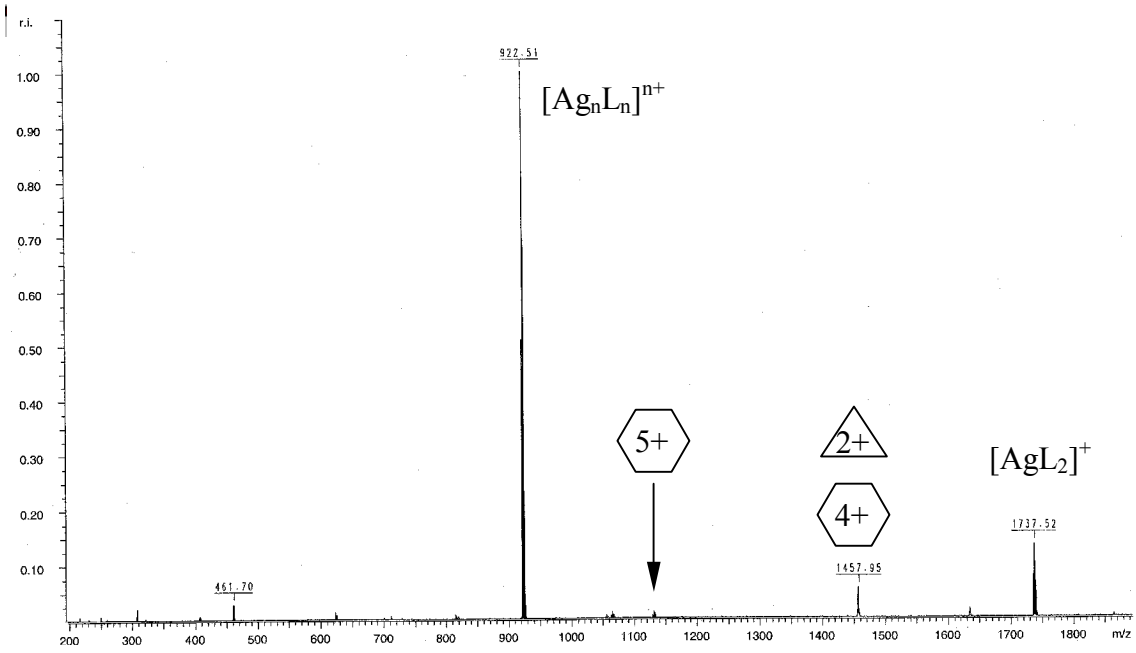

figure 46: electrospray mass spectroscopy of **C3**.

The results from NMR and ESI-MS investigations have to be interpreted with caution. The formation of the circular helicates is strongly dependent on the concentration. While the NMR-technique is applicable for concentration in the range 0.01M to 0.1M, the maximum concentration for ESI-MS is around 10^{-3}M. The species observed in the ESI-MS are more stable at low concentration, but they are only minor species or not even observed in the NMR.

2.1.3 Characterization of the copper(I)-complexes C4, C5 and C6

The copper(I)-complexes of **L11** (**C4**) (scheme 25), **L12** (**C6**) (scheme 27) and **L13** (**C5**) (scheme 26) show similar behaviour in solution, which have already been observed for their analogue **C2**.[51]

The ^{1}H-NMR spectra of these complexes show highly symmetrical, polynuclear species (mononuclear ones are inhibited by the geometry of the ligands). All copper(I)-complexes show sharp signals in the ^{1}H-NMR-spectra, which is in contrast to the silver(I)-complexes (**C4** in figure 43c, **C5** in figure 47b). No broadening occurs through exchange by various species. Otherwise the spectra show similar characteristics as compared to its silver(I)-analogue. The signals of the protons at the bridge are sharp and show again a large upfield shift ($\Delta\delta$ = 1.50 ppm for **C4**, $\Delta\delta$ = 1.60 ppm for **C5**, $\Delta\delta$ = 1.69 ppm for **C6**). Protons 7 and 8 are shifted significantly to high field.

The spectra of **C5** and **C6** show an additional phenomenon. The protons of the 6'-subsituents are strongly shifted highfield ($\Delta\delta$ = 1.04 ppm for 8', $\Delta\delta$ = 0.78 ppm for 9' in both ligands and $\Delta\delta$ = 0.38 ppm for 10' in **L12**, figure 47).

All protons signal of **C4** are shifted by nearly the same amount as compared to its analogue **C2**, again the largest differences occur by protons 6' and 4', induced by the methoxy-phenyl group at 5' (table 8).

The comparison of **C2** with the complexes **C5** and **C6** shows remarkable differences in the chemical shifts (table 8), especially for the protons 3', 4', 3, 7 and both 1''. An explanation for this could be the slightly different geometries of the ligands. The 6'-substituents (themselves shifted to high field) are pointing towards the metal centre. Therewith it influences strongly the second ligand coordinated to the same centre.

	6'	5'	4'	3'	3''	3	4	7	8	9a	9b	10	12	13	1a''	1b''
C2	8.17	7.40	7.98	8.31	5.70	8.3	7.87	2.69	1.33	1.59	2.54	3.02	1.12	0.02	2.27	3.68
C4	8.48	---	8.16	8.33	5.78	8.32	7.88	2.77	1.40	1.63	2.58	3.05	1.17	0.09	2.33	3.80
Δδ	0.31	---	0.18	0.02	0.08	0.02	0.01	0.08	0.07	0.04	0.04	0.03	0.05	0.07	0.06	0.12
C5	---	7.28	7.68	7.68	5.69	8.12	7.9	2.93	1.45	1.77	2.64	3.1	1.12	0.14	2.56	4.26
Δδ	---	-0.12	-0.30	-0.63	-0.01	-0.18	0.03	0.24	0.12	0.18	0.1	0.08	0.00	0.12	0.29	0.58
C6	---	7.35	7.71	7.71	5.69	8.1	7.91	2.92	1.45	1.75	2.63	3.12	1.21	0.14	2.57	4.26
Δδ	---	-0.05	-0.27	-0.60	-0.01	-0.20	0.04	0.23	0.12	0.16	0.09	0.10	0.09	0.12	0.30	0.58

table 8: comparison of the chemical shifts of **C2**[51] and **C4**, **C5** and **C6**.

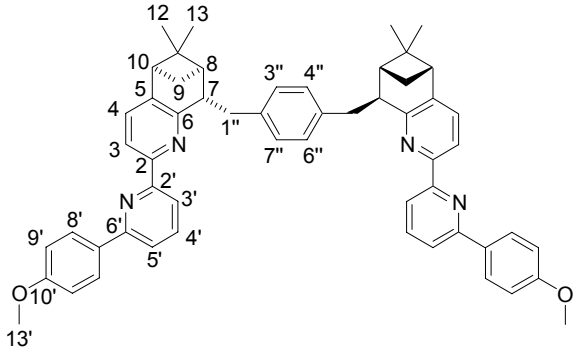

chart 9: numbering of the ligand **L13**.

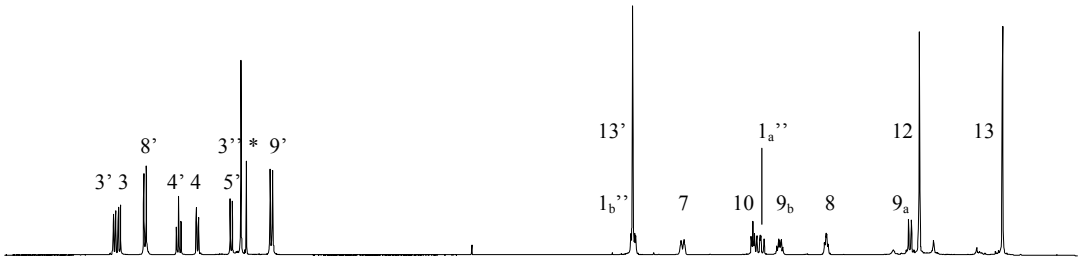

a) free ligand **L13**

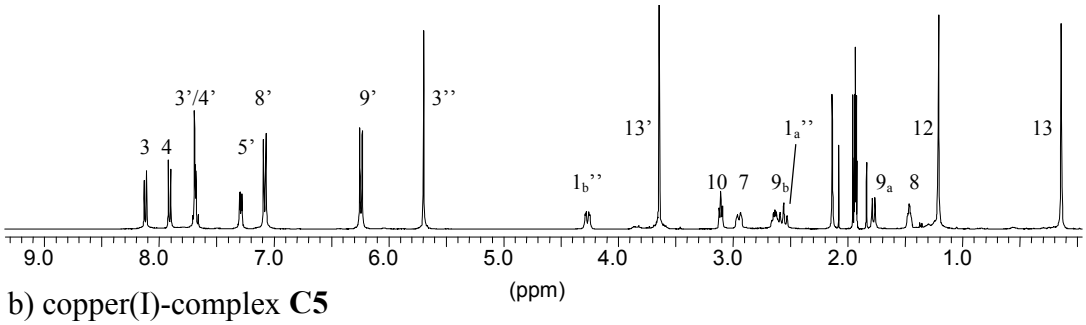

b) copper(I)-complex **C5**

figure 47: ^{1}H-NMR-spectra of the ligand **L13** and its copper(I)-complex **C5**.

The electrospray mass spectrum of **C2** does not show a peak corresponding to the hexanuclear species, which is in contrast with the X-ray analysis (figure 48)[111]. Only peaks of the penta- ($[Cu_5\mathbf{L39}_5]PF_6^{4+}$ at 869.4 and $[Cu_5\mathbf{L39}_5](PF_6)_2^{3+}$ at 1207.4), tetra- ($[Cu_4\mathbf{L39}_4]PF_6^{3+}$ at 936.6) and trinuclear ($[Cu_3\mathbf{L39}_3]PF_6^{2+}$ at 1071.8) species could be observed (figure 48). Peaks corresponding to $Cu\mathbf{L39}^+$ ($\hat{=}[Cu_n\mathbf{L39}_n]^{n+}$ at 666.5) and $[Cu\mathbf{L39}_2]^+$ (at 1270.6.5) are also present. These results are in accordance with the concentration dependence observed for the silver(I)-complexes. At low concentration several species with different nuclearities, but mostly with the ligand/metal ratio of 1:1 are in equilibrium.

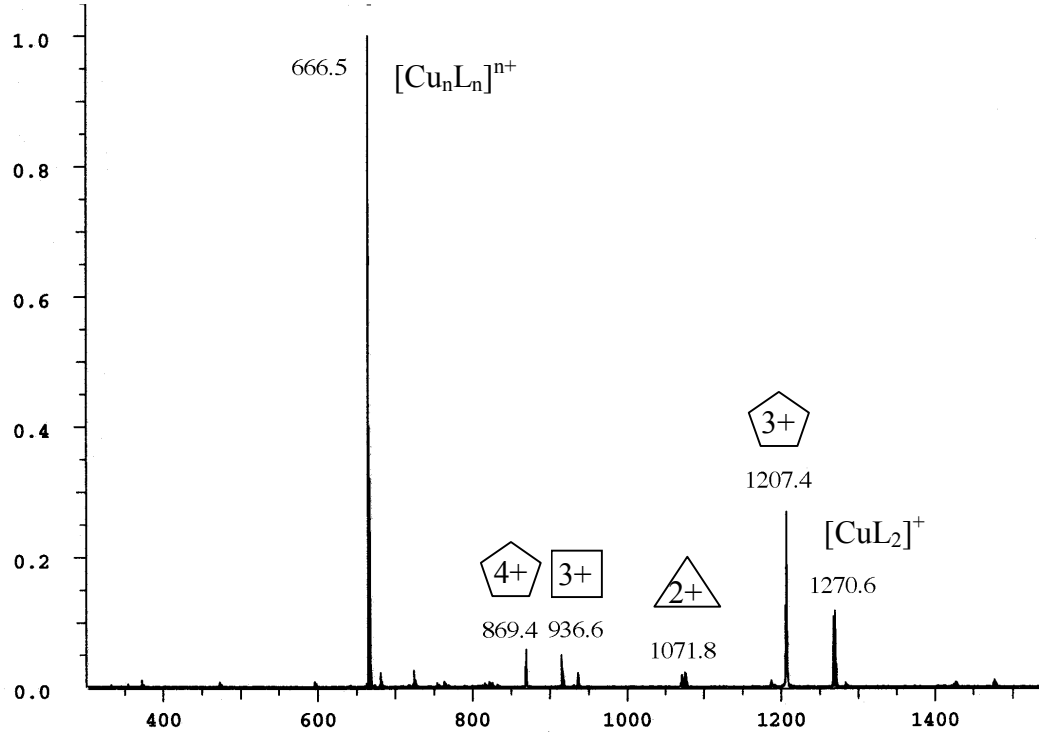

figure 48: ESI-MS of **C2**[111]

A similar behaviour was observed for the complexes **C4**, **C5** (figure 49) and **C6**. In each case, the major peak $[Cu\mathbf{L}]^+$ (the isotopic pattern show again the superposition of several charged species $[Cu_n\mathbf{L}_n]^{n+}$) and the peaks corresponding to $[CuL_2]^+$ and $[Cu_2L]^{2+}$ are present (table 9). The pentanuclear species can be observed in each case, whereas peaks of the tetranuclear complex in **C4** and the trinuclear complex in **C4** and **C6** are present. The ESI-mass spectra were recorded at different concentrations (not determined), which could explain the absence of some peaks in several spectra. But it is apparent, that at low concentration several species are in equilibrium.

	$[Cu_5\mathbf{L}_5]X^{4+}$	$[Cu_5\mathbf{L}_5]X_2^{3+}$	$[Cu_4\mathbf{L}_4]X^{3+}$	$[Cu_3\mathbf{L}_3]X^{2+}$	$[Cu_n\mathbf{L}_n]^{n+}$	$[Cu\mathbf{L}_2]^{+}$	$[Cu_2\mathbf{L}]^{2+}$
C2	869.4	1207.4	936.6	1071.8	666.5	1270.6	---
C4	1134.4	1560.9	1219.8	1390.0	879.4	1693.8	470.2
C5	1133.4	1560.6	---	---	879.4	1691.8	470.12
C6	1048.0	1430.50	---	1277.5	817.38	1573.6	441.2
For the complexes **C2**,[111]1 **C4** and **C5** the counterions X^- is PF_6^-, for **C6** ClO_4^-.							

table 9: peaks observed in the ESI-mass spectroscopy for the complexes **C2**, **C4-C6**.

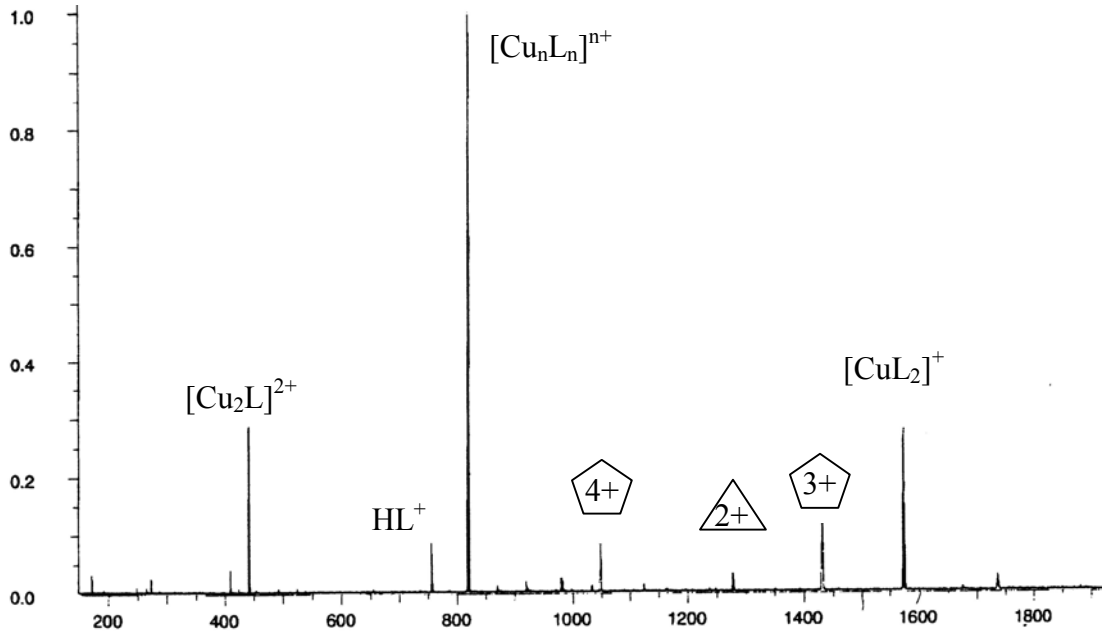

figure 49: ESI-MS of **C6**.

2.1.4 Characterization of the complexes C3 to C6 (UV/Vis- and CD)

With the knowledge, that several species are in equilibrium at low concentration, the UV/Vis and CD-spectroscopy should be interpreted with caution. Several species can be in equilibrium at the concentration used for UV/Vis and CD-spectroscopy. The UV/Vis spectra are similar (ε_{max} at similar λ) to those of the free ligands (figure 50).

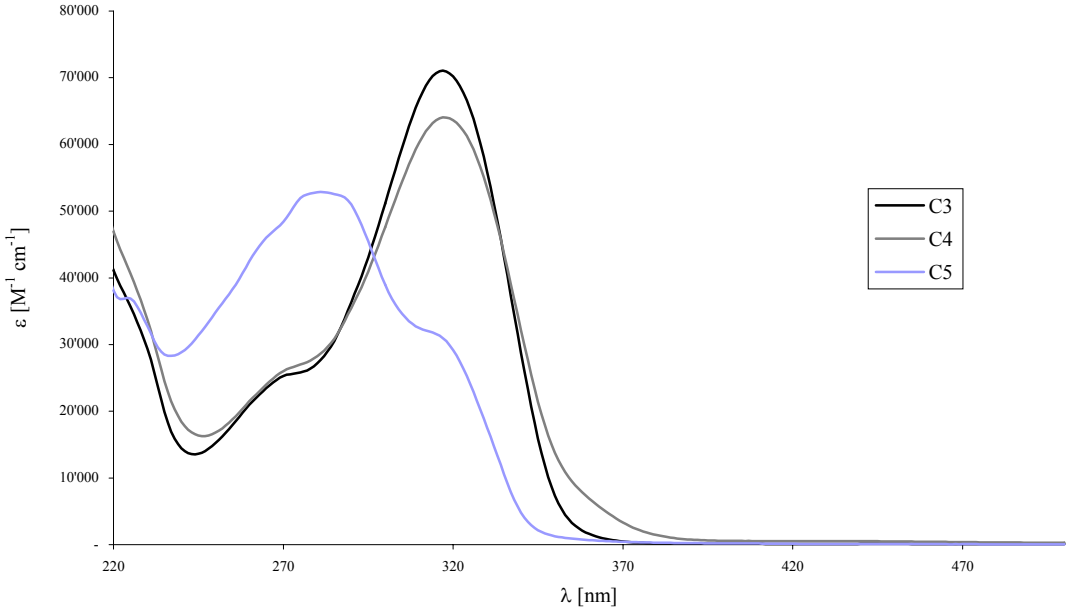

figure 50: UV/Vis spectra of **C3**, **C4** and **C5**.

The MLCT band for **C4**, **C5**and **C6** was not observed due to low concentration of the solutions.

From the CD-spectra, the configuration at the metal centres can be assigned (figure 51). The bands around 345 nm for **C3** and **C4**, around 317 nm for **C5** and around 306 nm for **C6** are in the positive range. The exciton coupling theory predicts for this effect an absolute configuration *Λ*, which is in line with the configuration found in the crystal structure of **C2**. [51]

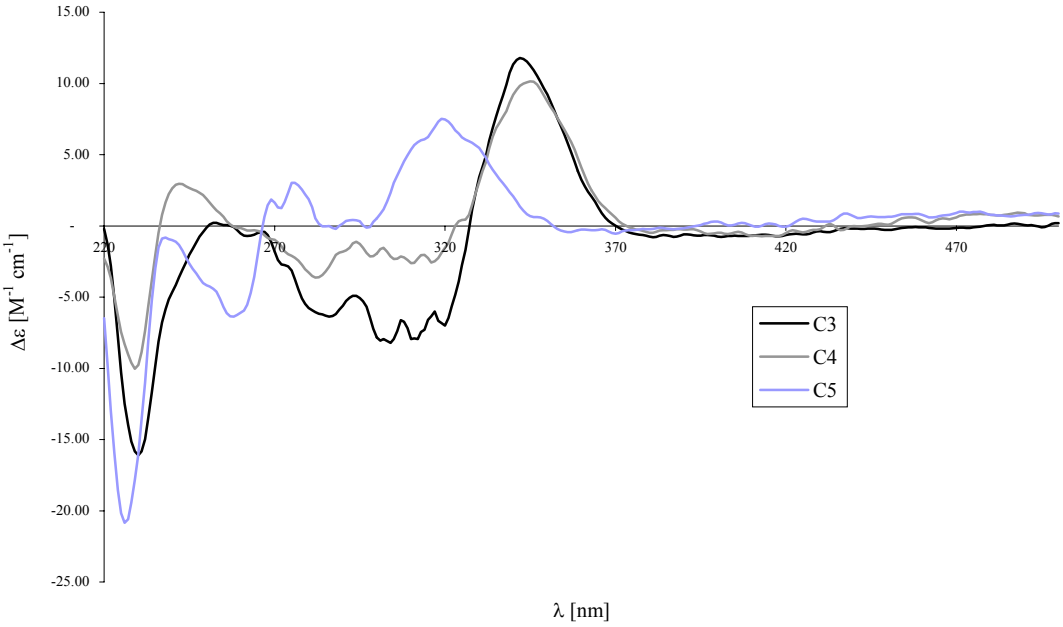

figure 51: CD-spectra of **C3**, **C4** and **C5**.

2.2. Complexes with CHIRAGEN[0]-derivatives

2.2.1 Synthesis

The [5,6]-CHIRAGEN[0] is designed for the formation of mononuclear complexes, as metal cations can fit into the cavity, which is defined by the two pinene-bpy units. Complexes **C8** and **C9** are synthesised by adding a solution of $AgPF_6$ in acetonitrile to an equimolar solution of the ligands **L16** and **L18** in mixtures of chloroform and acetonitrile. After stirring the solution for several minutes, the solvent was removed and the solid obtained in a nearly quantitative yield was analysed without further purification.

2.2.2 NMR-spectroscopy

The ^{1}H-NMR-spectra of both complexes **C8** and **C9** show symmetrical species, the C_2-symmetry of the ligand is not broken and therefore the silver(I)-complexes are still C_2-symmetric (figure 52b). The broad signals (protons 3', 7 and 9_a) in the free ligand (see figure 52a) become sharper upon complexation, indicating that the conformation of the ligand is fixed.

Compared to the published complex **C7**[60], only slight changes in the chemical shifts are observed (table 10). In complex **C8**, the signals of the protons 6' and 4' are influenced by the methoxy-phenyl group attached to 5' and show a slight difference of the chemical shift as compared to **C7**.

In complex **C9**, proton 5' nearby the methoxy-phenyl group shows a similar behaviour. Other differences can be explained by the geometry of the complex. The 6'-substituents are pointing towards the metal centre. Therewith it influences strongly the second ligand coordinated to the same centre. This phenomenon has already been observed for the analogous hexanuclear species. Furthemore, the protons of the methoxy-phenyl group are shifted to high field ($\Delta\delta$ = 0.76 ppm for 8', $\Delta\delta$ = 0.54 ppm

for 9') as compared to the free ligand (also observed in the hexanuclear species, figure 47).

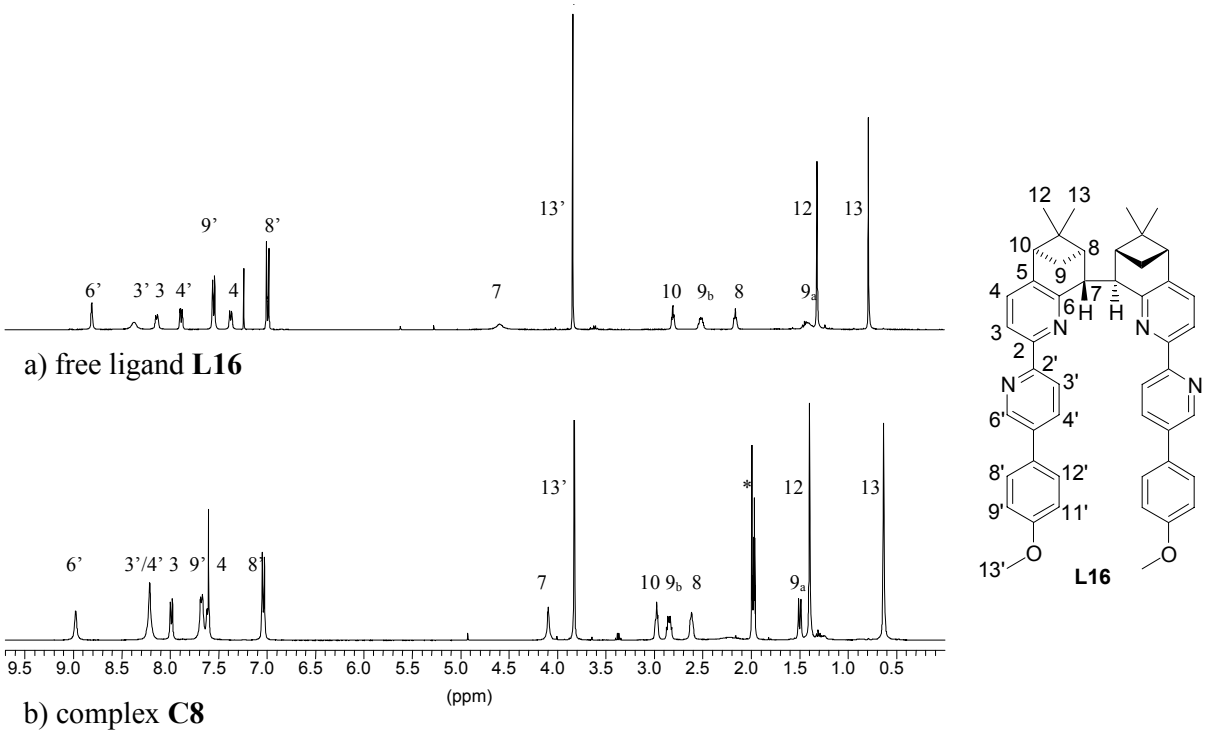

figure 52: ^{1}H-NMR of the free ligand **L16** and its complex **C8.**

	6'	5'	4'	3'	3	4	7	8	9a	9b	10	12	13
C7	8.76	7.57	8.06	8.19	7.93	7.58	3.98	2.61	1.47	2.81	2.94	1.35	0.56
C8	8.98	---	8.21	8.21	7.99	7.55	4.10	2.61	1.51	2.85	2.98	1.40	0.63
Δδ	0.22	---	0.15	0.02	0.06	-0.03	0.12	0.00	0.04	0.04	0.04	0.05	0.07
C9	---	7.79	7.95	8.16	8.15	7.52	4.08	2.6	1.46	2.81	3.01	1.39	0.65
Δδ	---	0.22	-0.11	-0.03	0.22	-0.06	0.10	-0.01	-0.01	0.00	0.07	0.04	0.09

table 10: comparison of the chemical shifts of **C7**, **C8** and **C9**.

2.2.3 ESI-mass-spectroscopy

The electrospray mass spectra of both complexes (**C8** and **C9**) is in accordance with the observations from the NMR-experiments (figure 53). For both complexes the main peak corresponds to the mononuclear species AgL^+. The isotopic pattern of these peaks are almost identical to the calculated one (figure 54).

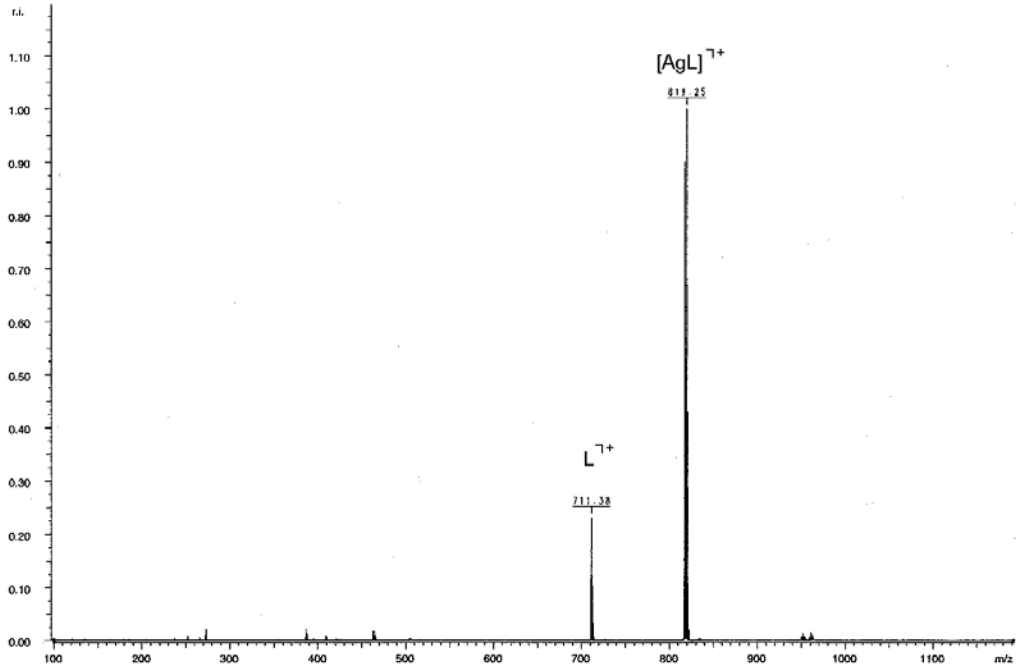

figure 53: ESI-MS of complex **C9**.

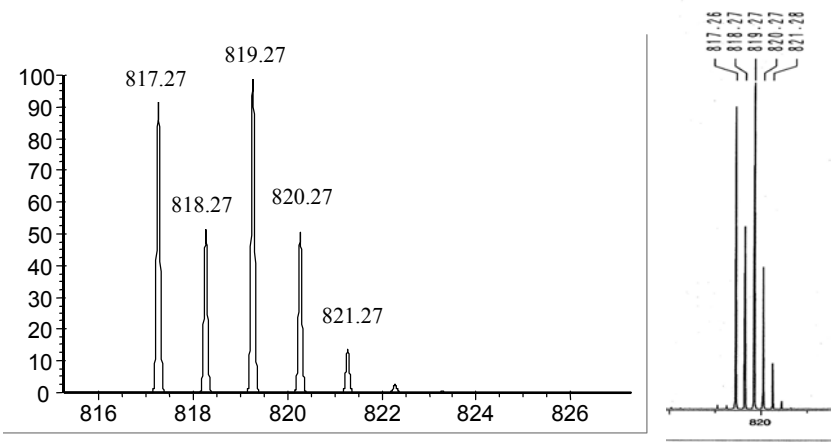

figure 54: calculated (left) and measured (right) isotopic pattern at 819.27 of C**8**.

2.2.4 UV/VIS- and CD-spectroscopy

From the CD-spectra measured in acetonitrile the absolute configuration can be attributed to *Δ* (negative effect of the exciton couplets at 337 nm, figure 55). While ligand **L16** already show intenses CD-activity (figure 42) assuming a similar structure as in the complex by π-π-stacking, complex **C9** shows a much larger CD-effect than the free ligand **L18**, which implies a conformation change. The corresponding UV-spectra are shown in figure 56.

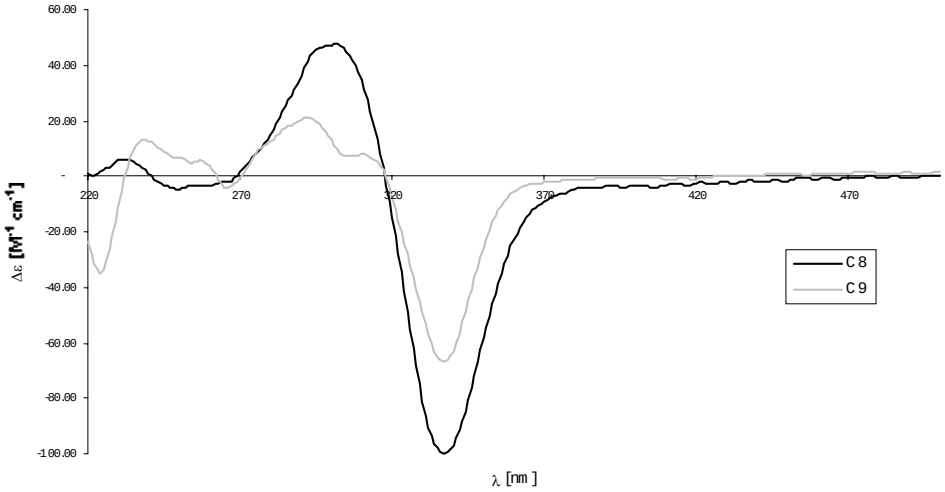

figure 55: CD-spectra of **C8** and **C9**.

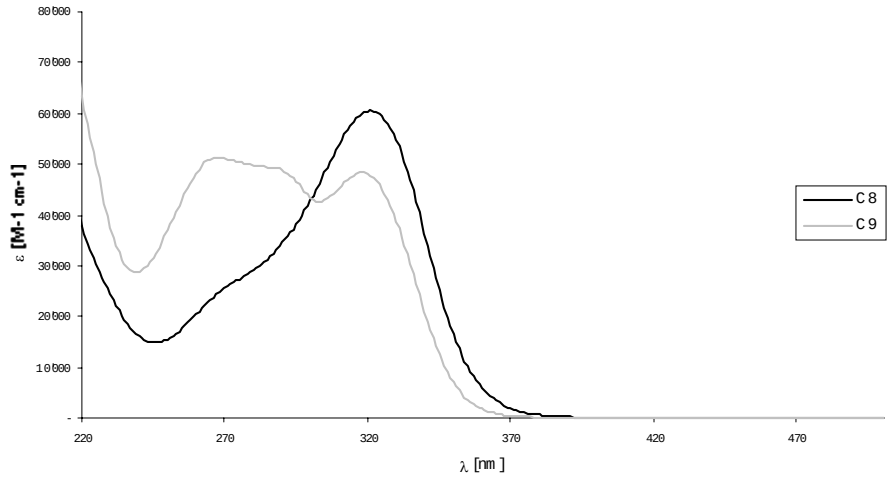

figure 56: UV/Vis spectra of **C8** and **C9**.

3. Protonation Studies

The ability of **L15** (chart 10) to form mononuclear complexes with several metal cations has been well studied in our group.[60,111] Cations such as Ag(I), Pd(II), Cu(II) and Zn(II) fit into the cavity defined by both pinene-bpy-units. Ligand **L15** wraps around the metal in a helical fashion. This was the motivation to investigate the protonation behaviour of the ligand **L15**. Can the proton, as smallest cation, act as a complexing agent and fix the conformation of the ligand? If the ligand can be fixed in one conformation, does it correspond to a helical conformation comparable to that one in metal complexes?

In order to understand the protonation behaviour of **L15**, an extended study was carried out not only for **L15,** but also for bpy, **L1**, **L19** and **L20** (chart 10).

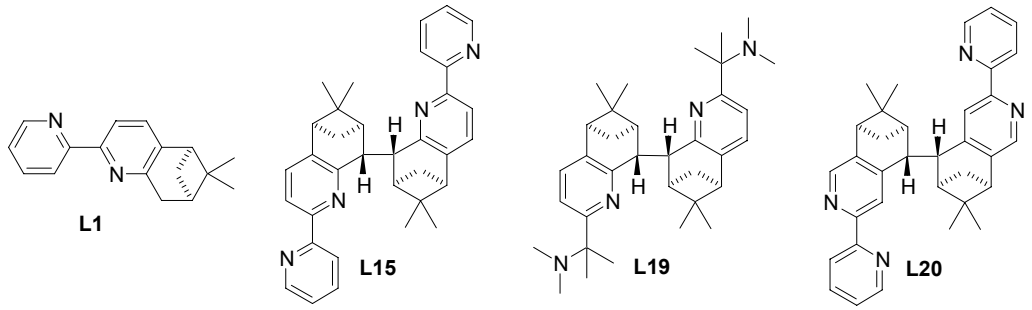

chart 10: ligands used for extended protonation studies.

Since ligand **L1** has a similar structure to bpy, similar protonation behaviour should be observed and was used as a reference for the latter ones (**L15**, **L19** and **L20)**.

L15 and **L20** have similar structures, both consist of two directly linked pinene-bpy-moieties. While in **L15** all four nitrogen donor atoms can point into the cavity and therefore can bind cations in this cavity, the nitrogen atoms in **L20** are arranged to be outside this cavity and both bpy units react independently.

L19 with its two dimethylamino-functions was designed as analogue to the proton sponge (1,8-bis-(dimethylamino)-naphthalene, scheme 7) and it should show a more pronounced basicity than the ligands containing two bipyridine moieties (**L15** and **L20**). (pK_a –values of py, bpy , trimethylamine (TMA) and the proton sponge (PS) are

pK_a(py) = 5.3;[112] pK_a(bpy) = 4.5;[113] pK_a(TMA) = 9.8[112] and pK_a(PS) = 12.4[66]).

The methods to study the protonation behaviour were spectrophotometric titration's (UV/Vis and CD-spectroscopy) and NMR-experiments. In the latter, several nuclei were the object of the observation. ^{1}H-NMR were used to gain an initial insight into the protonation behaviour. The use of NMR-inverse-detection techniques allowed the observation of other nuclei (^{13}C, ^{15}N), obtaining results in a reasonable time and with small amounts of product.

3.1. Protonation behaviour of [5,6]-pinene-bpy (L1) and bpy

First of all, [5,6]-pinene-bpy (**L1**) and bpy will be discussed. Both ligands contain two nitrogen donor atoms, which can be protonated. From bpy it is known, that the first protonation changes the conformation from *trans* to *cis*. The proton is shared between both nitrogens.[114-116] The second protonation leads again to a *trans*-conformation. The pK_a-value for the mono–protonated bpy in water is pK_a = 4.5, but varies depending on the percentage of organic solvents in aqueous solution and the ionic strength.[113,115,117-127] The UV-spectra of bpy and [5,6]-pinene-bpy (**L1**) were measured in 60% (v/v) methanol/water solution with an ionic strength of 0.1M (NaCl). Hydrochloric acid was used as proton source (figure 57). Since both ligands show similar behaviour upon protonation, only **L1** will be discussed.

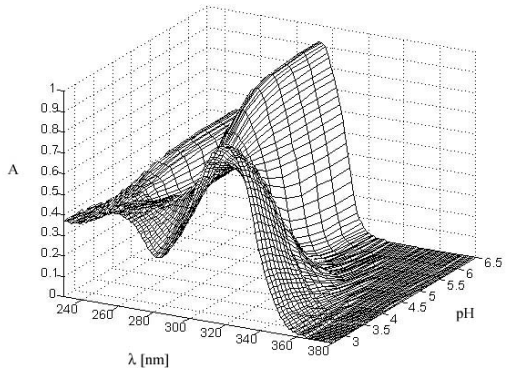

figure 57: UV/Vis spectra **L1** upon protonation.

The UV-spectrum of the free ligand **L1** shows an absorption maximum at 293 nm (figure 57). Upon protonation a bathochromic shift appears (from 293 nm to 312 nm). An analogous phenomenon was described for bpy in several publications.[114,115,127-130] The UV-spectra were recorded in a pH-range from 10 to 2, in which only mono-protonated species can be formed.[113-115] The pK_a were calculated with the programme Specfit. (pK_a = 3.9±0.1 for bpy; pK_a = 4.2±0.1 for **L1**), which is in accordance with the literature.[126]

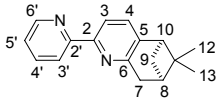

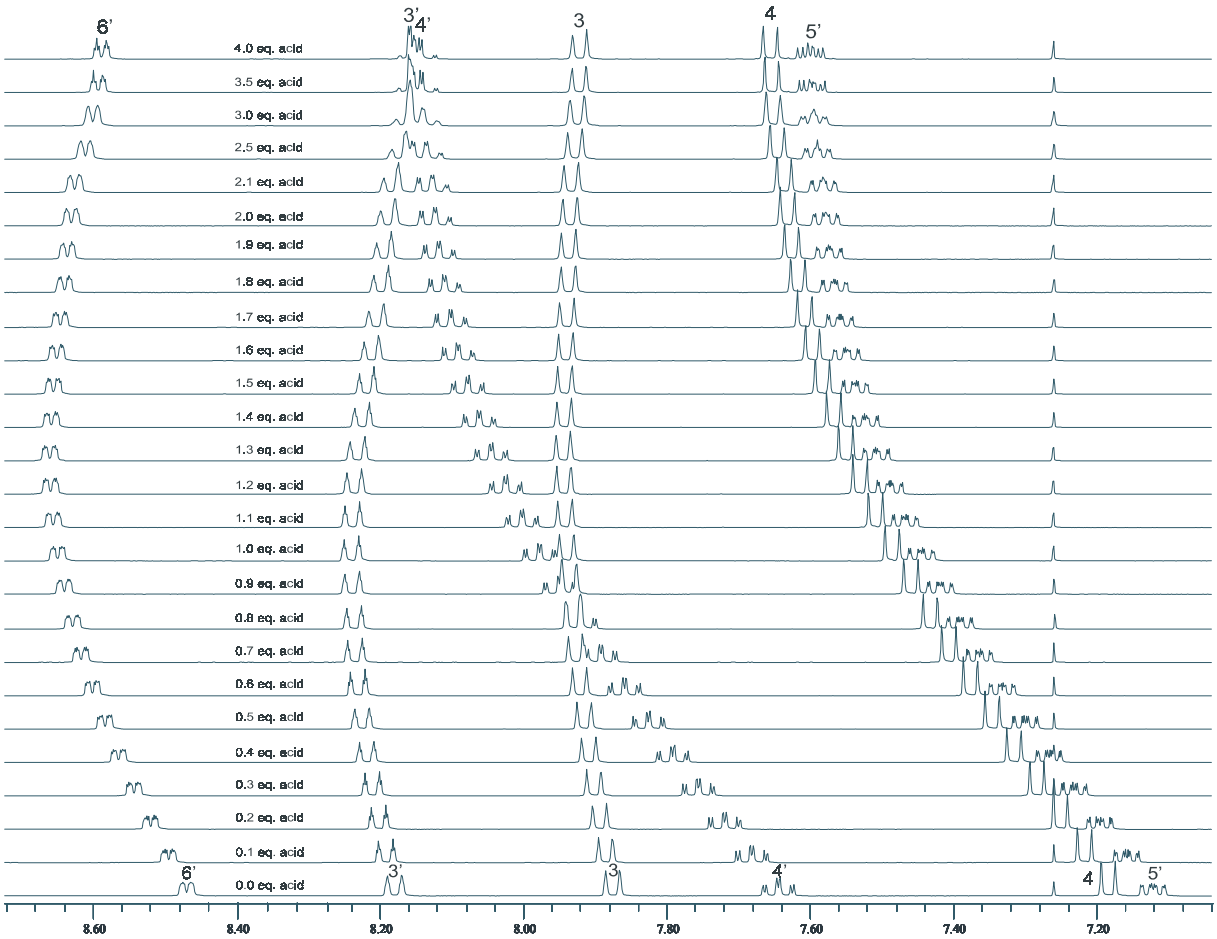

figure 58: ^{1}H-NMR-titration of **L1**.

The NMR protonation studies were carried out for **L1**. A ^{1}H-NMR-spectrum was recorded after each addition of 0.1 equivalent of the trifluoroacetic acid solution to the ligand **L1** (figure 58).

Large shifts in the spectra were observed until the addition of two equivalents of acid. Only the aromatic protons show a remarkable shift, whereas the aliphatic ones are almost uninfluenced (complete spectra shown in the Appendix). The signals of the protons in *para*-position (4, 4') with regard to the nitrogen and in *meta*-position (5') show similar downfield shifts (figure 58). Proton 6' in *ortho*-position shows a less pronounced downfield shift. The protons 3 and 3' in *meta*-positions show initially a slight downfield shift but afterwards they return to their original position.

The chemical shifts of the carbons were recorded by indirect detection (^{1}H-^{13}C-HMQC for the short range couplings $^{1}J_{C,H}$ and ^{1}H-^{13}C-HMBC for long range couplings $^{2}J_{C,H}$ to $^{4}J_{C,H}$). Knowing from the ^{1}H-NMR that only the aromatic protons show remarkable shifts upon protonation, the ^{13}C-spectra were recorded in the region from 100-170 ppm. Due to the much larger acquisition times for 2D-spectra, measurements were recorded after additions of 1.0 equivalents of the acid solutions.

All signals corresponding to carbons, which are in *para*- or in *meta*-position (3, 3', 4, 4', 5 and 5') with regard to the nitrogens showed downfield shifts upon the addition of two equivalents of acid (figure 59). Further additions of acid did not influence the chemical shifts further. Carbons in *ortho*-positions were shifted upfield (2, 2' and 6') or remained at the same chemical shifts (in case of 6).

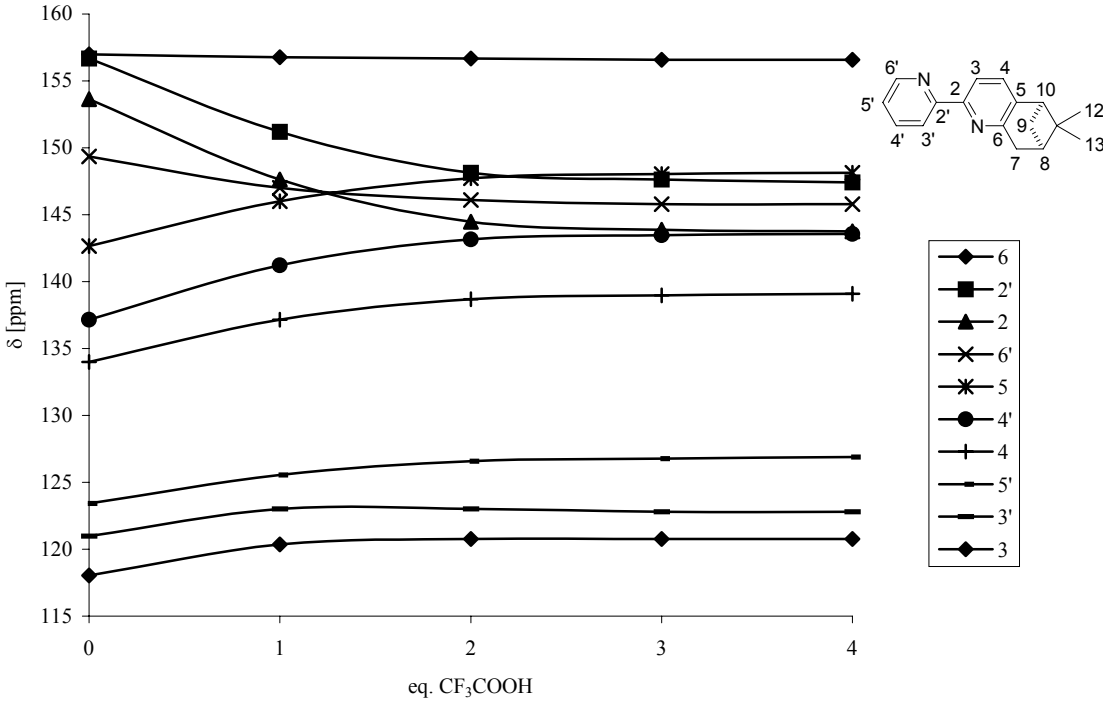

figure 59: ^{13}C-chemical shifts of **L1** upon protonation.

Finally, the most important information about protonation can be obtained by the observation of the chemical shift of ^{15}N. ^{1}H-^{15}N-HMBC were recorded either on a 700 MHz Bruker Avance DRX spectrometer[‡‡], which allowed these 2D indirect-detection experiments to be measured in a short time, or on a 400 MHz Bruker Avance DRX with the ^{15}N-labelled product ^{15}N-**L1**.

The chemical shifts of the nitrogens in the free ligand are at –77 and –72 ppm for N(A) and N(B) respectively (nitromethane used as reference). They are shifted upfield (–134 ppm) upon protonation (figure 60).

[‡‡] These measurements were carried out at Bruker Biospin in Fällanden.

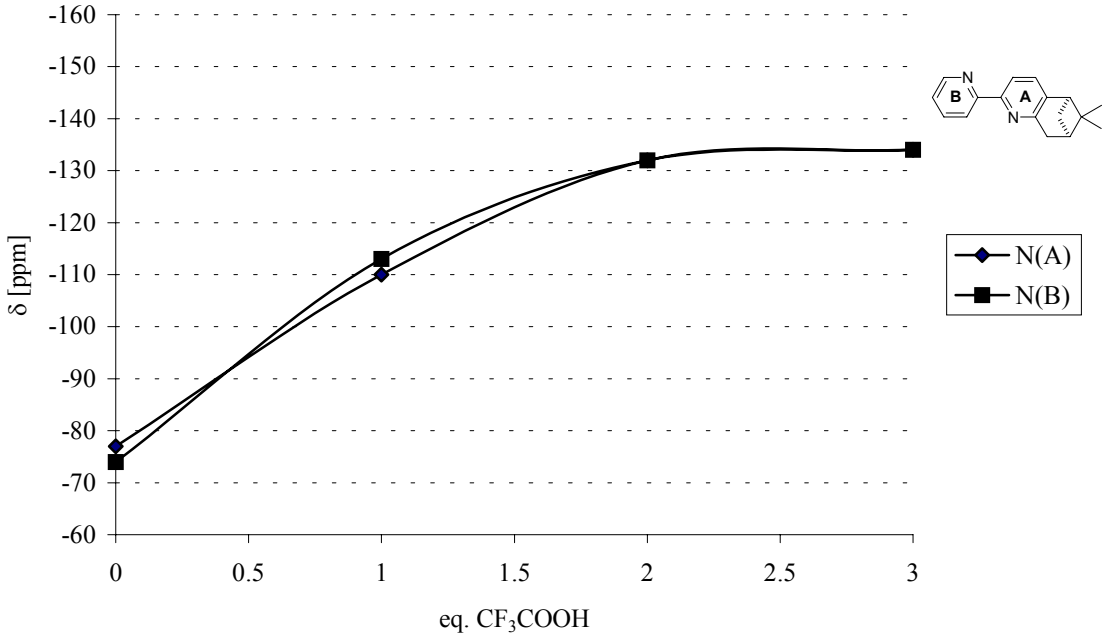

figure 60: ^{15}N-chemical shifts of **L1** upon protonation.

All these observations lead to the following conclusion: The free ligand **L1** and the mono-protonated species are in equilibrium upon protonation, as it can be seen in the UV-spectra (figure 57). The mono-protonated form is stabilised in the *cis*-conformation of the ligand by hydrogen bonding (scheme 28) and the proton is shared between both nitrogens, which is in accordance with the ^{15}N-experiments (figure 60).

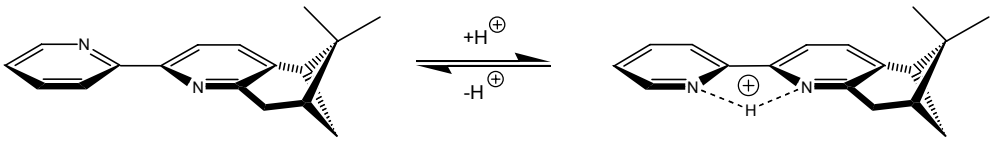

scheme 28: equilibrium between **L1** and its mono-protonated form H**L1**$^{+}$.

This is in accordance with the bathochromic shift observed in the UV-spectra. This bathochromic shift can be explained as follows. Although the free ligand is mostly in the *trans*-conformation, it can rotate around the bond between both pyridine rings. Therefore in the experimental time scale, the aromatic system is not conjugated over both rings. Upon protonation the coplanar *cis*-conformation is stabilised and π-

conjugation through both pyridine rings occurs (scheme 29).[115] Therefore the energy difference of the π-π*-transition is reduced, and a red-shift is observed.

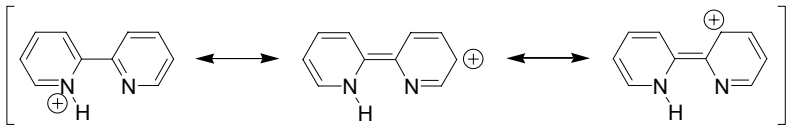

scheme 29: π-conjugation of the mono-protonated bpy.[115]

By analysing the NMR-spectra, it is not easy to determine if **L1** is protonated once or twice upon the addition of two equivalents of acid. Nevertheless, it should be taken into account, that the solvent is not water and therefore the acid/base behaviour changes. In water TFA is a strong acid (pK_a = -2), but in acetonitrile (a protophobic solvent) this behaviour changes dramatically. TFA with a pK_a of 12.65, in acetonitrile, is no longer a strong acid and it is less acidic than the protonated pyridinium cation (pK_a = 12.33).[131] In addition, TFA forms with its conjugated base a dimeric species (HA_2^-).[§§] In the solvent used in the present investigation ($CHCl_3/CH_3CN$: 3/1) the acid strength of TFA is probably even lower. Therefore, the protonation of **L1** follows the equilibrium:

This is in agreement with all NMR-titrations, where always two equivalents of TFA were needed to reach the mono-protonated species.

The conclusion with a mono-protonated species in a *cis*-conformation is in line with the ^{15}N-NMR-spectra. The identical chemical shift of both nitrogen atoms is consistent with a sharing of the proton between them (scheme 30).

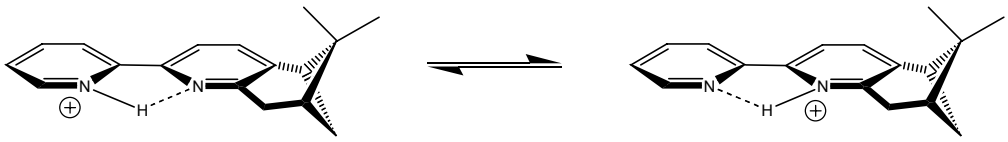

scheme 30: sharing of the proton between both nitrogen donor atoms in **L1**.

[§§] Equilibrium constant of the dimerisation in acetonitrile is $\log K^f(HA_2^-) = 3.88$.[131]

From the ^{1}H-NMR-spectra it can be seen, that the protons in *meta* (5')- and *para* (4, 4')-positions are influenced strongly upon protonation, whereas proton 6' undergoes only a slight downfield shift (figure 58). This is in accordance with the chemical shifts observed for pyridine and its protonated form. [132] The exceptions are represented by proton 3 and 3'. The expected downfield shift upon protonation is cancelled by other effects. The conformational change can be a explanation, since 3' and 3 are influenced by each other in the *cis*-conformation.
In the ^{13}C-spectra, the carbons in *meta*- and *para*-position are shifted to low field, these in *ortho*-position to high field (figure 59). This is as well in accordance with observations for pyridine and the pyridinium cation. [133]

3.2. Protonation behaviour of [4,5]-CHIRAGEN[0] (L20)

Ligand **L20** represents an analogous case to the [5,6]-pinene-bpy (**L1**), which consists of two [4,5]-pinene-bpy moieties linked directly together. The four nitrogen donor atoms of both bpy-units are orientated in such a way, that the formation of mononuclear complexes is inhibited (chart 10, p.78). The protonation behaviour is expected to be similar to that of the [5,6]-pinene-bpy (**L1**). No intramolecular proton transfer between the two bpy units can take place and therefore each bpy-unit will be independently protonated. In addition to the techniques (UV/Vis and NMR-spectroscopy) used for [5,6]-pinene-bpy (**L1**), CD-spectroscopy was performed to study the protonation behaviour.
The spectrophotometric titration's were carried out under the same conditions as those described for the [5,6]-pinene-bpy (**L1**). Only the solvent mixture was changed to methanol/water (90% v/v) because of solubility reasons. The UV-spectra (figure 61) show a bathochromic shift from 288 nm for the free ligand to 312 nm in the protonated species. In the pH-range of 10 to 1.5, **L20** can be protonated twice.

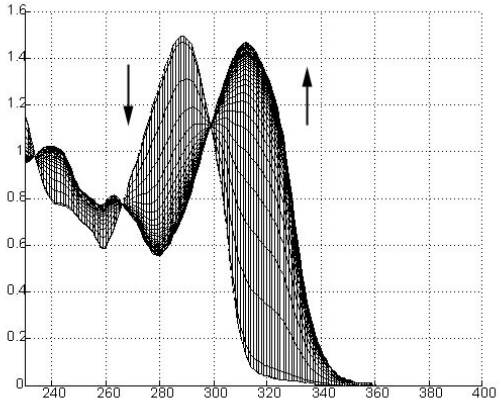

figure 61: UV-spectra of the free ligand **L20** and its protonated species. The arrows indicate spectral changes upon protonation.

The CD-spectra of **L20** show as well an analogous bathochromic shift (from 295 for the free ligand to 324 nm for the protonated species). The nature and the intensity of the CD-signals do not change upon protonation.

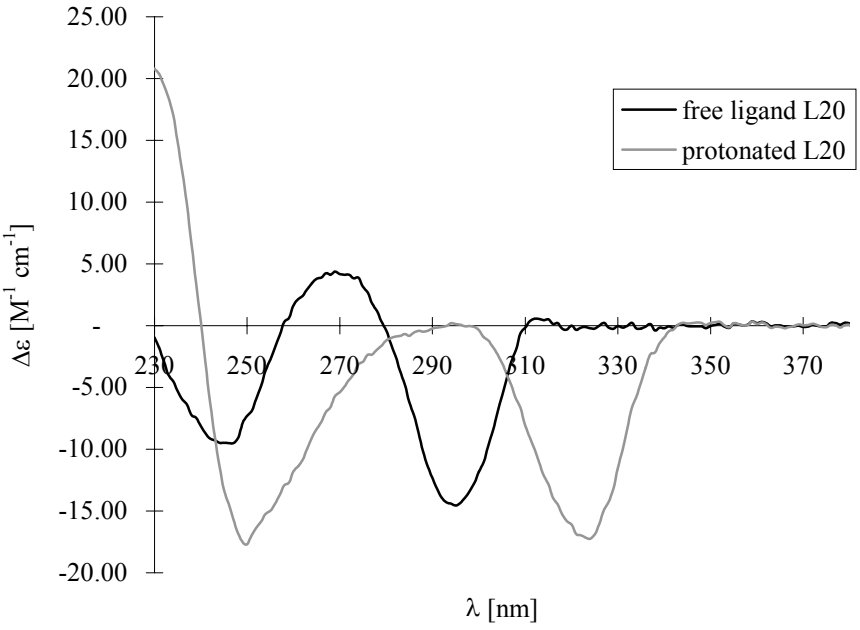

figure 62: CD-spectra of the free ligand **L20** and its protonated species.

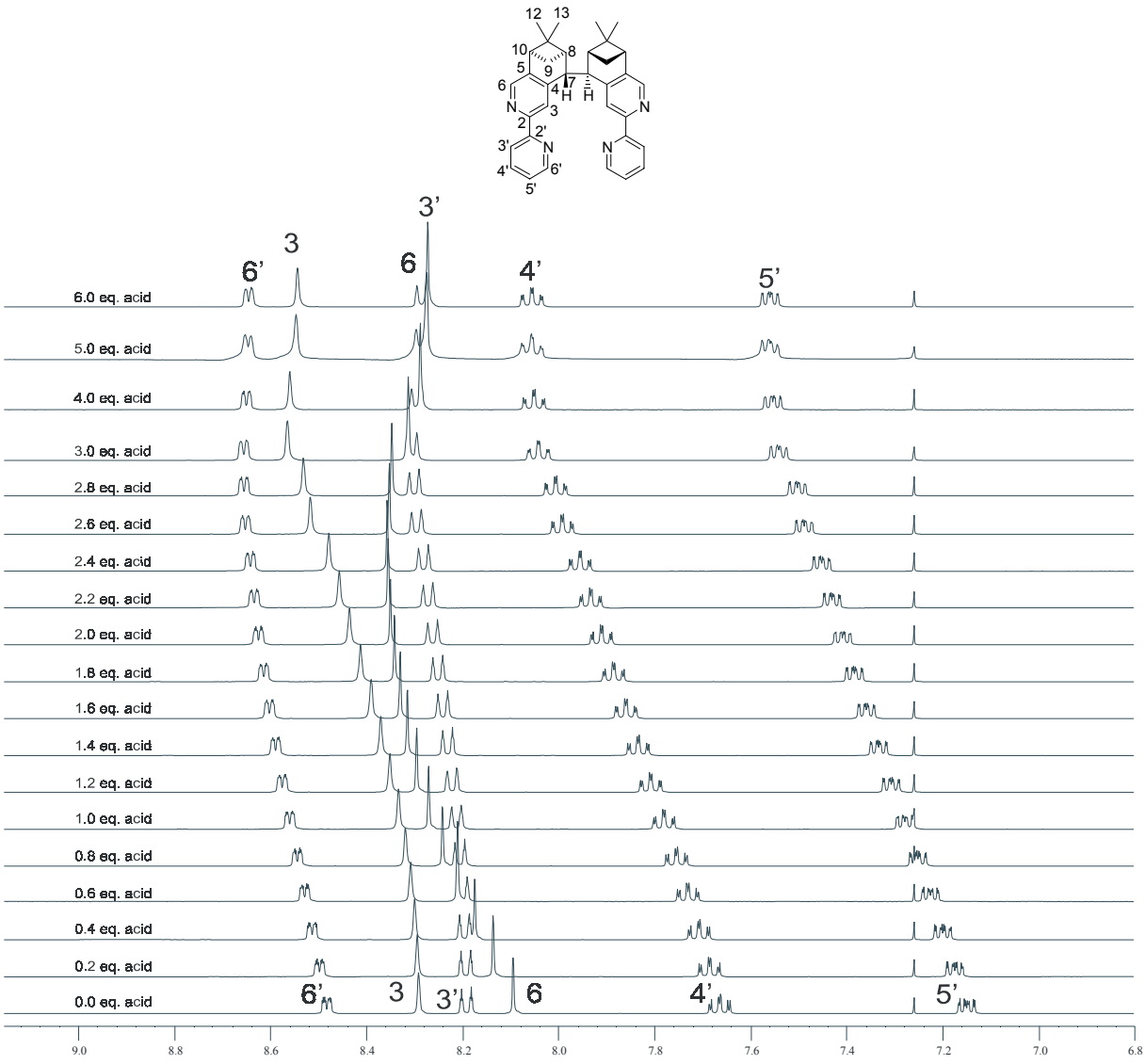

figure 63: ^{1}H-NMR-titration of **L20**.

The ^{1}H-NMR-titrations were carried out in the same manner as for [5,6]-pinene-bpy (**L1**). After each addition of the acid solution which corresponds to 0.2 equivalents, a ^{1}H-NMR-spectrum was recorded (figure 63). After 3 equivalents, the addition were made in 1.0 equivalent steps.

The ^{1}H-NMR-spectra do not show any doubling of the signals, ligand **L20** keeps its C_2-symmetry upon protonation due to the fast proton exchange between both bpy units on the NMR time scale. Large changes in the spectra can be observed upon the addition of 4-5 equivalents of acid (figure 64), mostly in the aromatic part (complete spectra shown in the Appendix). The proton in *para*-position (4', $\Delta\delta$ = 0.39 ppm) and in *meta*-position (5', $\Delta\delta$ = 0.40 ppm) are shifted downfield upon protonation. The

protons in *ortho*-position (6, Δδ = 0.19 ppm; 6', Δδ = 0.17 ppm) show a less pronounced downfield shift, but proton 6 is more influenced upon protonation (firstly, to lowfield and then back to highfield). Proton 3' (*meta*-position) remains at the same chemical shift (Δδ = 0.11 ppm), whereas 3 is slightly shifted to low field (Δδ = 0.27 ppm). The proton at the bridge (7) show a slight high field shift upon protonation (Δδ = 0.28 ppm, cf. Appendix).

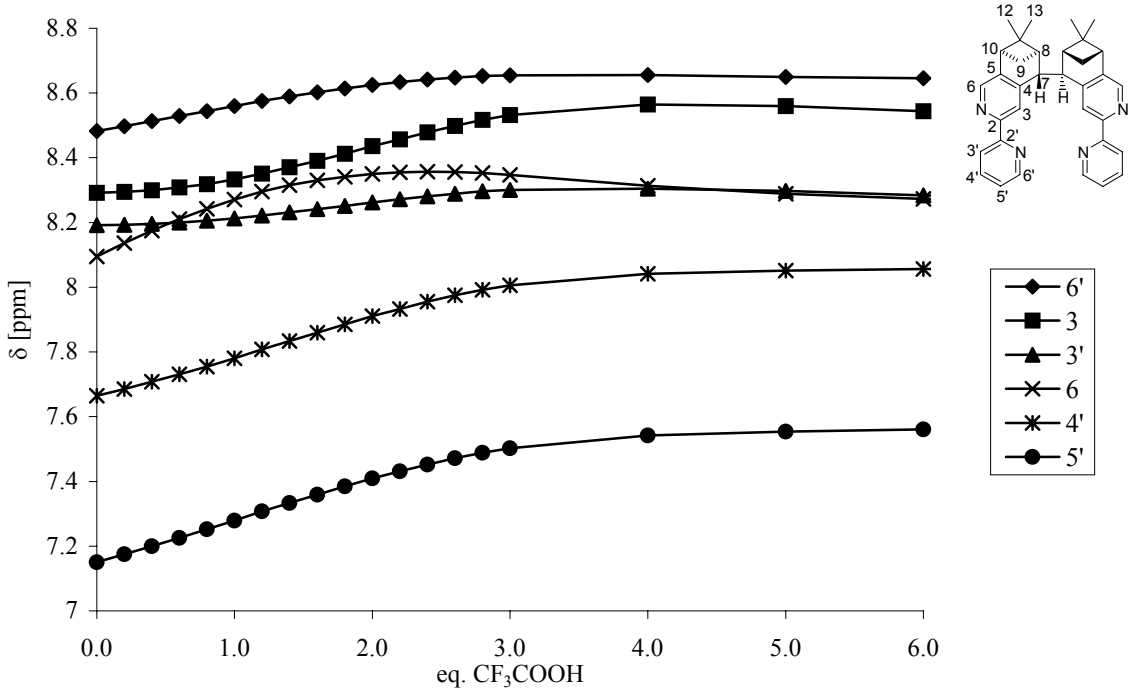

figure 64: ^{1}H-chemical shifts of **L20** upon protonation.

The inverse detected ^{13}C-experiments reveal, that all carbons in *meta*- and *para*-position are shifted to lowfield, the carbons in the *ortho*-postion are shifted highfield. Carbons 6' show a less pronounced highfield shift as compared to the other ones (figure 65).

From the ^{1}H-^{15}N-HMBC-experiment, the chemical shifts of the nitrogens can be determined (figure 66). Both nitrogens of the two bpy-moieties show a large shift to high field. The nitrogen N(A) (up to –158 ppm) is more influenced than N(B) (up to –112 ppm).

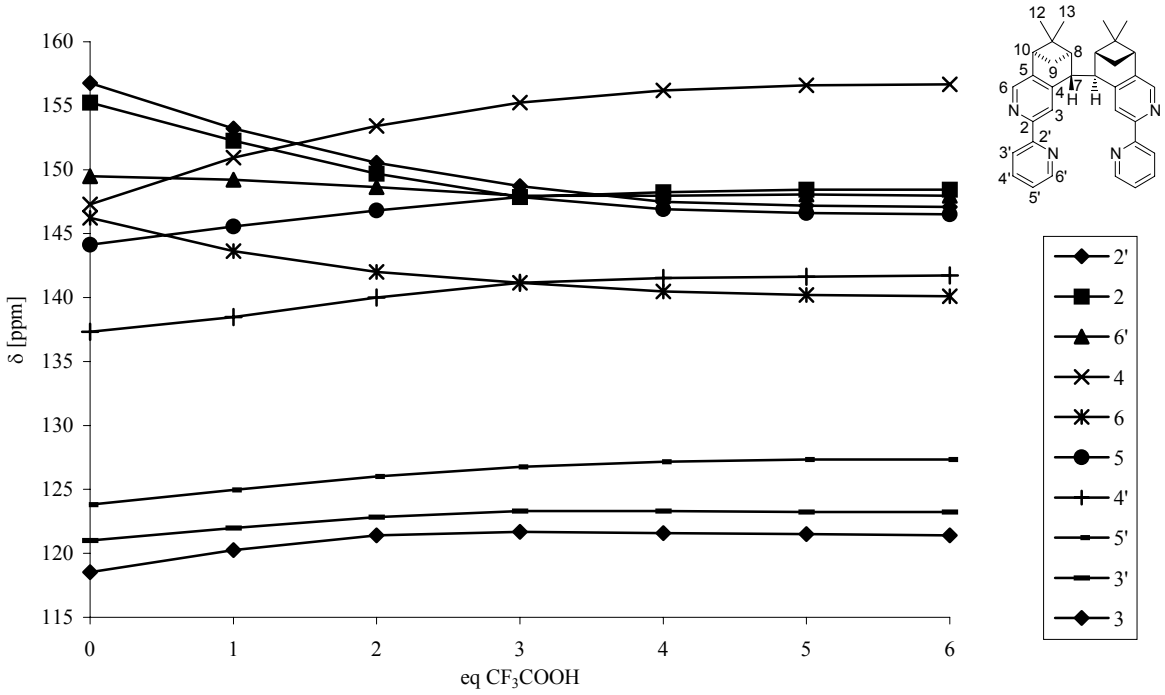

figure 65: ^{13}C-chemical shifts of **L20** upon protonation.

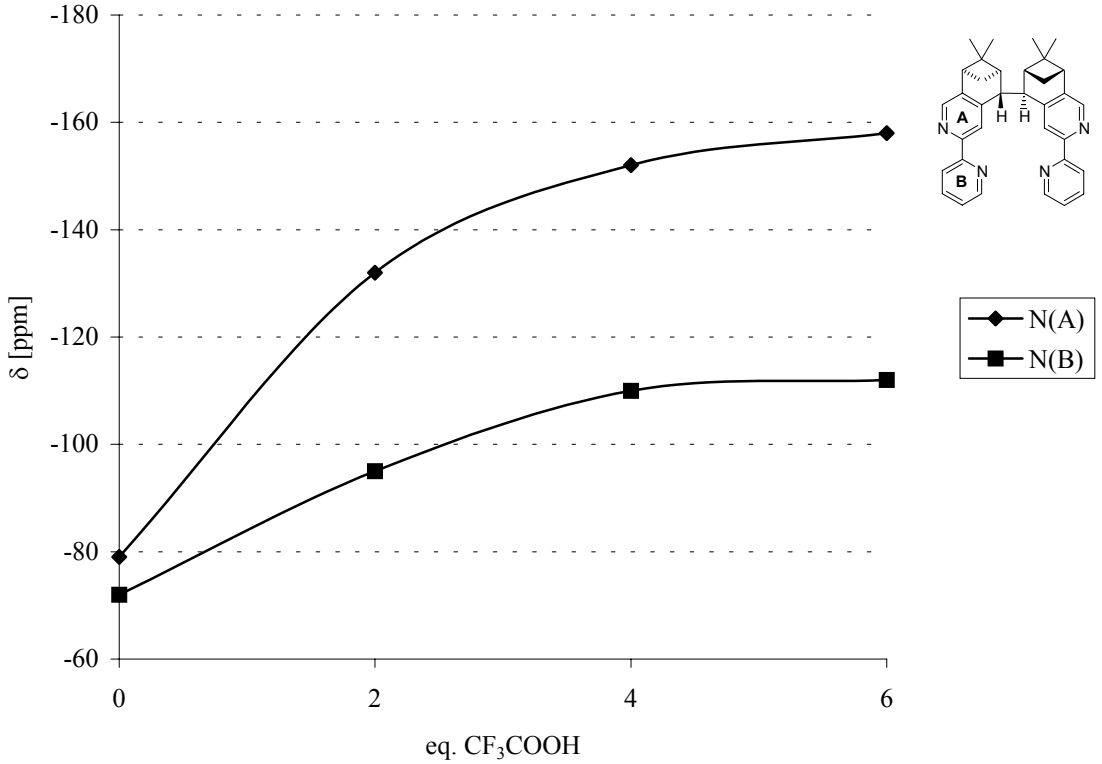

figure 66: ^{15}N-chemical shifts of **L20** upon protonation.

All these observations lead to the following conclusion: Upon protonation, the free ligand and the diprotonated species are in equilibrium. Both bpy units of the diprotonated species are in the *cis*-conformation. This protonation takes place via several other equilibria, where mono-protonated species can be present (scheme 31).

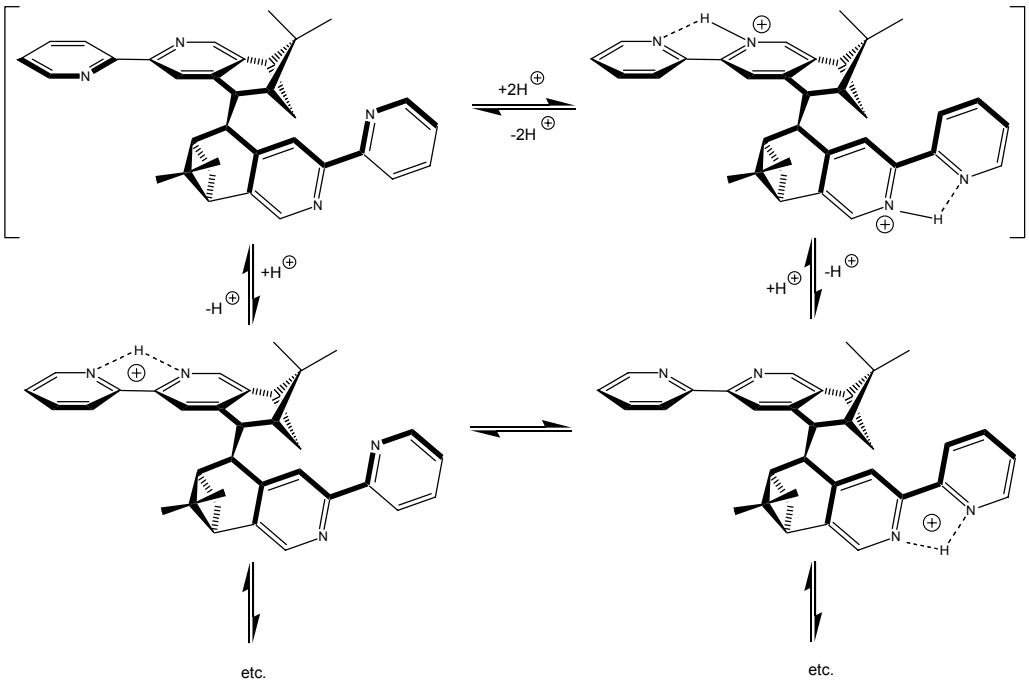

scheme 31: equilibria between **L20** and its protonated forms.

This is in accordance with the UV/Vis- (figure 61) and CD-measurements (figure 62), where no intermediate spectrum can be attributed to a mono-protonated form. The bathochromic shift in the UV-spectra (figure 61) and also in the CD-spectra (figure 62) can be explained by the *cis*-conformation of both bpy-moieties (analogous to [5,6]-pinene-bpy (**L1**), figure 57). The protonated ligand retains in a similar conformation as the free ligand (open form), since the intensity and the nature of the CD-signal does not change. If **L20** did change the conformation, which is comparable to metal complexes described with **L15** [60,111] a similar large CD-signal should appear, due to a strong exciton coupling.

The information obtained from the NMR-experiments supports the conclusion. As in the previous case (**L1**), twice the number of acid equivalents are needed, due to the formation of the relatively stable dimer:

$$4\ HA + \mathbf{L20} \rightleftharpoons H_2\mathbf{L20}^{2\oplus} + 2\ H(A)_2^{\ominus}$$

The ^{15}N-experiments indicate that the acidic proton is favourably located on the nitrogen N(A) (larger shift to high field, figure 66). But a sharing of the proton between the nitrogens N(A) and N(B) can be taken into account. (scheme 32).
This is in agreement with the ^{1}H-NMR, where the protons 3 and 6 show a more pronounced shift compared to 3' and 6'.

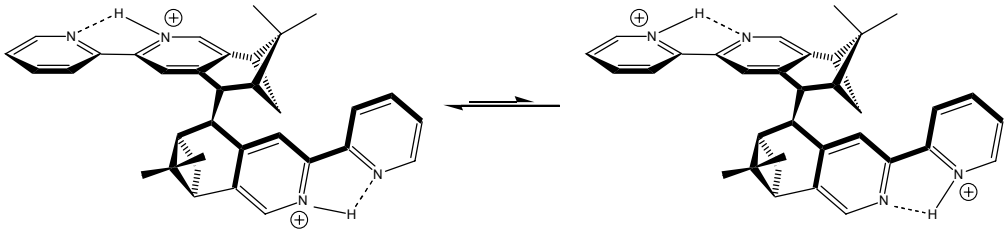

scheme 32: equilibrium of two diprotonated species.

The similarities of the proton and carbon-spectra for **L20** and **L1** support the model, where each bpy unit is independently mono-protonated. No intramolecular proton exchange between both bpy units of **L20** is observed.

3.3. Protonation behaviour of [5,6]-CHIRAGEN[0] (L15)

L15 is the most interesting case of all three pinene-bpy derivatives. Its geometry allows a proton exchange between both bpy-moieties and therefore a particular protonation behaviour is expected.
L15 is the least soluble of all pinene-bpy derivatives. In the solvent mixture used for **L1** and bpy (methanol/water 60% v/v), it was impossible to dissolve **L15**. The solvent mixture used for UV/Vis and CD-titration was methanol/water (90% v/v). But also for NMR-measurements solubility problems occurred. The free ligand is only soluble in chloroform, the protonated species in acetonitrile. A solvent mixture ($CDCl_3$, CD_3CN; 3:1) was finally used for these NMR-investigations.

In spectrophotometric titrations, two different protonation steps could be observed. In the UV-titration (figure 67), a hypochromic effect appears upon the first protonation, but with the addition of more acid a bathochromic effect leads to the final spectrum. All these spectra were fitted with the programme Specfit and the pK_a values were calculated (pK_{a1} = 8.2±0.1, pK_{a2} = 2.5±0.1 (methanol/water 90% v/v).

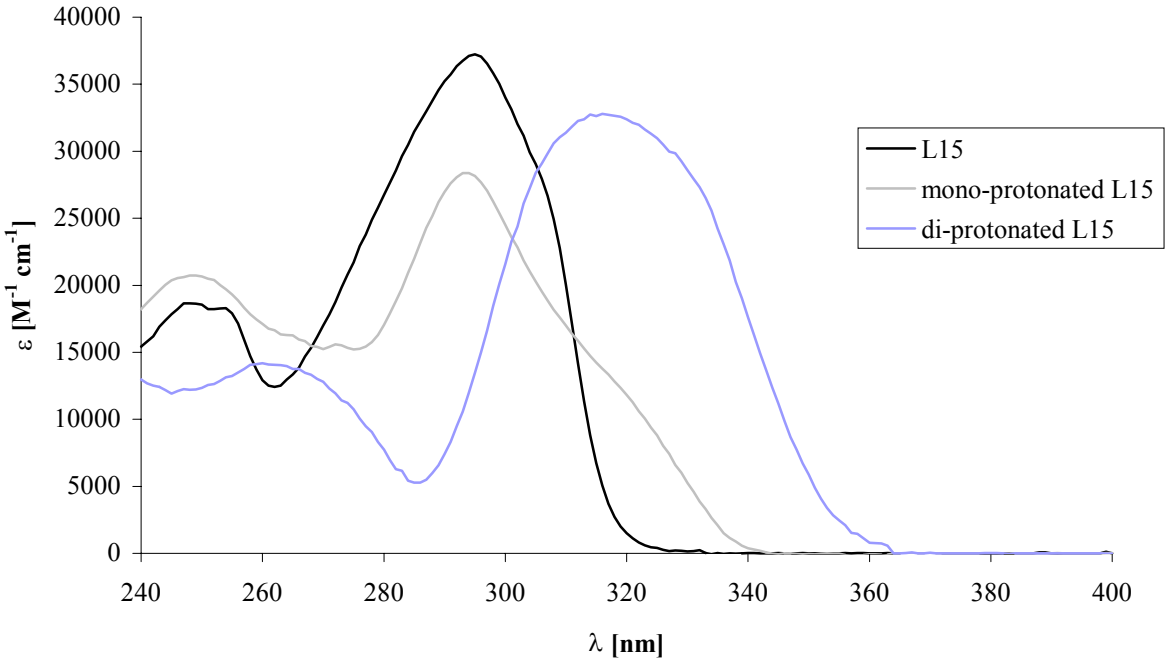

figure 67: UV-spectra of the **L15** and its mono- and diprotonated species. The arrows indicate spectral changes upon protonation.

An interesting effect was observed in the CD-spectra (figure 68). While the free ligand shows only slight CD-activity, a large intensity increase is observed upon protonation.

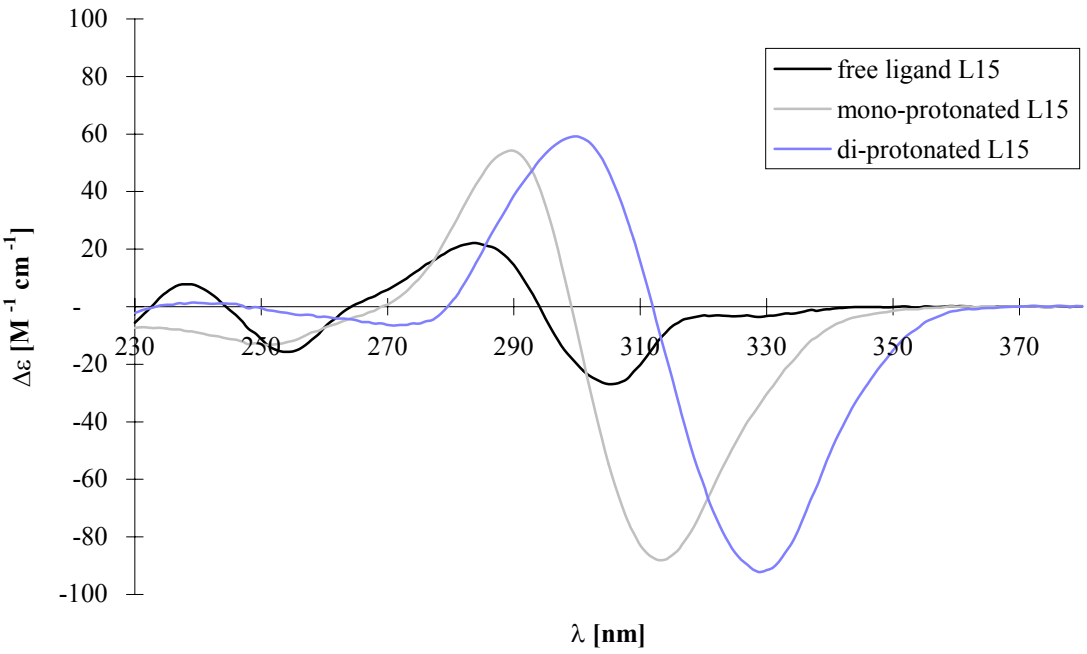

figure 68: CD-spectra of **L15** and its mono- and di-protonated species.

The second protonation leads to the bathochromic shift, which was already observed in the UV-spectra. The CD-signal does not change its intensity upon the second protonation. Analogous UV- and CD-spectra were observed for the same solvent mixture and acid (TFA) used in the NMR-spectroscopy.

The ^{1}H-NMR-titrations (and all other NMR-experiments) were carried out in the same manner as described previously. The ^{1}H-NMR-spectra (figure 69) do not show a doubling of the signals. Ligand **L15** keeps its C_2-symmetry upon protonation due to the fast proton exchange between both bpy-moieties on the NMR time scale. Two opposite trends are observable in the ^{1}H-NMR-titrations (figure 69). Up to the addition of two equivalents, most of the proton signals are shifted upfield. An opposite effect leads to a low field shift of these protons by adding six equivalents of acid. These protons are 6', 5', 4', 3' and 7. Proton 4 shows the opposite shift (first to low field and then back to high field). The broad signals of the protons 3', 7 and 9_a in the free ligand sharpens upon protonation (complete spectra shown in the Appendix).

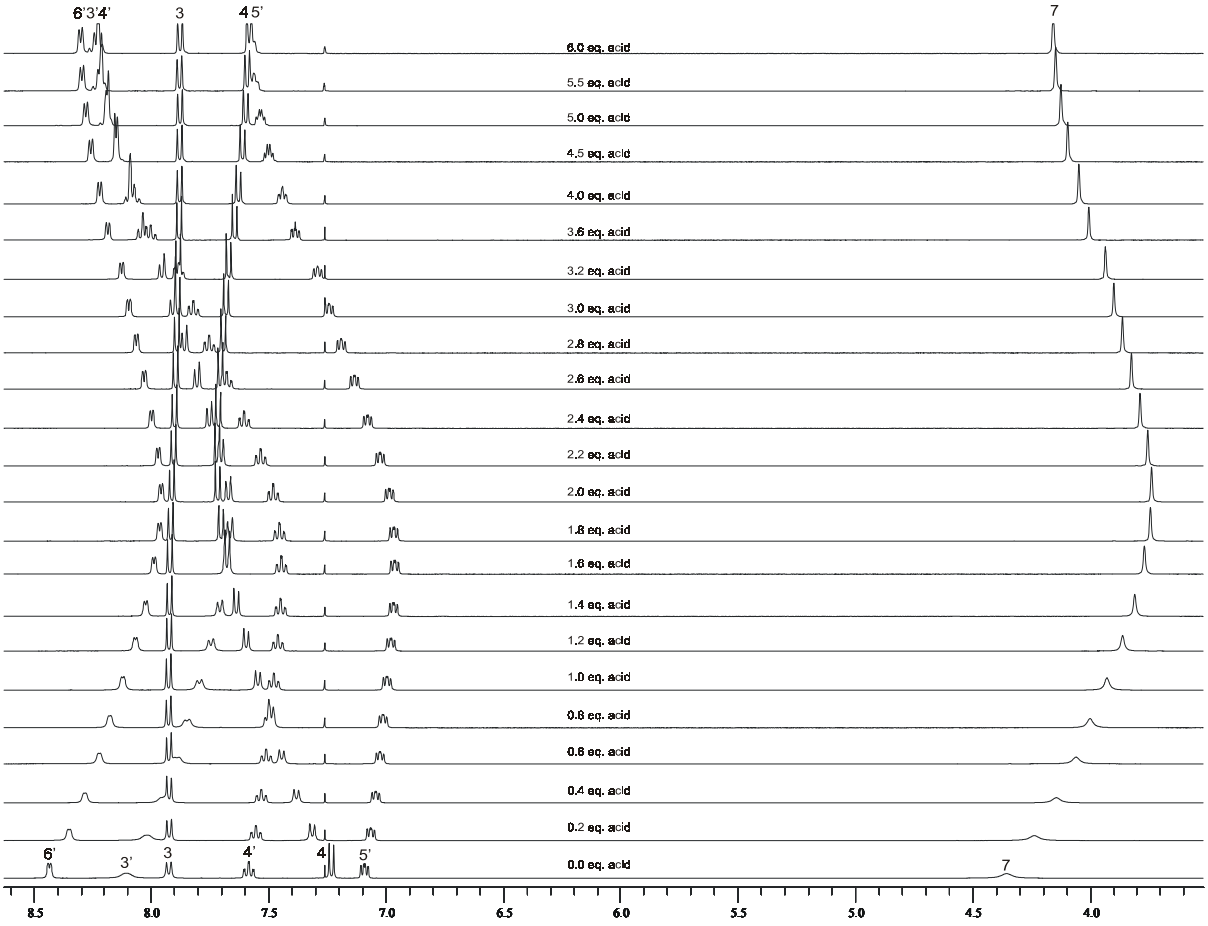

figure 69: ^{1}H-NMR-titration of **L15**.

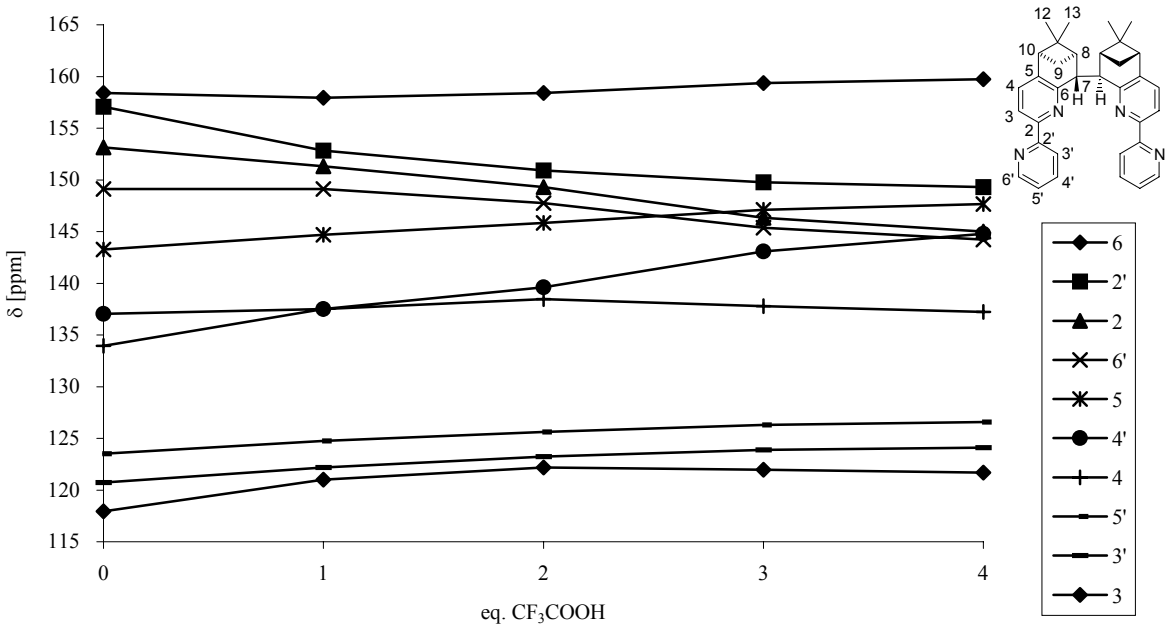

figure 70: ^{13}C-chemical shifts of **L15** upon protonation.

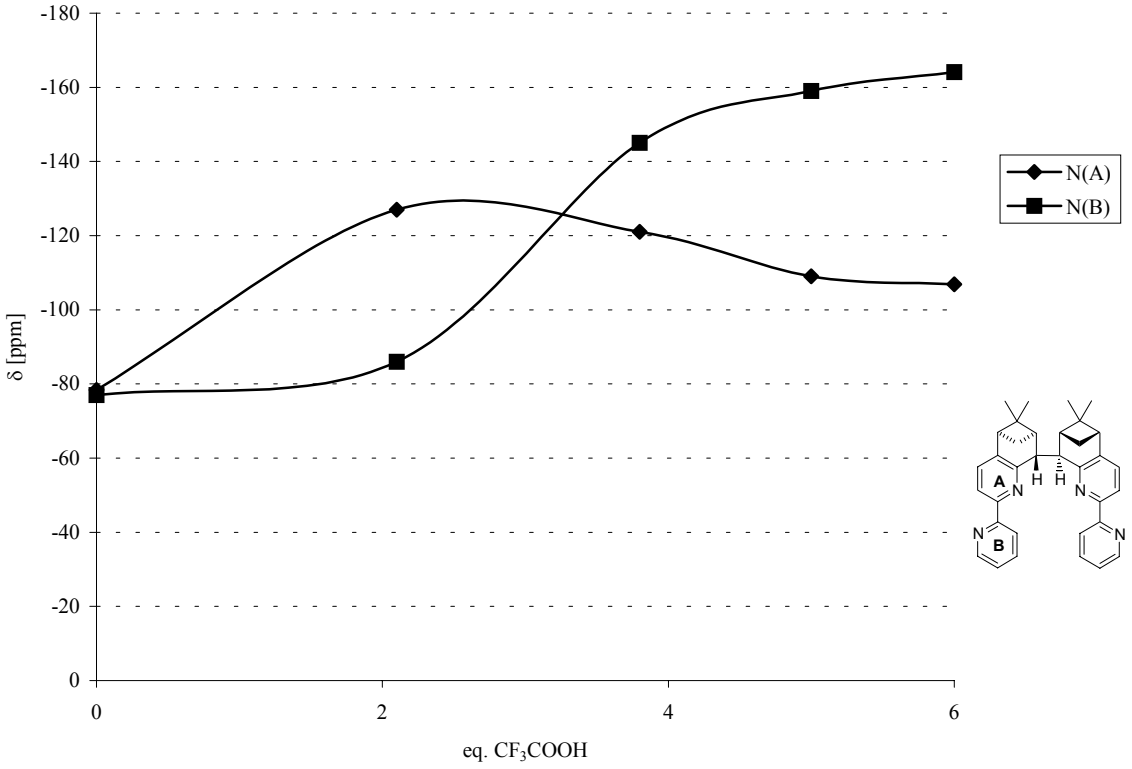

figure 71: ^{15}N-chemical shifts of **L15** upon protonation.

The most important and significant experiments were again the indirect detected ^{1}H-^{15}N-HMBC-experiments (figure 71). The two nitrogen atoms N(A) and N(B) show quite different behaviour. While the signal of the nitrogen N(A) is first shifted to highfield (-125 ppm) the second signal corresponding to N(B) is not influenced upon the first protonation.

The opposite effect occurs in the second protonation step. N(B) is shifted dramatically to highfield ($\Delta\delta$ = -164 ppm), whereas N(A) is slightly shifted back to low field ($\Delta\delta$ = -107 ppm).

All these observations lead to the following conclusions: The first protonation leads to a change of the conformation of the ligand (closed form). The second protonation does not influence this closed conformation, but leads to the *cis*-conformer of both bpy units (scheme 33).

This is consistent with the UV-spectra (figure 67). The first protonation leads only to a slight hypochromic effect. The pyridine rings B can still freely rotate and therefore no π-conjugation over both pyridine rings of each bpy unit is taking place. The large

change in the CD-activity upon the first protonation is due to a strong exciton coupling (figure 68). Similarly, this exciton coupling is observed in the metal complexes with **L15**, where the cation is fixed in the cavity of the ligand. The proton is therefore able to play a similar role, as the metals.

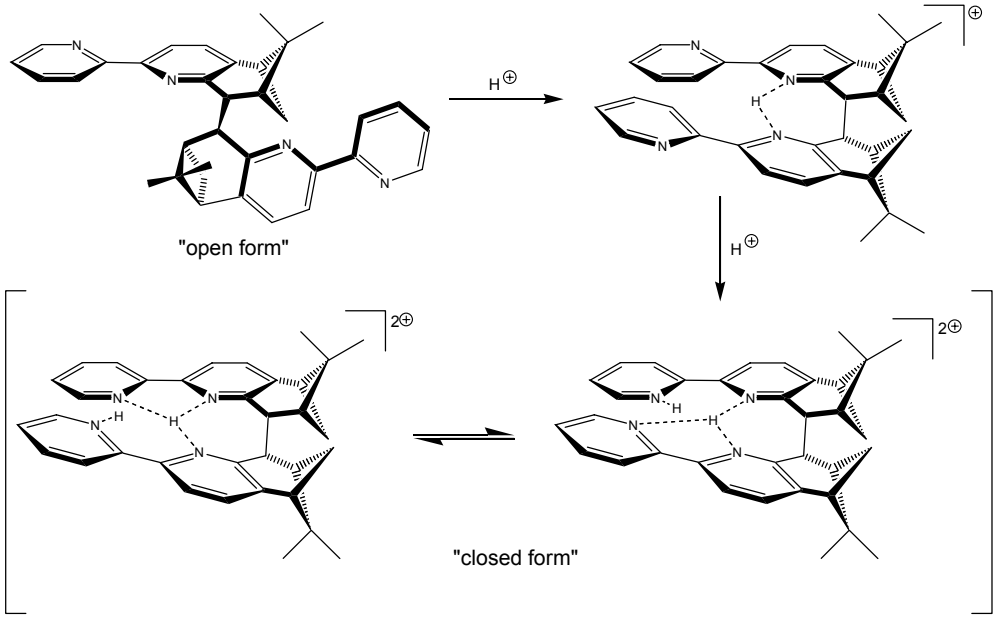

scheme 33: conformation change of **L15** upon protonation.

In contrast to the metal complexes, where the cations are bound to all four nitrogen donor atoms, the proton is only bound to the two N(A) nitrogen atoms near to the bridge. This can be explained by the large chemical shift of N(A) in the ^{15}N-experiment, whereas N(B) is not influenced by this proton. Both nitrogen atoms N(A) share the proton.

^{1}H-NMR-spectra are in accordance with the explanation described above (figure 69). Protons 4 and 3, attached to the pyridine ring (A), where the first protonation occurs, show comparable influences as these of the previously studied ligands **L1** and **L20**. Proton 4 is shifted lowfield (cf. proton 4 of **L1** in figure, and proton 4 of **L20** in figure), whereas proton 3 remains unchanged. The protons of the unprotonated pyridine rings are shifted to highfield, which can be explained by the conformation change to the closed form. Another indication for a fixed conformation is given by the protons 3', 7 and 9_a. All these signals are broad in the free ligand and give sharp signals upon protonation.

The second protonation leads to the *cis*-conformation of the bpy moieties (bathochromic shift in the UV- (figure 67) and CD-spectra (figure 68)). The bpy-moieties are now conjugated through both pyridine rings in a similar way as already seen in **L1** (figure 57) and **L20** (figure 61). The conservation of the large CD-intensity can be explained by an analogous conformation as in the mono-protonated species. Despite of an expected strong electronic repulsion of the two positive charges in the cavity, no reopening of the ligand occurs. One reason could be the distribution of the positive charges by π-conjugation (scheme 29).

The ^{15}N-chemical shifts show a strong highfield shift of N(B) upon the second protonation. The slight shift to low field of N(A) can be explained by a small participation of N(B) at the proton mainly bound to N(A). This is another reason for the *cis*-conformation of the bpy-moieties (scheme 33).

A second proton distribution **II** can be taken into account, where the two protons are bound in the cavity (scheme 34).

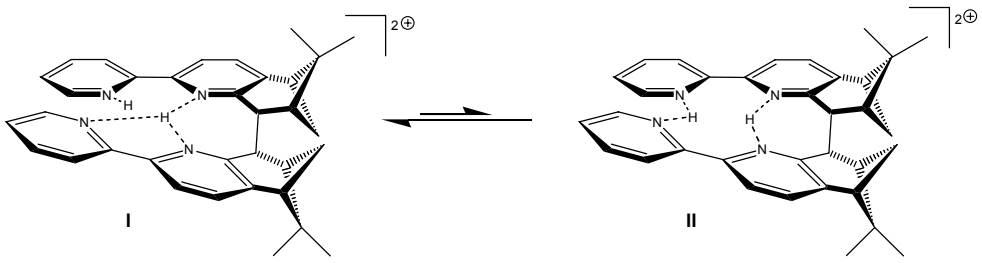

scheme 34: two possible proton distribution in the closed form of **L15**.

This distribution **II** would lead to a sharing of the two protons over all four nitrogen atoms (the same chemical shift of N(A) and N(B) is expected (table 11). From the chemical shifts observed in ^{15}N-experiments, the following distribution of the two protons can be assumed (table 11), which is in line with the proposed one (**I**).

The protons of the pyridine ring B (3', 4', 5' and 6') are downfield shifted upon the second protonation (figure 69). This is in accordance with the ^{15}N-experiments, where nitrogen B is strongly downfield shifted (figure 71). The protons in ligand **L1** (figure 58) and **L20** (**figure 63**) behave in a similar way. Proton 4 is slightly shifted back to high field (figure 69), which is in line with the chemical shift of nitrogen N(A)(figure 71).

I		II	
N(A)1: 0.4	N(A)2: 0.4	N(A)1: 0.5	N(A)2: 0.5
N(B)1: 1.0	N(B)2: 0.2	N(B)1: 0.5	N(B)2: 0.5

table 11: estimated distribution of the two proton.

3.4. Protonation behaviour of {2-DAMI}-[5,6]-CHIRAGEN[0] (L19)

L19 was designed as a combination of the previously described [5,6]-CHIRAGEN[0] (**L19**) and the proton sponge (1,8-bis-(dimethylamino)-naphthalene, scheme 35). The skeleton of the [5,6]-CHIRAGEN[0] is represented in the pinene-py-units and the dimethylamino-function should provide a higher basicity.

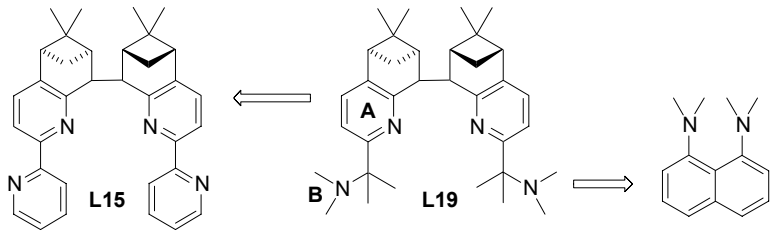

scheme 35: L19 as combination of **L15** and the proton sponge.

While the CHIRAGEN[0] derivatives (such as **L15** and **L20**) consist of two chromophors (bpy-units), which lead to exciton couplings in the CD-spectra, no information about the conformation can be obtained for **L19** from UV- and CD-spectroscopy, because of the lack of suitable π-π*-transitions. Therefore only NMR-studies gave some information about the protonation behaviour of **L19**.

The NMR-titrations were recorded in the same manner as for the other ligands. Due to even lower solubility, the solvent mixture was changed ($CDCl_3$/ CD_3CN : 5/1).

In the ^{1}H-NMR-titration, not only the aromatic protons are shifted, but also the aliphatic ones show some changes upon protonation. In the aromatic part two trends are observable. Both protons (3 and 4) are shifted downfield upon the addition of two equivalents of acid (figure 72). Then proton 3 is shifted back to high field, whereas proton 4 is still shifted downfield. The protons 7 and 9_a are broad in the free ligand and

sharpen at the addition of around 4 acid equivalents (figure 73). The other aliphatic protons of the pinene system are not significantly shifted upon addition of acid. The methyl groups attached to N(B) and to carbon 2' show large changes upon protonation. The methyl groups at N(B) show a sharp singlet at 2.07 ppm in the free ligand. This signal is shifted to lowfield and is split after the addition of almost two equivalents of acid, indicating the fixing of the nitrogen inversion. The splitting can be attributed to the diastereotopicity of the methyl groups at the protonated aliphatic nitrogen. No significant change is observed afterwards. Two broad signals were observed for the other two methyl groups (at C(2')). By adding acid, these signals merge to a broad singlet, which is shifted to lowfield. After addition of two equivalents no further changes of the chemical shifts is observed, but they split into two sharp singlets at about four equivalents (figure 73).

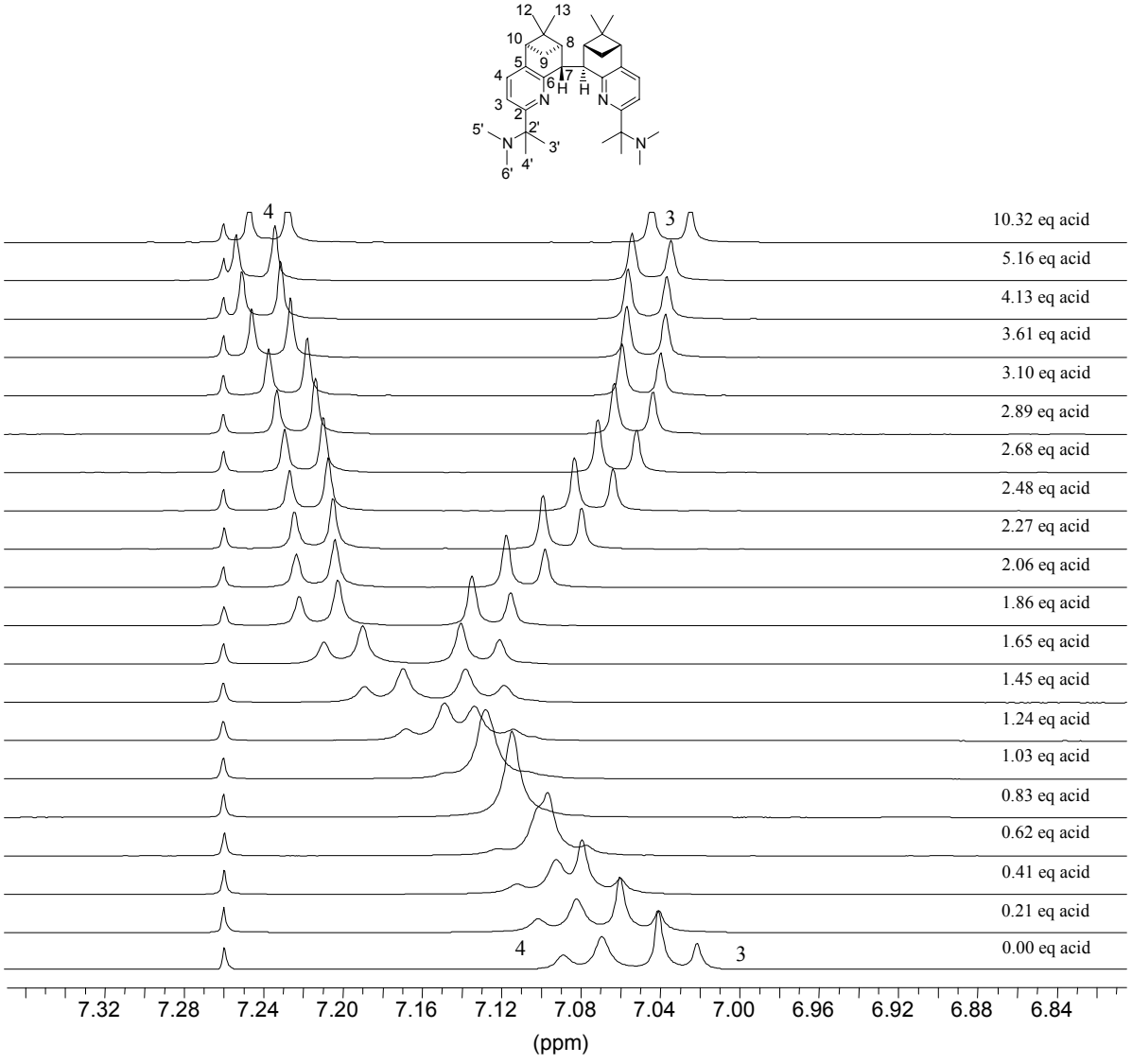

figure 72: aromatic protons of **L19**.

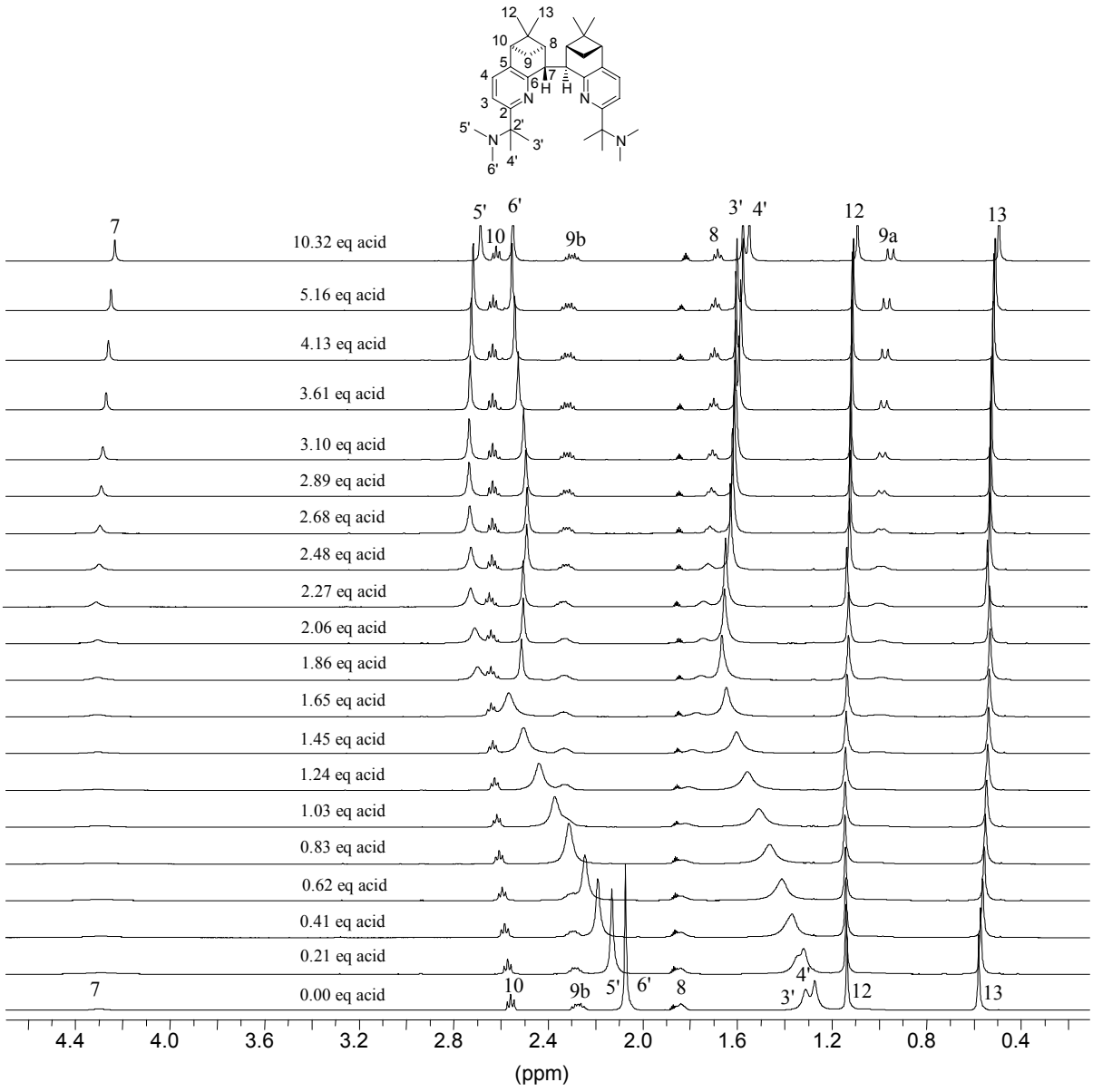

figure 73: aliphatic protons of **L19**.

The low solubility of **L19** poses a problem for the measurements of the 2D-inverse experiments. The acquisition time was kept short, so that no precipitation could occur during the acquisition time. Therefore not all signals (especially the broad ones) could be observed for each measurement.

While in the ^{1}H-NMR-titrations, no significant variation after one equivalent could be observed, the chemical shifts for the aromatic carbons (figure 74) are changing significantly.

^{1}H-^{15}N-HMBC-experiments were recorded twice. Once in the range of –50 ppm to –100 ppm for the pyridine nitrogen N(A) and once in the range of –300 ppm to –350

ppm for the tertiary amine N(B). N(A) shows only a slight downfield shift upon protonation (figure 75).

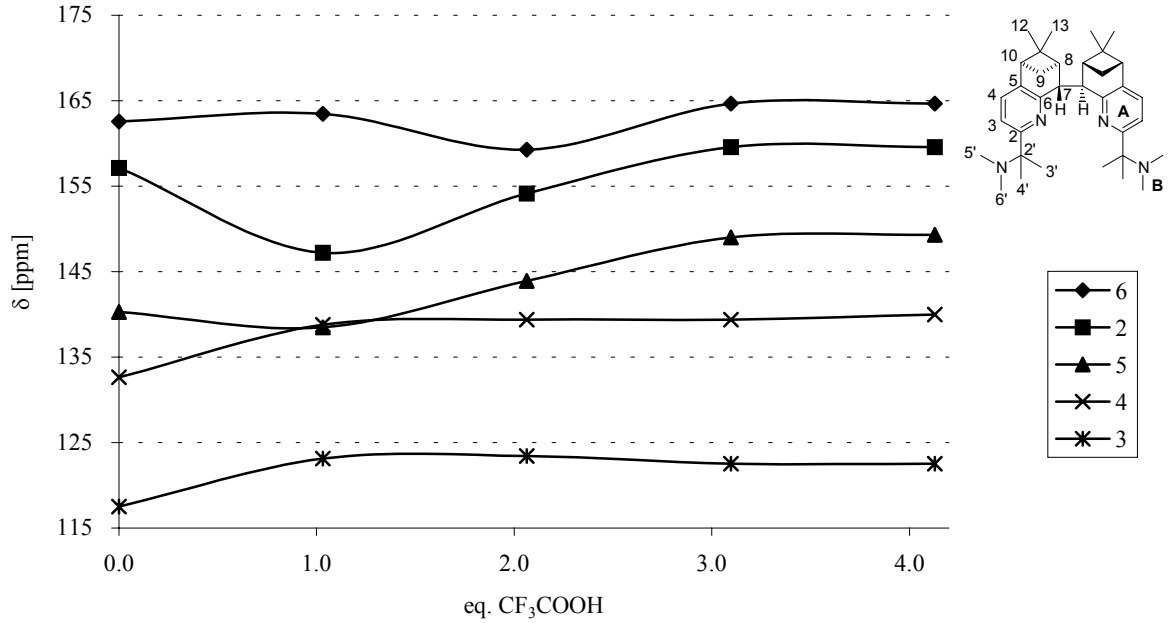

figure 74: chemical shifts of the aromatic carbons of **L19** upon protonation.

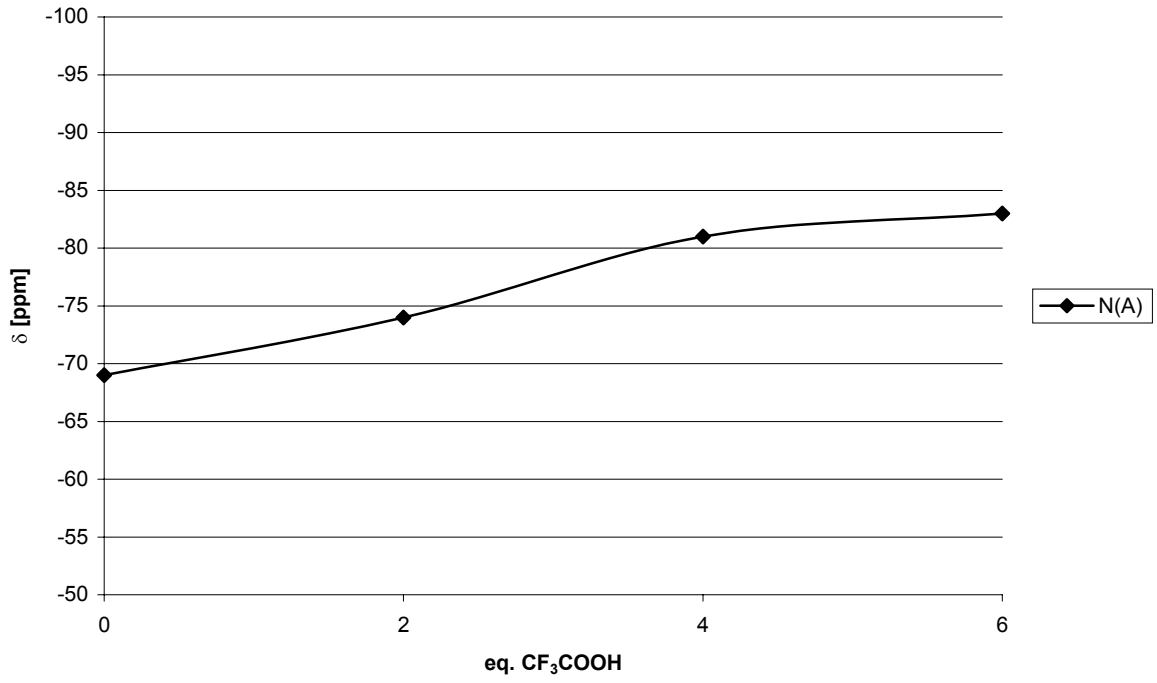

figure 75: chemical shift of N(A) upon protonation.

A correlation to the amine nitrogen was only observed at 0.0 equivalents of acid (δ = -340 ppm) and then again at four equivalents (δ = -325 ppm). In between, the signals of methyl groups are too broad (cf ^{1}H-NMR, figure 73) and a much longer acquisition time would be needed to observe the correlations (even on the 700 MHz spectrometer). The information of all these NMR-titrations was not sufficient to give a complete and final conclusion. Even tough, it seems to be evident, that the two dimethylamino-functions are protonated after addition of two equivalents of acid (scheme 36). The dimethylamino function is much more basic than pyridine and bpy and can even be protonated by TFA. After the addition of two equivalents the protonation is complete. This is indicated by the splitting of the corresponding signals (N-inversion is inhibited). Although the ^{1}H-^{15}N-correlation at two equivalents was not observed, the chemical shift at four equivalents (δ = -325 ppm) indicates strongly this protonation. Chemical shifts of analogous amines and their protonated species are given in table 12 and are comparable.

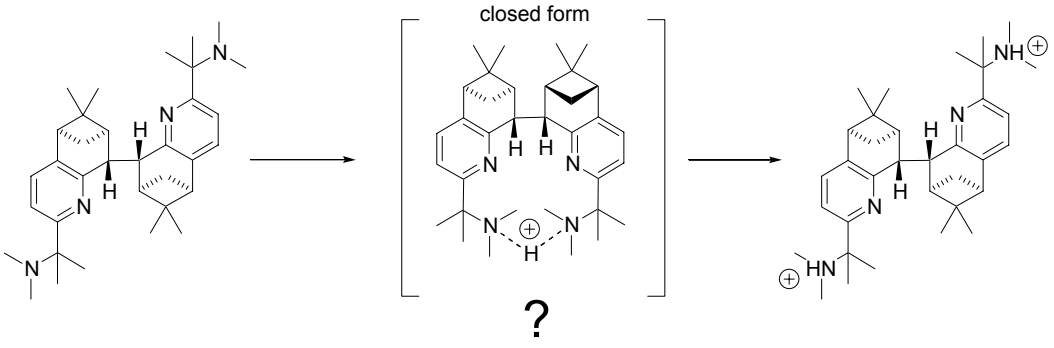

scheme 36: protonation of the dimethylamino groups.

The original reason for the design of this ligand was the binding of a proton between the two dimethylamino-functions. The pronounced change of the ^{13}C-chemical shifts at one equivalent of acid could be an indication of such a closed form (scheme 36). In contrast to that is the continuous shift of the proton signals up to two equivalents. No special effect at one equivalent could be observed. Therefore it cannot be proven, if the mono-protonated species is in a closed or in an open conformation.

R–N	Amine $\delta^{15}N$ (ppm/CH_3NO_2)	Hydrochloride $\delta^{15}N$ (ppm/CH_3NO_2)
CH_3	-363.1	-349.4
C_2H_5	-315.3	-340.0
n-C_3H_7	-352.8	-340.9
$(CH_3)_2CH$	-347.5	-333.7
n-C_4H_9	-352.8	-340.9
CH_3CH_2-$CH(CH_3)$	-349.6	-333.6
$(CH_3)_2CH$-CH_2	-354.8	-342.3
$(CH_3)_3$	**-339.8**	**-326.5**
$CH_3)_2CH$-CH_2-CH_2	-352.9	-340.8
CH_3CH_2-$C(CH_3)_2$	**-344.9**	**-326.7**

table 12: tri-substituted amine and the corresponding hydrochlorides.[143]

The sharpening of the protons 7 and 9_a and the splitting of the methyl groups at C(2') at four equivalents is an indication of a fixed conformation (figure 73). ^{15}N-shifts of the pyridine nitrogen atoms are not very pronounced, a complete protonation does not occur. Whether it adopts a closed conformation or a fixed open conformation cannot be determined.

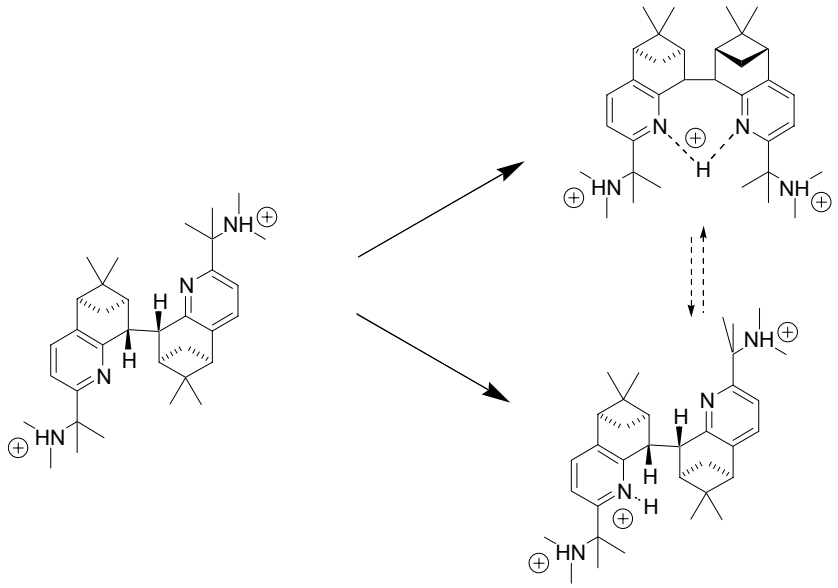

scheme 37: possibilities for a third protonation.

4. Conclusion

A series of new enantiopure pinene-bpy derivatives **L3**-**L9** were synthesised and fully characterized. The {6'-bromo}-pinene-bpy derivatives **L5** and **L6** are important key molecules for the synthesis of other 6'-substituted pinene-bpy ligands. They are available from these key molecules in one step via Suzuki cross-coupling reactions.
A combination of the pinene-bpy moiety and the proton sponge lead to ligand **L10**, which consists of a pinene-py-unit and a dimethylamino-function.
With the ligands **L3** to **L10** new tetradentate ligands were synthesised in one step. These CHIRAGEN derivatives can be divided into two families. In the first one, both pinene-bpy moieties are linked together via an bridge such as *p*-xylyl or *m*-xylyl giving the CHIRAGEN[bridge] derivatives **L11-L14**, in the second one, both pinene-bpy- or pinene-*N*-py-moieties are directly linked giving CHIRAGEN[0] derivatives **L16** to **L19**.

The CHIRAGEN[*p*-xyl]-derivatives **L11** to **L13** were further used for the formation of hexanuclear circular helicates. The structures of these complexes were analysed in solution and can be attributed to circular helicates.
Mononuclear silver(I)-complexes were synthesised from the CHIRAGEN[0]-derivatives **L16** and **L18**. These complexes were characterized in solution.

An extended protonation study was carried out with the non-substituted ligands **L1**, **L15** and **L20**, but also the ligand **L19** was examined.
L1 show the same protonation behaviour as bpy. Upon protonation, the free ligand **L1** is in equilibrium with its mono-protonated analogue. The mono-protonated species is stabilised in the *cis*-conformation by hydrogen bonding.
L20 consists of two pinene-bpy moieties, which are arranged in such a way, that no proton exchange can take place between them. Both pinene-bpy moieties are independently mono-protonated upon protonation. The conformation of the ligands does not change considerably.

L15 has the ability to form helical mononuclear complexes with several metal cations. But not only are metal cations able to fit into the cavity of the ligand, but also a proton, as the smallest cation, can fix the ligand in a helical conformation. Upon a first protonation, the ligand changes its conformation to a closed form, where the proton is shared between the two nitrogen atoms near the bridge. Upon the second protonation, the bpy-moieties are arranged in the *cis*-conformation, but the ligand keeps its conformation in a closed form.

L19 can be easily protonated twice due to the strong basicity of the dimethylamino-function. The conformation of the triply-protonated **L19** could not be determined.

EXPERIMENTAL PART

EXPERIMENTAL PART

1. General

1.1. Reagents

Solvents and reagents were purchased from Fluka, Merck, Acros, Aldrich and Strem chemicals. Pyridine was dried over KOH and freshly distilled prior to use. Ammonium acetate was dried for several days under vacuum. Diethyl ether and THF were distilled from sodium/benzophenone prior to use.

1.2. Measurements

NMR spectra were recorded on a 'Varian Gemini 300' (300.08 MHz for ^{1}H; 75.4 MHz for ^{13}C) or on a 'Bruker Avance DRX400' (400.13 MHz for ^{1}H; 100.62 MHz for ^{13}C) spectrometer. Chemical shifts are given in ppm using the solvent as internal standard, coupling constants *J* are given in Hertz. The assignment of the ^{1}H- and ^{13}C signals was performed by ^{1}H,^{1}H-COSY, DEPT, and ^{1}H-^{13}C-HECTOR, ^{1}H-^{13}C-HMQC/HMBC-techniques. The diastereotopic protons are generally labelled as H_a and H_b. The diastereotopic protons at carbon 9 of the pinene-bpy derivatives are labelled as H_a for the *endo*-oriented protons and H_b for the *exo*-oriented protons. The *exo* methyl groups of the pinene-moieties are assigned as 12, the *endo* oriented ones as 13. For the methoxy-phenyl derivatives, the protons 8', 9', 11' and 12' form a spin-coupling system AA'XX', but are labelled as doublets with the coupling constant $^{3}J_{A,X}$. Mass spectral data was acquired either on a 'VG Instrument 7070E' equipped with a FAB inlet system, on a Hewlett Packard 5988A quadrupol mass spectrometer with an electron ionization (EI) source and or on a Bruker FTMS 4.7 T BioApex II using a standard electrospray ion source (ESI). UV/Visible spectra were measured on a Perkin Elmer Lambda 40 spectrometer. Wavelengths are given in nm and molar absorption coefficients (ε) in M^{-1} cm^{-1}. Circular dichroism (CD) spectra were recorded on a Jasco J-715 spectropolarimeter and the results are given in $\Delta\varepsilon$ [M^{-1} cm^{-1}]. Elemental analyses were obtained from EIF (Ecole d'ingénieurs de Fribourg, Switzerland). X-ray measurements were carried out at the university of Neuchâtel, Switzerland.

2. Precursor syntheses

2.1. Synthesis *R,R*-(+)-Pinocarvone (1)

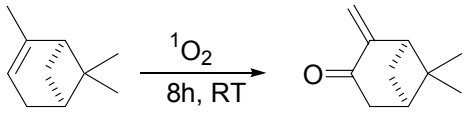

R,R-(+)-pinocarvone (**1**) was synthesized according to the published method of Mihelich *et al*.[71] Starting from (-)-*α*-pinene (52.28 g, 0.38 mole), a slightly yellow liquid (48.44 g; 85%) is obtained after distillation under high vacuum. The spectral properties of *R,R*-(+)-pinocarvone (**1**) correspond to those reported by Mihelich.[71]

^{1}H-NMR (300 MHz, $CDCl_3$): δ 5.91(d, 1H, H(10_a), $^2J_{10a,\ 10b}$ = 1.7 Hz); 4.95 5.91(d, 1H, H(10_b), $^2J_{10b,\ 10a}$ = 1.7 Hz); 2.71 (dd, 1H, H(1), $^3J_{1,7b}$ =6.0 Hz, $^4J_{1,5}$ = 6.0 Hz); 2.67-2.57 (m, 2H, H(7_b), H(4)); 2.46 (dd, 1H, H(4_b), $^2J_{4b,4a}$ = 19.2 Hz, $^3J_{4b,5}$=3.1 Hz); 2.15 (m, 1H, H(5)); 1.31 (s, 3H, H(8)); 1.24 (d, 1H, H(7_a),$^2J_{7a,7b}$ = 10.3 Hz); 0.75 (s, 3H, H(9)).

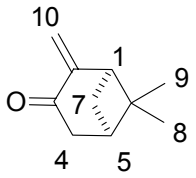

$C_{10}H_{14}O$
150.22

2.2. 1-(2-Acetylpyridyl)-pyridinium bromide (4)

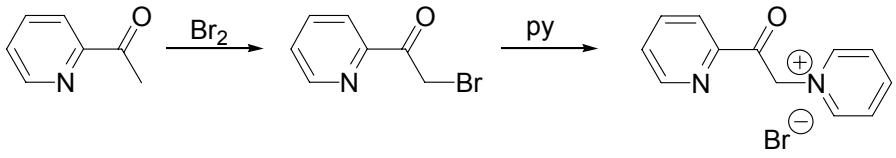

The synthesis of 1-(2-acetylpyridyl)-pyridinium bromide (**4**) was performed following the published procedure.[70] After the bromination, using acetylpyridine (36.1 g, 0.3 mole), the intermediate bromo-compound was used without isolation to from the corresponding pyridinium bromide with a slightly better yield (61%) compared to the published method. The spectral data corresponds to the published ones[37,69,70,134]

^{1}H-NMR (300 MHz, DMSO-d_6): δ = 9.02 (dd, 2H, H(10), $^3J_{10,11}$ = 6.7 Hz, $^4J_{10,12}$ = 1.3 Hz), 8.86 (ddd, 1H, H(6), $^3J_{6,5}$ = 4.7 Hz, $^4J_{6,4}$ = 1.6 Hz, $^5J_{6,3}$ = 1.0 Hz), 8.72 (tt, 1H, H(12), $^3J_{12,11}$ = 7.8 Hz, $^4J_{12,10}$ = 1.3 Hz), 8.27 (dd, 2H, H(11), $^3J_{11,10}$ = 6.7 Hz, $^3J_{11,12}$ = 7.8 Hz), 8.12 (ddd, 1H, H(4), $^3J_{4,3}$ = 7.5 Hz, $^3J_{4,5}$ = 7.5 Hz, $^4J_{4,6}$ = 1.6 Hz), 8.06 (ddd, 1H, H(3), $^3J_{3,4}$ = 7.5 Hz, $^4J_{3,5}$ = 1.5 Hz, $^5J_{3,6}$ = 1.0 Hz), 7.85 (ddd, 1H, H(5), $^3J_{5,4}$ = 7.5 Hz, $^3J_{5,6}$ = 4.7 Hz, $^4J_{5,3}$ =1.5 Hz), 6.51 (s, 2H, H(8)).

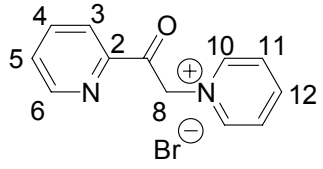

$C_{12}H_{11}BrN_2O$
279.13

2.3. 2-Acetyl-5-(*p*-methoxyphenyl)-pyridine (12)

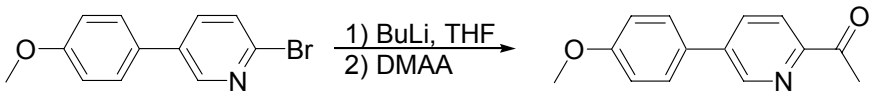

The introduction of the acetyl function starting from 2-bromo-5-(p-methoxyphenyl) pyridine (**20**) was carried out in similar manner as described for compound **13**. [87,88]. 2-Bromo-5-(p-methoxyphenyl)-pyridine (**20**) (2g, 7.6 mmole) was dissolved in dry diethyl ether (250 ml) under argon and cooled to –60°C, *n*-butyllithium (5 ml, 1.6M in hexane) was added dropwise over 45 minutes. After stirring for 1 ¼ hours, *N,N*-dimethylacetamide (0.75 ml, 8mmole) in diethyl ether (10 ml) was added over an hour. Overnight, the solution was allowed to warm to room temperature, quenched with saturated ammonium chloride solution and extracted five times with diethyl ether. Further purification was carried out by column chromatography (Hexane/ ethyl acetate/ trimethylamine: 8/1/0.5) yielding a white solid (1.04 g, 60 %). The spectral data was in accordance to the literature.[76]

^{1}H-NMR (400 MHz, $CDCl_3$): δ 8.88 (d, 1H, H(6), $^4J_{6,4}$ = 2.2 Hz, $^5J_{6,3}$ = 1.0 Hz), 8.07 (dd, 1H, H(4), $^3J_{4,3}$ = 8.1 Hz, $^4J_{4,6}$ = 2.2 Hz), 7.94 (d, 1H, H(3), $^3J_{3,4}$ = 8.1 Hz $^5J_{3,6}$ = 1.1 Hz), 7.62 (d, 2H, H(9), H(11), $^3J_{8,9}$ = 8.9 Hz), 7.04 (d, 2H, H(8), H(12), $^3J_{9,8}$ = 8.9 Hz), 3.87 (s, 3H, H(13)), 2.75 (s, 3H, H(15)).

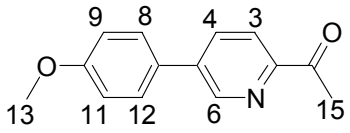

$C_{14}H_{13}NO_2$
227.26

2.4. 2-Acetyl-6-bromopyridine (13)

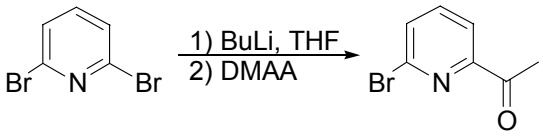

The introduction of the acetyl function starting from 2,6-dibromo-pyridine (**21**) was carried out according to the literature. [87,88,135]. 2,6-Dibromo-pyridine (**21**) (61.8 g, 0.26 mol) were transformed into 2-acetyl-6-bromopyridine (**13**) (31.6 g, 60 %), purified by recrystallisation in diethyl ether / pentane. The spectral properties correspond to those reported.

^{1}H-NMR (400 MHz, $CDCl_3$): 7.95 (dd, 1H, H(5), $^3J_{5,4}$ = 7.2 Hz, $^4J_{5,3}$ = 1.3 Hz); 7.65 (dd, 1H, H(4), $^3J_{4,5}$ = 7.2 Hz, $^3J_{4,3}$ = 7.9 Hz); 7.63 (dd, 1H, H(3), $^3J_{3,4}$ = 7.9 Hz, $^4J_{3,5}$ = 1.3 Hz); 2.69 (s. 3H, C(8)).

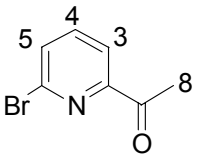

C_7H_6BrNO
200.03

2.5. 2-Acetyl-6-phenyl pyridine (14)

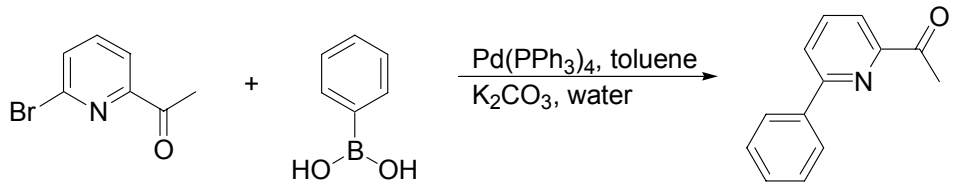

The synthesis was carried out according to the published method.[135] 2-Acetyl-6-bromopyridine (**13**) (7.75 g, 38.74 mmole) was dissolved in dry xylene (75 ml). Phenylboronic acid (7.09 g, 58.11 mmole), freshly purified $Pd(PPh_3)_4$ (5% eq) and potassium carbonate (10.71 g, 77.48 mmole) were added, stirred for 2hours at room temperature. Water (500 ml) was added and the reaction mixture was extracted by dichloromethane (500 ml). The resulting organic layers were dried over sodium sulfate and the solvent was evaporated to afford, after recrystallisation in hexane/ethylacetate, the desired compound (6.95 g, 91%).

^{1}H-NMR (300 MHz, $CDCl_3$): δ 8.03 (dd, 2H, H(8), (12)), 7.91-7.8 (m, 3H, H(3), H(4), H(5)), 7.44-7.38 (m, 3H, H(9), H(10), H(11)), 2.75 (s, 3H, H(14));

MS-EI: 197(100), 154(80), 127(25), 77(15).

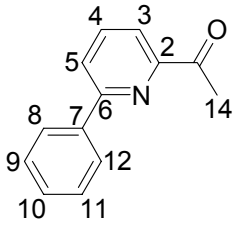

$C_{13}H_{11}NO$
197.23

2.6. 2-Acetyl-6-(*p*-methoxyphenyl)-pyridine (15)

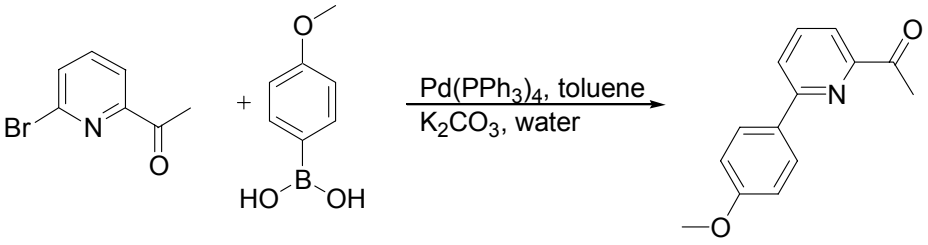

A mixture of 2-acetyl-6-bromopyridine (**13**) (2.00 g, 10 mmole), *p*-methoxyphenylboronic acid (347 mg, 10 mmole), and $Pd(PPh_3)_4$ (0.2% eq, 0.02 mmole) as catalyst, was heated at 120°C for 15 hours in a solvent mixture of toluene (100 ml) and an aqueous solution of K_2CO_3 ((50 ml, 8.5 M). After cooling to room temperature the two layers were separated and the aqueous layer extracted three times with dichloromethane. The combined organic layers were washed with water until pH=7 with water, dried over magnesium sulfate and the solvent was evaporated. Further purifications by recrystallization (ethylacetate/hexane: 1/4) yielded compound **15** (1.45 g, 64%).

^{1}H-NMR (300 MHz, $CDCl_3$): δ 8.04 (d, 2H, H(8), H(12)), $^3J_{8,9}$ = 8.9 Hz); 7.89 (dd, 1H, H(4); ^3J = 6.0 Hz, ^3J = 2.8 Hz); 7.83 (d, 1H, H(5) or H(3), ^3J = 2.5 Hz); 7.81 (d, 1H, H(3) or H(5) ^3J = 6.0 Hz); 7.01 (d, 2H, H(9), H(11), $^3J_{10,11}$ = 8.9 Hz); 3.87 (s, 3H, H(13)); 2.80 (s, 3H, H(15)).

^{13}C-NMR (75 MHz, $CDCl_3$): 200.8 (Cq, C(14)); 160.9 (Cq); 156.2 (Cq); 153.3 (Cq); 137.5 (CH, C(5) or C(3)); 131.1 (Cq); 128.2 (CH, C(8), C(12)); 122.7 (CH, C(3) or C(5)); 119.1 (CH, C(4)); 114.3 (CH, C(9), C(11)); 55.4 (CH_3, C(13)); 25.8 (CH_3, C(15)).

MS-EI: m/z = 227 (100%); 199 (51%); 170 (58%); 142 (16%).

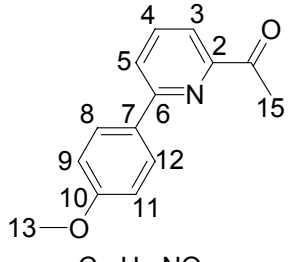

$C_{14}H_{13}NO_2$
227.26

2.7. 2-*N*,*N*-Dimethylamino-2-methyl-butan-3-one (16)

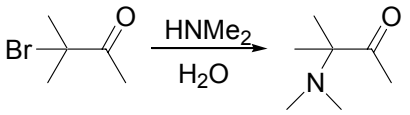

The synthesis was carried out according the published procedure by Gaset.[136] To a to 0 °C cooled solution of 2-bromo-2-methyl-butan-3-one (**23**) (10g, 0.06 mmole), dimethylamine (22 ml, 0.12 mmole, 5.6 M in ethanol) was added over a period of 5 minutes. The reaction solution was stirred overnight at 0 °C, then warmed to 40 °C for 70 minutes. After cooling to room temperature the reaction mixture was filtered and the residual solid was washed with cold ethanol. To the filtrate hydrochloric acid (66 ml, 4M) was added. Ethanol was removed under reduced pressure. To the acidic solution, sodium hydroxide (2M) was added, until the pH > 7. The alkaline solution was extracted three times with diethyl ether. The combined organic extracts were dried over magnesium sulfate and the solvent was removed under reduced pressure. The desired product was obtained (5.87 g, 76%). The spectral properties correspond to those reported.

^{1}H-NMR (300 MHz, $CDCl_3$): δ 2.18 (s, 3H, H(4)), 2.13 (s, 6H, H(6), H(8)), 1.06 (s, 6H, H(1), H(5)).

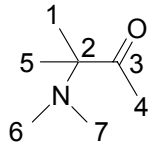

$C_7H_{15}NO$
129.20

2.8. 2-Amino-5-iodopyridine (18)

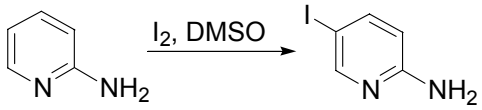

The synthesis was carried out according to a published method.[77] 2-amino-pyridine (**17**) (10 g, 0.11 mole) and iodine (54 g, 0.21 mole) were dissolved in dimethyl sulfoxide (200 ml) and heated for 3h at 100 °C. Overnight, the solution was allowed to cool to room temperature. The excess of iodine was destroyed by addition of a solution of sodium thiosulfate (5%). The pH was adjusted to 4, to remove the side product (2-amino-3,5-diiodopyridine) by extraction with diethyl ether (three times), then the pH was raised to 14 and the aqueous solution was extracted three times with diethyl ether, yielding a pure, white product (17.4 g, 74%). The spectral properties correspond to those reported.[77]

^{1}H-NMR (400 MHz, DMSO-d_6): δ 8.21 (d, 1H, H(6), $^4J_{6,4}$ = 2.1 Hz), 7.61 (dd, 1H, H(4), $^3J_{4,3}$ = 8.7 Hz, $^4J_{4,6}$ = 2.1 Hz), 6.82 (d, 1H, H(3), $^3J_{3,4}$ = 8.7 Hz), 6.34 (s, broad, 2H, NH_2).

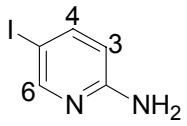

$C_5H_5IN_2$
220.01

2.9. 2-Bromo-5-iodopyridine (19)

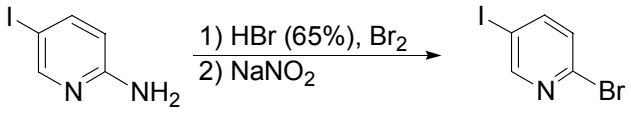

The synthesis was carried out according to published methods.[79-82] Starting from 2-amino-5-iodopyridine (**18**) (5.0,g 23 mmole), the desired pure product was obtained (3.7g, 57%). The spectral properties correspond to those reported.

^{1}H-NMR (400 MHz, $CDCl_3$): δ 8.59 (d, 1H, H(6), $^4J_{6,4}$ = 2.6 Hz), 7.82 (dd, 1H, H(4), $^3J_{4,3}$ = 8.0 Hz, $^4J_{4,6}$ = 2.6 Hz), 7.29 (d, 1H, H(3), $^3J_{3,4}$ = 8.7 Hz).

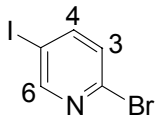

C_5H_3BrIN
283.89

2.10. 2-Bromo-5-(*p*-methoxyphenyl) pyridine (20)

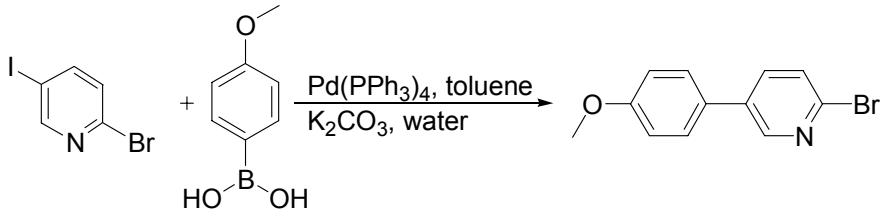

A mixture of 2-bromo-5-iodopyridine (**19**) (5.67 g, 20 mmole), *p*-methoxyphenyl-boronic acid (3.34 g, 20 mmole) and $Pd(PPh_3)_4$ (0.02 mmole) as catalyst, was heated at 120 °C for 4 days in a mixture of toluene (80 ml) and an aqueous solution of K_2CO_3 (80 ml, 80g, 8.5 M). After cooling to room temperature, the two layers were separated and the aqueous layer extracted three times with dichloromethane. The combined organic layers were washed until pH = 7 with water, dried over magnesium sulfate and the solvent was evaporated. Further purification was carried out by column chromatography (Hexane/ ethyl acetate/ trimethylamine: 5/1/0.1), yielding the desired product (5.3g, 99 %) .

^{1}H-NMR (400 MHz, $CDCl_3$): δ 8.55 (d, 1H, H(6), $^4J_{6,4}$ = 2.6 Hz), 7.69 (dd, 1H, H(4), $^3J_{4,3}$ = 8.0 Hz, $^4J_{4,6}$ = 2.6 Hz), 7.51 (d, 1H, H(3), $^3J_{3,4}$ = 8.0 Hz), 7.47 (d, 2H, H(9), H(11), $^3J_{9,8}$ = 8.0 Hz), 7.01(d, 2H, H(8), H(12), $^3J_{8,9}$ = 8.0 Hz), 3.85 (s, 3H, H(13)).

MS(EI): m/z = 265, 263 (M^+, 100%, 96%), 250, 248 (M^+- CH_3, 30%, 31 %), 222, 220 (M^+-C_2H_3O, 27%, 28%), 184 (M^+- Br, 19%), 169 (M^+- CH_3, 21%).

Elemental analysis calculated C: 54.57%, H:3.82% , N:5.30% , found C: 54.80%, H: 3.92%, N: 5.15%.

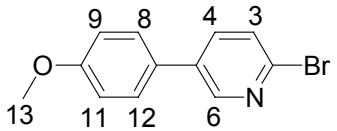

$C_{12}H_{10}BrNO$
264.12

2.11. 2-Bromo-2-methyl-butan-3-one (23)

To a solution of 2-methylbutan-3-one (**22**) (25.85 g, 0.3 mole) in carbon tetrachloride (120 ml), bromine (48.0 g, 0.3 mole) in carbon tetrachloride (30 ml) was added dropwise under reflux over a period of 2 hours. After the addition the reaction mixture was kept under reflux for another 2 hours, then cooled to room temperature. Unreacted bromine was destroyed with sodium thiosulfate solution (10%). The organic layer was separated, dried with magnesium sulfate, the solvent was removed under reduced pressure. The crude product was further purified by vacuum distillation (100 mbar, 60°C), yielding a colourless liquid (30.1 g, 60%). The spectral properties correspond to those reported.[137]

^{1}H-NMR (300 MHz, $CDCl_3$): δ 2.43 (s, 3H, H(4)), 1.84 (s, 6H, H(1), H(5)).

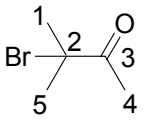

C_5H_9BrO
165.03

2.12. 1-Bromo-1,1-diphenyl-propan-2-one (25)

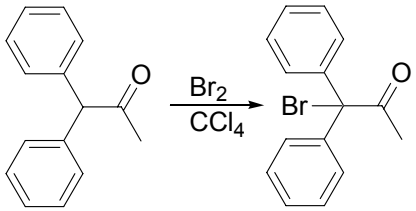

To a solution of 1,1-diphenyl-propan-2-one (**24**) (15.0 g, 71mmole) in carbon tetrachloride (80 ml), bromine (12.5 g, 78 mmole) in carbon tetrachloride (20 ml) was added dropwise under reflux over a period of 2 hours. After the addition the reaction mixture was kept under reflux for another 2 hours, then cooled to room temperature. Unreacted bromine was destroyed with sodium thiosulfate. The organic layer was separated, dried with magnesium sulfate, the solvent was removed under reduced pressure. The crude product was further purified by recrystallization, yielding a colourless solid (18.23 g, 82%).

^{1}H-NMR (300 MHz, $CDCl_3$): δ 7.25-7.38 (m, 10H, H(5), H(6), H(7)), 2.47 (s, 3H, H(1))

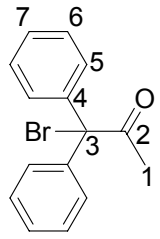

$C_{15}H_{13}BrO$
289.17

2.13. *N,N*-dimethyl- 3,3-diphenyl-propionamide (26)

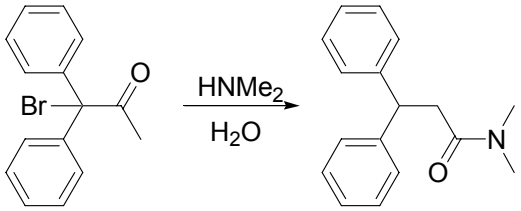

To a to 0 °C cooled solution of 1-bromo-1,1-diphenyl-propan-2-one (**25**) (2.0 g, 6.9 mmole), dimethylamine (2.5 ml, 13.8 mmole, 5.6 M in ethanol) was added over a period of 5 minutes. The reaction solution was stirred overnight at 0 °C, then warmed to 40 °C for 70 minutes. After cooling to room temperature, hydrochloric acid (50 ml, 4M) was added to the reaction mixture. Ethanol was removed under reduced pressure. To the acidic solution, sodium hydroxide (2M) was added, until the pH > 7. The alkaline solution was extracted three times with diethyl ether. The combined organic layers were dried over magnesium sulfate and the solvent was removed under reduced pressure, yielding product **26** (1.66 g 95%). The spectral properties correspond to those reported.[90,91]

^{1}H-NMR (300 MHz, $CDCl_3$): δ 7.16-7.29 (m, 10H, H(5), H(6), H(7)), 4.68 (t, 1H, H(3), $^3J_{3,2}$ = 7.4 Hz), 3.03 (d, 2H, H(2), $^3J_{2,3}$ = 7.4 Hz), 2.84 (s, 6H, H(8)).

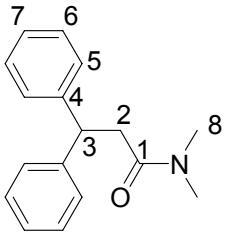

$C_{17}H_{19}NO$
253.34

2.14. 1-(2-Acetyl-5-(*p*-methoxyphenyl)-pyridyl)-pyridinium iodide (31)

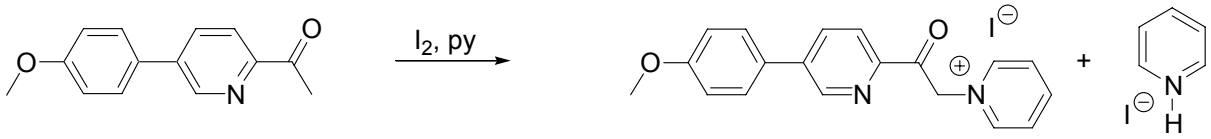

A mixture of pyridine (10 ml), iodine (280 mg, 1.1 mmole) and 2-acetyl-5-(*p*-methoxyphenyl)-pyridine (**12**) (210 mg, 0.925 mmole) was kept at 100 °C for 2 hours and at 0 °C for 20 min. After addition of dry diethyl ether, the desired product and pyridinium iodide precipitated and was filtered. The crude product (305 mg) was used without further purification: The ratio between **31** (1.3 eq, 223 mg, 59%) and the pyridinium iodide (1eq, 82 mg) was determined by ^{1}H-NMR-spectroscopy.

^{1}H-NMR (400 MHz, DMSO-d_6): δ 9.19 (d, 1H, H(6), $^{4}J_{6,4}$ = 2.0 Hz), 9.01 (d, 2H, H(16), $^{3}J_{16,17}$ = 5.7 Hz), 8.73 (dd, 1H, H(18), $^{3}J_{18,17}$ = 7.8 Hz), 8.37 (dd, 1H, H(4), $^{3}J_{4,3}$ = 8.3 Hz, $^{4}J_{4,6}$ = 2.0 Hz), 8.27 (dd, 2H, H(17), $^{3}J_{17,18}$ = 7.8 Hz), 8.09 (d, 1H, H(3), $^{3}J_{3,4}$ = 8.3 Hz), 7.88 (d, 2H, H(9), H(11), $^{3}J_{9,8}$ = 8.8 Hz), 7.13 (d, 2H, H(8), H(12), $^{3}J_{8,9}$ = 8.8 Hz), 6.52 (s, 2H, H(14)), 3.84 (s, 3H, H(13')).

MS(ESI): m/z = 305.14 M^{+}-I^{-}

Pyridinium iodide: ^{1}H-NMR (400 MHz, DMSO-d_6): δ 8.91 (d, 2H, H(a), $^{3}J_{a,b}$ = 6.6 Hz); 8.55 (dd, 1H, H(c), $J_{c,b}$ = 7.7 Hz); 8.03 (dd, 1H, H(b), $^{3}J_{b,a}$ = 6.6 Hz, $^{3}J_{b,c}$ = 7.7 Hz).

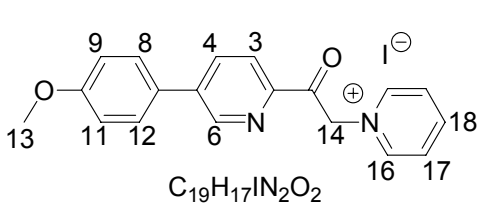

$C_{19}H_{17}IN_2O_2$
432.26

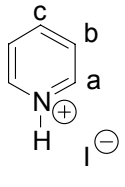

C_5H_6IN
207.01

2.15. 1-(2-Acetyl-6-bromopyridyl)-pyridinium iodide (32)

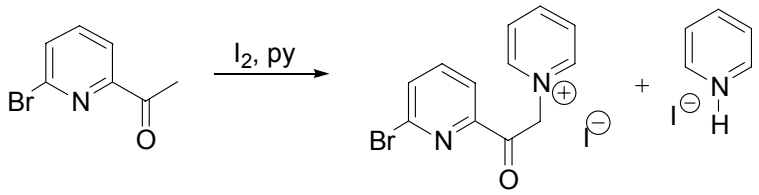

A mixture of pyridine (200 ml), iodine (40.1g, 0.16 mol) and 2-acetyl-6-bromopyridine (**13**) (31.2 g, 0.16 mol) was kept at 130 °C for 3 hours and then at 0 °C for 20 min. The pyridine was then removed by distillation (75 °C at 240 mbar). After addition of dry diethyl ether, the desired product and pyridinium iodide precipitated and was filtered. The crude product (84.5 g) was used without further purification: The ratio between **32** (1.1 eq, 57.9g, 92%) and pyridinium iodide (1 eq, 26.6 g) was determined by ^{1}H-NMR-spectroscopy.

^{1}H-NMR (300 MHz, DMSO-d_6): δ 8.96 (d, 1H, H(10), $^{3}J_{10,11}$ = 5.5 Hz); 8.74 (m, 1H, H(12)); 8.28 (dd, 1H, H(11), $^{3}J_{11,10}$ = 5.5 Hz, $^{3}J_{11,12}$ = 6.8 Hz); 8.10 (m, 3H, H(3), H(4), H(5)); 6.46 (s, 2H, H(8)).

MS-FAB (Matrix: NBA) : m/z = 279, 277 (M^{+}-I^{-}, 100%); 198, 200 (M^{+}-py, 30%, 20%) ; 154 (40%); 136 (48%)

Pyridinium iodide: cf. 3.2.14 p.16

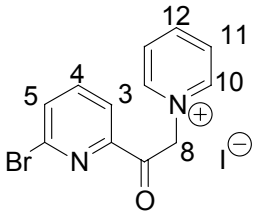

$C_{12}H_{10}BrIN_2O$
405.03

2.16. 1-(2-Acetyl-6-phenylpyridyl)-pyridinium iodide (33)

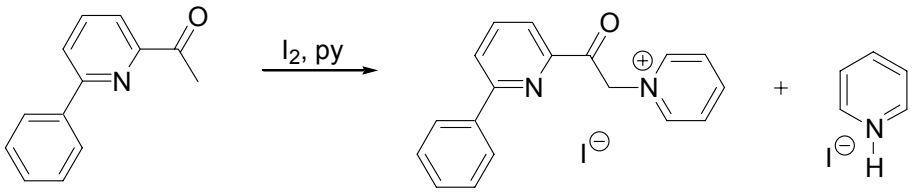

A mixture of pyridine (5 ml), iodine (0.64 g, 2.5 mmole) and 2-acetyl-6-phenylpyridine (**14**) (0.5 g, 2.5 mmole) was kept at 120 °C for 3 hours and then at 0 °C for a night. The pyridine was evaporated under reduced pressure. The residual solid was suspended in dry diethyl ether and filtered to yield a black solid (1.36 g). The ratio between **33** (1.2 eq, 0.95 g, 93%) and pyridinium iodide (1eq, 0.41 g) was determined by ^{1}H-NMR-spectroscopy.

^{1}H-NMR (300 MHz, DMSO-d_6): δ 9.02 (dd, 2H, H(16), $^{3}J_{16,17}$ = 6.6 Hz, $^{4}J_{16,17}$ = 1.2 Hz), 8.74 (dd, 1H, H(6), $^{3}J_{17,16}$ = 7.8 Hz, $^{4}J_{17,15}$ = 1.2 Hz), 8.42 (dd, 1H, (H(arom)), 8.33-8.25 (m, 4H, H(arom)), 8.22 (dd, 1H, H(arom)), 7.96 (dd, 1H, H(arom)), 7.64-7.51 (m, 3H, H(arom)), 6.69 (s, 2H, H(2)).

Pyridinium iodide: cf. 3.2.14 p.16

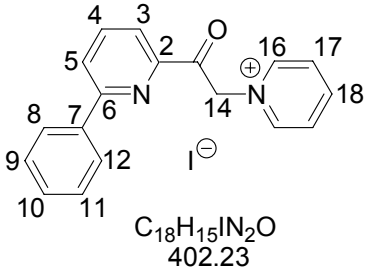

$C_{18}H_{15}IN_2O$
402.23

2.17. 1-(3-*N,N*-Dimethylamino-3-methyl-2-oxo-butyl)-pyridinium iodide (34)

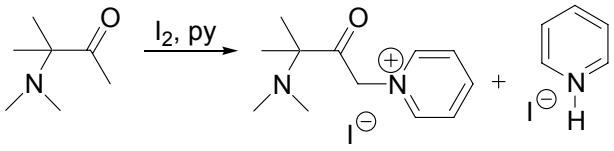

A mixture of pyridine 160 ml), iodine (36.0 g, 142 mmole) and 2-*N,N*-dimethylamino-2-methyl-butan-3-one (**16**) (17.6 g, 136 mmole) was kept at 130 °C for 3 hours and then at 0 °C for 20 min. After addition of dry diethyl ether the desired product and pyridinium iodide precipitated and was filtered. The crude product was used without further purification: The ratio between **34** (1 eq, 16.2, 36 %) and pyridinium iodide (2.2 eq, 22.1 g) was determined by ^{1}H-NMR-spectroscopy.

^{1}H-NMR (400 MHz, DMSO-d_6): δ 9.10 (d, 2H, H(8), $^{3}J_{8,9}$ = 5.6 Hz), 8.78 (dd, 1H, H(10), $^{3}J_{10,9}$ = 7.8 Hz), 8.31 (dd, 2H, H(9), $^{3}J_{9,10}$ = 7.8 Hz), 6.43 (s, 2H, H(1)), 2.77 (s, 6H, H(6), H(7)), 1.72 (s, 6H, H(4), H(5)).

MS(ESI): m/z = 207.16 M^{+}-I^{-}

Pyridinium iodide: cf. 3.2.14 p.16

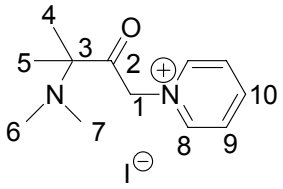

$C_{12}H_{19}IN_2O$
334.20

3. Ligand syntheses

3.1. [5,6]-Pinene-bpy (L1)***

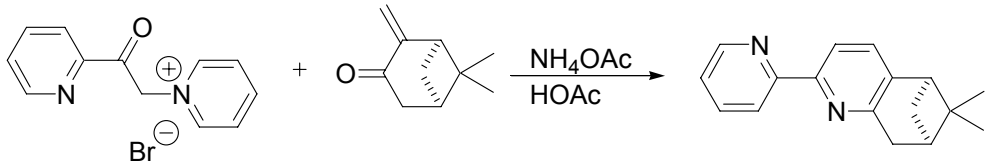

The synthesis of [5,6]-pinene-bpy (**L1**) was performed following the published procedure[134]. A mixture of 1-(2-acetylpyridyl)-pyridinium bromide (**4**) (22.5, 80 mmole), ammonium acetate (53.4 g, dried under vacuum) and *R,R*-(+)-pinocarvone (**1**) (12.2 g, 81 mmole) was suspended in acetic acid (100 ml) and slowly heated over 20 hours from 50 °C up to 115 °C. After addition of water, the pH was adjusted to 9 by addition of sodium carbonate. The aqueous solution was extracted ten times with hexane and the combined organic layers were washed with water and dried over magnesium sulfate with activated charcoal. The solvent was evaporated under reduced pressure. The residual solid was further purified by column chromatography (hexane/diethyl ether/trimethylamine: 14/6/1, yielding of pure **L1** (14.8 g, 74%). The spectral properties correspond to those reported.

^{1}H-NMR (300 MHz, $CDCl_3$): δ = 8.64 (ddd, 1H, H(6'), $^3J_{6',5'}$ = 4.8 Hz, $^4J_{6',4'}$ =1.8 Hz, $^5J_{6',3'}$ = 0.9 Hz), 8.32 (ddd, 1H, H(3'), $^3J_{3',4'}$ = 8.0 Hz, $^4J_{3',5'}$ = 1.1 Hz, $^5J_{6',3'}$ = 0.9 Hz), 8.02 (d, 1H, H(3), $^3J_{3,4}$ = 7.8 Hz), 7.76 (ddd, 1H, H(4'), $^3J_{4',3'}$ = 8.0 Hz, $^3J_{4',5'}$ =7.5 Hz, $^4J_{4',6'}$ = 1.8 Hz), 7.31 (d, 1H, H(4), $^3J_{4,3}$ = 7.8 Hz), 7.23 (ddd, 1H, H(5'), $^3J_{5',4'}$ = 7.5 Hz, $^3J_{5',6'}$ = 4.8 Hz, $^4J_{5',3'}$ = 1.2 Hz), 3.17 (d, 1H, H(7), $^3J_{7,8}$ = 2.8 Hz); 2.79 (dd, 1H, H(10), $^3J_{10,9b}$ = 5.7 Hz, $^4J_{10,8}$ = 5.7 Hz); 2.68 (ddd, 1H, $H(9_b)$, $^2J_{9b,9a}$ = 9.6 Hz, $^3J_{9b,10}$ =

*** *R,R*-[5,6]-pinene-bpy: (5*R*, 7*R*)-5,6,7,8-tetrahydro-6,6-dimethyl-2(2'-pyridyl)-5,7-methano-quinoline.

5.7 Hz, $^{3}J_{9b,8}$ = 5.7 Hz); 2.38 (ddt, 1H, H(8) $^{3}J_{8,9b}$ = 5.7 Hz, $^{4}J_{8,10}$ = 5.7 Hz, $^{3}J_{8,7}$ = 2.8 Hz); 1.40 (s, 3H, H(12)); 1.29 (d, 1H, H(9_a), $^{2}J_{9a,9b}$ = 9.6 Hz);0.66 (s, 3H, H(13)).

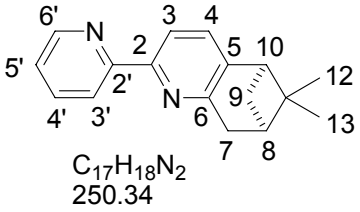

$C_{17}H_{18}N_2$
250.34

3.2. ^{15}N-[5,6]-Pinene-bpy (^{15}N-L1)

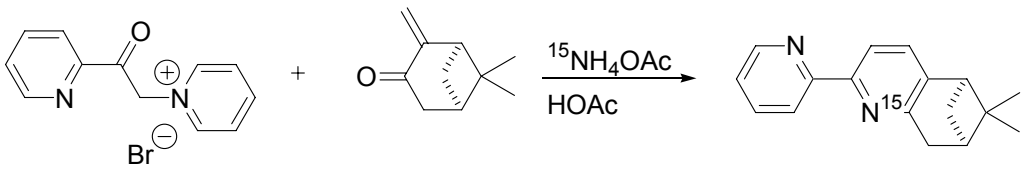

The synthesis was carried out according the procedures described for **L1**. The ammonium acetate used was a mixture of 99 %^{15}N-labelled ammonium acetate, (0.2 g) and unlabelled ammonium acetate, (1.8 g), yielding a 10 % ^{15}N-labelled [5,6]-pinene-bpy (^{15}N-**L1**). 1-(2-acetylpyridyl)-pyridinium bromide (**4**), (1.45 g, 5.2 mmole), ammonium acetate, (2.0 g, 26 mmole, 10% ^{15}N-labelled) and *R,R*-(+)-pinocarvone (**1**), (1.45g, 81 mmole) form pure the compound ^{15}N-**L1** (0.7 g, 53 %). The spectral properties correspond to those of the analogous non-labelled **L1.**

3.3. [4,5]-Pinene-bpy (L2)[†††]

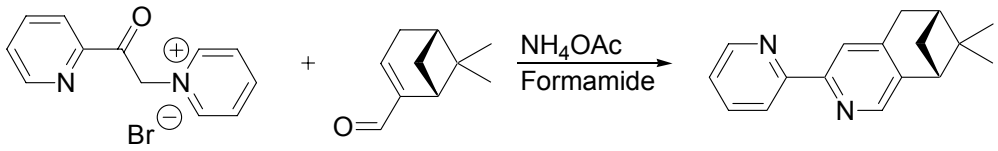

The synthesis of [4,5]-pinene-bpy (**L2**) was performed following the improved procedure[70]. A mixture of 1-(2-acetylpyridyl)-pyridinium bromide (**4**) (18.6, 66.7 mmole), ammonium acetate (10.3 g, dried under vacuum) and *R,R*-(-)-myrtenal (**2**) (10.0 g, 66.7 mmole) was suspended in formamide (80 ml) and slowly heated over 20 hours from 50 °C up to 115 °C. After addition of water, the solution was extracted ten times with hexane and the combined organic layers were washed with water and dried over magnesium sulfate with activated charcoal. The solvent was evaporated under reduced pressure. The residual solid was further purified by column chromatography (hexane/ethyl acetate/ trimethylamine: 2/1/0.1), yielding pure **L2** (10.8 g, 65%). The spectral properties correspond to those reported.

^{1}H-NMR (300 MHz, $CDCl_3$): δ = 8.62 (dd, 1H, H(6'), $^3J_{6',5'}$ = 4.0 Hz, $^4J_{6',4'}$ =1.8 Hz), 8.31 (dd, 1H, H(3'), $^3J_{3',4'}$ = 8.0 Hz, $^4J_{3',5'}$ = 1.1 Hz), 8.17 (s, 1H, H(3)), 8.15 (d, 1H, H(6)), 7.75 (ddd, 1H, H(4'), $^3J_{4',3'}$ = 8.0 Hz, $^3J_{4',5'}$ =7.5 Hz, $^4J_{4',6'}$ = 1.8 Hz), 7.23 (ddd, 1H, H(5'), $^3J_{5',4'}$ = 7.5 Hz, $^3J_{5',6'}$ = 4.0 Hz, $^4J_{5',3'}$ = 1.1 Hz), 3.01 (d, 1H, H(7)); 2.83 (dd, 1H, H(10), $^3J_{10,9b}$ = 5.5 Hz, $^4J_{10,8}$ = 5.5 Hz); 2.67 (ddd, 1H, H(9_b), $^2J_{9b,9a}$ = 9.5 Hz, $^3J_{9b,10}$ = 5.5 Hz, $^3J_{9b,8}$ = 5.5 Hz); 2.27 (ddt, 1H, H(8) $^3J_{8,9b}$ = 5.5 Hz, $^4J_{8,10}$ = 5.5 Hz); 1.37 (s, 3H, H(12)); 1.20 (d, 1H, H(9_a), $^2J_{9a,9b}$ = 9.5 Hz);0.61 (s, 3H, H(13)).

[†††] *R,R*-[4,5]-Pinene-bpy: IUPAC name: (*6R*, *8R*)-5,6,7,8- tetrahydro-7,7-dimethyl-3-(2'-pyridyl)-6,8-methano-isoquinoline.

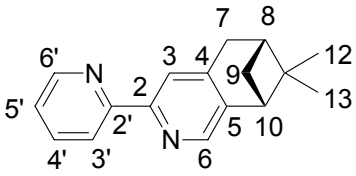

$C_{17}H_{18}N_2$
250.34

3.4. {5'-*p*-Methoxyphenyl}-[5,6]-pinene-bpy (L3)

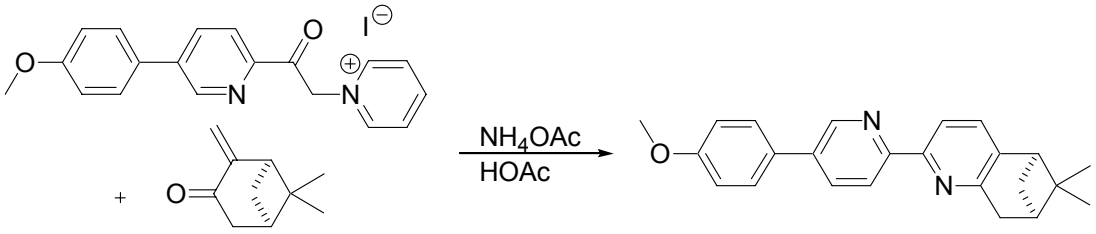

A mixture of 1-(2-acetyl-5-(*p*-methoxyphenyl)-pyridyl)-pyridinium iodide (**31**) (3.8 g, 8.79 mmole), ammonium acetate (6.93 g, dried under vacuum) and *R,R*-(+)-pinocarvone (**1**) (1.35 g, 9.0 mmole) was suspended in acetic acid (5 ml) and slowly heated over 42 hours from 50 °C up to 115 °C. After addition of water, the pH was adjusted to 9 by addition of sodium carbonate. This aqueous solution was extracted ten times with hexane and the combined organic layers were washed with water and dried over magnesium sulfate with activated charcoal. The solvent was evaporated under reduced pressure. The residual solid was further purified by column chromatography (hexane/ ethyl acetate/ trimethylamine: 8/1/0.1) yielding a slightly yellow product **L3** (936mg, 30%) .

^{1}H-NMR (400 MHz, $CDCl_3$): δ 8.84 (d, 1H, H(6'), $^4J_{6',4'}$ = 2.0 Hz); 8.35 (d, 1H, H(3'), $^3J_{3',4'}$ = 8.3 Hz); 8.04 (d, 1H, H(3), $^3J_{3,4}$ = 7.8 Hz); 7.91 (dd, 1H, H(4'), $^3J_{4',3'}$ = 8.3 Hz, $^4J_{4',6'}$ = 2.0 Hz) ; 7.56 (d, 2H, H(9'), H(11'), $^3J_{9',8'}$ = 8.8 Hz); 7.30 (d, 1H, H(4), $^3J_{4,3}$ = 7.8 Hz); 6.99 (dd, 2H, H(8'), H(12'), $^3J_{8',9'}$ = 8.8 Hz); 3.84 (s, 3H, H(13')); 3.18 (d, 1H, H(7), $^3J_{7,8}$ = 2.8 Hz); 2.82 (dd, 1H, H(10), $^3J_{10,9b}$ = 5.7 Hz, $^4J_{10,8}$ = 5.7 Hz); 2.69 (ddd, 1H, H(9_b), $^2J_{9b,9a}$ = 9.6 Hz, $^3J_{9b,10}$ = 5.7 Hz, $^3J_{9b,8}$ = 5.7 Hz); 2.38 (ddt, 1H, H(8) $^3J_{8,9b}$ = 5.7 Hz, $^4J_{8,10}$ = 5.7 Hz, $^3J_{8,7}$ = 2.8 Hz)); 1.40 (s, 3H, H(12)); 1.30 (d, 1H, H(9_a), $^2J_{9a,9b}$ = 9.6 Hz); 0.66 (s, 3H, H(13)).

^{13}C-NMR (100 MHz, $CDCl_3$): δ 160.2 (Cq); 157.0 (Cq); 155.4 (Cq); 153.8 (Cq); 147.6 (CH, C(6')); 142.6 (Cq); 135.8 (Cq); 135.0 (CH, C(4')); 134.2 (CH, C(4)); 130.7 (Cq); 128.5 (CH, C(9'), C(11')); 121.1 (CH, C(3')); 118.2 (CH, C(3)); 115.0 (CH, C(8'), C(12')); 55.8 (CH_3, C(13')); 47.0 (CH, C(10)); 40.7 (CH, C(8)); 40.0 (Cq, C(11)); 37.2 (CH_2, C(7)); 32.4 (CH_2, C(9)); 26.5 (CH_3, C(12)); 21.7 (CH_3, C(13)).

MS(EI): m/z = 356 (M^+, 54%), 341 (M^+-CH_3, 12%), 313 (M^+-$COCH_3$; 100%), 298 (M^+-C_3H_6O,18%).

UV/Vis: ($CHCl_3$): 317nm ($3.3*10^4$), 273 nm ($1.3*10^4$; sh).

Elemental analysis calculated C: 80.87%, H 6.79 %, N: 7.86 %, found C: 80.41%, H: 6.68%, N: 7.75%.

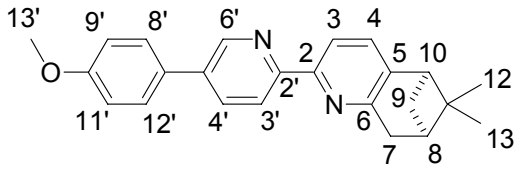

X-ray crystallography

Suitable crystals of **L3** were obtained as colourless blocks from a Chloroform/methanol solution. The intensity data was collected at 153K on a Stoe Image Plate Diffraction System[138] using MoKα graphite monochromated radiation. Image plate distance 70mm, ϕ oscillation scans 0 - 200°, step Δϕ = 1.5°, 2θ range 3.27 – 52.1°, d_{max} -d_{min} = 12.45 - 0.81 Å. The structure was solved by Direct methods and Fourier expansion using the programme SHELXS-97.[139] The refinement and all further calculations were carried out using SHELXL-97.[140] The H-atoms were located from Fourier difference maps and refined isotropically. The non-H atoms were refined anisotropically, using weighted full-matrix least-squares on F^2.

3.5. {5'-*p*-Methoxyphenyl}-[4,5]-pinene-bpy (L4)

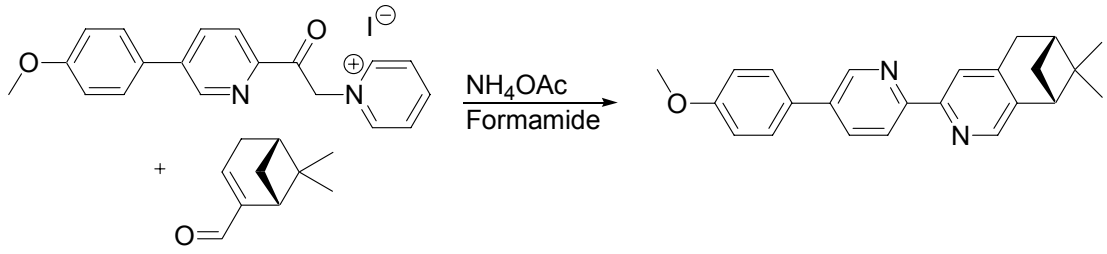

A mixture of 1-(2-acetyl-5-(*p*-methoxyphenyl)-pyridyl)-pyridinium iodide (**31**) (223 mg, 0.52 mmole), ammonium acetate (560 mg, dried under vacuum) and *R,R*-(-)-myrtenal (**2**) (90mg, 0.6 mmole) was suspended in formamide (20 ml) and stirred at room temeparture for 5 days, then it was slowly heated over 24 hours from 50 °C up to 100 °C. To the reaction mixture 50 ml of water was added and extracted five times with hexane and the combined organic layers were washed with water and dried over magnesium sulfate with activated charcoal. The solvent was evaporated under reduced pressure. The residual solid was further purified by column chromatography (hexane/ ethyl acetate/ trimethylamine: 4/1/0.25), yielding the desired product(85 mg, 24 %).

^{1}H-NMR (400 MHz, $CDCl_3$): δ 8.84 (d, 1H, H(6'), $^{4}J_{6',4'}$ = 2.0 Hz); 8.35 (d, 1H, H(3'), $^{3}J_{3',4'}$ = 8.3 Hz); 8.20 (s, 2H, H(3), H(6)); 7.93 (dd, 1H, H(4'), $^{3}J_{4',3'}$ = 8.3 Hz, $^{4}J_{4',6'}$ = 2.0 Hz); 7.57 (d, 2H, H(9'), H(11'), $^{3}J_{9',8'}$ = 8.8 Hz); 7.00 (d, 2H, H(8'), H(12'), $^{3}J_{8',9'}$ = 8.8 Hz); 3.85 (s, 3H, H(13')); 3.05 (d, 1H, H(7), $^{3}J_{7,8}$ = 2.7 Hz); 2.86 (dd, 1H, H(10), $^{3}J_{10,9b}$ = 5.7 Hz, $^{4}J_{10,8}$ = 5.7 Hz); 2.70 (ddd, 1H, $H(9_b)$, $^{2}J_{9b,9a}$ = 9.6 Hz, $^{3}J_{9b,10}$ = 5.7 Hz, $^{3}J_{9b,8}$ = 5.7 Hz); 2.30 (ddt, 1H, H(8) $^{3}J_{8,9b}$ = 5.7 Hz, $^{4}J_{8,10}$ = 5.7 Hz, $^{3}J_{8,7}$ = 2.7 Hz)); 1.41 (s, 3H, H(12)); 1.23 (d, 1H, $H(9_a)$, $^{2}J_{9a,9b}$ = 9.6 Hz); 0.65 (s, 3H, H(13)).

^{13}C-NMR (100 MHz, $CDCl_3$): δ 159.8 (Cq); 154.8 (Cq); 154.2 (Cq); 147.0 (CH, C(6')); 145.6 (CH, C(6)); 145.5 (Cq); 142.9 (Cq); 135.6 (Cq); 134.6 (CH, C(4')); 130.1 (Cq); 128.1 (CH, C(9'), C(11')); 120.7 (CH, C(3')); 120.4 (CH, C(3)); 114.6 (CH, C(8'), C(12')); 55.4 (CH_3, C(13')); 44.5 (CH, C(10)); 40.1 (CH, C(8)); 39.3 (Cq, C(11)); 32.9 (CH_2, C(7)); 31.8 (CH_2, C(9)); 26.0 (CH_3, C(12)); 21.4 (CH_3, C(13)).

MS(ESI): m/z = 357 (M^+).

UV/Vis: ($CHCl_3$), λ (ε): 314 nm ($2.9*10^4$), 274 nm ($1.2*10^4$; sh).

Elemental analysis calculated C: 80.87%, H: 6.79%, N: 7.86% , found C:79.82%, H:6.59%, N: 7.73%.

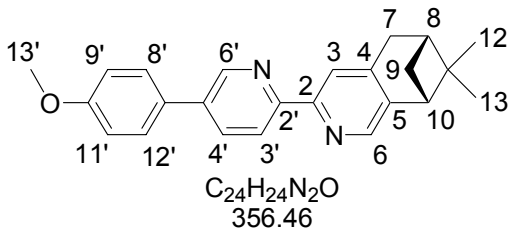

3.6. {6'-Bromo}-[5,6]-pinene-bpy (L5)

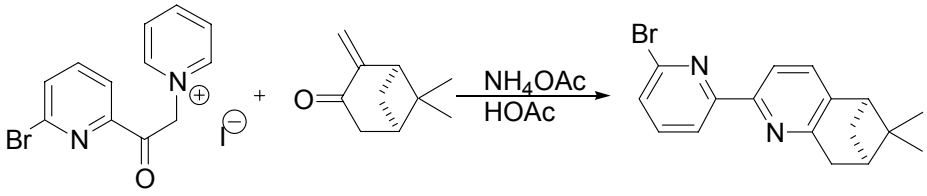

A mixture of 1-(2-acetyl-6-bromopyridyl)-pyridinium iodide (**32**) (27.75 g, 47 mmole), ammonium acetate (31.3 g, dried under vacuum) and *R,R*-(+)-pinocarvone (**1**) (7.0 g, 47 mmole) was suspended in acetic acid (60 ml) and slowly heated over 20 hours from 50 °C up to 115 °C. After addition of water, the pH was adjusted to 9 by addition of sodium carbonate. This aqueous solution was extracted ten times with hexane and the combined organic layers were washed with water and dried over magnesium sulfate with activated charcoal. The solvent was evaporated under reduced pressure. After filtration over silica gel (chloroform), a white powder of **L5** (7.69 g, 50%) was obtained.

^{1}H-NMR (400 MHz, $CDCl_3$): δ 8.34 (d, 1H, H(3'), $^3J_{3',4'}$ = 7.8 Hz); 8.07 (d, 1H, H(3), $^3J_{3,4}$ = 7.8 Hz); 7.61 (dd, 1H, H(4'), $^3J_{4',3'}$ = 7.8 Hz, $^3J_{4',5'}$ = 7.8 Hz); 7.42 (d, 1H, H(5'), $^3J_{5',4'}$ = 7.8 Hz); 7.31; (d, 1H, H(4), $^3J_{4,3}$ = 7.8 Hz); 3.16 (d, 1H, H(7), $^3J_{7,8}$ = 2.8 Hz); 2.81 (dd, 1H, H(10), $^3J_{10,9b}$ = 5.7 Hz, $^4J_{10,8}$ = 5.7 Hz); 2.69 (ddd, 1H, H(9_b), $^2J_{9b,9a}$ = 9.6 Hz, $^3J_{9b,8}$ = 5.7 Hz, $^3J_{9b,10}$ = 5.7 Hz); 2.38 (ddt, 1H, H(8), $^3J_{8,9b}$ = 5.7 Hz, $^4J_{8,10}$ = 5.7 Hz, $^3J_{8,7}$ = 2.8 Hz); 1.40 (s, 3H, H(12)); 1.28 (d, 1H, H(9_a), $^2J_{9a,9b}$ = 9.6 Hz); 0.65 (s, 3H, H(13)).

^{13}C-NMR (100 MHz, $CDCl_3$)**:** δ 158.0 (Cq); 156.6 (Cq); 151.8 (Cq); 143.0 (Cq); 141.5 (Cq); 139.0 (CH, C(4')); 133.8 (CH, C(4)); 127.2 (CH, C(5')); 120.7 (CH, C(6)); 119.4 (CH, C(3')); 118.4 (CH, C(3)); 46.5 (CH, C(10)); 40.2 (CH, C(8)); 39.5 (Cq, C(11)); 36.6 (CH_2, C(7)); 31.9 (CH_2, C(9)); 26.0 (CH_3, C(12)); 21.3 (CH_3, C(13)).

MS-FAB (Matrix: NBA) : m/z = 331,329 (M^+, 100%) ; 285,287 (M^+-i-Pr, 40%), 154 ($C_{11}H_8N^+$, 50%), 136 (30%).

UV/Vis: ($CHCl_3$), λ (ε): 303 nm ($2.0*10^4$), 252 nm ($0.9*10^4$).

Elemental analysis calculated C: 62.02%, H: 5.20%, N: 8.51%, found C: 61.57%, H: 5.22%, N: 7.91%.

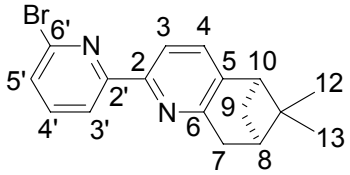

$C_{17}H_{17}BrN_2$
329.23

X-ray crystallography

Suitable crystals of **L5** were obtained as colourless rod-like crystals by slow evaporation from a solution in chloroform. The intensity data was collected at 153K on a Stoe Image Plate Diffraction System[138] using MoKα graphite monochromated radiation. Image plate distance 70mm, ϕ oscillation scans 0 - 185°, step Δϕ = 1.5°, 2θ range 3.27 – 52.1°, d_{max} -d_{min} = 12.45 - 0.81 Å. The structure was solved by Patterson and Fourier methods using the programme SHELXS-97.[139] The refinement and all further calculations were carried out using SHELXL-97.[140] The H-atoms were located from Fourier difference maps and refined isotropically. The non-H atoms were refined anisotropically, using weighted full-matrix least-squares on F^2. An empirical absorption correction was applied using the DIFABS routine in PLATON.[141] The coordinates correspond to the absolute structure of the molecule in the crystal.

3.7. {6'-Bromo}-[4,5]-pinene-bpy (L6)

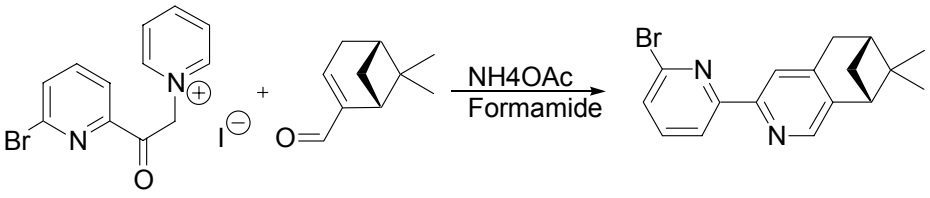

A mixture of 1-(2-acetyl-6-bromopyridyl)-pyridinium iodide (**32**) (3.0 g, 7.4 mmole), ammonium acetate (6.0g, dried under vacuum) and *R,R*-(-)-myrtenal (**2**) (1.1 g, 7.5 mmole) was suspended in formamide (100 ml) and stirred at room temperature for 4d, then slowly heated over 24 hours from 50 °C up to 115 °C. To the reaction mixture of water (75 ml) was added and extracted five times with hexane and the combined organic layers were washed with water and dried over magnesium sulfate with activated charcoal. The product was obtained after purification by column chromatography (hexane/ ethyl acetate/ trimethylamine: 5/1/0.1) as a white powder (706 mg, 29 %).

^{1}H-NMR (400 MHz, $CDCl_3$): δ 8.30 (dd, 1H, H(3'), $^{3}J_{3',4'}$ = 7.8 Hz, $^{3}J_{3',5'}$ = 0.8 Hz); 8.19 (s, 2H, H(3), H(6)); 7.61 (dd, 1H, H(4'), $^{3}J_{4',3'}$ = 7.8 Hz, $^{3}J_{4',5'}$ = 7.8 Hz); 7.42 (d, 1H, H(5'), $^{3}J_{5',4'}$ = 7.8 Hz, $^{3}J_{5',3'}$ = 0.8 Hz); 3.01 (d, 1H, H(7), $^{3}J_{7,8}$ = 2.7 Hz); 2.84 (dd, 1H, H(10), $^{3}J_{10,9b}$ = 5.5 Hz, $^{4}J_{10,8}$ = 5.5 Hz) ; 2.68 (ddd, 1H, H(9_b), $^{2}J_{9b,9a}$ = 9.6 Hz, $^{3}J_{9b,8}$ = 5.7 Hz, $^{3}J_{9b,10}$ = 5.7 Hz)); 2..29 (ddt, 1H, H(8)), $^{3}J_{8,9b}$ = 5.7 Hz, $^{4}J_{8,10}$ = 5.8 Hz, $^{3}J_{8,7}$ = 2.7 Hz); 1.39 (s, 3H, H(12)); 1.19 (d, 1H, H(9_a), $^{2}J_{9a,9b}$ = 9.6 Hz); 0.61 (s, 3H, H(13)).

^{13}C-NMR (100 MHz, $CDCl_3$): δ 157.9 (Cq); 152.7 (Cq); 145.6 (Cq); 145.5 (CH, C(3) or C(6)); 143.7 (Cq); 141.4 (Cq); 139.1 (CH, C(4')); 127.4 (CH, C(5')); 120.8 (CH, C(6) or C(3)); 119.4 (CH, C(3')); 118.4 (CH, C(3)); 44.5 (CH, C(10)); 40.1 (CH, C(8)); 39.2 (Cq, C(11)); 32.9 (CH_2, C(7)); 31.7 (CH_2, C(9)); 26.0 (CH_3, C(12)); 21.3 (CH_3, C(13)).

UV/Vis: ($CHCl_3$), λ (ε): 297 nm ($2.0*10^4$), 253 nm ($1.0*10^4$).

Elemental analysis calculated C: 62.02%, H: 5.2%, N:8.51%, found C: 62.35%, H: 5.30%, N: 8.28%.

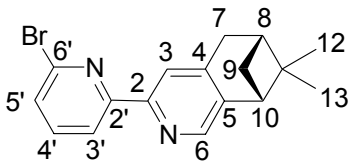

$C_{17}H_{17}BrN_2$
329.23

X-ray Crystallography

Suitable crystals of **L6** were grown from a chloroform/methanol mixture as large colourless blocks. Intensity data was collected at room temperature (293K) on a Stoe AED2 4-circle diffractometer[138] using CuKα graphite monochromated radiation (λ = 1.54186 Å) with ω/2Θ scans in the 2Θ range 5 - 125°. The structure was solved by direct methods using the programme SHELXS-97.[139] The refinement and all further calculations were carried out using SHELXL-97.[140] H-atoms are placed in calculated positions and refined as riding atoms using SHELXL-97 default parameters. The non-H atoms were refined anisotropically, using weighted full-matrix least-squares on F^2 .

The compound crystallises in the non-centrosymmetric space group $P2_12_12_1$ [Flack parameter x = 0.01(3)]. An absorption correction was applied using PSI-scans (T_{min}=0.140, T_{max}=0.283). The coordinates correspond to the absolute structure of the molecule in the crystal.

3.8. {6'-Phenyl}-[5,6]-pinene-bpy (L7)

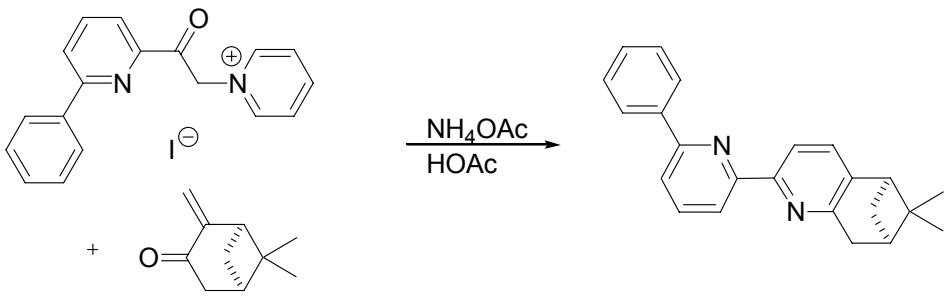

The synthesis of {6'-phenyl}-[5,6]-pinene-bpy (**L7**) was performed following the published procedure.[135] A mixture of 1-(2-acetyl-6-phenylpyridyl)-pyridinium iodide (**33**) (1.02 g, 2.5 mmole), ammonium acetate (1.7 g, dried under vacuum) and *R,R*-(+)-pinocarvone (**1**) (0.38 g, 2.5 mmole) was suspended in acetic acid (5 ml) and slowly heated over 20 hours from 50 °C up to 110 °C. Then the solution was cooled to room temperature and water (15ml) was added. The aqueous solution was extracted five times with dichloromethane. The combined organic layers were washed with water and dried over magnesium sulfate with activated charcoal. The solvent was evaporated under reduced pressure. The residual solid was further purified by recrystallization yielding a yellow powder (586 mg 71%).

^{1}H-NMR (300 MHz, $CDCl_3$): δ 8.37 (d, 1H, H(3'), $^3J_{3',4'}$ = 8.0 Hz); 8.31 (d, 1H, H(3), $^3J_{3,4}$ = 8.0 Hz); 8.13 (dd, 2H, H(8'), H(12'), $^3J_{8',9'}$ = 8.0 Hz, $^4J_{8',10'}$ = 2.1 Hz,); 7.85 (dd, 2H, H(4'), ^3J = 7.4 Hz,); 7.72 (dd, 1H, H(5'), $^3J_{5',4'}$ = 7.8 Hz, ^4J = 0.8 Hz); 7.48 (dd, 2H, H(9'),H(11'), ^3J = 7.4 Hz); 7.42 (dd, 1H, H(10'), ^3J = 7.9 Hz,); 7.37 (d, 1H, H(4), ^3J = 8.0 Hz); 3.22 (m, 2H, H(7)); 2.83 (dd, 1H, H(10), ^3J = 5.6 Hz); 2.71 (ddd, 1H, $H(9_b)$); 2.40 (ddt, 1H, H(8), ^3J = 3.2 Hz); 1.42 (s, 3H, H(12)); 1.32 (d, 1H, $H(9_a)$, $^3J_{9a,9b}$ = 9.5Hz); 0.68 (s, 3H, H(13)).

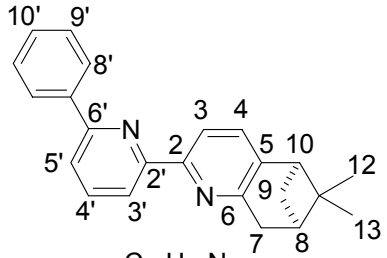

X-ray crystallography

Suitable crystals of **L7** were grown from acetone as colourless blocks. Intensity data was collected at room temperature on a Stoe AED2 4-circle diffractometer using MoKα graphite monochromated radiation (λ = 0.71073 Å) with ω/2Θ scans in the 2Θ range 5 - 55°. The structure was solved by direct methods using the programme SIR-97.[142] The refinement and all further calculations were carried out using SHELXL-97.[141] H-atoms were located from difference Fourier maps and refined isotropically. The non-H atoms were refined anisotropically, using weighted full-matrix least-squares on F^2 .

The absolute structure of the molecule in the crystal was assigned to the known absolute configuration of the pinene-moiety. The bond distances and angles are normal within experimental error.

3.9. {6'-Phenyl}-[4,5]-pinene-bpy (L8)

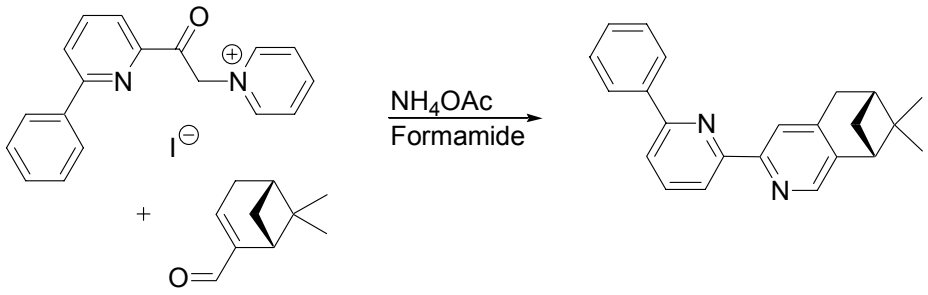

A mixture of (2-acetyl-6-phenylpyridyl)-pyridinium iodide (**33**) (0.80 g, 2.0 mmole), ammonium acetate (0.8 g, dried under vacuum) and *R,R*-(-)-myrtenal (**2**) (0.30 g, 2.0 mmole) was suspended in formamide (10 ml) and slowly heated over 20 hours from 50°C up to 115°C. To the reaction mixture, water (50 ml) was added and extracted five times with dichloromethane. The combined organic layers were washed with water and dried over magnesium sulfate with activated charcoal. The solvent was evaporated under reduced pressure. The residual solid was further purified by column chromatography: (hexane/ ethyl acetate/ trimethylamine: 4/1/0.25) giving 0.19 g (52 %) of the desired product **L8**.

^{1}H-NMR (300 MHz, $CDCl_3$): δ 8.41 (s, 1H, H(3)); 8.33 (d, 1H, H(3'), $^{3}J_{3',4'}$ = 7.8 Hz); 8.21 (s, 1H, H(6)); 8.14 (dd, 2H, H(8'), H(12'), $^{3}J_{8',9'}$ = 8.2 Hz); 7.85 (dd, 2H, H(4'), $^{3}J_{4',5'}$ = 7.8 Hz. $^{3}J_{4',3'}$ = 7.8 Hz); 7.72 (d, 1H, H(5'), $^{3}J_{5',4'}$ = 7.8 Hz); 7.50 (dd, 2H, H(9'), H(11'), $^{3}J_{9',8'}$ = 8.2 Hz, $^{3}J_{9',10'}$= 8.2 Hz); 7.42 (dd, 1H, H(10'), $^{3}J_{10',9'}$ = 8.2 Hz); 3.09 (d, 1H, H(7), $^{3}J_{7,8}$ = 2.8 Hz); 2.87 (dd, 1H, H(10), $^{3}J_{10,9b}$ = 5.6 Hz, $^{4}J_{10,8}$ = 5.6 Hz); 2.70 (ddd, 1H, $H(9_b)$, $^{2}J_{9b,9a}$ = 9.6 Hz, $^{3}J_{9b,8}$ = 5.6 Hz, $^{3}J_{9b,10}$ = 5.6 Hz); 2.33 (ddt, 1H, H(8), $^{3}J_{8,9b}$ = 5.5 Hz, $^{4}J_{8,10}$ = 5.6 Hz, $^{3}J_{8,7}$ = 2.8 Hz); 1.42 (s, 3H, H(12)); 1.25 (d, 1H, $H(9_a)$, $^{3}J_{9a\text{-}9b}$ = 9.6 Hz); 0.66 (s, 3H, H(13)).

^{13}C-NMR (100MHz, $CDCl_3$): δ 156.4 (Cq); 156.1 (Cq); 154.5 (Cq); 145.5 (Cq); 145.3 (CH, C(6)); 143.1 (Cq); 139.5 (Cq); 137.6 (CH, C(4')); 128.9 (CH, C(10')); 128.7 (CH, C(9'), C(11')); 127.0 (CH, C(8'), C(12')); 120.7 (CH, C(3)); 119.9 (CH, C(5')); 119.1 (CH, C(3')); 44.6 (CH, C(10)); 40.1 (CH, C(8)); 39.3 (Cq, C(11)); 33.1 (CH_2, C(7)); 31.8 (CH_2, C(9)); 26.0 (CH_3, C(12)); 21.4 (CH_3, C(13)).

MS(ESI): m/z = 327 (M^+)

UV/Vis: ($CHCl_3$), λ (ε): 300 nm ($1.7*10^4$), 253 nm ($2.4*10^4$).

Elemental analysis calculated C: 84.63% H: 6.79% N: 8.58%, found C: 84.47%, H: 7.05%, N: 8.48%.

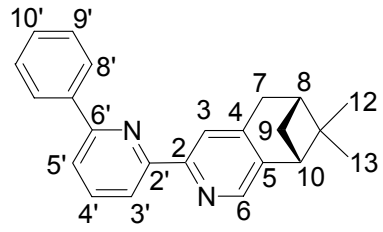

$C_{23}H_{22}N_2$
326.43

3.10. {6'-*p*-Methoxyphenyl}-[5,6]-pinene-bpy (L9)

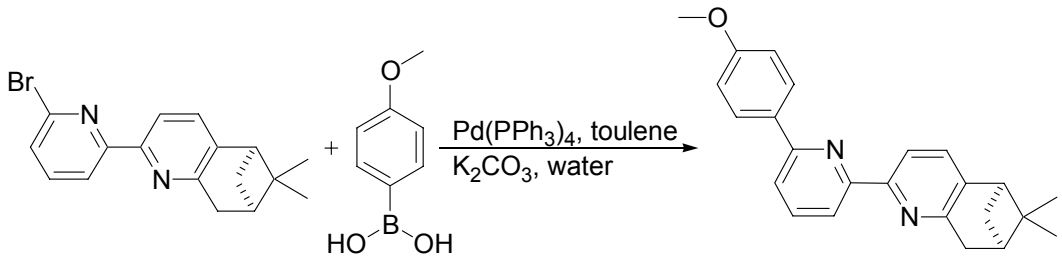

A mixture of {6'-bromo}-[5,6]-pinene-bpy (**L5**) (3.3 g, 10 mmole), *p*-methoxyphenylboronic acid (1.65 g, 10 mmole) and $Pd(PPh_3)_4$ (0.2% eq) as catalyst, was heated at 120 °C for 4 days in a mixture of toluene (100 ml) and an aqueous solution of K_2CO_3 (50 ml, 8.5 M). After cooling to room temperature the two layers were separated and the aqueous layer extracted three times with dichloromethane. The combined organic layers were washed until pH=7 with water, dried over magnesium sulfate and the solvent was evaporated. Without further purification pure **L9** (3.59 g, 99%) was obtained.

^{1}H-NMR (400 MHz, $CDCl_3$): δ 8.29 (d, 1H, H(3), $^3J_{3,4}$ = 7.8 Hz); 8.28 (d, 1H, H(3'), $^3J_{3',4'}$ = 7.8 Hz,) 8.10 (d, 2H, H(8'), H(12'), $^3J_{8',9'}$ = 8.8 Hz); 7.81 (dd, 1H, H(4'), $^3J_{4',5'}$ = 7.8 Hz, $^3J_{4',3'}$ = 7.8 Hz); 7.42 (d, 1H, H(5'), $^3J_{5',4'}$ = 7.8 Hz); 7.35 (d, 1H, H(4), $^3J_{4,3}$ = 7.8 Hz); 7.01 (d, 2H, H(9'), H(11'), $^3J_{9',11}$ = 8.8 Hz); 3.87 (s, 3H, H(13')); 3.19 (d, 1H, H(7), $^3J_{7,8}$ = 2.8 Hz); 2.82 (dd, 1H, H(10), $^3J_{10,9b}$ = 5.8 Hz, $^4J_{10,8}$ = 5.8 Hz); 2.71 (ddd, 1H, H(9_b), $^2J_{9b,9a}$ = 9.6 Hz, $^3J_{9b,10}$ = 5.8 Hz, $^3J_{9b,8}$ = 5.8 Hz); 2.40 (ddt, 1H, H(8) $^3J_{8,9b}$ = 5.8 Hz, $^4J_{8,10}$ = 5.8 Hz, $^3J_{8,7}$ = 2.8 Hz); 1.42 (s, 3H, H(12)); 1.32 (d, 1H, H(9_a), $^2J_{9a,9b}$ = 9.6 Hz); 0.69 (s, 3H, H(13)).

^{13}C-NMR (100 MHz, $CDCl_3$): δ 160.4 (Cq); 156.2 (Cq); 156.1 (Cq); 155.9 (Cq); 153.8 (Cq); 142.2 (Cq); 137.4 (CH, C(4')); 133.7 (CH, C(4)); 132.2 (Cq); 128.2 (CH, C(8'), C(12')); 118.9 (CH, C(5')); 118.3 (CH, C(3)); 118.0 (CH, C(3')); 114.0 (CH, C(9'), C(11')); 55.3 (CH_3, C(13')); 46.5 (CH, C(10)); 40.3 (CH, C(8)); 39.5 (Cq, C(11)); 36.7 (CH_2, C(7)); 31.9 (CH_2, C(9)); 26.1 (CH_3, C(12)); 21.3 (CH_3, C(13)).

UV/Vis: ($CHCl_3$), λ (ε): 281 nm ($2.8*10^4$).

MS-FAB (Matrix: NBA) : m/z = 357 (M^+, 100%) ; 154 ($C_{11}H_8N^+$, 10%), 136 (6%).

Elemental analysis calculated C: 80.87%, H: 6.79%, N : 7.86%, found C: 81.22%, H: 6.80%, N: 7.45%.

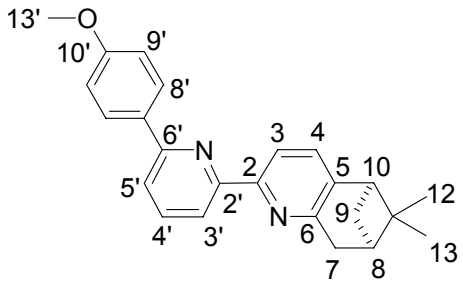

$C_{24}H_{24}N_2O$
356.46

X-ray crystallography

Suitable crystals of **L9 * $CHCl_3$ solvate** were obtained as colourless plates by slow evaporation. The intensity data was collected at 153K on a Stoe Image Plate Diffraction System[138] using MoKα graphite monochromated radiation. Image plate distance 70mm, ϕ oscillation scans 0 - 200°, step Δϕ = 1.0°, 2θ range 3.27 – 52.1°, d_{max} -d_{min} = 12.45 - 0.81 Å. The structure was solved by direct methods using the programme SHELXS-97.[139] The refinement and all further calculations were carried out using SHELXL-97.[140] The H-atoms were located from Fourier difference maps and refined isotropically. The non-H atoms were refined anisotropically, using weighted full-matrix least-squares on F^2.

Owing to the anomalous dispersion of the chlorine atoms in the $CHCl_3$ solvate molecule, present per molecule of **L9**, the absolute configuration of the molecule in the crystal could be determined.

3.11. {2-DAMI}-[5,6]-pinene-py (L10)

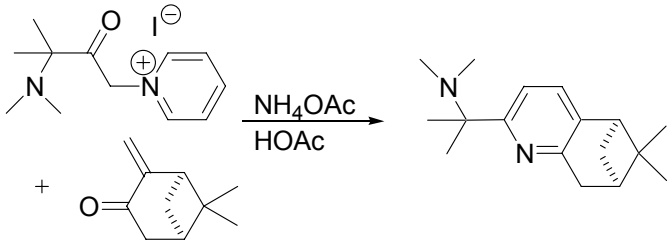

A mixture of 1-(3-dimethylamino-3-methyl-2-oxo-butyl)-pyridinium iodide (**34**) (8.6 g, 25 mmole), ammonium acetate (23.1 g, dried under vacuum) and *R,R*-(+)-pinocarvone (**1**) (4.5 g, 47 mmole) was suspended in acetic acid (100 ml) and slowly heated over 20 hours from 50 °C up to 115 °C. After addition of water, the pH was adjusted to 9 by addition of sodium carbonate. This aqueous solution was extracted ten times with hexane and the combined organic layers were washed with water and dried over magnesium sulfate with activated charcoal. A viscous liquid (1.6 g, 29 %) was obtained after purification by column chromatography: (hexane/ ethyl acetate/ trimethylamine: 5/1/0.1).

^{1}H-NMR (400 MHz, $CDCl_3$): δ = 7.2 (d, 1H, H(3), $^3J_{3,4}$ = 7.8 Hz); 7.09 (d, 1H, H(4), $^3J_{4,3}$ = 7.8 Hz); 3.06 (d, 1H, H(7), $^3J_{7,8}$ = 2.7 Hz); 2.69 (dd, 1H, H(10), $^3J_{10,9b}$ = 5.7 Hz, $^4J_{10,8}$ = 5.7 Hz); 2.62 (ddd, 1H, H(9_b), $^2J_{9b,9a}$ = 9.2 Hz, $^3J_{9b,10}$ = 5.7 Hz, $^3J_{9b,8}$ = 5.7 Hz); 2.38 (ddt, 1H, H(8) $^3J_{8,9b}$ = 5.7 Hz, $^4J_{8,10}$ = 5.7 Hz, $^3J_{8,7}$ = 2.8 Hz); 2.18 (s, 6H, H(5'), H(6')); 1.38 (s, 6H, H(2'), H(3')); 1.37 (s, 3H, H(12)); 1.25 (d, 1H, H(9_a), $^2J_{9a,9b}$ = 9.2 Hz); 0.61 (s, 3H, H(13)).

MS(ESI): m/z = 259.2(HM^+).

Elemental analysis calculated C: 79.02%, H: 10.14%, N: 10.84%, found C: 79.52%, H: 10.1%, N: 11.91%.

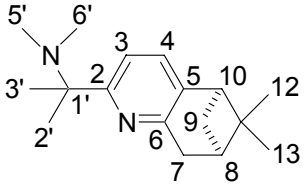

$C_{17}H_{26}N_2$
258.40

3.12. {5'-*p*-Methoxyphenyl}-[5,6]-CHIRAGEN[*p*-xyl] (L11)

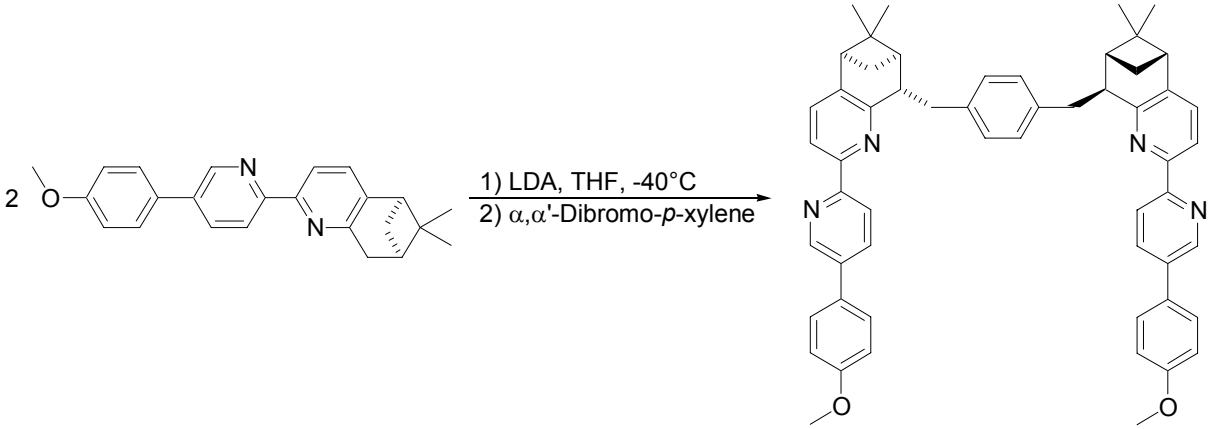

To dry THF (40 ml) at –40 °C diisopropylamine (0.2 ml, 1.4 mmole) was added, followed by *n*-butyllithium (0.85 ml, 1.35 mmole, 1.6 M in hexane). The temperature was allowed to increase to 0 °C for 30 minutes and then lowered to –40 °C. {5'-*p*-Methoxyphenyl}-[5,6]-pinene-bpy (**L3**) (400 mg, 1.12 mmole) dissolved in dry THF (10 ml) was added dropwise over 1 hour. After stirring the solution at –40 °C for 2 hours, *α,α'*-dibromo-*p*-xylene (148 mg, 0.56 mmole) dissolved in THF (10 ml) was injected slowly (1 hour). The solution was warmed gradually to room temperature, quenched by water (50 ml). The aqueous solution was extracted three times with diethyl ether. The combined organic layers were dried over magnesium sulfate, and the solvent was evaporated. The residual solid was further purified by column chromatography or recrystallization (hexane/ethyl acetate/trimethylamine: 1/1/0.5), yielding a slightly yellow powder (303 mg, 64%) .

^{1}H-NMR (400 MHz, $CDCl_3$): δ 8.86 (dd, 2H, H(6'), $^4J_{6',4'}$ = 2.4 Hz, $^5J_{6',3'}$ = 0.6 Hz); 8.50 (b, 2H, H(3') $^3J_{3',4'}$ = 8.3 Hz, $^5J_{3',6'}$ = 0.6 Hz); 8.14 (d, 2H, H(3), $^3J_{3,4}$ = 7.8 Hz); 7.94 (dd, 2H, H(4'), $^3J_{4',3'}$ = 8.3 Hz, $^4J_{4',6'}$ = 2.4 Hz); 7.59 (d, 2H, H(9'), H(11'), $^3J_{9',8'}$ = 8.7 Hz); 7.35 (d, 2H, H(4), $^3J_{4,3}$ = 7.8 Hz); 7.28 (s, 4H, H(3''), H(4''), H(5''), H(6'')); 7.01 (d, 4H, H(8'), H(12'), $^3J_{8',9'}$ = 8.8 Hz); 3.86 (m, 2H, H(1_b'')); 3.85 (s, 6H, H(13')); 3.43 (ddd, 2H, H(7) $^3J_{7,1a''}$ = 10.8 Hz, $^3J_{7,1b''}$ = 2.7 Hz, $^3J_{7,8''}$ = 2.7 Hz); 2.82 (dd, 2H, H(10), $^3J_{10,9b}$ = 5.6 Hz, $^4J_{10,8}$ = 5.6 Hz); 2.76 (dd, 2H, H(1_a''), $^2J_{1a'',1b''}$ = 13.6 Hz, $^3J_{1a'',7}$ = 10.8 Hz); 2.59 (ddd, 2H, H(9_b), $^2J_{9b,9a}$ = 9.8 Hz, $^3J_{9b,10}$ = 5.6Hz, $^3J_{9b,8}$ = 5.6 Hz); 2.18

(ddd, 2H, H(8), $^{3}J_{8,9b}$ = 5.6 Hz, $^{4}J_{8,10}$ = 5.6 Hz, $^{3}J_{8,7}$ = 2.7 Hz); 1.45 (d, 2H, H(9_a), $^{2}J_{9a,9b}$ = 9.8 Hz); 1.36 (s, 6H, H(12)); 0.64 (s, 6H, H(13)).

^{13}C-NMR (100 MHz, $CDCl_3$): δ 159.7 (Cq); 158.8 (Cq); 155.1 (Cq); 153.1 (Cq); 147.1 (CH, C(6')); 142.2 (Cq); 138.6 (Cq); 135.4 (Cq)); 134.5 (CH, C(4')); 133.7 (CH, C(4)); 130.3 (Cq); 129.3 (CH, C(3'')); 128.1 (CH, C(9'), C(11')); 120.7 (CH, C(3')); 117.8 (CH, C(3)); 114.6 (CH, C(8'), C(12')); 55.4 (CH_3, C(13')); 46.9 (CH, C(10)); 46.2 (CH, C(7)); 42.7 (CH_2, C(8)); 41.2 (Cq, C(11)); 38.5 (CH_2, C(1'')); 28.4 (CH_2, C(9)); 26.3 (CH_3, C(12)); 20.9 (CH_3, C(13)).

MS(ESI): m/z = 815 (M^+)

UV/Vis: ($CHCl_3$), λ (ε): 317 nm ($7.1*10^4$), 272 nm ($2.6*10^4$; sh).

Elemental analysis calculated C:82.52%; H:7.10%, N: 6.87% , found C:81.59%, H:7.10%, N: 6.63%.

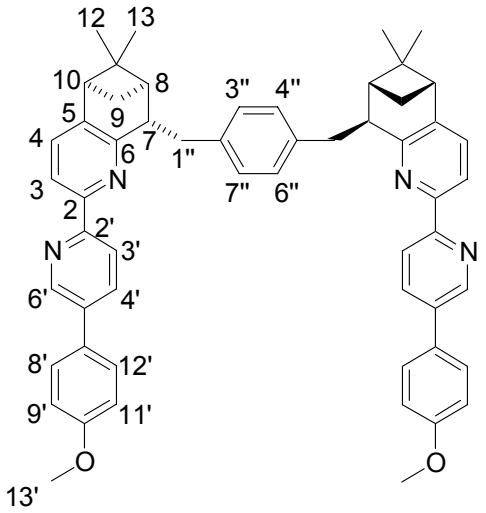

3.13. {6'-Phenyl}-[5,6]-CHIRAGEN[*p*-xyl] (L12)

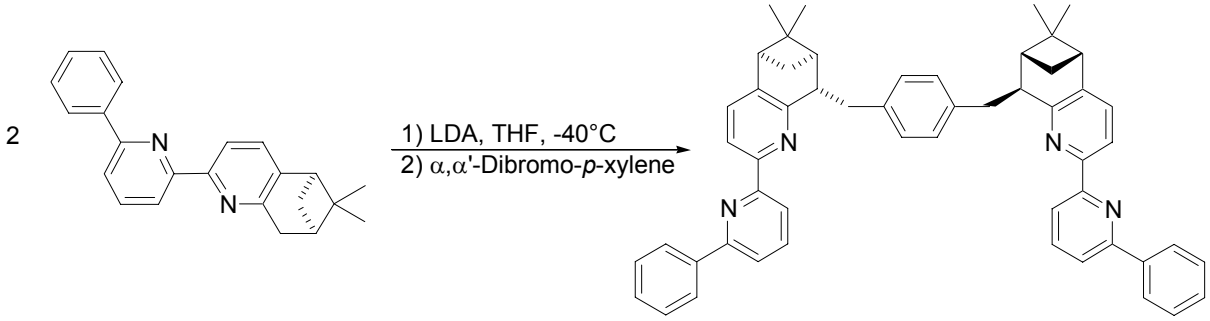

To dry THF (5 ml) at –20 °C diisopropylamine (0.41 ml, 2.9 mmole) was added, followed by *n*-butyllithium (1.6 ml, 1.9 mmole, 1.2 M in hexane). The temperature was allowed to increase to room temperature for 20 minutes and then lowered to –40 °C. {6'-phenyl}-[5,6]-pinene-bpy (**L7**) (500 mg, 1.53 mmole) dissolved in 5 ml dry THF was added dropwise over 1 hour). After stirring the solution at –40 °C for 3 hours, *α,α'*-dibromo-*p*-xylene (202 mg, 0.77 mmole) dissolved in THF (8 ml) was injected slowly (1 hour). The solution was warmed gradually to room temperature, quenched by water (3 ml). The solvent was removed under reduced pressure and a saturated aqueous solution of $NaHCO_3$ (10ml) was added to the resulting solid. The aqueous solution was extracted three times with dichloromethane. The combined organic layers were dried over magnesium sulfate, and the solvent was evaporated under reduced pressure. The residual solid was further purified by column chromatography (hexane/ ethyl acetate/ trimethylamine: 2/1/0.1) yielding the desired product **L12** (395 mg, 68%).

^{1}H-NMR (300 MHz, $CDCl_3$): δ 8.48 (d, 2H, H(3'), $^3J_{3',4'}$ = 7.7 Hz); 8.39 (d, 2H, H(3), $^3J_{3,4}$ =7.7 Hz); 8.17 (dd, 4H, H (8'), H(12'), $^3J_{8',9'}$ = 7.0 Hz); 7.90 (dd, 2H, H (4'), $^3J_{4',3'}$ = 7.7 Hz, $^3J_{4',5}$ = 7.8 Hz); 7.76 (d, 2H, H (5') $^3J_{5',4'}$ = 7.8 Hz); 7.52 (dd, 4H, H (9'), H(11'), $^3J_{9',10'}$ = 7.8 Hz, $^3J_{9',8'}$ = 7.0 Hz); 7.47-7.36 (m, 2H, H(10'), $^3J_{10',9'}$ = 7.8 Hz); 7.38 (s, 4H, H(3''), H(4''), H(5''), H(6'')); 3.87 (dd, 2H, H (1''b), $^2J_{1b'',\,1a''}$ = 13.5 Hz, $^3J_{1b'',7}$ = 3.6 Hz); 3.44 (d (broad), 2H, H(7) $^3J_{7,1a''}$ = 11.0 Hz, $^3J_{7,\,1b''}$ = 3.6 Hz); 2.83 (dd, 2H, H (10), $^3J_{10,9b}$ = 5.5 Hz, $^3J_{10,8}$ = 5.5 Hz); 2.75 (dd, 2H, H(1''a), $^2J_{,\,1a'',\,1b''}$ = 13.5 Hz, $^3J_{,\,1a'',7}$ = 11.0 Hz); 2.58 (ddd 2H, H(9b), $^2J_{9b,9a}$ = 9.9 Hz, $^3J_{9b,8}$ = 5.5 Hz, $^3J_{9b,10}$

= 5.5 Hz); 2.18 (m, 2H, H(8)); 1.46 (d, 2H, H(9a), $^{2}J_{9a,9b}$ = 9.9 Hz); 1.37 (s, 6H, H(12)); 0.70 (s, 6H, H(13));

^{13}C-NMR (75.4 MHz, $CDCl_3$): δ 158.8 (Cq); 156.5 (Cq); 153.6 (Cq); 142.6 (Cq); 139.8 (Cq); 138.8 (Cq); 137.7 (CH, C(4')); 134.0 (CH, C(4)); 132.4 (Cq); 129.5 (CH, C(3'')); 129.1 (CH, C(8')); 128.9 (CH, C(10')); 127.1 (CH, C(3')); 119.9 (CH, C(5')); 119.4 (CH, C(3)); 118.5 (CH, C(9')); 47.2 (CH, C10); 46.4 (CH, C7); 43.0 (CH, C8); 41.4 (Cq, C11); 38.7 (CH_2, C1''); 28.6 (CH_2, C9); 26.5 (CH_3, C12); 21.2 (CH_3, C13);

FAB-MS (Matrix: NBA): m/z = 755 (M^+); 325 (M^+-$C_{24}H_{28}N_2$).

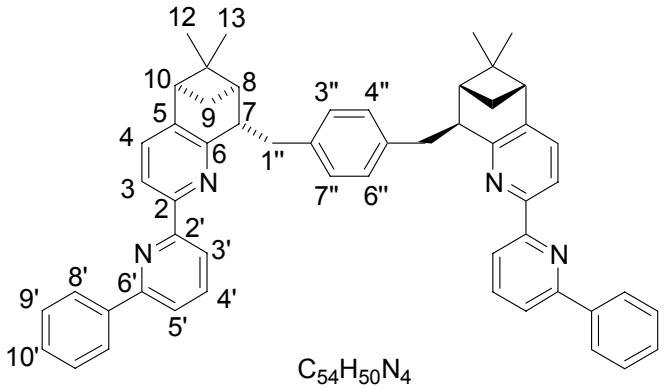

X-ray crystallography

Suitable crystals of **L12** were grown from methanol/dichloromethane as colourless rods. Intensity data was collected at 153K on a Stoe Image Plate Diffraction system equipped with a ϕ circle, using MoKα graphite monochromated radiation. Image plate distance 70mm, ϕ oscillation scans 0 - 200°, step Δϕ = 1°, 2θ range 3.27 – 52.1°, d_{max} - d_{min} = 12.45 - 0.8 1 Å. The structure was solved by direct methods using the programme SHELXS-97.[139] The refinement and all further calculations were carried out using SHELXL-97.[140] The H-atoms were located from difference Fourier maps and refined isotropically. The non-H atoms were refined anisotropically, using weighted full-matrix least-squares on F^2. The absolute structure of the molecule in the crystal was assigned to the known absolute configuration of the pinene-moiety.

3.14. {6'-*p*-Methoxyphenyl}-[5,6]-CHIRAGEN[*p*-xyl] (L13)

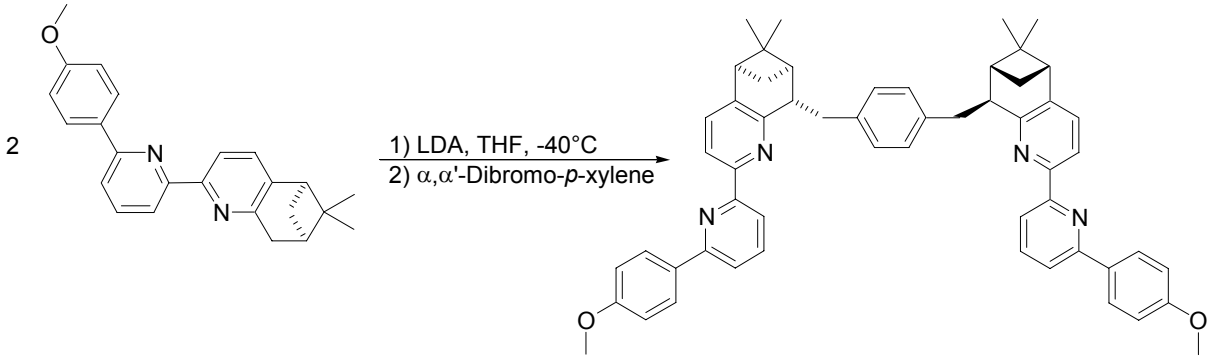

To dry THF (20 ml) at –20 °C diisopropylamine (0.6 ml, 4 mmole) was added, followed by *n*-butyllithium (2.1 ml, 3.4 mmole, 1.6 M in hexane). The temperature was allowed to increase to 0 °C for 30 minutes and then lowered to –40 °C. {6'-*p*-Methoxyphenyl}-[5,6]-pinene-bpy (**L9**) (1.0 g, 2.8 mmole) dissolved in dry THF (10 ml) was added dropwise over 1 hour. After stirring the solution at –40 °C for 2 hours *α,α'*-dibromo-*p*-xylene (0.37 g, 1.4 mmole) dissolved in THF (8 ml) was injected slowly (1 hour). The solution was warmed gradually to room temperature, quenched by water (3 ml), followed by addition of dichloromethane and a saturated aqueous solution of $NaHCO_3$. The aqueous solution was extracted three times with dichloromethane. The combined organic layers were dried over magnesium sulfate, and the solvent was evaporated. The residual solid was further purified by filtration over over silica gel (hexane/ethyl acetate/triethylamine : 8/1/0.5), yielding of **L19** (1.35 g, 95%).

^{1}H-NMR (400 MHz, $CDCl_3$): δ 8.39 (d, 2H, H(3'), $^3J_{3',4'}$ = 7.8 Hz); 8.35 (d, 2H, H(3), $^3J_{3,4}$ = 7.8 Hz); 8.12 (d, 4H, H(8'), H(12'), $^3J_{8',9'}$ = 8.8 Hz); 7.83 (dd, 2H, H(4'), $^3J_{4',3'}$ = 7.8 Hz, $^3J_{4',5'}$ = 7.8 Hz); 7.67 (d, 2H, H(5'), $^3J_{5',4'}$ = 7.8 Hz); 7.37 (d, 2H, H(4), $^3J_{4,3}$ = 7.8 Hz); 7.29 (s, 4H, H(3''), H(4''), H(6''), H(7'')); 7.02 (d, 4H, H(9'), H(11''), $^3J_{9',8'}$ = 8.8 Hz); 3.87 (s, 6H, H(13')); 3.86 (m, 2H, H(1_b'')); 3.43 (ddd, 2H, H(7), $^3J_{7,1b''}$ = 10.8 Hz, $^3J_{7,1a''}$ = 2.7 Hz, $^3J_{7,8}$ = 2.7 Hz); 2.82 (dd, 2H, H(10), $^3J_{10,9b}$ = 5.6 Hz, $^4J_{10,8}$ = 5.6 Hz); 2.74 (dd, 2H, H(1a''), $^2J_{1a'',1b''}$ = 13.6 Hz, $^3J_{1a'',7}$ = 10.8 Hz); 2.59 (ddd, 2H, H(9_b), $^2J_{9b,9a}$ = 9.8 Hz, $^3J_{9b,\ 10}$ = 5.6 Hz, $^3J_{9b,\ 8}$ = 5.6 Hz); 2.18 (ddd, 2H, H(8), $^3J_{8,9b}$ = 5.6

Hz, $^{4}J_{8,10}$ = 5.6 Hz, $^{3}J_{8,7}$ = 2.7 Hz); 1.45 (d, 2H, H(9a) $^{2}J_{9a,9b}$ = 9.8 Hz); 1.37 (s, 6H, H(12)); 0.65 (s, 6H, H(13)).

^{13}C-NMR (75MHz, $CDCl_3$): δ160.4 (Cq); 158.6 (Cq); 156.2 (Cq); 155.9 (Cq); 153.6 (Cq); 142.2 (Cq); 138.6 (Cq); 137.4 (CH, C(4')); 133.6 (CH, C(4)); 132.3 (Cq); 129.2 (CH, C(3'), C(4'), C(6'), C(7')); 128.2 (CH, C(8'), C(12')); 118.9 (CH, C(5')); 118.4 (CH, C(3')); 118.1 (CH, C(3)); 114.0 (CH, C(9'), C(11')); 55.4 (CH_3, C(13')); 47.0 (CH, C(10)); 46.2 (CH, C(7)); 42.7 (CH, C(8)); 41.2 (Cq, C(11)); 38.5 (CH_2, C(1'')); 28.4 (CH_2, C(9)); 26.3 (CH_3, C(12)); 20.9 (CH_3, C(13)).

MS-FAB (Matrix: NBA): m/z = 816 (MH^+, 82%); 355 (M^+/2-bridge, 100%); 341 (M^+/2-bridge- CH_2, 95%); 154 ($C_{11}H_8N^+$, 23%)

UV/Vis: ($CHCl_3$), λ (ε): 279 nm ($5.2*10^4$)

Elemental analysis calculated C: 82.52%, H: 6.68%, N: 6.87%, found C: 82.40%, H: 6.76%, N: 6.2%.

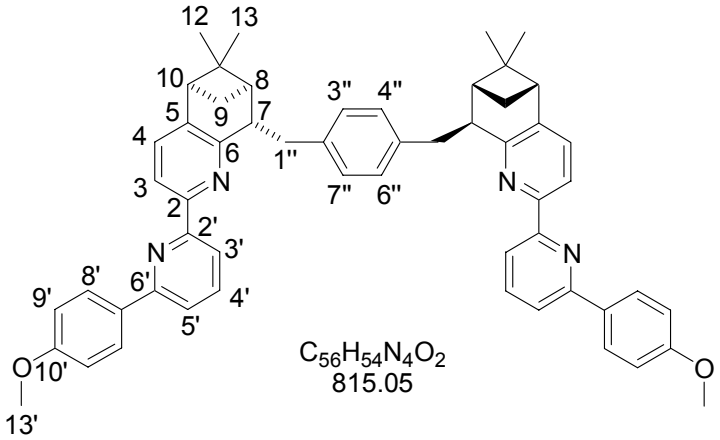

3.15. {6'-*p*-Methoxyphenyl}-[5,6]-CHIRAGEN[*m*-xyl] (L14)

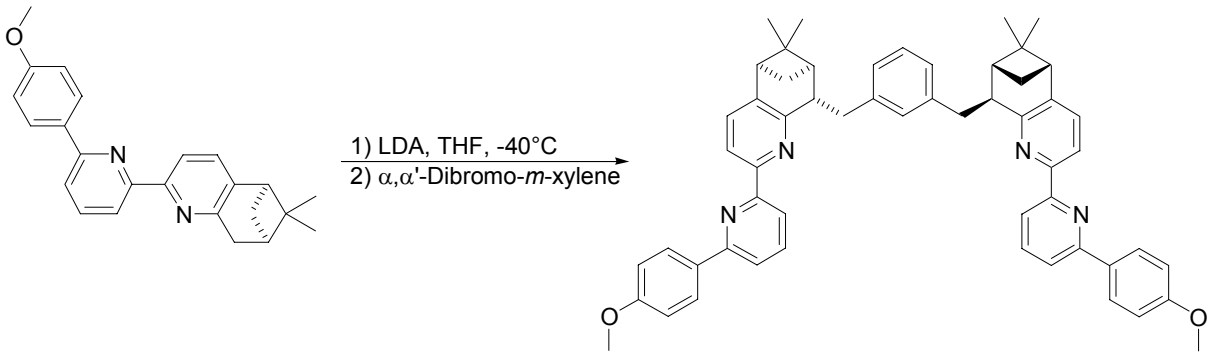

To dry THF (20 ml) at –20 °C diisopropylamine (0.6 ml, 4 mmole) was added, followed by *n*-butyllithium (2.1 ml, 3.4 mmole, 1.6 M in hexane). The temperature was allowed to increase to 0 °C for 30 minutes and then lowered to –40 °C. {6'-*p*-Methoxyphenyl}-[5,6]-pinene-bpy (**L9**) (1.0 g, 2.8 mmole) dissolved in dry THF (10 ml) was added dropwise over 1 hour. After stirring the solution at –40 °C for 2 hours *α,α'*-dibromo-*m*-xylene (0.37 g, 1.4 mmole) dissolved in THF (8 ml) was injected slowly (1 hour). The solution was warmed gradually to room temperature, quenched by water (3 ml), followed by addition of dichloromethane and a saturated aqueous solution of $NaHCO_3$. The aqueous solution was extracted three times with dichloromethane. The combined organic layers were dried over magnesium sulfate, and the solvent was evaporated. After several purifications via column chromatography (Hexane/ ethyl acetate/ trimethylamine: 8/1/0.5) and via recrystallisation (chloroform/methanol) white crystals of **L14** (0.15g 13%) were obtained.

^{1}H-NMR (300 MHz, $CDCl_3$): δ8.39 (d, 2H, H(3'), $^3J_{3',4'}$ = 7.2 Hz); 8.34 (d, 2H, H(3), $^3J_{3,4}$ = 8 Hz); 8.12 (d, 4H, H(8'), H(12'), $^3J_{8',9'}$ = 8.8 Hz); 7.82 (dxd, 2H, H(4'), $^3J_{4',3'}$ = 7.1 Hz, $^3J_{4',5'}$ = 7.2 Hz); 7.66 (d, 2H, H(5'), $^3J_{5',4'}$ = 7.1 Hz); 7.37 (d, 2H, H(4), $^3J_{4,3}$ = 8 Hz); 7.32-7.25 (broad, 3H, H(3''), H(5''), H(7'')); 7.17 (d, 1H, H(6''), $^3J_{6'',5''}$ = 7.1 Hz); 7.02 (d, 4H, H(9'), H(11'), $^3J_{9',8'}$ = 8.8 Hz); 3.90 (m, 2H, H(1_b'')); 3.87 (s, 6H, H(13')); 3.43 (ddd, 2H, H(7), $^3J_{7,1a''}$ = 10.8 Hz, $^3J_{7,1b''}$ = 2.8 Hz, $^3J_{7,8}$ = 2.8 Hz); 2.82 (dxd, 2H, H(10), $^3J_{10,9b}$ = 5.6 Hz, $^4J_{10,8}$ = 5.6 Hz); 2.73 (dxd, 2H, H(1_a''), $^2J_{1a'',1b''}$ =

13.8 Hz, $^{3}J_{1a'',7}$ = 10.8 Hz); 2.57 (ddd, 2H, H(9b), $^{2}J_{9b,9a}$ = 9.6 Hz, $^{3}J_{9b,10}$ = 5.6 Hz, $^{3}J_{9b,8}$ = 5.6 Hz); 2.14 (ddd, 2H, H(8), $^{3}J_{8,9b}$ = 5.6 Hz, $^{4}J_{8,10}$ = 5.6 Hz, $^{3}J_{8,7}$ = 2.8 Hz); 1.47 (d, 2H, H(9_a), $^{2}J_{9a,9b}$ = 9.6 Hz); 1.36 (s, 6H, H(12)); 0.64 (s, 6H, H(13)).

UV/Vis: ($CHCl_3$), λ (ε): 280 nm ($4.9*10^4$)

Elemental analysis: calculated C: 82.52%, H: 6.68%, N: 6.87%, found C: 81.88%, H: 6.63%, N: 6.28%.

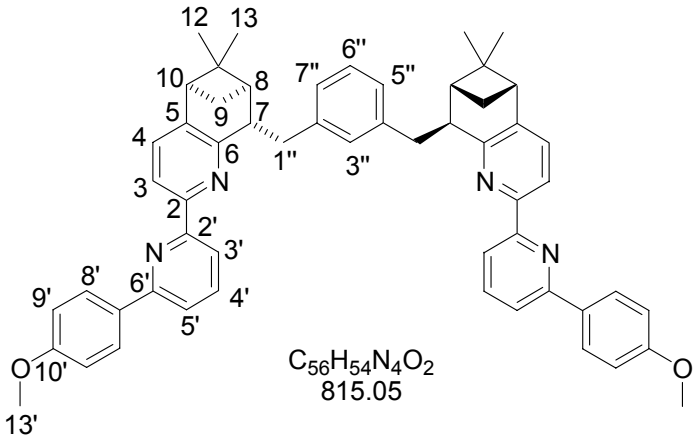

3.16. [5,6]-CHIRAGEN[0] (L15)

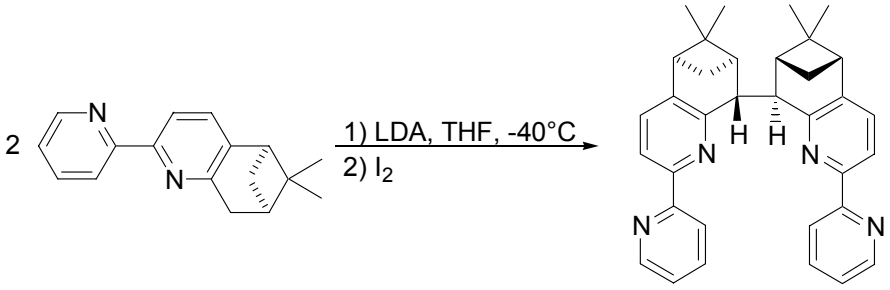

The synthesis of **L15** was carried out according to the published procedure. [60] To dry THF (20 ml) at –20 °C diisopropylamine (1.2 ml, 7.0 mmole) was added, followed by *n*-butyllithium (4.2 ml, 6.6 mmole 1.6 M in hexane). The temperature was allowed to increase to 0 °C for 30 minutes and then lowered to –40 °C. **L1** (1.5 g, 6 mmole) dissolved in dry THF (20 ml) was added dropwise over 1 hour. After stirring the solution at –40 °C for 2 hours of iodine (0.79 g, 3.1 mmole) dissolved in THF (20 ml) was injected slowly (1 hour). The solution was warmed gradually to room temperature, quenched by water (3 ml), followed by addition of dichloromethane and a saturated aqueous solution of $NaHCO_3$. The aqueous solution was extracted three times with dichloromethane. The combined organic layers were dried over magnesium sulfate, and the solvent was evaporated. The residual solid was further purified by recrystallization (chloroform/methanol) yielding pure **L15** (0.8 g, 54 %). The spectral properties correspond to those reported

^{1}H-NMR (300 MHz, $CDCl_3$): δ = 8.61 (ddd, 2H, H(6'), $^3J_{6',5'}$ = 4.8 Hz, $^4J_{6',4'}$ =1.8 Hz, $^5J_{6',3'}$ = 0.8 Hz), 8.33 (ddd, 2H, H(3'), $^3J_{3',4'}$ = 7.8 Hz), 8.02 (d, 2H, H(3), $^3J_{3,4}$ = 7.8 Hz), 7.71 (ddd, 2H, H(4'), $^3J_{4',3'}$ = 7.8 Hz, $^3J_{4',5'}$ =6.0 Hz, $^4J_{4',6'}$ = 1.8 Hz), 7.34 (d, 2H, H(4), $^3J_{4,3}$ = 7.8 Hz), 7.21 (ddd, 2H, H(5'), $^3J_{5',4'}$ = 6.0 Hz, $^3J_{5',6'}$ = 4.8 Hz, $^4J_{5',3'}$ = 1.2 Hz), 4.58 (s, broad, 2H, H(7)), 2.78 (dd, 2H, H(10), $^3J_{10,9b}$ = 5.7 Hz, $^4J_{10,8}$ = 5.7 Hz); 2.49 (ddd, 2H, H(9_b), $^2J_{9b,9a}$ = 9.6 Hz, $^3J_{9b,10}$ = 5.7 Hz, $^3J_{9b,8}$ = 5.7 Hz); 2.13 (dd, 2H, H(8) $^3J_{8,9b}$ = 5.7 Hz, $^4J_{8,10}$ = 5.7 Hz); 1.38 (d, 2H, H(9_a), $^2J_{9a,9b}$ = 9.6 Hz); 1.30 (s, 6H, H(12)), 0.76 (s, 6H, H(13)).

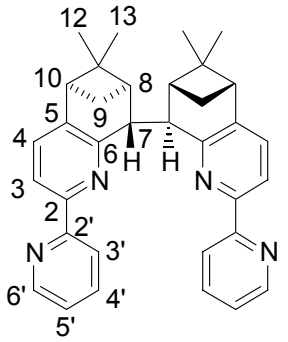

$C_{34}H_{34}N_4$
498.66

3.17. ^{15}N-[5,6]-CHIRAGEN[0] (^{15}N-L15)

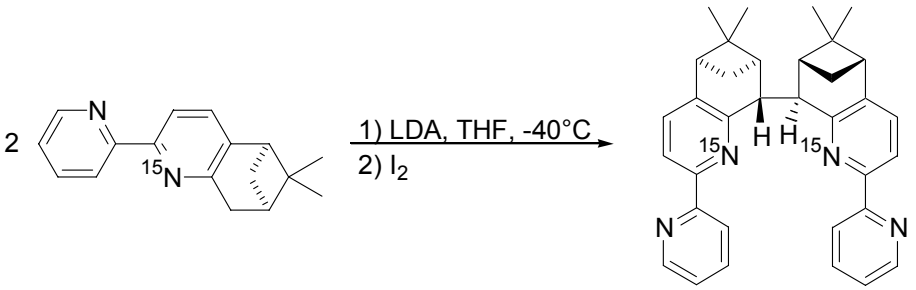

The same procedure as described above was used for the synthesis of the ^{15}N-**L15**, using ^{15}N-**L1** as starting material. ^{15}N-**L1** (0.4 mg, 1.6 mmole) lead after recrystallisation to the desired product ^{15}N-**L15** (290 mg,73%). The spectral data corresponds to that of the non-labelled compound (**L15**).

3.18. {5'-*p*-Methoxyphenyl}-[5,6]-CHIRAGEN[0] (L16)

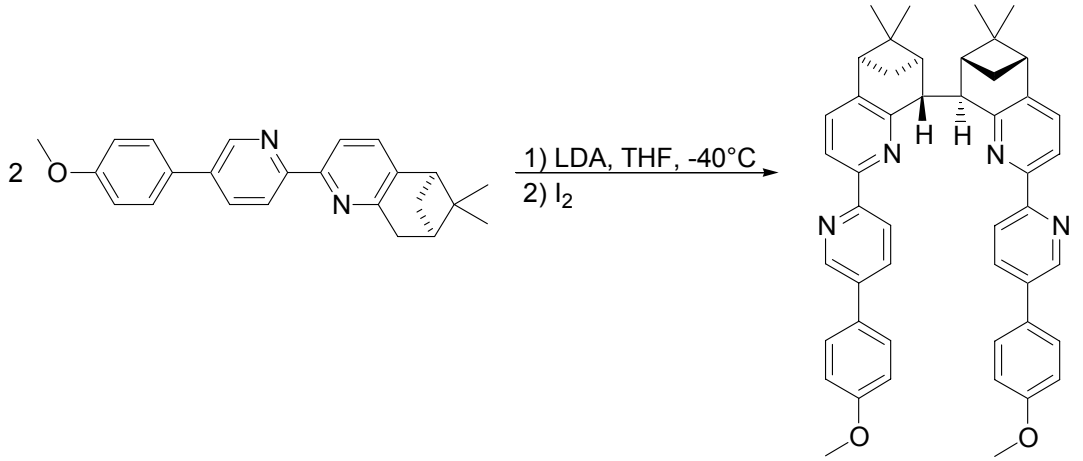

To dry THF (40 ml) at –40 °C diisopropylamine (0.2 ml, 1.4 mmole) was added, followed by *n*-butyllithium (0.85 ml, 1.35 mmole, 1.6 M in hexane). The temperature was allowed to increase to 0 °C for 30 minutes and then lowered to –40 °C. {5'-*p*-Methoxyphenyl}-[5,6]-pinene-bpy (**L3**) (400 mg, 1.12 mmole) dissolved in dry THF (10 ml) was added dropwise over 45 minutes. After stirring the solution at –40°C for 2 hours of iodine (148 mg, 0.56 mmole) dissolved in THF (10 ml) was injected slowly (1 hour). The solution was warmed gradually to room temperature, quenched by water (50 ml), followed by addition of dichloromethane and a saturated aqueous solution of $NaHCO_3$. The aqueous solution was extracted three times with diethyl ether. The combined organic layers were dried over magnesium sulfate, and the solvent was evaporated. The residual solid was further purified by column chromatography (Hexane/ ethyl acetate/ trimethylamine: 1/1/0.5) and recrystallisation yielding the desired product (63 mg, 16%) .

^{1}H-NMR (400 MHz, $CDCl_3$): δ 8.81 (br, 2H, H(6')); 8.37 (br, 2H, H(3')); 8.14 (d, 2H, H(3), $^3J_{3,4}$ = 7.7 Hz); 7.89 (dd, 2H, H(4'), $^3J_{4',3'}$ = 8.3 Hz, $^4J_{4',6'}$ = 2.2 Hz); 7.55 (d, 4H, H(9'), H(11'), $^3J_{9',8'}$ = 8.7 Hz); 7.37 (d, 2H, H(4), $^3J_{4,3}$ = 7.7 Hz); 6.99 (d, 4H, H(8'), H(12'), $^3J_{8',9'}$ = 8.7 Hz); 4.60 (br, 2H, H(7)); 3.84 (s, 6H, H(13')); 2.81 (dd, 2H, H(10), $^3J_{10,9b}$ = 5.5 Hz, $^4J_{10,8}$ = 5.5 Hz); 2.51 (m, 2H, H(9_b)); 2.16 (dd, 2H, H(8) $^3J_{8,9b}$ = 5.5 Hz, $^4J_{8,10}$ = 5.5 Hz); 1.43 (d, 2H, H(9_a)); 1.34 (s, 6H, H(12)); 0.79 (s, 6H, H(13)).

^{13}C-NMR (100 MHz, $CDCl_3$): δ 159.7 (Cq); 158.3 (Cq); 155.1 (Cq); 152.6 (Cq); 146.8 (CH, C(6')); 143.0 (Cq); 135.4 (Cq); 134.6 (CH, C(4')); 133.6 (CH, C(4)); 130.2 (Cq); 128.0 (CH, C(9'), C(11')); 120.7 (CH, C(3')); 117.6 (CH, C(3)); 114.5 (CH, C(8'), C(12')); 55.4 (CH_3, C(13')); 46.5 (CH, C(7)); 46.2 (CH, C(10)); 42.70 (Cq, C(11)); 41.9 (CH, C(8)); 29.0 (CH_2, C(9)); 26.3 (CH_3, C(12)); 21.0 (CH_3, C(13)).

MS(ESI): m/z = 711 (M^+)

UV/Vis: ($CHCl_3$), λ (ε): 319 nm ($7.1*10^4$), 274 nm ($2.5*10^4$; sh).

CD: ($CHCl_3$), λ (Δε): 332 (-87), 300 (61)

Elemental analysis calculated C: 81.10%, H: 6.52%, N: 7.88% , found C: 79.93%, H: 6.72%, N: 7.70% .

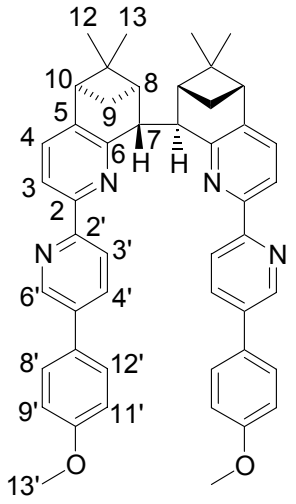

3.19. {6'-Phenyl}-[5,6]-CHIRAGEN[0] (L17)

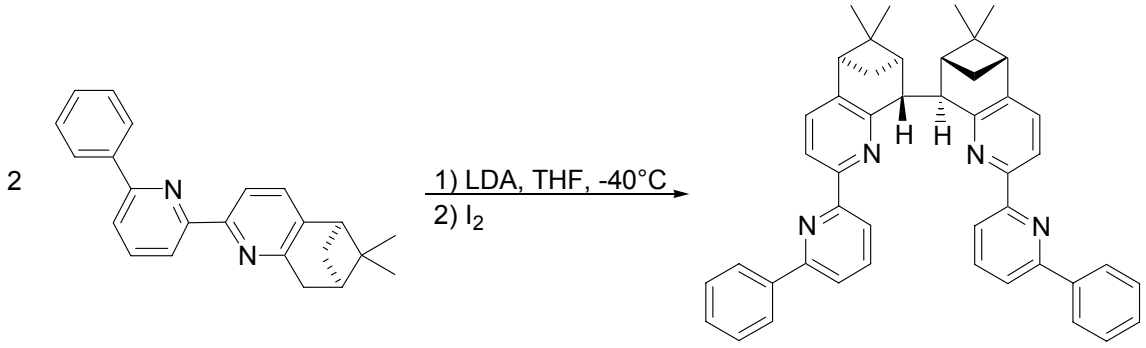

To dry THF (5 ml) at –20 °C diisopropylamine (0.33 ml, 2.3 mmole) was added, followed by *n*-butyllithium (1.9 ml, 2.1 mmole, 1.1 M in hexane). The temperature was allowed to increase to room temperature for 15 minutes and then lowered to –40 °C. {6'-Phenyl}-[5,6]-pinene-bpy (**L7**) (494 mg, 1.5 mmole) dissolved in dry THF (5 ml) was added dropwise over 1 hour). After stirring the solution at –40 °C for 4 hours iodine (192 mg, 0.76 mmole) dissolved in THF (5 ml) was injected slowly (15 minutes). The solution was warmed to room temperature overnight, quenched by water (2 ml). The solvent was removed under reduced pressure and a saturated aqueous solution of $NaHCO_3$ (10 ml) was added to the resulting solid. The aqueous solution was extracted three times with dichloromethane. The combined organic layers were dried over magnesium sulfate, and the solvent was evaporated under reduced pressure. The residual solid was further purified by recrystallization (methanol/ dichloromethane) yielding the pure compound **L17**(345 mg, 70 %) .

^{1}H-NMR (300 MHz, $CDCl_3$): δ 8.32 (d, 2H, H(3) $^3J_{3,4}$ = 7.8 Hz); 8.31 (br, 2H, H(3')); 8.14 (d, 4H, H(8'), H(12') , $^3J_{8',9'}$ = 7.3 Hz); 7.80 (dd, 2H, H(4'), $^3J_{4',3'}$ =7.8 Hz, $^3J_{4',5'}$ = 7.8 Hz); 7.69 (d, 2H, H(5'),$^3J_{5',4'}$ = 7.8 Hz); 7.49 (dd, 4H, H(9'), H(11'),$^3J_{9',8'}$ = 7.3 Hz, $^3J_{9',10'}$ =7.3 Hz); 7.41 (dd, 2H, H(10')); $^3J_{10',9'}$ =7.3 Hz); 7.38 (d, 2H, H(4) $^3J_{4,3}$ = 7.8 Hz); 4.65 (m, 2H, H(7)); 2.81 (dd, 2H, H(10), $^3J_{10,9b}$ = 5.6 Hz, $^4J_{10,8}$ = 5.6 Hz); 2.50 (ddd, 2H, H(9_b), $^2J_{9b,9a}$ = 9.8 Hz, $^3J_{9b,10}$ = 5.6Hz, $^3J_{9b,8}$ = 5.6 Hz)); 2.16 (dd, 2H, H(8), $^3J_{8,9b}$ = 5.6 Hz, $^4J_{8,10}$ = 5.6 Hz); 1.38 (b, 2H, H-C(9a)); 1.31 (s, 6H, H-C(12)); 0.79 (s, 6H, H(13)).

^{13}C-NMR (75 MHz, $CDCl_3$): δ 158.2 (Cq); 156.7 (Cq); 156.7.2 (Cq); 153.3 (Cq); 143.1 (Cq); 139.6 (Cq); 137.4 (CH, C(4')); 133.4 (CH, C(4)); 128.9 (CH, C(10')); 128.6 (CH, C(9'), C(11')); 126.9 (CH, C(8'), C(12')); 119.5 (CH, C(5')); 119.1 (CH, C(3')); 117.9 (CH, C(3)); 46.3 (CH, C(7)); 46.2 (CH, C(10)); 42.6 (CH, C(8)); 41.9 (Cq, C(11)); 29.1 (CH_2, C(9)); 26.3 (CH_3, C(12)); 21.0 (CH_3, C(13)).

FAB-MS (matrix: NBA): m/z = 651.6 (M^+); 575.3 (M-$C_6H_5^+$); 557.7 (M-$C_{12}H_{10}^+$); 326.4 ($C_{23}H_{21}N_2$, M/2$^+$); 283.3 (M/2-$C_3H_7^+$); 218.2 ($C_{14}H_{14}N_2^+$); 154.1 ($C_{10}H_6N_2^+$).

Elemental analysis calculated for $C_{46}H_{42}N_4$: C 84.89%, H 6.50%, N 8.61%; found C 83.33%, H 6.55%, N 8.43%.

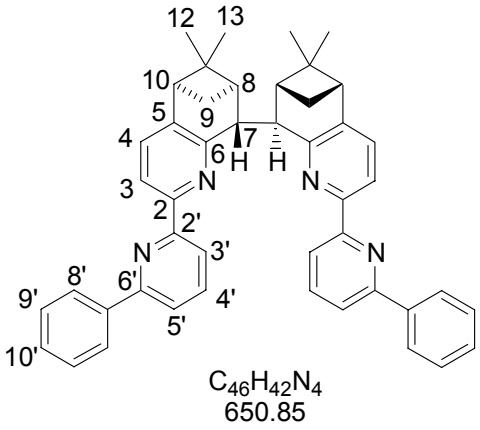

3.20. {6'-*p*-Methoxyphenyl}-[5,6]-CHIRAGEN[0] (L18)

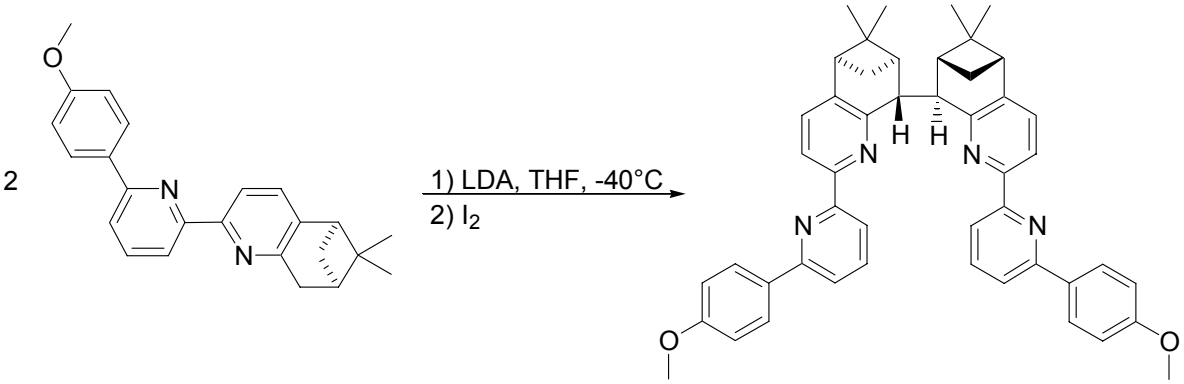

To dry THF (20 ml) at –20 °C diisopropylamine (0.6 ml, 4 mmole) was added, followed by *n*-butyllithium (2.1 ml, 3.4 mmole, 1.6 M in hexane). The temperature was allowed to increase to 0 °C for 30 minutes and then lowered to –40°C. {6'-*p*-Methoxyphenyl}-[5,6]-pinene-bpy (**L9**) (1.0 g, 2.8 mmole) dissolved in dry THF (10 ml) was added dropwise over 1 hour. After stirring the solution at –40 °C for 2 hours iodine (0.37 g, 1.4 mmole) dissolved in THF (8 ml) was injected slowly (1 hour). The solution was warmed gradually to room temperature, quenched by water (3 ml), followed by addition of dichloromethane and a saturated aqueous solution of $NaHCO_3$. The aqueous solution was extracted three times with dichloromethane. The combined organic layers were dried over magnesium sulfate, and the solvent was evaporated. The residual solid was further purified by recrystallization (methanol/chloroform), yielding white crystals (0.53 g, 53%)

^{1}H-NMR (400 MHz, $CDCl_3$): δ 8.31 (d, 2H, H(3), $^{3}J_{3,4}$ = 7.8 Hz); 8.25 (b, 2H, H(3')); 8.11 (d, 4H, H(8'), H(12'), $^{3}J_{8',9'}$ = 8.8 Hz); 7.76 (dd, 2H, H(4'), $^{3}J_{4',3'}$ = 7.8 Hz, $^{3}J_{4',5'}$ = 7.8 Hz); 7.62 (d, 2H, H(5'), $^{3}J_{5',4'}$ = 7.8 Hz); 7.37 (d, 2H, H(4), $^{3}J_{4,3}$ = 7.8 Hz); 7.01 (d, 4H, H(9'), H(11'), $^{3}J_{9',8'}$ = 8.8 Hz); 4.65 (b, 2H, H(7)); 3.87 (s, 6H, H(13'); 2.80 (dd, 2H, H(10), $^{3}J_{10,9b}$ = 5.6 Hz, $^{4}J_{10,8}$ = 5.6 Hz); 2.50 (ddd, 2H, H(9_b), $^{2}J_{9b,9a}$ = *9.8 Hz,* $^{3}J_{9b,10}$ = 5.6 Hz, $^{3}J_{9b,8}$ = 5.6 Hz); 2.16 (dd, 2H, H(8), $^{3}J_{8,10}$ = 5.6 Hz, $^{3}J_{8,9b}$ = 5.6 Hz), 1.38 (b, 2H, H(9_a)); 1.31 (s, 6H, H(12)); 0.79 (s, 6H, H(13)).

^{13}C-NMR (100 MHz, $CDCl_3$): δ 160.4 (Cq); 158.2 (Cq); 156.5 (Cq); 155.8 (Cq); 153.3 (Cq); 143.0 (Cq); 137.4 (CH, C(4')); 133.4 (CH, C(4)); 132.3 (Cq); 128.2 (CH,

C(8'), C(12')); 118.8 (CH, C(5'); 118.4 (CH, C(3')); 117.8 (CH, C(3)); 114.0 (CH, C(9'), C(11')); 55.4 (CH_3, C(13'); 46.3 (CH, C(7)); 46.2 (CH, C(10)); 42.6 (CH, C(8)); 41.8 (Cq, C(11)); 29.1 (CH_2, C(9)); 26.3 (CH_3, C(12)); 21.0 (CH_3,C(13)).

MS-FAB (Matrix: NBA) : m/z = 712 (M^+, 58%); 341 (M^+/2-Me, 26%); 307 (52%); 154 ($C_{11}H_8N^+$, 100%), 136 (93%).

UV/Vis: ($CHCl_3$), λ (ε): 280 ($5.3*10^4$).

CD: ($CHCl_3$), λ (Δε): 310 (-22), 287 (+32), 266 (-21.5)

Elemental analysis calculated: C: 81.10%, H: 6.52%, N: 7.88%, found C: 80.37%, H: 6.41%, N: 7.37%.

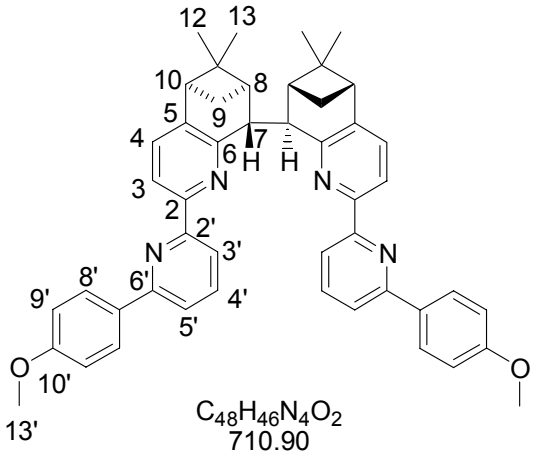

X-ray crystallography

Suitable crystals of **L18** were obtained as colourless rod-like crstals by evaporation of a chloroform solution. The intensity data was collected at 153K on a Stoe Image Plate Diffraction System[138] using MoKα graphite monochromated radiation. Image plate distance 70mm, ϕ oscillation scans 0 - 200°, step Δϕ = 1.0°, 2θ range 3.27 – 52.1°, d_{max} -d_{min} = 12.45 - 0.81 Å. The structure was solved by direct methods using the programme SHELXS-97.[139] The refinement and all further calculations were carried out using SHELXL-97.[140] The H-atoms were located from Fourier difference maps and refined isotropically. The non-H atoms were refined anisotropically, using weighted full-matrix least-squares on F^2.

The molecule possesses C_2 crystallographic symmetry. The absolute structure of the molecule in the crystal was assigned to the known absolute configuration of the pinene-moiety.

3.21. {2-DAMI}-[5,6]-CHIRAGEN[0] (L19)

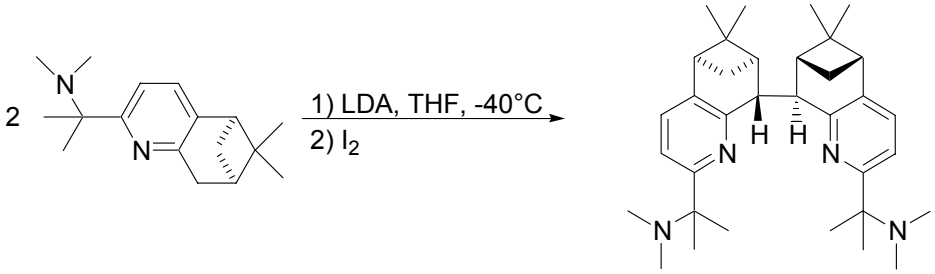

To dry THF (20 ml) at –20 °C diisopropylamine (1.6 ml, 11.3 mmole) was added followed by *n*-butyllithium (5.8 ml, 9.3 mmole, 1.6 M in hexane). The temperature was allowed to increase to 0 °C for 30 minutes and then lowered to –40 °C. {2-DAMI}-[5,6]-pinene-py (**L10**) (0.8 g, 3.1 mmole) dissolved in dry THF (10 ml) was added dropwise over 1 hour. After stirring the solution at –40 °C for 2 hours iodine (0.5 g, 0.2 mmole) dissolved in 8 ml THF was injected slowly (1 hour). The solution was warmed gradually to room temperature, quenched by water (3 ml), followed by addition of dichloromethane and a saturated aqueous solution of $NaHCO_3$. The aqueous solution was extracted three times with dichloromethane. The combined organic layers were dried over magnesium sulfate, and the solvent was evaporated. The residual solid was further purified by recrystallization (methanol/chloroform), yielding white crystals (0.16 g, 20%).

^{1}H-NMR (400 MHz, $CDCl_3/CD_3CN$): δ = 7.08 (d, 2H, H(3), $^3J_{3,4}$ = 7.8 Hz), 7.03 (d, 2H, H(4), $^3J_{4,3}$ = 7.8 Hz), 4.30 (s, br, 2H, H(7)), 2.56 (dd, 2H, H(10), $^3J_{10,9b}$ = 5.6 Hz, $^4J_{10,8}$ = 5.6 Hz), 2.27 (ddd, 2H, H(9b), $^2J_{9b,9a}$ = 9.4 Hz, $^3J_{9b,10}$ = 5.6 Hz, $^3J_{9b,8}$ = 5.6 Hz), 2.07 (s, 12H, H(6'), H(5')), 1.92-1.76 (m, 2H, H(8)), 1.31 (s, 6H, H(3')), 1.27 (s, 6H, H(4')), 1.14 (s, 6H, H(12)), 1.08 (s, br, 2H, H(9a)), 0.58 (s, 6H, H(13)).

^{13}C-NMR ($CDCl_3/CD_3CN$, 400 MHz): δ = 163.54 (Cq, C(6)), 157.15 (Cq, C(2)), 140.28 (Cq, C(5)), 132.64 (CH, C(4)), 117.51 (CH, C(3)), 62.00 (Cq, C(2')), 46.11 (CH, C(10)), 41.52 (Cq, C(11)), 39.65 (CH_3, C(5'), C(6')), 26.54 (CH_3, C(12)), 24.72 (CH_3, C(3')), 22.71 (CH_3, C(4')), 31.30 (CH_3, C(13)).

MS(ESI): m/z = 515.5 (HM^+)

UV/Vis: ($CHCl_3$), λ (ε): 276 ($1.1*10^4$).

CD: ($CHCl_3$), λ (Δε): 269 (13.7).

Elemental analysis calculated: C: 79.33%, H: 9.79%, N: 10.88%, found C: 79.7%, H: 9.86%, N: 10.74%.

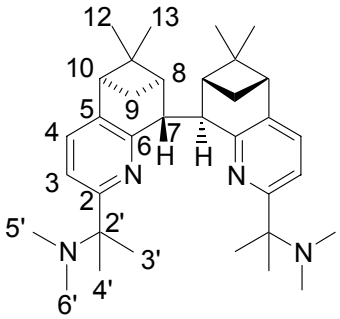

$C_{34}H_{50}N_4$
514.79

X-ray crystallography

Suitable crystals of **L19** were obtained as colourless rod-like crystals by slow evaporation of a Chloroform/methanol solution. The intensity data was collected at 153K on a Stoe Image Plate Diffraction System[138] using MoKα graphite monochromated radiation. Image plate distance 70mm, ϕ oscillation scans 0 - 198°, step $\Delta\phi$ = 1.0°, 2θ range 3.27 – 52.1°, d_{max} -d_{min} = 12.45 - 0.81 Å. The structure was solved by Direct methods using the programme SHELXS-97.[139] The refinement and all further calculations were carried out using SHELXL-97.[140] The H-atoms were included in calculated positions and treated as riding atoms using SHELXL default parameters. The non-H atoms were refined anisotropically, using weighted full-matrix least-squares on F^2. The molecule possesses C_2 symmetry. The absolute structure of the molecule in the crystal was assigned to the known absolute configuration of the pinene-moiety.

3.22. [4,5]-CHIRAGEN[0] (L20)

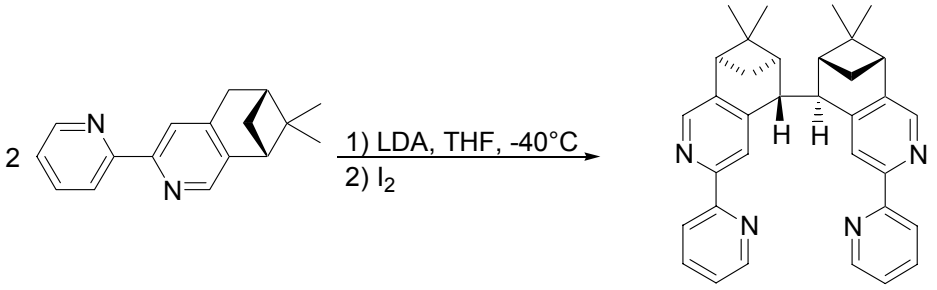

The synthesis was carried out according to the published method[36], giving a slightly better yield. To dry THF (15 ml) at –20 °C diisopropylamine (0.15 ml, 1 mmole) was added, followed by *n*-butyllithium (0.6 ml, 0.96 mmole,1.6 M in hexane). The temperature was allowed to increase to 0 °C for 30 minutes and then lowered to –40 °C. [4,5]-Pinene-bpy (**L2**) (200 mg, 0.8 mmole) dissolved in dry THF(10 ml) was added dropwise over 1 hour. After stirring the solution at –40 °C for 2 hours, iodine (0.13 g, 0.5 mmole) dissolved in THF (10 ml) was injected slowly (1 hour). The solution was warmed gradually to room temperature, quenched by water (3 ml), followed by addition of dichloromethane and a saturated aqueous solution of $NaHCO_3$. The aqueous solution was extracted three times with dichloromethane. The combined organic layers were dried over magnesium sulfate, and the solvent was evaporated. The residual solid was further purified by recrystallization (methanol/chloroform), yielding of pure product (135 mg, 69%).

^{1}H-NMR (300 MHz, $CDCl_3$,): δ = 8.65 (ddd, 2H, H(6'), $^3J_{6',5'}$ = 3.9 Hz, $^4J_{6',4'}$ = 1.7 Hz), 8.45 (s, 2H, H(3), 8.36 (ddd, 2H, H(3'), $^3J_{3',4'}$ = 8.0 Hz), 8.26 (s, 2H, H(6)), 7.79 (ddd, 2H, H(4'), $^3J_{4',3'}$ = 8.0 Hz, $^3J_{4',5'}$ = 8.0 Hz, $^4J_{4',6'}$ = 1.7 Hz), 7.26 (ddd, 2H, H(5'), $^3J_{5',4'}$ = 6.0 Hz, $^3J_{5',6'}$ = 4.8 Hz, $^4J_{5',3'}$ = 1.2 Hz), 4.03 (s, 2H, H(7)), 2.82 (dd, 2H, H(10), $^3J_{10,9b}$ = 5.5 Hz, $^4J_{10,8}$ = 5.5 Hz); 2.50 (ddd, 2H, H(9_b), $^2J_{9b,9a}$ = 9.8 Hz, $^3J_{9b,10}$ = 5.5 Hz, $^3J_{9b,8}$ = 5.5 Hz); 2.09 (dd, 2H, H(8) $^3J_{8,9b}$ = 5.5 Hz, $^4J_{8,10}$ = 5.5 Hz); 1.28 (s, 6H, H(12)), 1.24 (d, 2H, H(9_a), $^2J_{9a,9b}$ = 9.8 Hz); 0.70 (s, 6H, H(13)).

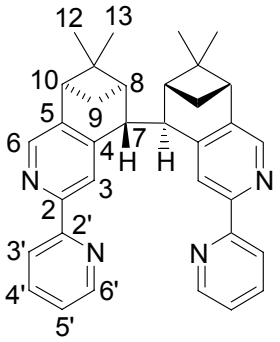

$C_{34}H_{34}N_4$
498.66

4. Complex syntheses

4.1. $[Ag_6L11_6](PF_6)_6$ (C3)

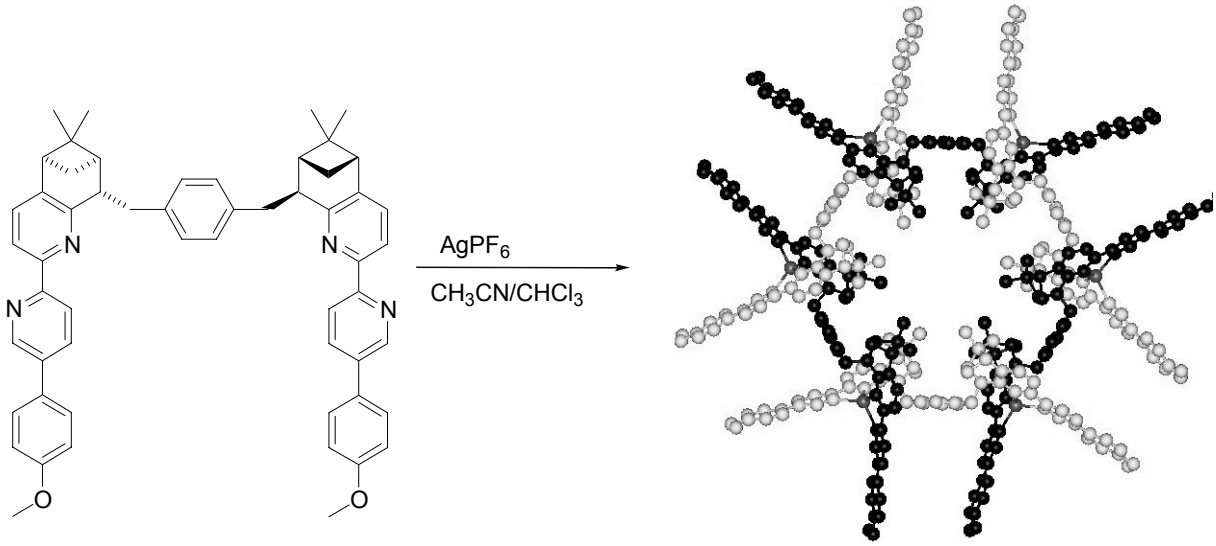

$AgPF_6$ (15.5 mg, 0.061 mmol) dissolved in acetonitrile (6 ml) was added to a solution of **L11** (50 mg, 0.061 mmol) in chloroform (2 ml) and acetonitrile (2 ml). This mixture was stirred for 10 minutes at room temperature and the solvent was evaporated under reduced pressure. The white solid (quantitative yield) was used without further purification for the analysis.

^{1}H-NMR (400 MHz, CD_3CN): δ 8.74 (d, 2H, H(6'), $^3J_{6',4'}$ = 2.0 Hz); 8.29 (d, 2H, H(3), $^3J_{3,4}$ = 8.3 Hz); 8.24 (d, 4H, H(3'), $^3J_{3',4'}$ = 8.2 Hz); 8.14 (d, 2H, H(4'), $^3J_{4',3'}$ = 8.2 Hz); 7.85 (d, 2H, H(4), $^3J_{4,3}$ = 8.3 Hz); 7.44 (d, 2H, H(9'), H(11'), $^3J_{9',8'}$ = 8.6 Hz); 6.89 (d, 2H, H(8'), H(12'), $^3J_{8',9'}$ = 8.6 Hz); 5.95 (s, 4H, H(3''), H(4''), H(6''), H(7'')); 3.83 (d, 2H, H(1_b''), $^2J_{1b'',1a''}$ = 12.6 Hz); 3.75 (s, 6H, H(13')); 2.97 (m, 2H, H(10)); 2.89 (m, 2H, H(7), $^3J_{7,1b''}$ = 10.5 Hz); 2.59 (m 2H, H(9_b), $^2J_{9b,9a}$ = 9.1 Hz); 2.46 (m, 2H, H(1a'')); 1.60 (d, 2H, H(9_a), $^2J_{9a,9b}$ = 9.1 Hz); 1.45 (m, 2H, H(8)); 1.22 (s, 6H, H(12)); 0.14 (s, 6H, H(13)).

^{13}C-NMR (100 MHz, CD_3CN): δ 161.5 (Cq); 160.1 (Cq); 151.3 (Cq); 149.1 (Cq); 146.0 (CH, C(6')); 138.4 (Cq); 137.8 (CH, C(4')); 137.4 (CH, C(4)); 137.3 (Cq); 129.2 (CH, C(3'')); 128.9 (CH, C(9'), C(11')); 123.5 (CH, C(3')); 122.1 (CH, C(3)); 115.6 (CH, C(8'), C(12')); 56.1 (CH_3, C(13')); 49.6 (CH, C(7)); 47.4 (CH, C(10));

43.2 (CH, C(8)); 41.6 (Cq, C(11)); 38.5 (CH_2, C(1'')); 28.2 (CH_2, C(9)); 26.6 (CH_3, C(12)); 21.8 (CH_3, C(13)).

ESI-MS (CH_3CN): m/z = 1737.52 (1+, $[Ag\mathbf{L11}_2]^+$); 1457.96 (4+, $[Ag_6\mathbf{L11}_6](PF_6)_2^{4+}$; 2+, $[Ag_3\mathbf{L11}_3]PF_6^{2+}$); 1136.53 (5+, $[Ag_6\mathbf{L11}_6](PF_6)_2^{5+}]^+$); 922.51 (1+, $[Ag\mathbf{L11}]^+$).

UV/Vis: (c= $9.7*10^{-6}$ M for $[Ag\mathbf{L11}]PF_6$, CH_3CN, λ (ε)): 317 ($7.1*10^4$), 273 ($2.6*10^4$).

CD: (c= $9.7*10^{-6}$ M for $[Ag\mathbf{L11}]PF_6$, CH_3CN, λ(Δε)): 342 (11.8), 303 (-8.0), 230 (-16.1).

Elemental analysis calculated C: 62.98%, H: 5.10%, N: 5.25%, found C: 62.4%, H: 4.96, N: 4.58%.

4.2. $[Cu_6\mathbf{L11}_6](PF_6)_6$ (C4)

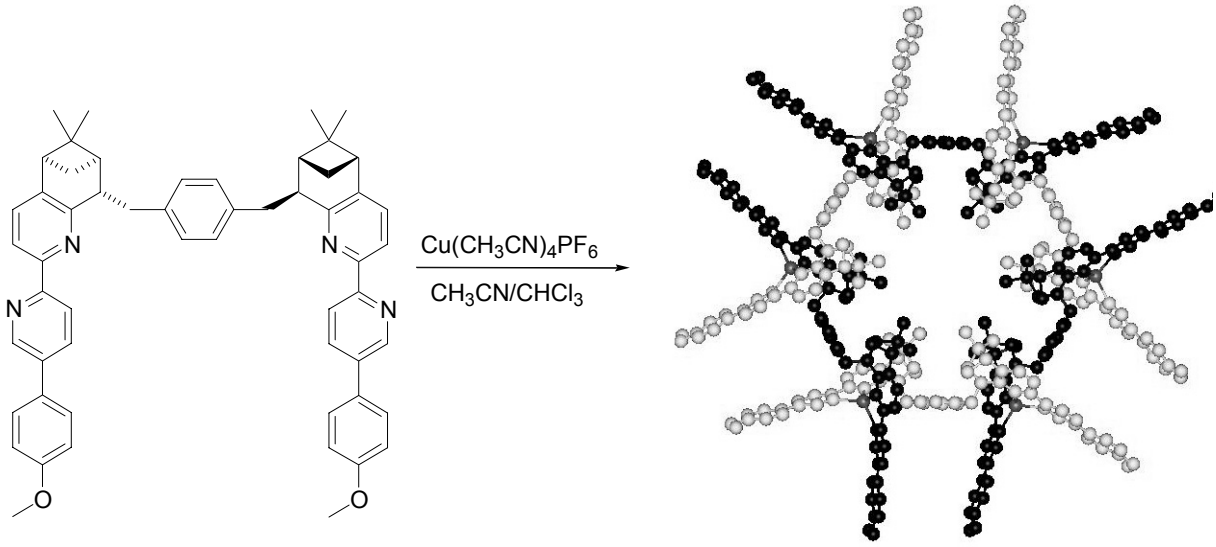

$[Cu(CH_3CN)_4]PF_6$[108] (22.8 mg, 0.061 mmol) dissolved in acetonitrile (6 ml) was added to a solution of (50 mg, 0.061 mmol) **L11** in chloroform (2 ml) and acetonitrile (2 ml). Immediately the solution became orange-red. This colored mixture was stirred for 10 minutes at room temperature and the solvent was evaporated under reduced pressure. The red solid (60.5mg, 97%) was used without further purification for the analysis.

^{1}H-NMR (400 MHz, CD_3CN): δ 8.48 (d, 2H, H(6'), $^{4}J_{6',4'}$ = 2.0 Hz); 8.33 (d, 2H, H(3'), $^{3}J_{3',4'}$ = 8.5 Hz); 8.32 (d, 4H, H(3), $^{3}J_{3,4}$ = 8.1 Hz); 8.16 (d, 2H, H(4'), $^{3}J_{4',3'}$ = 8.5 Hz, $^{4}J_{4',3'}$ = 2.0 Hz); 7.88 (d, 2H, H(4), $^{3}J_{4,3}$ = 8.1 Hz); 7.40 (d, 2H, H(9'), H(11'), $^{3}J_{9',8'}$ = 8.6 Hz); 6.90 (d, 2H, H(8'), H(12'), $^{3}J_{8',9'}$ = 8.6 Hz); 5.78 (s, 4H, H(3''), H(4''), H(6''), H(7'')); 3.80 (d, 2H, $H(1_b'')$, $^{2}J_{1b'',1a''}$ = 12.6 Hz); 3.75 (s, 6H, H(13')); 3.05 (dd, 2H, H(10), $^{3}J_{10,9b}$ = 5.7 Hz, $^{4}J_{10,8}$ = 5.7 Hz); 2.77 (d, 2H, H(7), $^{3}J_{7,1b''}$ = 11.7 Hz); 2.58 (ddd 2H, $H(9_b)$, $^{2}J_{9b,9a}$ = 10.1 Hz, $^{3}J_{9b,10}$ = 5.7 Hz, $^{3}J_{9b,8}$ = 5.7 Hz); 2.33 (m, 2H, H(1a'')); 1.63 (d, 2H, $H(9_a)$, $^{2}J_{9a,9b}$ = 10.1 Hz); 1.40 (m, 2H, H(8)); 1.17 (s, 6H, H(12)); 0.09 (s, 6H, H(13)).

^{13}C-NMR (100 MHz, CD_3CN): δ 160.7 (Cq); 159.0 (Cq); 151.4 (Cq); 150.9 (Cq); 145.9 (CH, C(6')); 138.7 (Cq); 136.6 (CH, C(4')); 135.9 (CH, C(4)); 135.5 (Cq); 128.7 (CH, C(3'')); 128.5 (CH, C(9'), C(11')); 121.8 (CH, C(3')); 120.9 (CH, C(3)); 114.8 (CH, C(8'), C(12')); 55.4 (CH_3, C(13')); 49.0 (CH, C(7)); 46.7 (CH, C(10)); 42.6 (CH, C(8)); 41.8 (Cq, C(11)); 37.3 (CH_2, C(1'')); 27.4 (CH_2, C(9)); 25.8 (CH_3, C(12)); 21.7 (CH_3, C(13)).

ESI-MS (CH_3CN): m/z = 1693.76 (1+, $[Cu\mathbf{L11}_2]^{+}$); 1560.88 (3+, $[Cu_5\mathbf{L11}_5](PF_6)_2^{3+}$); 1390.02 (2+, $[Cu_3\mathbf{L11}_3]PF_6^{2+}$); 1219.79 (2+, $[Cu_4\mathbf{L11}_4]PF_6^{3+}$); 1134.42 (4+, $[Cu_5\mathbf{L11}_5]PF_6^{4+}$); 879.35 (1+, 3+, 6+, $[Cu_n\mathbf{L11}_n]^{n+}$); 815.43 (1+, $[H\mathbf{L11}]^{+}$); 470.15 (2+, $[Cu_2\mathbf{L11}]^{2+}$); 439.18 (2+, $[Cu\mathbf{L11}]^{2+}$).

UV/Vis: (c= 1.44*10^{-6} M for $[Cu\mathbf{L11}]PF_6$, CH_3CN, λ (ε)): 317 (6.4*10^{4}).

CD: (c= 1.44*10^{-6} M for $[Cu\mathbf{L11}]PF_6$, CH_3CN, λ(Δε)): 345 (10.1), 282 (-3.6), 242 (3.0), 229 (-10.0).

4.3. $[Cu_6L13_6](PF_6)_6$ (C5)

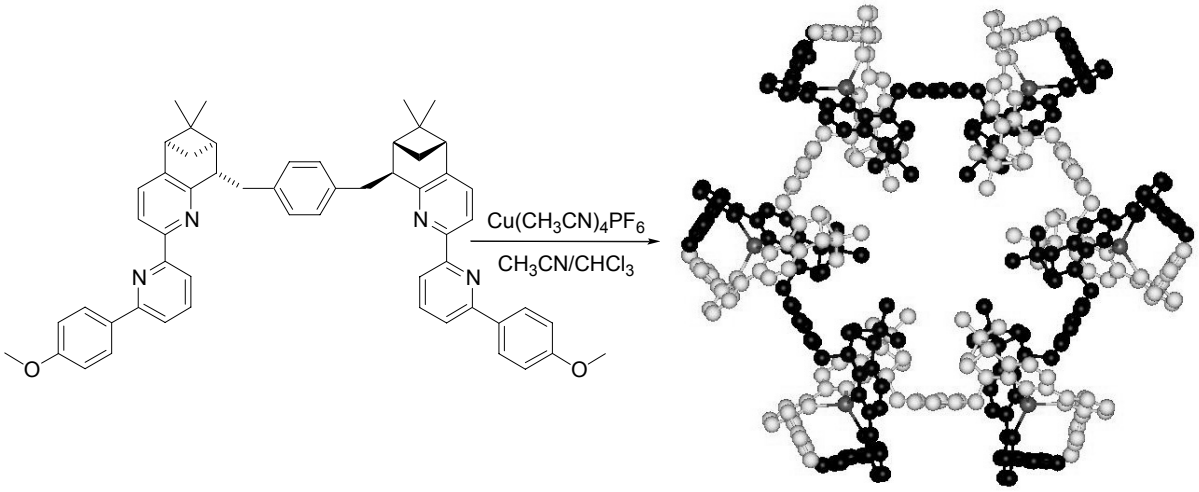

$[Cu(CH_3CN)_4]PF_6$[108] (22.9 mg, 0.061 mmol) dissolved in acetonitrile (6 ml) was added to a solution of **L13** (50 mg, 0.061 mmol) in chloroform (2 ml) and acetonitrile (2 ml). Immediately the solution became orange-red. This colored mixture was stirred for 10 minutes at room temperature and then about 6 ml of the solvent was evaporated under reduced pressure. The remaining solution was precipitated with diethyl ether. The precipitate was filtrated over *Kieselgur*, washed with hexane and chloroform and redissolved in acetonitrile. The solvent was removed under reduced pressure. The orange-red powder was dried in vacuum, yielding the complex **C5** (49 mg, 78%).

^{1}H-NMR (400 MHz, CD_3CN): δ 8.12 (d, 2H, H(3), $^3J_{3,4}$ = 8.1 Hz); 7.90 (d, 2H, H(4), $^3J_{4,3}$ = 8.1 Hz); 7.68 (m, 4H, H(3'), H(4')); 7.28 (dd, 2H, H(5'), $^3J_{5',4'}$ = 7.3 Hz, $^3J_{5',3'}$ = 2.6 Hz); 7.08 (d, 2H, H(8'), H(12'), $^3J_{8',9'}$ = 8.6 Hz); 6.24 (d, 2H, H(9'), H(11'), $^3J_{9',8'}$ = 8.6 Hz); 5.69 (s, 4H, H(3''), H(4''), H(6''), H(7'')); 4.26 (dd, 2H, H(1_b''), $^2J_{1b'',1a''}$ = 12.5 Hz, $^3J_{1b'',7}$ = 3.6 Hz); 3.64 (s, 6H, H(13')); 3.10 (dd, 2H, H(10), $^3J_{10,9b}$ = 5.6 Hz, $^4J_{10,8}$ = 5.6 Hz); 2.93 (m, 2H, H(7), $^3J_{7,1b''}$ = 11.7 Hz); 2.64 (ddd, 2H, H(9_b), $^2J_{9b,9a}$ = 10.0 Hz, $^3J_{9b,\ 10}$ = 5.6 Hz, $^3J_{9b,\ 8}$ = 5.6 Hz); 2.56 (m, 2H, H(1a''), *J* = 12 Hz); 1.77 (d, 2H, H(9_a), $^2J_{9a,9b}$ = 10.0 Hz); 1.45 (m, 2H, H(8)); 1.21 (s, 6H, H(12)); 0.14 (s, 6H, H(13)).

ESI-MS (CH_3CN): m/z = 1691.75 (1+, [Cu**L13**$_2$]$^+$); 1560.55 (3+, [Cu_5**L13**$_5$](PF_6)$_2^{3+}$); 1133.43 (4+, [Cu_5**L13**$_5$]PF_6^{4+}); 879.36 (1+, 3+, 6+, [Cu_n**L13**$_n$]$^{n+}$); 815.43 (1+, [H**L13**]$^+$); 470.15 (2+, [Cu_2**L13**]$^{2+}$); 439.19 (2+, [Cu**L13**]$^{2+}$).

UV/Vis: (c= 1.45*10^{-6} M for [Cu**L13**]PF_6, CH_3CN, λ (ε)): 313 (sh, 3.2*10^4), 261 (5.3*10^4), 209 (6.4*10^4),

CD: (c= 1.45*10^{-6} M for [Cu**L13**]PF_6, CH_3CN, λ(Δε)): 318 (+7.5); 276 (3.0); 258 (-6.3), 226 (-20.9).

Elemental analysis calculated C: 65.71%, H: 5.32%, N: 5.47%, found C: 63.26%, H: 5.39%, N: 5.14%.

4.4. [Cu_6**L12**$_6$](ClO_4)$_6$ (C6)

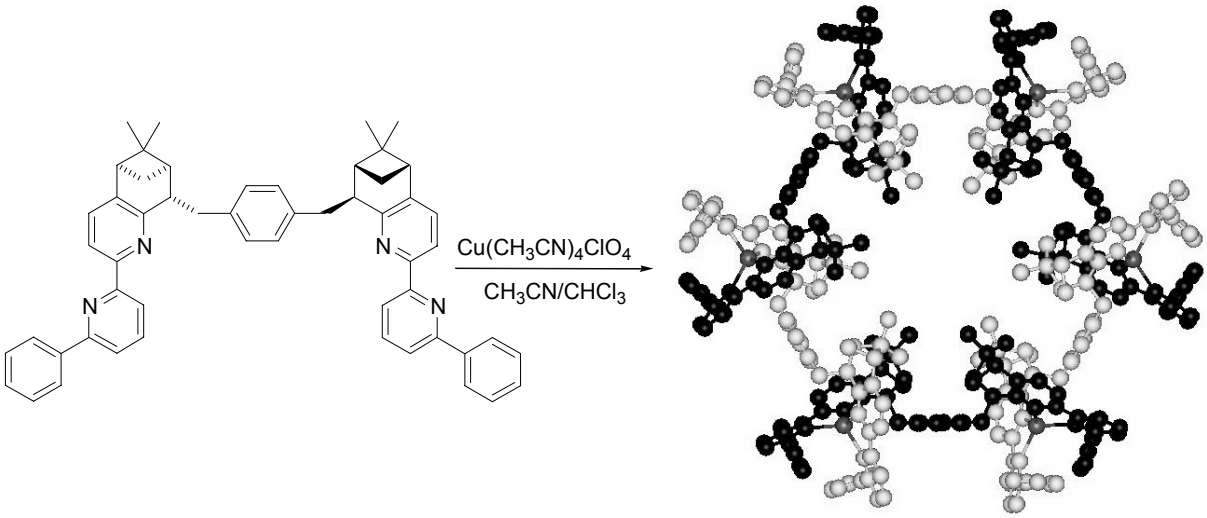

{6'-Phenyl}-[5,6]-pinene-CHIRAGEN[*p*-xyl] (**L12**) (50 mg, 0.066 mmol) was dissolved in dichloromethane (2 ml) and a solution of $Cu(CH_3CN)_4ClO_4$ (22,mg, 0.66 mmol) in acetonitrile (2 ml) was added. The colour changed from yellow to deep red. The mixture was stirred for 30 minutes and the solvent was removed under reduced pressure. The red residue was dissolved in acetonitrile and the complex was precipitated adding 5ml of diethyl ether. The red solid was filtered and dried in vacuo, yielding the complex **C6** (60 mg, 99%).

^{1}H-NMR (300 MHz, CD_3CN): δ 8.10 (d, 2H, H(3), $^{3}J_{3,4}$ = 8.1 Hz); 7.91 (d, 2H, H(4), $^{3}J_{4,3}$ = 8.1 Hz); 7.71 (m, 4H, H(3'), H(4')); 7.35 (dd, 2H, H(5'), $^{3}J_{5',4'}$ = 7.68 Hz, $^{3}J_{5',3'}$ = 2.6 Hz); 7.13 (d, 4H, H(8'), H(12'), $^{3}J_{8',9'}$ = 7.5 Hz); 7.02 (d, 2H, H(10'), $^{3}J_{10',9'}$ = 7.5 Hz); 6.76 (dd, 4H, H(9'), H(11'), $^{3}J_{9',8'}$ = 7.5 Hz, $^{3}J_{9',10'}$ = 7.5 Hz); 5.69 (s, 4H, H(3''), H(4''), H(6''), H(7'')); 4.26 (m, 2H, H(1_b'')); 3.12(dd, 2H, H(10), $^{3}J_{10,9b}$ = 5.5 Hz, $^{3}J_{10,8}$ = 5.5 Hz); 2.92 (m, 2H, H(7)); 2.66-2.52 (m, 2H, H(9_b), H(1_a'')); 1.75 (d, 2H, H(9_a), $^{2}J_{9a,9b}$ = 9.9 Hz); 1.45 (m, 2H, H(8)); 1.21 (s, 6H, H(12)); 0.14 (s, 6H, H(13)).

^{13}C-NMR (75.4 MHz, CD_3CN): δ 158.6 (Cq); 158.3 (Cq); 153.6 (Cq); 147.0 (Cq); 139.8 (Cq); 139.3 (Cq); 137.0 (CH, C(4')); 136.5 (CH, C(4)); 129.5 (Cq); 129.4 (CH, C(3'')); 128.5 (CH, C(8')); 128.2 (CH, C(10')); 126.3 (CH, C(3')); 122.4 (CH, C(5')); 121.9 (CH, C(3)); 118.2 (CH, C(9')); 48.4 (CH, C10); 47.4 (CH, C7); 43.3 (CH, C8); 41.0 (Cq, C11); 37.3 (CH_2, C1''); 27.9 (CH_2, C9); 26.5 (CH_3, C12); 22.8 (CH_3, C13);

ESI-MS (CH_3CN): m/z = 1573.55 (1+, [Cu**L12**$_2$]$^{+}$); 1430.50 (3+, [Cu_5**L12**$_5$]$(ClO_4)_2^{3+}$); 1277.54 (2+, [Cu_3**L12**$_3$]ClO_4^{2+}); 1048.03 (4+, [Cu_5**L12**$_5$]ClO_4^{4+}); 817.38 (1+, 2+, , [Cu_n**L12**$_n$]$^{n+}$); 755.45 (1+, [H**L12**]$^{+}$); 441.15 (2+, [Cu_2**L12**]$^{2+}$);

UV/Vis: (c= 2.01*10^{-5} M for [Cu**L12**]PF_6, CH_3CN, λ (ε)): 302 (3.92*10^4), 288 (3.21*10^4), 253 (4.8*10^4).

CD: (c= 2.01*10^{-6} M for [Cu**L12**]PF_6, CH_3CN, λ(Δε)): 306 (6.3), 252 (-6.0), 226 (-21.0).

4.5. [AgL16]PF_6 (C8)

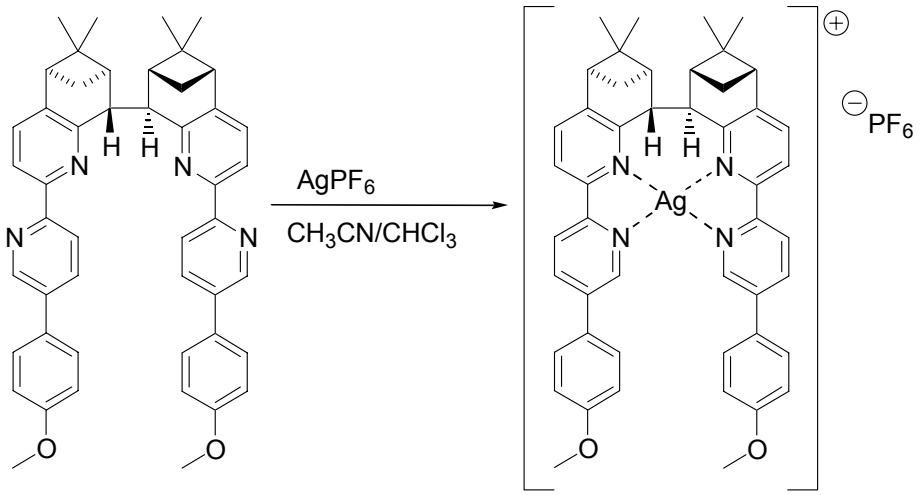

Under argon and light protection, $AgPF_6$ (11.2 mg, 0.045 mmol) dissolved in acetonitrile (6 ml) and added to a solution of 5,6-CHIRAGEN[0] (31.5 mg, 0.045 mmol) in chloroform (6 ml) and actonitrile (4 ml). This mixture was stirred for 30 minutes at room temperature. The solvent was removed under reduced pressure. After drying, a white solid was obtained (42.5 mg, quantitative yield) and was analysed without further purification.

^{1}H-NMR (400 MHz, CH_3CN): δ 8.98 (s, 2H, H(6')); 8.21 (br, 4H, H(3'), H(4')); 7.99 (d, 2H, H(3), $^3J_{3,4}$ = 7.8 Hz); 7.55 (br, 4H, H(9'), H(11')); 7.37 (br, 2H, H(4)); 7.03 (d, 4H, H(8'), H(12'), $^3J_{8',9'}$ = 8.7 Hz); 4.10 (br, 2H, H(7)); 3.83 (s, 6H, H(13')); 2.98 (m, 2H, H(10)); 2.85 (m, 2H, H(9_b)); 2.61 (m, 2H, H(8)); 1.51 (d, 2H, H(9_a), $^2J_{9a,9b}$ = 9.8 Hz); 1.40 (s, 6H, H(12)); 0.63 (s, 6H, H(13)).

^{13}C-NMR (100 MHz, CH_3CN): δ 161.5 (Cq); 160.7 (Cq); 151.5 (Cq); 150.6 (Cq); 149.2 (CH, C(6')); 145.3 (Cq); 137.3 (Cq); 136.6 (CH, C(4')); 135.2 (CH, C(4)); 133.1 (Cq); 128.7 (CH, C(9'), C(11')); 122.7 (CH, C(3')); 120.1 (CH, C(3)); 115.0 (CH, C(8'), C(12')); 55.4 (CH_3, C(13')); 47.7 (CH, C(7)); 46.0 (CH, C(10)); 41.8 (Cq, C(11)); 41.4 (CH, C(8)); 31.2 (CH_2, C(9)); 25.9 (CH_3, C(12)); 20.6 (CH_3, C(13)).

MS(ESI): m/z = 817.3 (1+, Ag**L16**-H^+), 711.3 (1+, **L16**$^+$).

UV/Vis: (CH_3CN), λ (ε): 321 nm ($6.1*10^4$), 271 nm ($2.2*10^4$; sh).

CD: (CH_3CN), λ (Δε): 337 (-100), 302 (47).

Elemental analysis calculated C: 59.82%, H: 4.81%, N: 5.81% , found C: 59.83%, H: 4.88%, N: 5.45% .

4.6. [AgL18]PF_6 (C9)

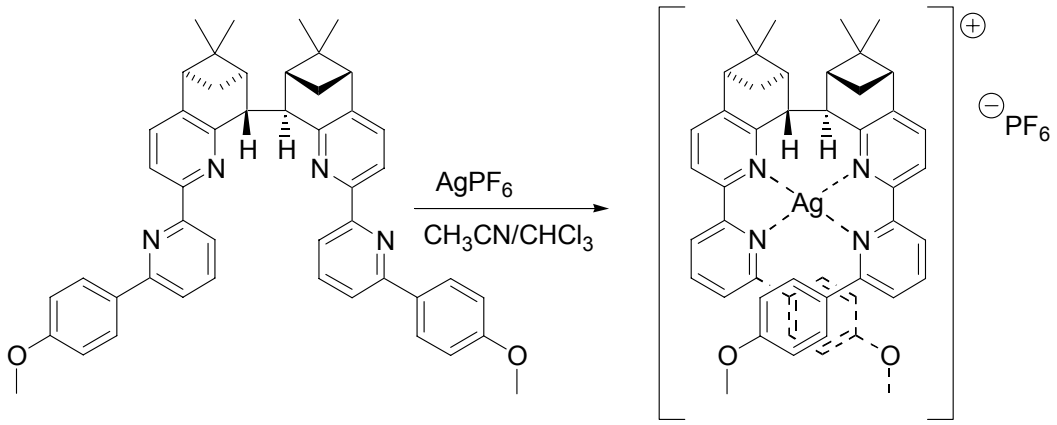

Under argon and light protection, $AgPF_6$ (17.7 mg, 0.07 mmol) dissolved in acetonitrile (6 ml) was added to a solution of 5,6-CHIRAGEN[0] (50 mg, 0.07 mmol) in chloroform (20 ml) and actonitrile (5 ml). This mixture was stirred for 3 hours at room temperature. The solvent was removed under reduced pressure. After drying, a white solid was obtained in quantitative yield, and was analysed without further purification.

^{1}H-NMR (400 MHz, CH_3CN): δ 8.16 (d, 2H, H(3), $^3J_{3,4}$ = 7.7 Hz)); 8.15 (d, 2H, H(3'), $^3J_{3',4'}$ = 7.8 Hz); 7.95 (dd, 2H, H(4'), $^3J_{4',3'}$ = 7.8 Hz, $^3J_{4',5'}$ = 7.8 Hz); 7.79 (d, 2H, H(5'), $^3J_{5',4'}$ = 7.8 Hz,); 7.52(d, 2H, H(4), $^3J_{4,4}$ = 7.7 Hz); 7.35 (d, 4H, H(8'), H(12'), $^3J_{8',9'}$ = 8.7 Hz); 6.47 (br, 4H, H(9'), H(11')); 4.08 (br, 2H, H(7)); 3.61 (s, 6H, H(13')); 3.01 (m, 2H, H(10)); 2.81 (m, 2H, H(9_b)); 2.60 (m, 2H, H(8));1.46 (d, 2H, H(9_a), $^2J_{9a,9b}$ = 9.8 Hz); 1.39 (s, 6H, H(12)); 0.65 (s, 6H, H(13)).

MS(ESI): m/z = 817.3 (1+, Ag**L18**-H$^+$), 711.3 (1+, **L18**$^+$).

UV/Vis: (CH_3CN), λ (ε): 318 nm (4.9*10^4), 267 nm (5.2 *10^4; sh).

CD: (CH_3CN), λ (Δε): 337 (-67), 292 (21), 224 (-35).

Elemental analysis calculated C: 59.82%, H: 4.81%, N: 5.81% , found C: 59.3%, H: 4.67%, N: 5.23% .

5. Protonation studies

5.1. NMR-Titrations

5.1.1 Measurements

The NMR-spectra (^{1}H, ^{1}H-^{13}C-HMQC, ^{1}H-^{13}C-HMBC, ^{1}H-^{15}N-HMBC) were measured either on a Bruker Avance DRX 400 or on a Bruker Avance DRX 700 NMR spectrometer. The spectrometers operate at 400.13 MHz or 700.13 MHz for ^{1}H, at 100.62 MHz for ^{13}C and at 40.54 MHz or 70.96 MHz for ^{15}N. $CDCl_3$ was used as internal reference for ^{1}H (7.26 ppm) and ^{13}C (77.0 ppm). For the ^{15}N-experiments nitromethane at (0.0 ppm) was used as internal reference.

5.1.2 Preparation of the solutions

From commercially available trifluoroacetic acid (Aldrich) a solution (2.7 M) in CD_3CN was freshly prepared for each acidic titration. The ligands **L1** (100.0 mM), **L15** (50.0 mM) and **L20** (50.0 mM) were dissolved in a mixture of $CDCl_3/CD_3CN$= 3:1. Ligand **L19** (48.6 mM) was dissolved in mixture of $CDCl_3/CD_3CN$= 5:1

5.1.3 Titrations

Titration with trifluoroacetic acid

Titrations were carried out by adding small aliquots (typically 2.23 µl) of the TFA-solution to the ligand solutions (0.6ml). 22.30µl of TFA solution corresponds to 1.0 equivalent of **L1**, 11.16µl to 1.0 equivalent of **L15** and **L20**. For **L19**, 11.15µl of the TFA-solution corresponds to 1.03 equivalents.

5.2. Spectrophotometric titrations

5.2.1 Measurements

UV/Visible spectra were measured on a Perkin Elmer Lambda 40 spectrometer. Wavelength are given in nm and molar absorption coefficients (ε) in M^{-1} cm^{-1}. Circular dichroism (CD) spectra were recorded on a Jasco J-715 spectropolarimeter and the results are given in $\Delta\varepsilon$ M^{-1} cm^{-1}. The pH was measured with a micro-combination pH electrode (Orion model 9863). UV-titrations were carried out with a Mettler Titrator DL21 with 1ml and 10ml burettes.

5.2.2 Calibration of the electrode

Assuming that hydrochloric acid is completely dissociated forming H_3O^+ in aqueous solution containing methanol. The calculated H^+-concentration were attributed to the measured potential E_{meas} according to the following equation: $pH = a*E_{meas} + b$. For further titrations the pH was calculated with the measured potential.

5.2.3 Preparation of the solutions

0.1 M HCl (methanol/water (60% v/v)), 1M HCl (methanol/water (60% v/v)), 0.1M (methanol/water (90% v/v)) and 1M (methanol/water (90% v/v)) were used for the titrations. The ligand solutions for **L1** and bpy consisted of 0.001M NaOH, 0.1M NaCl and $5*10^{-5}$M **L1** and bpy in a mixture of methanol water (60% v/v). The ligand solutions for **L15** and **L20** consisted of 0.001M NaOH, 0.1M NaCl and $2.5*10^{-5}$ M or $5*10^{-5}$ M of **L15** and **L20** in methanol water (90% v/v).

5.2.4 Titrations

In the pH-range from 10 to 3, HCl solution (0.1M) was added in 2µl steps to 2ml of the ligand solutions by the Mettler Titrator DL21 (1ml burette) for the UV/Vis-titration. In the pH-range from 3 to 1 HCl solution (1M) was used. pH of the stirred solution was measured directly in the cuvette by a micro electrode. The CD-titrations

were carried out by adding the corresponding aliquots of acid with a micropipette without pH-measurements. Acid solutions in methanol/water (60% v/v) were used for **L1** and bpy, acid solutions in methanol/water (90% v/v) for **L15** and **L20**.

All spectra represented in the previous chapter are baseline and volume corrected. Calculations of the equilibrium constants were carried out with the program Specfit®.

5.3. Additional spectral data of L1, L15, L19 and L20 (incl. protonation)

5.3.1 [5,6]-Pinene-bpy (L1)

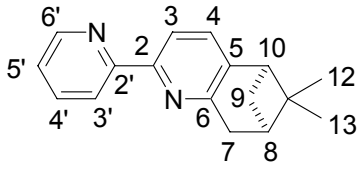

Free Ligand **L1**:

^{1}H-NMR (400 MHz, $CDCl_3/CD_3CN$): δ 8.47 (d, 1H, H(6')), 8.18 (ddd, 1H, H(3')), 7.87 (d, 1H, H(3), $^{3}J_{3,4}$ = 8.0 Hz), 7.64 (ddd, 1H, H(4')), 7.18 (d, 1H, H(4), $^{3}J_{4,3}$ = 8.0 Hz), 7.12 (d, 1H, H(5'), $^{3}J_{5',4'}$ = 7.1 Hz, $^{3}J_{5',6'}$ = 7.1 Hz, $^{4}J_{5',3'}$ = 2.0 Hz), 3.00 (m, 2H, H(7)), 2.67 (dd, 1H, H(10), $^{3}J_{10,9b}$ = 5.6 Hz, $^{3}J_{10,8}$ = 5.6 Hz), 2.56 (ddd, 1H, H(9_b), $^{2}J_{9b,9a}$ = 10.4 Hz, $^{3}J_{9b,10}$ = 5.8 Hz, $^{3}J_{9b,8}$ = 5.8 Hz), 2.24 (ddt, 1H, H(8), $^{3}J_{8,9b}$ = 5.8 Hz, $^{3}J_{8,10}$ = 5.8 Hz, $^{3}J_{8,7}$ = 2.8 Hz), 1.26 (s, 3H, H(12)), 1.13 (d, 1H, H(9_a), 0.51 (s, 3H, H(13)).

^{15}N-NMR (40 and 71 MHz, $CDCl_3/CD_3CN$): δ -77 (N), -74 (N').

UV/Vis: (MeOH/H_2O (60% v/v)), λ (ε): 293 ($1.9*10^4$).

Mono-protonated ligand **HL1^{+}** (3 eq. CF_3COOH)

^{1}H-NMR (400 MHz, $CDCl_3/CD_3CN$): δ 8.60 (d, 1H, H(6')), 8.17 (ddd, 1H, H(3')), 8.14 (ddd, 1H, H(4')), 7.93 (d, 1H, H(3), $^{3}J_{3,4}$ = 8.0 Hz), 7.65 (d, 1H, H(4), $^{3}J_{4,3}$ = 8.0 Hz), 7.60 (d, 1H, H(5'), $^{3}J_{5',4'}$ = 7.1 Hz, $^{3}J_{5',6'}$ = 7.1 Hz, $^{4}J_{5',3'}$ = 2.0 Hz), 3.16 (m, 2H, H(7)), 2.87 (dd, 1H, H(10), $^{3}J_{10,9b}$ = 5.6 Hz, $^{3}J_{10,8}$=5.6 Hz), 2.65 (ddd, 1H, H(9_b), $^{2}J_{9b,9a}$ = 10.4 Hz, $^{3}J_{9b,10}$ = 5.8 Hz, $^{3}J_{9b,8}$ = 5.8 Hz), 2.31 (ddt, 1H, H(8), $^{3}J_{8,9b}$ = 5.8 Hz, $^{3}J_{8,10}$ = 5.8 Hz, $^{3}J_{8,7}$ = 2.8 Hz), 1.29 (s, 3H, H(12)), 1.15 (d, 1H, H(9_a), $^{2}J_{9a,9b}$ = 10.4 Hz), 0.51 (s, 3H, H(13)).

^{15}N-NMR (40 and 71 MHz, $CDCl_3/CD_3CN$): δ –134 (N, N').

UV/Vis: (MeOH/H_2O (60% v/v)), λ (ε): 312 ($2.0*10^4$).

5.3.2 [5,6]-CHIRAGEN[0] (L15)

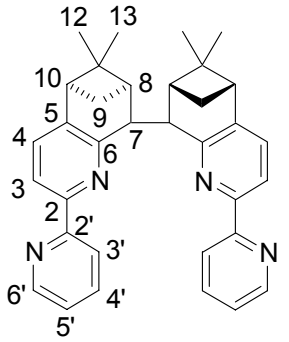

Free Ligand **L15**:

^{1}H-NMR (400 MHz, $CDCl_3/CD_3CN$): δ 8.43 (d, 2H, H(6')), 8.10 (s, br, 2H, H(3')), 7.93 (d, 2H, H(3), $^{3}J_{3,4}$ = 7.6 Hz), 7.59 (ddd, 2H, H(4'), $^{3}J_{4',3'}$ = 7.8 Hz, $^{3}J_{4',5'}$ = 5.8 Hz, $^{4}J_{4',6'}$ = 1.8 Hz), 7.23 (d, 2H, H(4), $^{3}J_{4,3}$ = 7.6 Hz), 7.09 (ddd, 2H, H(5'), $^{3}J_{5',4'}$ = 5.8 Hz, $^{3}J_{5',6'}$ = 4.8 Hz, $^{4}J_{4',3'}$ = 1.0 Hz), 4.36 (s, br, 2H, H(7)), 2.68 (dd, 2H, H(10), $^{3}J_{10,9b}$ = 5.6 Hz, $^{3}J_{10,8}$ = 5.6 Hz), 2.39 (ddd, 2H, H(9_b), $^{2}J_{9b,9a}$ = 9.6 Hz, $^{3}J_{9b,10}$ = 5.6 Hz, $^{3}J_{9b,8}$ = 5.6 Hz), 2.00 (dd, 2H, H(8), $^{3}J_{8,9b}$ = 5.6 Hz, $^{3}J_{8,10}$ = 5.6 Hz), 1.29 (s, br, 2H, H(9_a)), 1.17 (s, 6H, H(12)), 0.61 (s, 6H, H(13)).

^{15}N-NMR (40 and 71 MHz, $CDCl_3/CD_3CN$): δ –78 (N), -77 (N').

UV/Vis: (MeOH/H_2O (90% v/v)), λ (ε): 295 ($3.7*10^4$).

CD: (MeOH/H_2O (90% v/v)), λ (ε): 305 (-27), 284 (22).

Mono-protonated ligand **$HL15^+$** (2 eq. CF_3COOH)

^{1}H-NMR (400 MHz, $CDCl_3/CD_3CN$): δ 7.96 (d, 2H, H(6')), 7.91 (d, 2H, H(3), $^{3}J_{3,4}$ = 7.8 Hz), 7.67 (ddd, 2H, H(3'), $^{3}J_{3',4'}$ = 7.6 Hz), 7.72 (d, 2H, H(4), $^{3}J_{4,3}$ = 8.1 Hz), 7.48 (ddd, 2H, H(4'), $^{3}J_{4',3'}$ = 7.6 Hz, $^{3}J_{4',5'}$ = 7.6 Hz, $^{4}J_{4',6'}$ = 1.5 Hz), 6.98 (ddd, 2H, H(5'), $^{3}J_{5',4'}$ = 7.3 Hz), 3.74 (s, 2H, H(7)), 2.94 (dd, 2H, H(10), $^{3}J_{10,9b}$ = 5.6 Hz, $^{3}J_{10,8}$ = 5.6 Hz), 2.66 (ddd, 2H, H(9_b), $^{2}J_{9b,9a}$ = 10.1 Hz, $^{3}J_{9b,10}$ = 5.6 Hz, $^{3}J_{9b,8}$ = 5.6 Hz), 2.21 (dd, 2H, H(8), $^{3}J_{8,9b}$ = 5.6 Hz, $^{3}J_{8,10}$ = 5.6 Hz), 1.19 (d, 2H, H(9_a), $^{2}J_{9a,9b}$ = 10.1 Hz), 1.33 (s, 6H, H(12)), 0.61 (s, 6H, H(13)).

^{15}N-NMR (40 and 71 MHz, $CDCl_3/CD_3CN$): δ –127 (N), -87 (N').

UV/Vis: (MeOH/H_2O (90% v/v)), λ (ε): 294 ($2.7*10^4$).

CD: (MeOH/H_2O (90% v/v)), λ (ε): 313 (-88), 289 (54).

Di-protonated ligand **H_2L15^{2+}** (6 eq. CF_3COOH)

^{1}H-NMR (400 MHz, $CDCl_3/CD_3CN$): δ 8.30 (d, 2H, H(6')), 8.24 (ddd, 2H, H(3')), 8.24 (ddd, 2H, H(4')), 7.88 (d, 2H, H(3), $^3J_{3,4}$ = 7.8 Hz), 7.57 (ddd, 2H, H(5')), 7.48 (d, 2H, H(4)), 4.16 (s, 2H, H(7)), 2.83 (dd, 2H, H(10), $^3J_{10,9b}$ = 5.3 Hz, $^3J_{10,8}$ = 5.3 Hz), 2.52 (ddd, 2H, H(9_b), $^2J_{9b,9a}$ = 10.1 Hz, $^3J_{9b,10}$ = 5.6 Hz, $^3J_{9b,8}$ = 5.6 Hz), 2.02 (dd, 2H, H(8), $^3J_{8,9b}$ = 5.8 Hz, $^3J_{8,10}$ = 5.8 Hz), 1.20 (s, 6H, H(12)), 1.16 (d, 2H, H(9_a), $^2J_{9a,9b}$ = 10.1 Hz), 0.50 (s, 6H, H(13)).

^{15}N-NMR (40 and 71 MHz, $CDCl_3/CD_3CN$): δ -164 (N'), –107 (N).

UV/Vis: (MeOH/H_2O (90% v/v)), λ (ε): 312 (($2.9*10^4$).

CD: (MeOH/H_2O (90% v/v)), λ (ε): 329 (-92), 299 (59).

5.3.3 {2-DAMI}-[5,6]-CHIRAGEN[0] (L19)

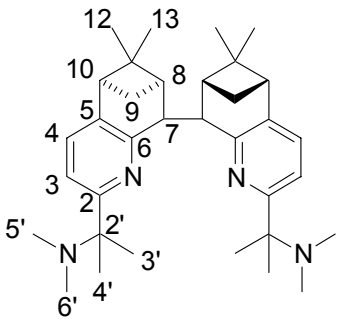

Free ligand **L19**

^{1}H-NMR (400 MHz, $CDCl_3/CD_3CN$): δ 7.08 (d, 2H, H(3), $^3J_{3,4}$ = 7.8 Hz), 7.03 (d, 2H, H(4), $^3J_{4,3}$ = 7.8 Hz), 4.30 (s, br, 2H, H(7)), 2.56 (dd, 2H, H(10), $^3J_{10,9b}$ = 5.6 Hz, $^4J_{10,8}$ = 5.6 Hz), 2.27 (ddd, 2H, H(9_b), $^2J_{9b,9a}$ = 9.4 Hz, $^3J_{9b,10}$ = 5.6 Hz, $^3J_{9b,8}$ = 5.6 Hz), 2.07 (s, 12H, H(5', 6')), 1.92-1.76 (m, 2H, H(8)), 1.31 (s, 6H, H(3')), 1.27 (s, 6H, H(4')), 1.14 (s, 6H, H(12)), 1.08 (s, br, 2H, H(9_a)), 0.58 (s, 6H, H(13)).

^{13}C-NMR ($CDCl_3/CD_3CN$, 100 MHz): δ 163.54 (Cq, C(6)), 157.15 (Cq, C(2)), 140.28 (Cq, C(5)), 132.64 (CH, C(4)), 117.51 (CH, C(3)), 62.00 (Cq, C(2')), 46.11 (CH,

C(10)), 41.52 (Cq, C(11)), 39.65 (CH_3, C(5'), C(6')), 26.54 (CH_3, C(12)), 24.72 (CH_3, C(3')), 22.71 (CH_3, C(4')), 31.30 (CH_3, C(13)).

^{15}N-NMR (40 and 71 MHz, $CDCl_3/CD_3CN$): δ -340 (N'), –69 (N).

Di-protonated ligand **H_2L15^{2+}** (2.22 eq. CF_3COOH):

^{1}H-NMR (400 MHz, $CDCl_3/CD_3CN$): δ 7.21 (d, 2H, H(3), $^3J_{3,4}$ = 7.8 Hz), 7.13 (d, 2H, H(4), $^3J_{4,3}$ = 7.8 Hz), 4.31 (s, br, 2H, H(7)), 2.70 (s, 6H, H(5')), 2.64 (dd, 2H, H(10), $^3J_{10,9b}$ = 5.6 Hz, $^4J_{10,8}$ = 5.6 Hz), 2.51 (s, 6H, H(6')), 2.33 (ddd, 2H, H(9_b), $^2J_{9b,9a}$ = 9.4 Hz, $^3J_{9b,10}$ = 5.6 Hz, $^3J_{9b,8}$ = 5.6 Hz), 1.76(m, 2H, H(8)), 1.67 (s, 12H, H(3', 4')), 1.13 (s, 6H, H(12)), 0.99 (s, br, 2H, H(9_a)), 0.53 (s, 6H, H(13)).

^{13}C-NMR ($CDCl_3$/ACN-d_3, 100 MHz): δ 159.25 (C(6)), 154.13 (C(2)), 143.90 (C(5)), 139.38 (C(4)), 123.42 (C(3)), 67.72 (C(2')), 50.56 (C(10)), 50.60 (C(7)), 44.23 (C(6')), 31.29 (C(12)), 26.47 (C(3', 4')), 26.17 (C(13)).

5.3.4 [4,5]-CHIRAGEN[0] (L20)

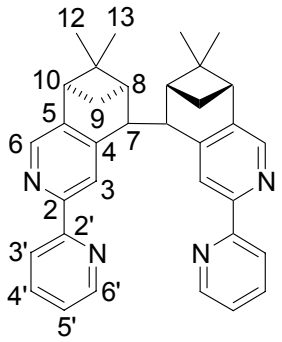

Free ligand **L20**:

^{1}H-NMR (400 MHz, $CDCl_3/CD_3CN$): δ 8.48 (ddd, 2H, H(6')), 8.29 (s, 2H, H(3)), 8.19 (ddd, 2H, H(3')), 8.10 (s, 2H, H(6), $^3J_{3,4}$ = 8.0 Hz), 7.66 (ddd, 2H, H(4'), $^3J_{4',3'}$ = 7.8 Hz, $^3J_{4',5'}$ = 7.8 Hz, $^4J_{4',6'}$ = 1.5 Hz), 7.15 (ddd, 2H, H(5'), $^3J_{5',4'}$ = 7.6 Hz, $^3J_{5',6'}$ = 5.3 Hz, $^4J_{5',3'}$ = 1.0 Hz), 3.88 (s, 2H, H(7)), 2.69 (dd, 2H, H(10), $^3J_{10,9b}$ = 5.3 Hz, $^3J_{10,8}$ = 5.3 Hz), 2.36 (ddd, 2H, H(9_b), $^2J_{9b,9a}$ = 10.4 Hz, $^3J_{9b,10}$ = 5.8 Hz, $^3J_{9b,8}$ = 5.8 Hz), 1.94 (dd,

2H, H(8), $^{3}J_{8,9b}$ = 5.6 Hz, $^{4}J_{8,10}$ = 5.6 Hz), 1.14 (s, 6H, H(12)), 1.09 (d, 2H, H(9_a), $^{2}J_{9a,9b}$ = 10.4 Hz), 0.54 (s, 6H, H(13)).

^{15}N-NMR (40 and 71 MHz, $CDCl_3/CD_3CN$): δ –79 (N), -72 (N').

UV/Vis: (MeOH/H_2O, 90% v/v), λ (ε): 288 ($3.0*10^4$).

CD: (MeOH/H_2O, 90% v/v), λ (ε): 295 (-15), 247 (-10).

Di-protonated ligand **H_2L20^{2+}** (5 eq. CF_3COOH)

^{1}H-NMR (400 MHz, $CDCl_3/CD_3CN$): δ 8.65 (ddd, 2H, H(6')), 8.56 (s, 2H, H(3)), 8.30 (ddd, 2H, H(3')), 8.29 (s, 2H, H(6), $^{3}J_{3,4}$ = 8.0 Hz), 8.05 (ddd, 2H, H(4'), $^{3}J_{4',3'}$ = 7.8 Hz, $^{3}J_{4',5'}$ = 7.8 Hz, $^{4}J_{4',6'}$ = 1.5 Hz), 7.55 (ddd, 2H, H(5'), $^{3}J_{5',4'}$ = 7.6 Hz, $^{3}J_{5',6'}$ = 5.3 Hz, $^{4}J_{5',3'}$ = 1.0 Hz), 4.16 (s, 2H, H(7)), 2.90 (dd, 2H, H(10), $^{3}J_{10,9b}$ = 5.3 Hz, $^{3}J_{10,8}$ = 5.3 Hz), 2.49 (ddd, 2H, H(9_b), $^{2}J_{9b,9a}$ = 10.4 Hz, $^{3}J_{9b,10}$ = 5.8 Hz, $^{3}J_{9b,8}$ = 5.8 Hz), 1.95 (dd, 2H, H(8), $^{3}J_{8,9b}$ = 5.6 Hz, $^{4}J_{8,10}$ = 5.6 Hz), 1.18 (s, 6H, H(12)), 1.09 (d, 2H, H(9_a), $^{2}J_{9a,9b}$ = 10.4 Hz), 0.56 (s, 6H, H(13)).

^{15}N-NMR (40 and 71 MHz, $CDCl_3/CD_3CN$): δ –158 (N), -112 (N').

UV/Vis: (MeOH/H_2O, 90% v/v), λ (ε): 312 ($3.0*10^4$).

CD: (MeOH/H_2O, 90% v/v), λ (ε): 324 (-17), 251 (-18).

REFERENCES

[1] "helix", 4th ed., The American Heritage® Dictionary of the English Language, Boston: Houghton Mifflin, **2000**.

[2] A. von Zelewsky, "Stereochemistry of Coordination Compounds", John Wiley & Sons Ltd, Chichester, **1995**.

[3] Lord Kelvin, "In *Baltimore Lectures*", Cambridge University Press, Cambridge, **1904**.

[4] J. H. Jung, Y. Ono, S. Shinkai, *Chem. Eur. J.* **2000**, *6*, 4552.

[5] K. P. Meurer, F. Vögtle, *Top. Curr. Chem.* **1985**, *127*, 1.

[6] H.-C. H. Wu, S. A;, *Carbohyde. Res.* **1978**, *61*, 27.

[7] W. Saenger, "Principles of Nucleic Acid Structure", Springer, New York, **1984**.

[8] J. D. Watson, F. C. H. Crick, *Nature* **1953**, *171*, 737.

[9] A. Fehrst, "Structure and Mechanism in Protein Science", W. H. Freeman, New York, **1998**.

[10] V. Berl, I. Huc, R. G. Khoury, M. J. Krische, J.-M. Lehn, *Nature* **2000**, *407*, 720.

[11] S. Hanessian, M. Simard, S. Roelens, *J. Am. Chem. Soc.* **1995**, *117*, 7630.

[12] S. Hanessian, A. Gomtsyan, M. Simard, S. Roelens, *J. Am. Chem. Soc.* **1994**, *116*, 4495.

[13] J.-M. Lehn, *Chem. Eur. J.* **2000**, *6*, 2097.

[14] A. E. Rowan, R. J. M. Nolte, *Angew. Chem., Int. Ed.* **1998**, *37*, 63.

[15] J.-M. Lehn, A. Rigault, J. Siegel, J. Harrowfield, B. Chevrier, D. Moras, *Proc. Natl. Acad. Sci. USA* **1987**, *84*, 2565.

[16] C. L. Atkin, J. B. Neilands, *Biochemistry* **1968**, *7*, 3734.

[17] R. C. Scarrow, D. L. White, K. N. Raymond, *J. Am. Chem. Soc.* **1985**, *107*, 6540.

[18] J. M. Lehn, J. P. Sauvage, J. Simon, R. Ziessel, C. Piccinni-Leopardi, G. Germain, J. P. Declercq, M. Van Meerssche, *Nouv. J. Chim.* **1983**, *7*, 413.

[19] G. C. Van Stein, H. Van der Poel, G. Van Koten, A. L. Spek, A. J. M. Duisenberg, P. S. Pregosin, *Chem. Commun.* **1980**, 1016.

[20] W. S. Sheldrick, J. Engel, *Chem. Commun.* **1980**, 5.

[21] C. J. Carrano, K. N. Raymond, *J. Am. Chem. Soc.* **1978**, *100*, 5371.

[22] G. Struckmeier, U. Thewalt, J. H. Fuhrhop, *J. Am. Chem. Soc.* **1976**, *98*, 278.

[23] C. Piguet, G. Bernardinelli, G. Hopfgartner, *Chem. Rev.* **1997**, *97*, 2005.

[24] M. Albrecht, *Chem. Rev.* **2001**, *101*, 3457.

[25] R. S. Cahn, C. Ingold, V. Prelog, *Angew. Chem.* **1966**, *78*, 413.

[26] T. Damhus, C. E. Schäfer, *Inorg. Chem.* **1983**, *22*, 2406.

[27] R. Krämer, J.-M. Lehn, A. Marquis-Rigault, *Proc. Natl. Acad. Sci. U.S.A.* **1993**, *90*, 5394.

[28] D. Caulder, K. N. Raymond, *Angew. Chem. Int. Ed.* **1997**, *36*, 1440.

[29] M. A. Masood, E. J. Enemark, T. D. P. Stack, *Angew. Chem. Int. Ed.* **1998**, *37*, 928.

[30] M. Albrecht, S. Kotila, *Chem. Comm.* **1996**, 2309.

[31] R. P. Thummel, C. Hery, D. Williamson, F. Lefoulon, *J. Am. Chem. Soc.* **1988**, *110*, 7894.

[32] D. A. Bardwell, F. Barigelletti, R. L. Cleary, L. Flamigni, M. Guardigli, J. C. Jeffery, M. D. Ward, *Inorg. Chem.* **1995**, *34*, 2438.

[33] J. H. Brewster, *Top. Curr. Chem.* **1974**, *47*, 29.

[34] V. Balzani, A. Juris, M. Venturi, S. Campagna, S. Serroni, *Chem. Rev.* **1996**, *96*, 759.

[35] N. C. Fletcher, F. R. Keene, H. Viebrock, A. von Zelewsky, *Inorg. Chem.* **1997**, *36*, 1113.

[36] N. C. Fletcher, F. R. Keene, M. Ziegler, H. Stoeckli Evans, H. Viebrock, A. Von Zelewsky, *Helv. Chim. Acta* **1996**, *79*, 1192.

[37] H. Muerner, P. Belser, A. von Zelewsky, *J. Am. Chem. Soc.* **1996**, *118*, 7989.

[38] J. Hamblin, L. J. Childs, N. W. Alcock, M. J. Hannon, *J.. Chem. Soc., Dalton Trans.* **2002**, 164.

[39] C. Provent, E. Rivara-Minten, S. Hewage, G. Brunner, W. A. F., *Chem. Eur. J.* **1999**, *5*, 3487.

[40] C. Provent, S. Hewage, G. Brand, G. Bernardinelli, L. J. Chrbonnière, A. F. Wiliams, *Angew. Chem., Int. Ed.* **1997**, *36*, 1287.

[41] H. Nishiyama, M. Kondo, T. Nakamura, K. Itoh, *Organometallics* **1991**, *10*, 500.

[42] S. G. Telfer, G. Bernardinelli, A. F. Williams, *Chem. Comm.* **2001**, *16*, 1498.

[43] P. N. W. Baxter, J.-M. Lehn, K. Rissanen, *Chem. Comm.* **1997**, *14*, 1323.

[44] G. Baum, E. C. Constable, D. Fenske, C. E. Housecroft, T. Kulke, *Chem. Comm.* **1999**, 195.

[45] C. Bonnefous, N. Bellec, R. Thummel, *Chem. Comm.* **1999**, *13*, 1243.

[46] B. Hasenknopf, J.-M. Lehn, N. Boumediene, A. Dupont-Gervais, A. Van Dorsselaer, B. Kneisel, D. Fenske, *J. Am. Chem. Soc.* **1997**, *119*, 10956.

[47] C. S. Campos-Fernández, R. Clérac, K. R. Dunbar, *Angew. Chem., Int. Ed.* **1999**, *38*, 3477.

[48] T. Bark, M. Dueggeli, H. Stoeckli-Evans, A. Von Zelewsky, *Angew. Chem., Int. Ed.* **2001**, *40*, 2848.

[49] R. Krämer, J.-M. Lehn, A. De Cian, J. Fischer, *Angew. Chem., Int. Ed.* **1993**, *32*, 703.

[50] B. Hasenknopf, J.-M. Lehn, N. Boumediene, E. Leize, A. Van Dorsselaer, *Angew. Chem., Int. Ed.* **1998**, *37*, 3265.

[51] O. Mamula, A. Von Zelewsky, G. Bernardinelli, *Angew. Chem., Int. Ed.* **1998**, *37*, 290.

[52] O. Mamula, F. J. Monlien, A. Porquet, G. Hopfgartner, A. E. Merbach, A. Von Zelewsky, *Chem. Eur. J.* **2001**, *7*, 533.

[53] P. L. Jones, K. J. Byrom, J. C. Jeffery, J. A. Mc Cleverty, M. D. Ward, *Chem. Comm.* **1997**, *15*, 1361.

[54] E. C. Constable, M. G. B. Drew, G. Forsith, M. D. Ward, *Chem. Comm.* **1988**, 1450.

[55] E. C. Constable, S. M. Elder, P. R. Raithby, M. D. Ward, *Polyhedron* **1991**, *10*, 1395.

[56] E. C. Constable, J. V. Walker, D. A. Tocher, M. A. M. Daniels, *Chem. Comm.* **1992**, 768.

[57] E. C. Constable, M. A. M. Daniels, M. G. B. Drew, D. A. Tocher, J. V. Walker, P. D. Wood, *J. Chem. Soc. Dalton Trans.* **1993**, 1947.

[58] K. A. Gheysen, K. T. Potts, H. C. Hurell, H. D. Abruna, *Inorg. Chem.* **1990**, *29*, 1589.

[59] Y. Fu, J. Sun, Q. Li, Y. Chen, W. Dai, D. Wang, T. C. W. Mak, W. Tang, H. Hu, *J. Chem. Soc. Dalton Trans.* **1996**, 2309.

[60] O. Mamula, A. Von Zelewsky, T. Bark, H. Stoeckli-Evans, A. Neels, G. Bernardinelli, *Chem. Eur. J.* **2000**, *6*, 3575.

[61] M. Cesario, O. C. Dietrich, A. Edel, J. Guilhem, J.-P. Kintzinger, C. Pacard, J.-P. Sauvage, *J. Am. Chem. Soc.* **1986**, *108*, 6250.

[62] N. Fatin-Rouge, S. Blanc, E. Leize, A. Van Drosselaer, P. Baret, J.-P. Pierre, A.-M. Albrecht-Gary, *Inorg. Chem.* **2000**, *39*, 5771.

[63] S. P. Meneghetti, P. J. Lutz, J. Fischer, J. Kress, *Polyhedron* **2001**, *20*, 2705.

[64] C.-M. Che, Z.-Y. Li, K.-Y. Wong, C.-K. Poon, T. C. W. Mak, S.-M. Peng, *Polyhedron* **1994**, *13*, 771.

[65] P. Hayoz, *Thesis No. 1022, University of Fribourg* **1992**.

[66] R. W. Alder, P. S. Bowman, W. R. S. Steele, D. R. Winterman, *Chem. Commun.* **1968**, 723.

[67] H. Mürner, A. von Zelewsky, G. Hopfgartner, *Inorg. Chim. Acta* **1998**, *271*, 36.

[68] H. Mürner, A. von Zelewsky, H. Stoeckli-Evans, *Inorg. Chem.* **1996**, *35*, 3931.

[69] P. Hayoz, A. Von Zelewsky, *Tetrahedron Lett.* **1992**, *33*, 5165.

[70] H. Mürner, *Thesis No. 1135, University of Fribourg* **1996**.

[71] E. D. Mihelich, D. J. Eickhoff, *J. Org. Chem.* **1983**, *48*, 4135.

[72] W. Zecher, F. Kröhnke, *Chem. Ber.* **1961**, *94*, 690.

[73] W. Zecher, F. Kröhnke, *Chem. Ber.* **1961**, *94*, 698.

[74] W. Zecher, F. Kröhnke, *Chem. Ber.* **1961**, *94*, 707.

[75] F. Kröhnke, *Synthesis* **1976**, 1.

[76] J.-P. Sauvage, M. Ward, *Inorg. Chem.* **1991**, *30*, 3869.

[77] M. V. Jovanovic, *Heterocycles* **1984**, *22*, 1195.

[78] Y. Hama, Y. Nobuhara, Y. Aso, T. Otsubo, F. Ogura, *Bull. Chem. Soc. Jpn* **1988**, *61*, 1683.

[79] P. M. Windscheif, F. Voegtle, *Synthesis* **1994**, 87.

[80] F. Vögtle, R. Hochberg, F. Kochendörfer, P.-M. Windscheif, M. Volkmann, M. Jansen, *Chem. Ber.* **1990**, *123*, 2181.

[81] H.-P. Hsieh, L. W. McLaughlin, *J. Org. Chem.* **1995**, *60*, 5356.

[82] F. H. Case, *J. Am. Chem. Soc.* **1946**, *68*, 2574.

[83] A. Suzuki, *Pure Appl. Chem.* **1985**, *57*, 1749.

[84] A. Suzuki, *Pure Appl. Chem.* **1991**, *63*, 419.

[85] A. Suzuki, *Pure Appl. Chem.* **1994**, *66*, 213.

[86] A. Suzuki, *J. Organomet. Chem.* **1999**, *576*, 147.

[87] M. A. Peterson, J. R. Mitchell, *J. Org. Chem.* **1997**, *62*, 8237.

[88] J. E. Parks, B. E. Wagner, R. H. Holm, *J. Org. Chem.* **1973**, *56*, 53.

[89] Gilbert, *J. Am. Chem. Soc.* **1955**, *77*, 4413.

[90] T. Yamashita, K. Shiomori, M. Yasuda, ;, S. Kensuke, *Bull. Chem. Soc. Jpn* **1991**, *64*, 366.

[91] T. Yamashita, M. Watanabe, R. Kojima, T. Shiragami, K. Shima, M. Yasuda, *J. Photochem. Photobiol., A* **1998**, *118*, 165.

[92] F. Pezet, I. Sasaki, J.-C. Daran, J. Hydrio, H. Aït-Haddou, G. Balavoine, *Eur. J. Inorg. Chem.* **2001**, 2669.

[93] M. Palacio, *unpublished results*.

[94] L.-E. Perret Aebi, A. von Zelewsky, *Synlett* **2002**, *5*, 773.

[95] B. Quinodoz, *unpublished results*.

[96] M. E. Huttenloch, J. Diebold, U. Rief, H. H. Brintzinger, *Organometallics* **1992**, *11*, 3600.

[97] M. Enders, G. Kohl, H. Pritzkow, *J. Org. Chem.* **2001**, *622*, 66.

[98] J. G. P. Delis, P. W. N. M. van Leeuwen, K. Vrieze, N. Veldman, A. L. Spek, J. Fraanje, K. Goubitz, *J. Org. Chem.* **1996**, *514*, 125.

[99] R. Arnold, S. A. Matchett, *Organometallics* **1988**, *7*, 2261.

[100] G. Baum, E. C. Constable, D. Fenske, T. Kulke, *Chem. Commun.* **1997**, 2043.

[101] G. Baum, E. C. Constable, D. Fenske, C. E. Housecroft, T. Kulke, *Chem. Eur. J.* **1999**, *5*, 1862.

[102] E. C. Constable, T. Kulke, G. Baum, D. Fenske, *Inorg. Chem. Commun.* **1998**, *1*, 80.

[103] A. V. Malkov, Bella Marco, V. Langer, P. Kocovsky, *Org. Lett.* **2000**, *2*, 3047.

[104] A. V. Malkov, I. R. Baxendale, M. Bella, V. Langer, J. Fawcett, D. R. Russel, D. J. Mansfield, M. Valko, P. Kocovsky, *Organometallics* **2001**, *20*, 673.

[105] L. L. Merritt, E. D. Schroeder, *Acta Crystallogr:* **1956**, 801.

[106] S. Rupprecht, H. Viebrock, A. Von Zelewsky, D. Abeln, *Z. Kristallogr.* **1997**, *212*, 317.

[107] A. Goeller, U.-W. Grummt, *Chem. Phys. Lett.* **2000**, 399.

[108] G. J. Kubas, *Inorg. Synth.* **1979**, *19*, 90.

[109] B. J. Hathaway, D. G. Holah, J. D. Postlethwaite, *J. Chem. Soc.* **1961**, 3215.

[110] G. Schaftenaar, J. H. Noordik, *J. Comput.-Aided Mol. Design* **2000**, *14*, 123.

[111] O. Mamula, *Thesis No. 1268, University of Fribourg* **1999**.

[112] "CRC Handbook of Chemistry and Physics", 59 ed., CRC Press, Inc, West Palm Beach, Florida, **1978**.

[113] P. Krumholz, *J. Am. Chem. Soc* **1951**, *73*, 3487.

[114] H. Uchimura, A. Tajiri, M. Hatano, *Bull. Chem. Soc. Jpn.* **1984**, *57*, 341.

[115] K. Nakamoto, *J. Phys. Chem.* **1960**, *64*, 1420.

[116] O. Borgen, B. Mestvedt, I. Skauvik, *Acta. Chem. Scand. A* **1976**, *30*, 43.

[117] D. K. Hazra, S. C. Lahiri, *Anal. Chim. Acta* **1975**, *79*, 335.

[118] L. H. Abdel-Rahman, G. G. Herman, A. M. Goeminne, M. Mahmoud, *Bull. Soc. Chim. Belg.* **1990**, *99*, 73.

[119] D. K. Hazra, S. C. Lahiri, *J. Indian Chem. Soc.* **1976**, *53*, 787.

[120] D. K. Hazra, S. C. Lahiri, *J. Indian Chem. Soc.* **1976**, *53*, 567.

[121] R. Mandal, S. C. Lahiri, *Z. Phys. Chem.* **1999**, *210*, 157.

[122] S. Bandyopadhyay, A. K. Mandal, S. Aditya, *J. Indian Chem. Soc* **1981**, *58*, 467.

[123] G. V. Budu, L. V. Nazarova, *Russ. J. Inorg. Chem. (Engl. Ed)* **1973**, *18*, 1574.

[124] S. K. Chakravorty, D. Sengupta, S. C. Lahiri, *Z. Phys. Chem.* **1986**, *267*, 969.

[125] S. C. Lahiri, C. C. Deb, D. K. Hazra, *Z. phys. Chem.* **1985**, *1*, 158.

[126] J. Fan, J. Wang, C. Ye, *Talanta* **1998**, *46*, 1285.

[127] D. H. Buisson, R. J. Irving, *J. Chem. Soc. Faraday Trans. I* **1977**, *73*, 157.

[128] M. Maestri, D. Sandrini, V. Balzani, A. von Zelewsky, C. Deuschel-Cornioley, P. Jolliet, *Helv. Chim. Acta* **1988**, *71*, 1053.

[129] N. N. Vlasova, N. K. Davidenko, V. I. Bogomaz, *Russ.J. Phys. Chem.* **1995**, *69*, 2001.

[130] C. C. Deb, D. K. Hazra, S. C. Lahiri, *Indian J. Chem.* **1992**, *21*, 26.

[131] K. Izutsu, "Acid-base dissociation constants in dipolar aprotic solvents", Blackwell Scientific Publications (IUPAC Chemical data Series No. 35)", Oxford, **1990**.

[132] M. Hesse, H. Meier, B. Zeeh;, "Spektroskopische Methoden in der organischen Chemie", 4. ed., Gerorge Thieme Verlag, Stuttgart, **1991**.

[133] H.-O. Kalinowksy, S. Berger, S. Braun, "^{13}C-NMR-Spektroskopie", Georg Thieme Verlag, Stuttgart, **1984**.

[134] P. Collomb, *Thesis No. 1174, University of Fribourg* **1997**.

[135] D. Lötscher, S. Rupprecht, H. Stoeckli-Evans, A. von Zelewsky, *Tetrahedron: Asymmetry* **2000**, *11*, 4341.

[136] A. Gaset, A. Verdier, A. Lattes, *Spectrochim. Acta, Part A* **1975**, *31A*, 727.

[137] F. Ros, J. de la Rosa, J. Enfedaque, *J.Org. Chem.* **1995**, *60*, 5419.

[138] Stoe, &, Cie, "IPDS Software", Stoe & Cie GmbH, Darmstadt, Germany, **2000**.

[139] G. M. Sheldrick, *Acta Crystallogr.* **1990**, *A46*, 467.

[140] G. M. Sheldrick, "SHELXL-97", Universität Göttingen, Göttingen, Germany, **1999**.

[141] A. L. Spek, *Acta Crystallogr.* **1990**, *A46*, C-34.

[142] Altomare, G. Cascarano, C. Giacovazzo, C. Guagliardi, A. G. G. Moliterni, M. C. Burla, G. Polidori, M. Camalli, R. Spagna, SIR97 - A package for crystal structure solution by direct methods and refinement, c/o Istituto di Ricerca per lo Sviluppo di Metodologie Cristallografiche, CNR, & Dipartimento Geomineralogico, Campus Universitario, Via Orabona 4, 70125 Bari., **1997**.

[143] G. J. Martin, M. L. Martin, J.-P. Gouesnard, "^{15}N-Spectroscopy", Springer Verlag, Berlin, **1981**.

APPENDIX

APPENDIX

1. Complete ^{1}H spectra of the titration of L1 with CF_3COOH

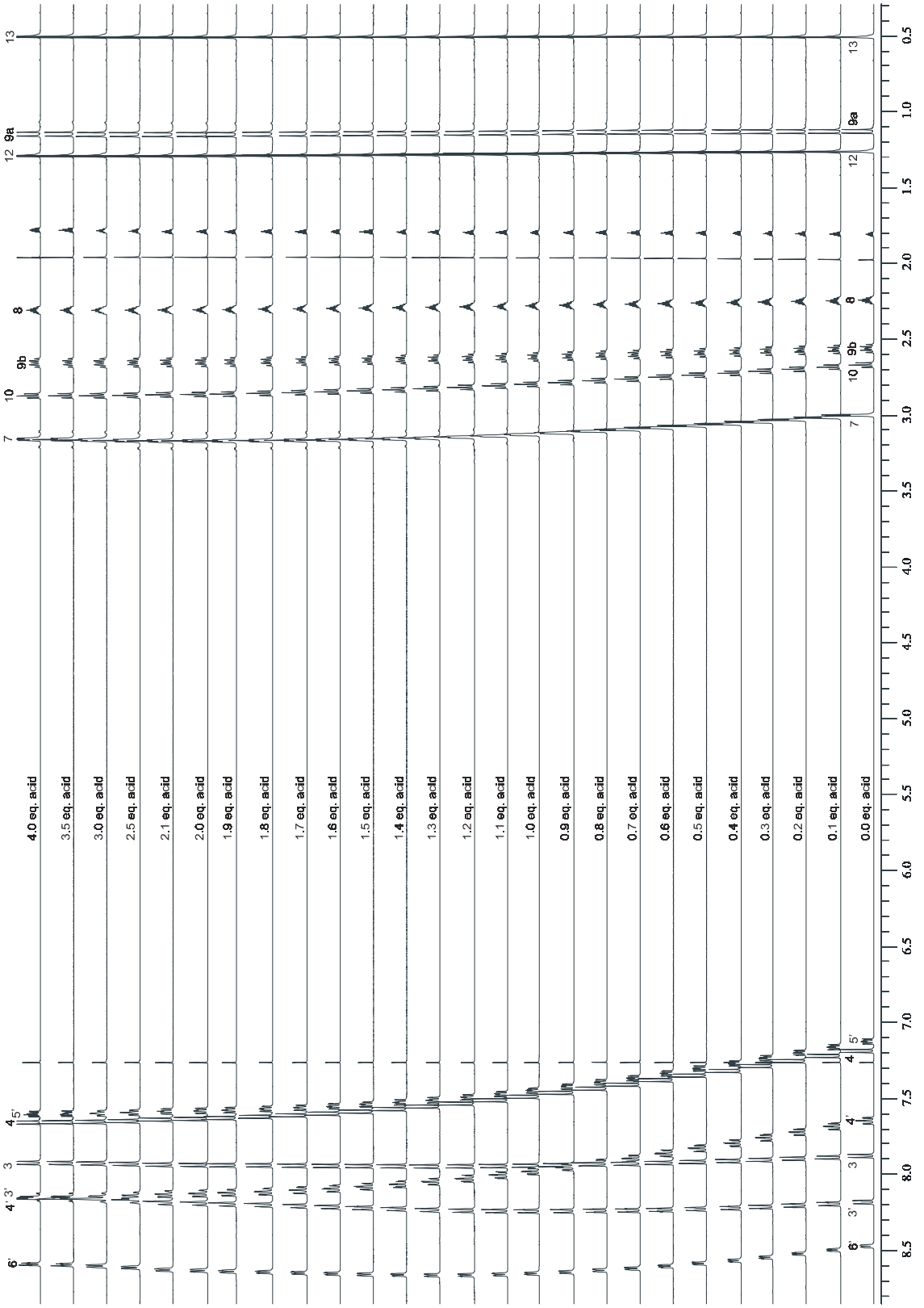

2. Complete ^{1}H spectra of the titration of L15 with CF_3COOH

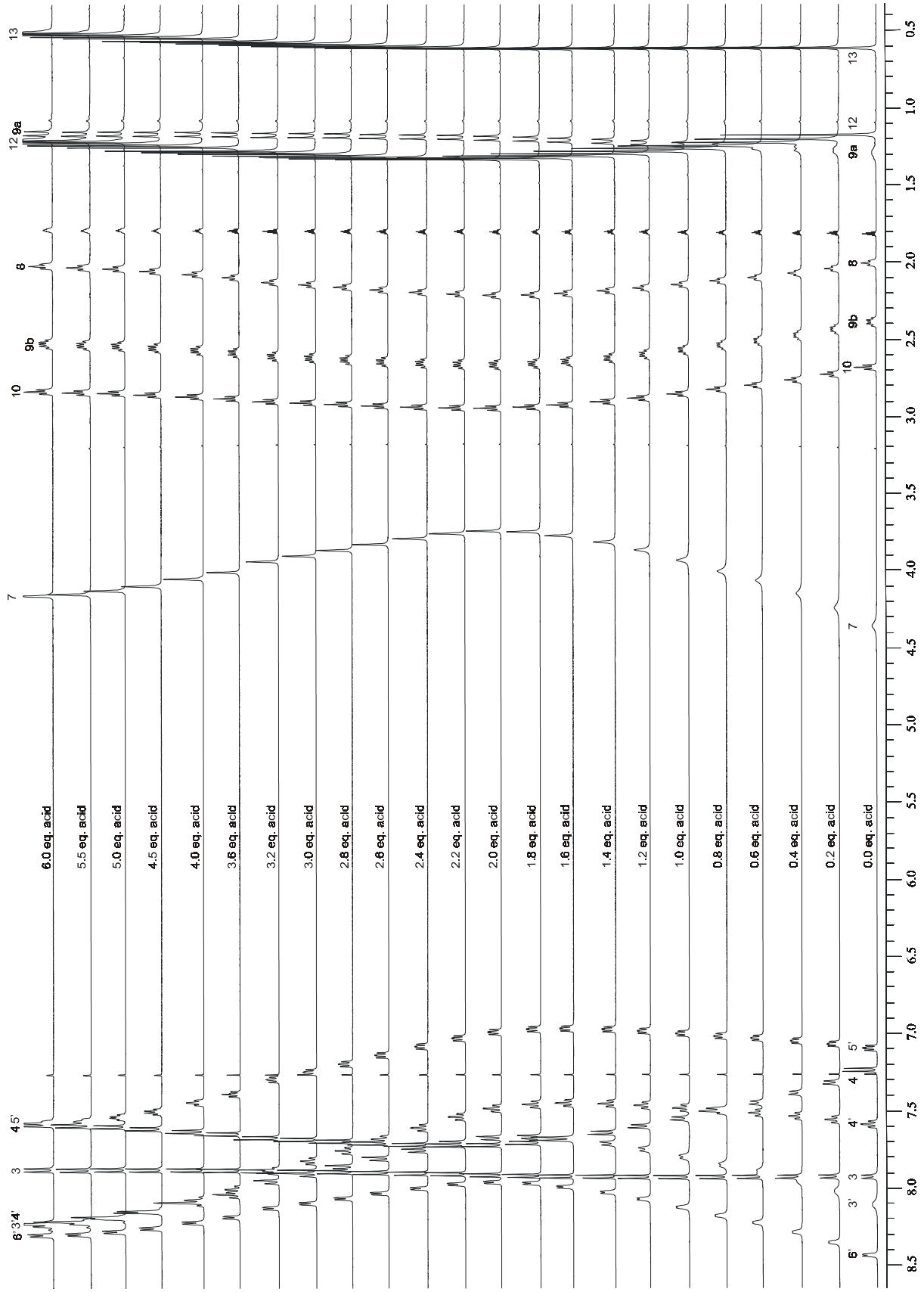

3. Complete ^{1}H spectra of the titration of L20 with CF3COOH

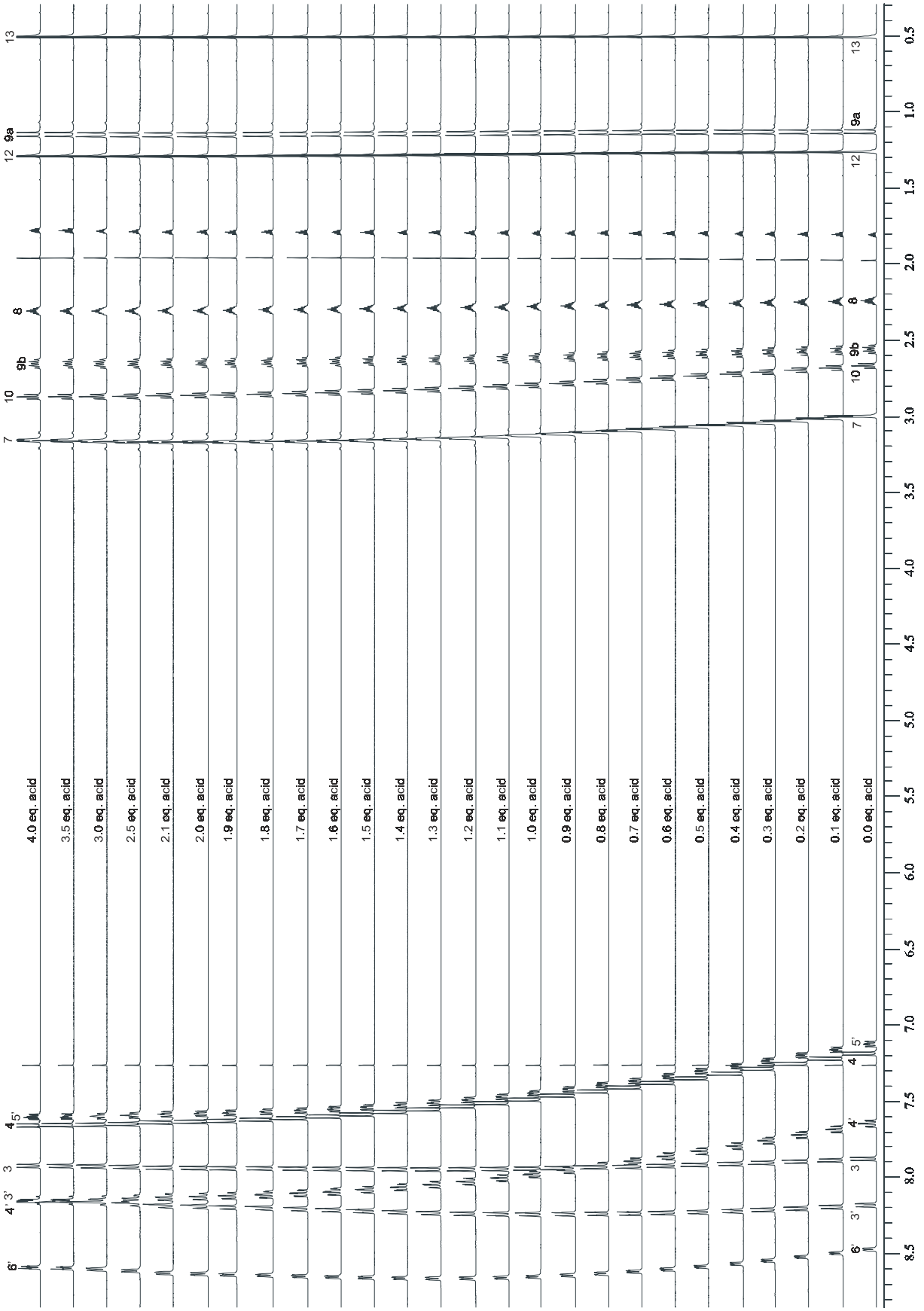

Curriculum Vitae

Personalien :

Name, Vorname:	Düggeli, Mathias
Geburtsdatum:	14.08.1973
Staatsangehörigkeit:	Schweizer
Heimatort:	Malters (LU)
Zivilstand:	ledig
Militär:	Fk Wm des Inf Rgt 19

Besuchte Schulen:

1980-1986	Primarschule in Malters
1986-1993	Kantonsschule in Reussbühl
1993-1997	Chemiestudium an der Universtät Freiburg
1998	Sprachschule in London (5 Monate)
1998- Juli 2002	Doktorat bei Prof. Dr. Alex von Zelewsky an der Univeristät Freiburg
ab August 2002	Postdoc bei Prof. Dr. Alex von Zelewsky an der Univeristät Freiburg

Erhaltene Diplome:

1993	Matura in Typus A (Latein und Altgriechisch)
1997	Diplom in Chemie mit Hauptfach anorganische Chemie und Nebenfach organische Chemie Diplomarbeit in anorganischer Chemie bei Prof. Dr. P. Belser: „Herstellung eines dinuklearen Ru-PCP-Os- Komplexes“
1998	Cambridge Certificate in Advanced English (CAE) Cambridge First Certificate in Englisch (FCE)
2002	Doktorat am Departement für Chemie der Universität Freiburg unter Leitung von Prof. Dr. A. von Zelewsky: “Complexation and Protoantion Behaviour of Chiral Tetradentate Polypyridines Derived from α-Pinene”

Berufserfahrungen:

1998	Praktikum bei CIBA SC in Marly (13 Wochen, mit Patent)
seit 1.10.1998	Assistent des Praktikum für anorganische und analytische Chemie (Erstjahrstudenten in Biochemie) durchgeführt in zwei Sprachen (deutsch und französisch) Betreuung von Diplomstudenten und 3. Jahreslehrlinge
seit 1.1.2001	NMR-Verantwortlicher für ein 400 MHz Bruker NMR-Spektrometer. Weiterbildungskurs bei Bruker (Oktober 2001).

Wissenschaftliche Publikationen:

”Yellow Pteridine having a Hue-Angle of at least 98”
Eichenberger, Thomas; Düggeli, Mathias, Hügin, Max (CIBA Speciality Chemicals Holding Inc., Switz). PCT Int. Appl., **1999**, 31.

”Designed Molecules for Self-Assembly: The Controlled Formation of Two Chiral Self-Assembled Polynuclear Species with Predetermined Configuration”
Bark, Thomas; Düggeli, Mathias; Stoeckli-Evans, Helen, von Zelewsky, Alexander, Angew. Chem., Int. Ed. **2001**, 40(15), 2848.

”Synthetic Routes for a New Family of Chiral Bipyridines Derived from Pinene”
Düggeli, Mathias; Goujon-Ginglinger, Catherine; Richard Ducotterd, Sarah; Mauron, David; Bonte, Christophe; von Zelewsky, Alexander, Stoeckli-Evans, Helen; in preparation.

Sprachliche Kenntnisse:

Muttersprache: Deutsch

Englisch-Kenntnisse: Sehr gut (Cambridge Certificate in Advanced English (CAE))

Französisch-Kenntnisse: Sehr gut (durch zweisprachiges Studium und Studentenbetreuung)

Besondere Kenntnisse:

Computerkenntnisse (Mac&PC) sehr gut
(MS-Office, Endnote, ChemOffice, IsisDraw, Adobe GoLive (Homepagedarstellung), Adobe Photoshop, MS Photodraw (Graphik)

[10] a) C. Cheadle, Y. Ivashchenko, V. South, G. H. Searfoss, S. French, R. Howk, G. A. Ricca, M. Jaye, *J. Biol. Chem.* **1994**, *269*, 24034 – 24039; b) A. B. Sparks, L. A. Quilliam, J. M. Thorn, C. J. Der, B. K. Kay, *J. Biol. Chem*. **1994**, *269*, 23853 – 23856; c) R. J. Rickles, M. C. Botfield, X. M. Zhou, P. A. Henry, J. S. Brugge, M. J. Zoller, *Proc. Natl. Acad. Sci. USA* **1995**, *92*, 10909 – 10913.

[11] a) T. Wöhr, F. Wahl, A. Nefzi, B. Rohwedder, T. Sato, X. Sun, M. Mutter, *J. Am. Chem. Soc.* **1996**, *118*, 9218 – 9227; b) M. Mutter, T. Wöhr, S. Gioria, M. Keller, *Biopolymers* **1999**, *51*, 121 – 128; c) A. Wittelsberger, M. Keller, L. Scarpellino, L. Patiny, H. Acha-Orbea, M. Mutter, *Angew. Chem*. **2000**, *112*, 1153 – 1156; *Angew. Chem. Int. Ed*. **2000**, *39*, 1111 – 1115.

[12] X. Wu, B. Knudsen, S. M. Feller, J. Zheng, A. Sali, D. Cowburn, H. Hanafusa, J. Kuriyan, *Structure* **1995**, *3*, 215.

[13] D. Bowtell, P. Fu, M. Simon, P. Senior, *Proc. Natl. Acad. Sci. USA* **1992**, *89*, 6511 – 6515; P. Chardin, J. H. Camonis, N. W. Gale, L. Van Aelst, M. H. Wigler, D. Bar-Sagi, *Science* **1993**, *60*, 1338 – 1343; M. Rozakis-Adcock, R. Fernley, J. Wade, T. Pawson, D. Bowtell, *Nature* **1993**, *363*, 83 – 85.

[14] The molecular graphics package INSIGHT II (version 97, Molecular Simulations, **1997**) was used. Energy minimizations and MD simulations were performed on a Silicon Graphics OCTANE by using the program CVFF/FDISCOVER (version 97, Molecular Simulations, **1997**). The simulations were performed with a cut-off distance of 12 Å, a time step of 1 fs, and a distance-dependent dielectricity constant ε of $4.00\,r$ (r = distance) The backbone coordinates of the N-terminal SH3 domain were restrained to their initial positions. Implicit treatment of solvation and conformational restraints permitted long run times of MD simulations within an appropriate time scale. After 5000 steps of steepest descent minimization, the system was heated to 298 K by applying the standard FDISCOVER protocol. After an initialization time of 10 ps, the simulation run was continued for 1 ns. Averaged structures were generated for the last 50 ps of the simulation and further minimized for 500 steps of steepest descent, followed by a conjugate gradient minimization until the rms gradient was < 0.01 kcal mol^{-1} Å^{-1}. After this procedure, the peptide ligand Val-Pro-Ser(Ψpro^{Ph,H})-Pro-Val-Ser(Ψpro^{Ph,H})-Pro-Arg-Arg-Arg was compared with Val-Pro-Pro-Pro-Val-Pro-Pro-Arg-Arg-Arg, the decameric native SoS peptide sequence 3gbq.[21] The fluctuation was analyzed for the last 500 ps of the simulation.

[15] M. Keller, M. Mutter, C. Lehmann, *Synlett* **1999**, *S1*, 935 – 939; M. Keller, C. Lehmann, M. Mutter, *Tetrahedron* **1999**, *55*, 413 – 422.

[16] J. M. Stewart, J. D. Young, *Solid Phase Peptide Synthesis*, 2nd ed., Pierce Chemical, Rockford, IL, **1984**.

[17] E. Klein, H. Ben-Bassat, H. Neumann, P. Ralph, J. Zeuthen, A. Polliack, F. Vanky, *Int. J. Cancer* **1976**, *18*, 421 – 431.

[18] G. Posern, J. Zheng, B. S. Knudsen, C. Kardinal, K. B. Muller, J. Voss, T. Shishido, D. Cowburn, G. Cheng, B. Wang, G. D. Kruh, S. K. Burell, C. A. Jacobson, D. M. Lenz, T. J. Zamborelli, K. Adermann, H. Hanafusa, S. M. Feller, *Oncogene* **1998**, *16*, 1903 – 1912.

[19] J. M. Word, S. C. Lovell, T. H. LaBean, H. C. Taylor, M. E. Zalis, B. K. Presley, J. S. Richardson, D. C. Richardson, *J. Mol. Biol.* **1999**, *285*, 1711 – 1733.

[20] P. Sieber, *Tetrahedron Lett*. **1987**, *28*, 2107.

[21] M. Wittekind, C. Mapelli, V. Lee, V. Goldfarb, M. S. Friedrichs, C. A. Meyers, L. Müller, *J. Mol. Biol*. **1997**, *267*, 933 – 952.

Designed Molecules for Self-Assembly: The Controlled Formation of Two Chiral Self-Assembled Polynuclear Species with Predetermined Configuration**

Thomas Bark, Mathias Düggeli, Helen Stoeckli-Evans, and Alex von Zelewsky*

Self-assembly reactions are not yet as predictable to the same degree as classical reaction sequences. Often, highly interesting structures are obtained through a combination of intuition, conjecture, and serendipity.[1] Herein, we report the formation of two closely related supramolecular structures that were obtained in a programmed way. Our intention is to fabricate supramolecular complexes of the type **A** from octahedrally coordinating metal ions.

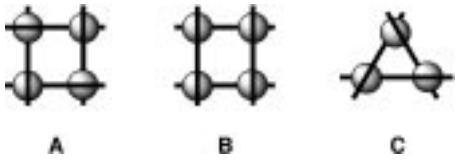

Complexes of this type are chiral (D_4 symmetry) as a consequence of the special way the ligand strands enfold the cations. Chirality is the main feature that distinguishes them from the related grid-type complexes **B** investigated by J.-M. Lehn and co-workers,[2a,b] and other recently reported molecular squares.[2c,d]

To achieve such structures we had to design a ligand that fulfils the following demands: 1) it must offer two terpyridine-type binding sites to cover each half of the coordination sphere of an OC-6 cation in a *mer* configuration; 2) it must be geometrically rigid, and define the side of a square in a tetranuclear self-assembled species; and 3) the orientation of the binding vectors of the two terpyridine (terpy) units must be antiparallel, in order to make the ligand coordinate to the metal ions once from "above" and once from "below" the plane defined by the four metal ions. These requirements, and especially the relative orientation of the binding sites, are fulfilled in ligand L^1, in which two 2,2′-bipyridin-6-yl groups are attached to a central pyrazine ring at positions 2 and 5.[3]

[*] Prof. Dr. A. von Zelewsky, T. Bark, M. Düggeli
Department of Chemistry
University of Fribourg
Pérolles, 1700 Fribourg (Switzerland)
Fax: (+41) 26-300-97-38
E-mail: alexander.vonzelewsky@unifr.ch

Prof. Dr. H. Stoeckli-Evans[+]
Institute of Chemistry
University of Neuchâtel
Avenue de Bellevaux 51, 2000 Neuchâtel (Switzerland)

[+] Crystal structure analysis.

[**] This work was financially supported by the Swiss National Science Foundation. We thank F. Nydegger for ESI-MS measurements and F. Fehr for conducting NOE experiments. Prof. C. W. Schläpfer and Prof. C. A. Daul are thanked for fruitful discussions.

Supporting information for this article is available on the WWW under http://www.angewandte.com or from the author.

  1433-7851/01/4015-2848 $ 17.50+.50/0

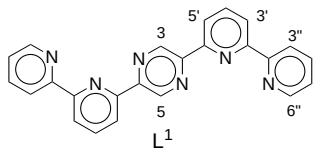

L^1

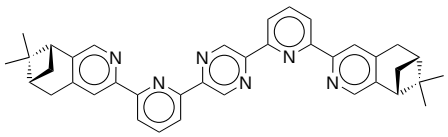

L^2

This ligand yields the desired tetrameric assembly with Zn^{2+} ions. The solution behavior of $[Zn_4(L^1)_4](PF_6)_8$ (**1**) in MeCN was investigated by electrospray-ionization mass spectrometry (ESI-MS) as well as by ^1H and ^{13}C NMR spectroscopy. The mass spectrum (Figure 1 a) reveals the tetrameric structure of **1** and displays peaks that are attributed unambiguously (from their isotopic distribution pattern) to fragments of the type $[Zn_4(L^1)_4](PF_6)_n$ ($n = 3-6$).

The ^1H NMR spectrum of the complex in CD_3CN displays one half-set of hydrogen atoms that originate from L^1; the symmetry of the ligand is thus not broken upon complexation. All resonances have been identified by 2D experiments ($^1H^1H$-COSY, NOE). The spectrum of **1** is always accompanied by a minor species with the same number of signals and the same coupling patterns. The relative amount of this minor species *increases* at lower overall concentrations of **1** and *decreases* at higher temperatures. Detailed studies revealed the existence of an equilibrium between a trimer[4] of type **C** and a tetramer, with the tetramer being the major species in the concentration range investigated. The thermodynamic parameters of this equilibrium are given in Figure 2.

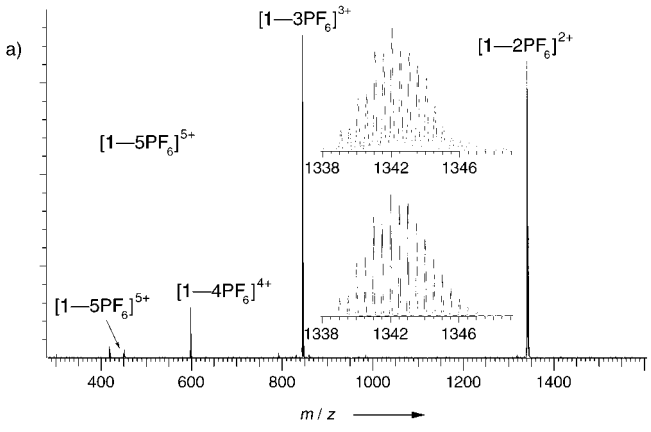

Figure 1. a) ESI mass spectrum of $[Zn_4(L^1)_4](PF_6)_8$ (a) and $[Zn_4(L^2)_4](PF_6)_8$ (b) in MeCN. Inset: found (top in both) and calculated (bottom in both) isotopic distribution for $\{[Zn_4(L^1)_4](PF_6)_6\}^{2+}$ and $\{[Zn_4(L^2)_4](PF_6)_5\}^{3+}$, respectively.

$$3\ [Zn_4(L^1)_4](PF_6)_8 \underset{MeCN}{\overset{K}{\rightleftharpoons}} 4\ [Zn_3(L^1)_3](PF_6)_6$$

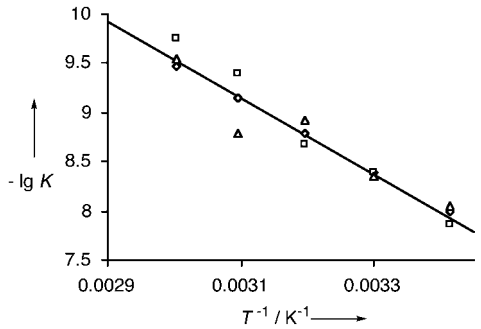

Figure 2. Temperature dependence of the tetramer/trimer equilibrium. The thermodynamic data were obtained by ^1H NMR spectroscopy. The equlibrium constants have been calculated from the integrals over three different protons (◇: H–C(3′); △: H–C(5′); □: H–C(3‴)). The resulting thermodynamic constants are: $\lg K^\circ(303\ K) = -(8.43 \pm 0.02)$; $\Delta H^\circ = -(74.5 \pm 10.0)\ kJ\,mol^{-1}$; $\Delta S^\circ = -(406 \pm 12)\ J\,mol^{-1}\,K^{-1}$.

The formation of the trimeric form from the tetramer is hence exothermic but endotropic. The negative ΔH° value must be the result of a better solvation of the trimeric complexes. The higher "ring strain" in the trimer resulting from a strong deviation from the ideal octahedral coordination geometry at the Zn^{2+} ions can probably be neglected because of the absence of ligand-field stabilization in Zn^{2+} ions. Thus the reduction of "void space" on going from the tetramer to the trimer dominates the reaction enthalpy. The negative reaction entropy is not easily understood, as both the number of complex ions and the configurational diversity increase upon the formation of the trimer. The same counter-intuitive behavior has been reported very recently for the equilibrium between the hexameric and tetrameric form of a silver-containing circular helicate.[5]

Complex **1** crystallizes[6] from $MeNO_2/Et_2O$ as a racemic compound in the centrosymmetrical space group *C*2/*c* (Figure 3). The symmetry of the complex in the crystal is C_2, and the zinc ions define a symmetrical trapezoid which is close to a square ($\alpha = 89.49(0.01)^\circ$, $\beta = 90.51(0.01)^\circ$). The lengths of the coordinative bonds are not unusual: Zn–N(pyridine) varies from 2.050 to 2.126 Å, while the bonds to the pyrazine nitrogen atoms are considerably longer (2.244–2.311 Å), probably as a result of electronic communication through the pyrazine ring. Two of the eight PF_6^- counterions are in close contact with the complex ion and occupy positions

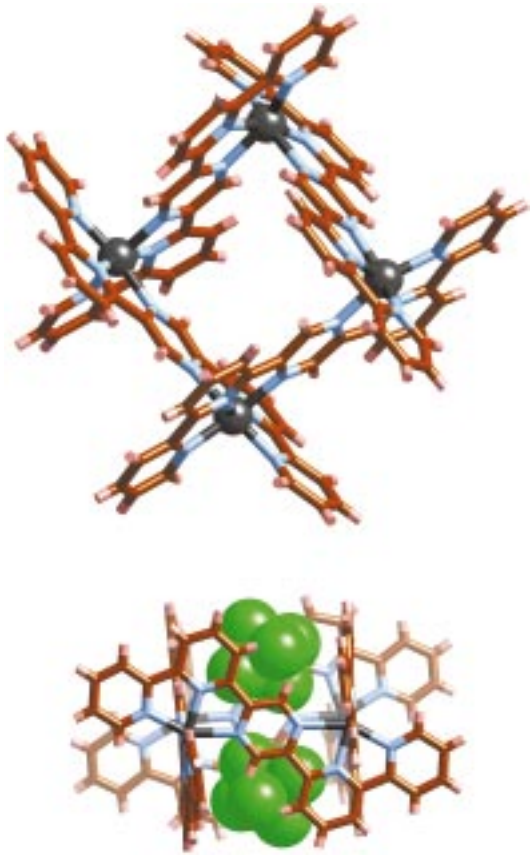

Figure 3. Crystal structure of the racemic compound $[Zn_4(L^1)_4](PF_6)_8$. Only the all-$\vec{\Delta}$ enantiomer is shown.

above and below the center of the square (Figure 3). Large numbers of disordered solvent molecules complicated the refinement of the structure. Related structures have been reported with the commercial ligand bispyridyltetrazine.[7]

After having obtained the racemic complex **1**, we envisaged the *stereoselective synthesis* of similar molecular assemblies. For this purpose we developed L^2, a chiral derivative of L^1. By rendering the ligand chiral, the all-$\vec{\Delta}$ and all-$\vec{\Lambda}$ isomers of the complex, which are enantiomers in the case of achiral L^1, will become diastereomers with L^2 (**D** and **E** in Scheme 1).

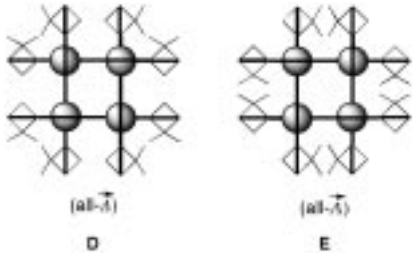

Scheme 1. Schematic representation of the two diastereomers of tetranuclear complexes with L^2. The methyl groups of the pinene moieties in **D** point to each other at the "corners" of the square, while in **E** their orientation is along the sides of the quadrangle.

The "chiralization" (that is, chiral derivatization) of the ligand was achieved quite straightforwardly by introducing pinene moieties, a technique used many times before for pyridine-type ligands.[8] The auto-assembly process delivers the tetranuclear Zn^{2+} complex (all-$\vec{\Delta}$)-$[Zn_4((R,R)\text{-}L^2)_4](PF_6)_8$ (**2**) as the major product with a high diastereomeric excess and in high yield.

The ^1H NMR spectrum shows that three minor species are also present; these species are presumably the other diastereomer of the tetramer and the two diastereomers of the trimer. Although further quantitative analysis of the NMR data is difficult because the signals are insufficiently separated, we can confirm that for a concentration suitable for NMR measurement (here 11.7 mmol L^{-1}), over 95% of the mass of complex **2** is present as the dominant diastereomer of the tetrameric complex, which is the same as that found in the solid state.

The crystal[9] contains only one diastereomer of **2** (type **D**, Scheme 1). The asymmetric unit comprises one complex molecule (Figure 4), and all the Zn^{2+} ions are thus crystallographically inequivalent. The parameters of the coordinative

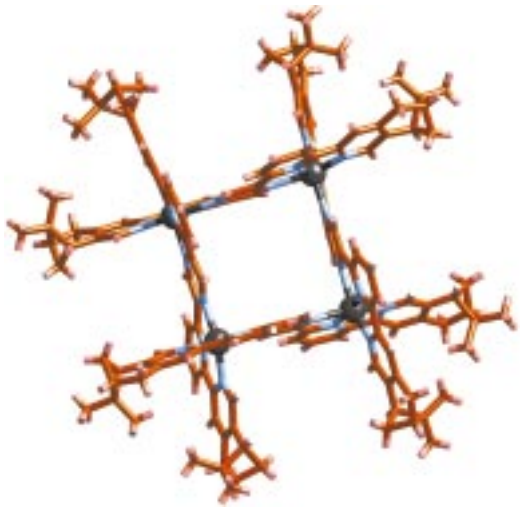

Figure 4. Crystal structure of $[Zn_4(L^2)_4](PF_6)_8$.

bonds are in the usual range (Zn–N(pyridine) 2.077 – 2.171 Å, Zn–N(pyrazine) 2.234 – 2.359 Å). Again, two PF_6^- ions are in close contact with the complex ion (not displayed). The X-ray structure analysis does not only establish the *relative* configuration of the complex (configuration of the ligand ↔ configuration at the metal centers), but it also confirms the *absolute configuration*; the Flack parameter[10] converged to 0.016(13) for the absolute structure containing the $(R,R)/\vec{\Delta}$ isomer of the complex.

In conclusion, we have reported a new type of chiral square complex and presented for the first time the configurational predetermination of the metal centers in such a tetramer by the use of a chiral ligand.

Experimental Section

The syntheses of L^1 and L^2 will be reported, together with isomeric and related pyrazine containing ligands, in a forthcoming publication.

rac-$[Zn_4(L^1)_4](PF_6)_8$ (**1**) was obtained by treating L^1 with a stoichiometric amount of $Zn(ClO_4)_2 \cdot 6H_2O$ in a small volume of MeCN. The ligand dissolved within a few minutes, and after one day at RT, the complex was isolated by precipitation from an aqueous NH_4PF_6 solution.

  1433-7851/01/4015-2850 $ 17.50+.50/0

$[Zn_4(L^2)_4](PF_6)_8$ (**2**) was prepared similarly, but the reaction mixture needed to be refluxed and the subsequent PF_6^- salt recrystallized from $MeCN/Et_2O$. The yields in both cases exceeded 95%. **ATTENTION**: The intermediate perchlorate salts of the complexes are explosive.

Received: March 19, 2001 [Z16796]

[1] a) B. Hasenknopf, J.-M. Lehn, B. O. Kneisel, G. Baum, D. Fenske, *Angew. Chem.* **1996**, *108*, 1987–1990; *Angew. Chem. Int. Ed. Engl.* **1996**, *35*, 1838–1840; b) O. Mamula, A. von Zelewsky, G. Bernadinelli, *Angew. Chem.* **1998**, *110*, 302–305; *Angew. Chem. Int. Ed.* **1998**, *37*, 289–293; c) O. Mamula, A. von Zelewsky, T. Bark, G. Bernadinelli, *Angew. Chem.* **1999**, *111*, 3129–3133; *Angew. Chem. Int. Ed.* **1999**, *38*, 2945–2948.

[2] a) M. Ruben, E. Breuning, J.-P. Gisselbrecht, J.-M. Lehn, *Angew. Chem.* **2000**, *112*, 4312–4315; *Angew. Chem. Int. Ed.* **2000**, *39*, 4139–4142; b) A. M. Garcia, F. J. Romero-Salguero, D. M. Bassani, J.-M. Lehn, G. Baum, D. Fenske, *Chem. Eur. J.* **1999**, *5*, 1803–1808, and references therein; c) S. Toyota, C. R. Woods, M. Benaglia, R. Haldimann, K. Wärnmark, K. Hardcastle, J. S. Siegel, *Angew. Chem.* **2001**, *113*, 773–776; *Angew. Chem. Int. Ed.* **2001**, *40*, 751–754; d) J. R. Galán-Mascarós, K. R. Dunbar, *Chem. Commun.* **2001**, 217–218.

[3] In contrast, the isomeric ligand 2,3-bis(2,2′-bipyridin-6-yl)pyrazine with Co^{2+} ions yields a dinuclear "metallocyclophane". F. Heirtzler, T. Weyhermüller, *J. Chem. Soc. Dalton Trans.* **1997**, 3653–3654.

[4] The solid-state structure of a related trimeric complex obtained from $ZnCl_2$ and 2,5-bis(2-pyridyl)pyrazine has been reported: A. Neels, H. Stoeckli-Evans, *Inorg. Chem.* **1999**, *38*, 6164–6170.

[5] O. Mamula, F. J. Monlien, A. Porquet, G. Hopfgartner, A. E. Merbach, A. von Zelewsky, *Chem. Eur. J.* **2001**, *7*, 533–539.

[6] Crystal data for **1**: $C_{109}H_{100}F_{48}N_{26}O_8P_8Zn_4$, $M_r = 3323.39$; pale yellow block, $0.40 \times 0.40 \times 0.30\ mm^3$, obtained from $MeNO_2$/EtOH/MeOH by the diffusion of Et_2O. $\mu = 0.947\ mm^{-1}$, $F(000) = 6688$. Monoclinic, space group $C2/c$, $a = 19.8633(12)$, $b = 31.1631(17)$, $c = 22.8036(12)$ Å, $\alpha = 90$, $\beta = 110.562(6)$, $\gamma = 90°$, $V = 13216.2(13)$ Å^3, $Z = 4$, $\rho_{calcd} = 1670\ kg\,m^{-3}$. Data collection at 153 K on a Stoe Image Plate Diffraction system, by using graphite-monochromated $Mo_{K\alpha}$ radiation ($\lambda = 0.71073$ Å). Image plate distance: 70 mm, ϕ oscillation scans 0–190°, step $\Delta\phi = 1°$, $2\theta = 3.27–52.1°$, $d_{max}/d_{min} = 12.45/0.81$ Å. A total of 49250 reflections of which 12828 were independent and used to refine 857 parameters. 6968 observed reflections with $I > 2\sigma(I)$. $R = 0.0748$, $wR_2 = 0.2002$ (observed); $R = 0.1216$, $wR_2 = 0.2214$ (all data). The structure was solved by direct methods (SHELXS-97) and refined anisotropically on F^2 (SHELXL-97). Hydrogen atoms were included in calculated positions and treated as riding atoms. Max./min. residual electron density $+1.274/-1.056$ e A^{-3}. One molecule of CH_3NO_2 was located in the asymmetric unit together with a considerable amount of highly disordered, and difficult to identify, solvent. The SQUEEZE routine in PLATON (A. L. Spek, *Acta Crystallogr. Sect. A* **1990**, *46*, C43) was used to modify the HKL data and indicated the presence of the equivalent of 515 electrons per unit cell. This value was equated to one MeOH, one EtOH, and two Et_2O molecules per molecule of complex. b) Crystallographic data (excluding structure factors) for the structures reported in this paper have been deposited with the Cambridge Crystallographic Data Centre as supplementary publication nos. CCDC-159770 (**1**) and -159771 (**2**). Copies of the data can be obtained free of charge on application to CCDC, 12 Union Road, Cambridge CB2 1EZ, UK (fax: (+44) 1223-336-033; e-mail: deposit@ccdc.cam.ac.uk).

[7] K. R. Dunbar and co-workers have reported the tetrameric complex $[Ni_4(bptz)_4(MeCN)_8](BF_4)_8$ (bptz = 3,6-bis(pyridyl)-1,2,4,5-tetrazine): C. S. Campos-Fernandez, R. Clérac, K. R. Dunbar, *Angew. Chem.* **1999**, *111*, 3685–3688; *Angew. Chem. Int. Ed.* **1999**, *38*, 3477–3479. The group of X.-H. Bu and M. Mitsuhiko obtained the tetrameric Zn^{2+} complex from the same ligand, and this complex resolved spontaneously into enantiomers upon crystallization: X.-H. Bu, M. Hiromasa, K. Tanaka, K. Biradha, S. Furusho, M. Shionoya, *Chem. Commun.* **2000**, 971–972.

[8] a) U. Knof, A. von Zelewsky, *Angew. Chem.* **1999**, *111*, 312–333; *Angew. Chem. Int. Ed.* **1999**, *38*, 302–322; b) A. von Zelewsky, O. Mamula, *J. Chem. Soc. Dalton Trans.* **2000**, 219–231.

[9] Crystal data for **2**: $C_{169}H_{199}F_{48}N_{31}O_{12}P_8Zn_4$, $M_r = 4277.83$; pale yellow rod, $0.30 \times 0.20 \times 0.15\ mm^3$, from $MeCN/MeOH/Et_2O$. $\mu = 0.605\ mm^{-1}$, $F(000) = 2198$. Triclinic, space group $P1$, $a = 13.7635(10)$, $b = 18.9612(11)$, $c = 21.8334(16)$ Å, $\alpha = 102.476(8)$, $\beta = 106.002(9)$, $\gamma = 90.240(8)°$, $V = 5335.5(6)$ Å^3, $Z = 1$, $\rho_{calcd} = 1331\ kg\,m^{-3}$, data collection (at 153 K) and refinement as for **1**. $2\theta = 3.72–51.82°$, $\phi = 0–200°$, $\Delta\phi = 1°$. In total 42111 reflections were collected of which 34862 were independent and used to refine 1622 parameters. $R = 0.0717$ and $wR_2 = 0.1604$ for 13535 observed reflections ($I > 2\sigma(I)$); $R = 0.1711$ and $wR_2 = 0.1871$ for all data. Disordered solvent was equated to 7 MeCN, 3 MeOH, and 11 H_2O molecules. The PF_6^- ions are disordered and suffer from thermal motion. Flack parameter[10] $x = 0.016(13)$. Max./min. residual electron density $+0.811/-0.441$ e Å^{-3}.[6b]

[10] H. D. Flack, *Acta Crystallogr. Sect. A* **1983**, *39*, 876–881.

By Overexpression in the Yeast *Pichia pastoris* to Enhanced Enantioselectivity: New Aspects in the Application of Pig Liver Esterase**

Anna Musidlowska, Stefan Lange, and Uwe T. Bornscheuer*

Dedicated to Professor Günter Schmidt-Kastner on the occasion of his 75th birthday

Lipases and esterases can be used as efficient biocatalysts for the preparation of a wide variety of optically pure compounds.[1] Whereas a range of lipases—especially of microbial origin—are commercially available, only a few esterases can be obtained for the kinetic resolution of racemates or desymmetrization. In the majority of publications, pig liver esterase[2] (PLE) is used, which is isolated from pig liver by extraction. Although it has been demonstrated that this preparation can convert a broad range of compounds at partially very high stereoselectivity, its application is connected with a number of disadvantages. Besides a variation of the esterase content between different batches, the presence of other hydrolases particularly has to be considered as problematic with respect to stereoselectivity.[3] Furthermore, it has been shown that PLE consists of several isoenzymes,[4] which in part differ considerably in their substrate specificity. Thus, electrophoretic separation by isoelectric focusing enabled access to PLE fractions that,

[*] Prof. Dr. U. T. Bornscheuer, A. Musidlowska
Institute of Chemistry and Biochemistry
Department of Technical Chemistry and Biotechnology
Greifswald University
Soldmannstrasse 16, 17487 Greifswald (Germany)
Fax: (+49) 3834-86-4373
E-mail: bornsche@mail.uni-greifswald.de
S. Lange
Institute of Technical Biochemistry
Stuttgart University (Germany)

[**] We thank the Konrad-Adenauer foundation (St. Augustin, Germany) for a stipend to A.M., Prof. R. D. Schmid (Institute of Technical Biochemistry, Stuttgart University) for his support and discussions, and A. Gollin for the synthesis of the acetates.